LOGISTICS AND SERVICE OPERATIONS UNDER DISRUPTIONS

OUYUANG XU

PhD

The Hong Kong Polytechnic University

2026

The Hong Kong Polytechnic University

Department of Industrial and Systems Engineering

Logistics and Service Operations under Disruptions

Ouyang Xu

A thesis submitted in partial fulfillment of the requirements for the degree of Doctor of Philosophy

August 2025

CERTIFICATE OF ORIGINALITY

I hereby declare that this thesis is my own work and that, to the best of my knowledge and belief, it reproduces no materials previously published or written, nor material that has been accepted for the award of any other degree or diploma, except where due acknowledgment has been made in the text.

____________________ (Signed)

__________OUYANG Xu__________ (Name of student)

Abstract

Over the past five years, various disruptions have frequently occurred in the world, calling for a new level of operational resilience from both public and private organizations. This thesis aims to address this need through a structured investigation presented in three original studies, which collectively examine this theme. The thesis is progressive and contains i) a review of the recent development of studies on logistics and service operations under disruptions, as well as the methodology of modeling uncertainties arising in disruptions. In particular, it establishes an understanding of the current research landscape and identifies a powerful tool for modeling uncertainties, i.e., distributionally robust optimization (DRO). Various applications of DRO in operations are reviewed, bridging theory and practice. Equipped with a comprehensive understanding of both the problem domain and key methodologies, the research then proceeds to practical applications. The first analytical study is ii) an investigation of targeted intercity travel restriction policies under pandemics, which applies the DRO framework to a critical public health logistics problem. To explore operational challenges under disruption in a competitive environment, the third study shifts focus to the service sector. This work is iii) an analytical study on the adoption of service downgrading strategies (SDS) under economic downturns, which examines competitive strategy using game theory, while also incorporating DRO to model demand uncertainty. The above study sequence provides a progressive exploration of operational resilience across different contexts.

Regarding i), the logistics and service sectors have recently struggled with major disruptions from events like the COVID-19 pandemic, geopolitical tensions, and extreme weather, creating critical operational challenges. To understand how to hedge against these impacts, we conduct a focused review of the latest literature. It identifies primary sources of disruption, classifies their effects on operational uncertainty, and demonstrates how classic problems like vehicle routing are being adapted. This review also surveys representative methodologies used to solve these problems. Among these methods, DRO has gained increasing attention for modeling under uncertainty. Therefore, we further illustrate the interface between DRO and specific operations problems. It begins with preliminary of DRO, presents its application in various scenarios like fleet operations and resource allocation, and uses the newsvendor model to deepen understanding. This work provides researchers and managers with insights into this vital tool for enhancing operational resilience.

Regarding ii), as an effective non-pharmaceutical tool, travel restrictions are often adopted to contain the early spread of severe infectious diseases (e.g., SARS, COVID-19, and monkeypox). This study examines targeted intercity travel restriction policies to hedge against potential pandemic deterioration. We consider the correlation of disease spread among cities in deteriorating scenarios, modeled by DRO. The problem is formulated by a nonlinear huge-scale DRO model and then reduced to a mixed-integer linear equivalence of moderate scales. We develop a Benders decomposition algorithm, utilizing a special relation

between master- and sub-problem variables. Experiments show our model "mean-variance dominates" a classic robust optimization model that ignores the correlation of spread, in terms of higher pandemic control performance and lower performance variation. In the case study, targeted policies exhibit two to five times the pandemic control performance (i.e., infections reduced or human lives saved) against uniform travel restriction policies adopted in the real world. Policymakers are advised to impose targeted intercity travel restrictions as early as possible, since pandemic control performance is more obvious at the early outbreak stage. Targeted restriction policies are promising for developing countries because of comparable pandemic control performance under limited budgets, compared with those with adequate budgets.

Regarding iii), in recent years, facing economic downturns and intense competition, many companies in the service industry (e.g., *American Airlines* in aviation and *Hilton* in hospitality) have downgraded certain services to cut operating costs (e.g., *Hilton* cancelled free breakfasts in some places). We term this emerging practice the *Service Downgrade Strategy* (SDS). While SDS lowers operating expenses, it impairs customer experience, risking demand loss. To offset this, some companies innovatively pair SDS with loyalty programs. Loyalty programs reward customers with "points" redeemable for gifts or other perks, which foster engagement, retention, and repeat purchases in a cost-efficient manner. However, when to implement SDS and how to design the corresponding loyalty program in a competitive environment remain unexplored. To fill this gap, we develop a Stackelberg game model where two service companies compete in SDS commitment and associated loyalty program investments. Our model reveals the following insights: i) The *expected post-SDS market size* (EPSM) is the key determinant for the two companies' equilibrium outcomes. ii) SDS always requires higher loyalty program investments to offset demand loss. iii) Unexpectedly, low competition would drive the adoption of SDS for both companies. iv) Market power asymmetry shapes equilibrium outcomes. Specifically, the same operational efforts (i.e., cost-saving ability during SDS implementation) could exhibit opposite effects on the leader and the follower. In extensions, we generalize our analysis and examine the findings' robustness by considering three operational features, namely a quadratic cost structure of loyalty program investments, the distributional ambiguity of the post-SDS market size and companies' risk attitudes, and the game of one leader and more than two followers.

In conclusion, this thesis contributes to the literature by exploring the operational challenges posed by disruptions. It progresses from broad literature surveys to focused methodological reviews and, finally, to the application of these advanced methods in critical logistics and service operations contexts. The collective findings provide valuable insights and decision-support tools for both public policymakers and private-sector managers aiming to enhance operational resilience in an increasingly uncertain world.

Publications Arising from the Thesis

Papers and Book Chapters

1. **Ouyang X**, Chung SH, Choi TM (2025) Optimal targeted intercity travel restriction policies. Under journal review.
2. **Ouyang X**, Wen X, Choi TM, Chung SH (2025) "Less is more" in service operations: When is it wise to offer less? Under journal review.
3. **Ouyang X**, Chung SH (2025) Logistics and service operations under disruptions: A review. *IEEE Transactions on Engineering Management*, published online.
4. **Ouyang X**, Chung SH (2025) DRO in operations: An introduction. *Encyclopedia in Operations Management*, Elsevier, published online.

Conference Proceedings

1. **Ouyang X** (presenter) (with Wen X, Choi TM, Chung SH) "Less is more" in service operations: When is it wise to offer less? *INFORMS M&SOM Conference 2025*, London, UK, 27 to 29 June 2025.
2. **Ouyang X** (presenter) (with Choi TM, Chung SH) Optimal targeted intercity travel restriction policies. 2025 *INFORMS Annual Meeting*, Atlanta, US, 25 to 29 October 2025.

Acknowledgements

First and foremost, I would like to express my deepest appreciation to my supervisors, Professor Nick Sai-Ho Chung at PolyU and Professor Jason Tsan-Ming Choi at ULMS. They offered me the opportunity to pursue my doctoral studies during a particularly harsh period of my life. Had I not encountered them at that pivotal moment, I might have sought immediate employment rather than embarking on this academic journey. Throughout my doctoral studies, they provided not only meticulous academic guidance, helping me refine my research through numerous revisions, but also profound life lessons. They are, and will always be, my lifelong mentors.

I would also like to extend my gratitude to my friends, Dr. Weikun Xu, Dr. Fan Zhang, Dr. Yonghuan He, Dr. Junting Li, and Dr. Qiangxiang Zhao, among others. My thanks also go to those who created happy memories with me, including many whose names I do not even know.

Last, I am grateful to my family. I want to thank my father, Rujin Ou, and my mother, Shengying Xie, for their unconditional support. They never pressure me regarding my career or lifestyle choices, but instead encourage every interest and decision I make. I want to thank Dr. William Wang, who stands by me through countless challenges, creates wonderful memories with me, and supports any of my interests and decisions.

Before the end of this journey, I wish everyone who has helped me during my doctoral journey happiness and health. Thank you.

Table of Contents

Chapter 1. Introduction

1.1. Background

The outbreak of the COVID-19 pandemic in early 2020 exposed the logistics and service sectors to various disruptions (Gupta et al. 2022). The closure of manufacturing facilities, strict travel restrictions between and within cities, and widespread labor shortages created substantial challenges for operators (Birge et al. 2023). For example, during the pandemic, the Los Angeles Port, which is a vital hub of global shipping, failed to function as usual, and over 100 container ships were stuck there, leading to billions of dollars in losses[1]. These disruptions severely hampered daily operations, and various activities, including production, delivery, and service, were interrupted. It is thus crucial to devise resilient operational strategies to hedge against unexpected disruptions like the COVID-19 pandemic.

Infectious diseases are just one instance of potential disruptive events. Natural disasters (e.g., earthquakes and hurricanes) also incur significant threats to humans for a long time, with increasing frequency and intensity (Chen et al. 2023). For example, Hurricane Katrina in 2005 caused damage of over USD 100 billion and crippled supply chains in the Gulf Coast region for months[2]. The 2021 Texas Winter Storm led to the shutdown of petrochemical plants, causing a domestic energy shortage that affected various industries, including transportation, aviation, and hospitality, resulting in an economic loss of millions of dollars[3]. More recently, the 2023 earthquakes in Turkey and Syria resulted in over 55,000 deaths and left millions homeless, creating a humanitarian catastrophe that was far beyond local response abilities[4].

Except for natural disasters, operational activities have become increasingly vulnerable to human-caused disruptions in recent years (Charpin and Cousineau 2025). The US-China trade war, which began in 2018 and re-intensified in 2025, has introduced a new dimension of disruptions (i.e., geopolitical risk and regulatory uncertainty). The high tariffs and policy uncertainty forced players in international trade to reshape their global sourcing strategies (Huang et al. 2023). Another example that merges international politics, economy, and geographical conflicts is the Russo-Ukrainian War. The 2022 invasion of Russia not only triggered a humanitarian crisis but also sent disruptions throughout Central European supply chains[5]. The resulting adverse impacts were profound; energy supply became a tool of statecraft, food security was threatened, and countless facilities were severely damaged or destroyed (Sheth and Uslay 2023). These two

[1] https://www.bbc.co.uk/news/58926842/. Accessed 20 Jul 2025.
[2] https://www.britannica.com/event/Hurricane-Katrina/. Accessed 20 Jul 2025.
[3] https://www.dallasfed.org/research/swe/2021/swe2102/swe2102c/. Accessed 20 July 2025.
[4] https://www.redcross.org.uk/stories/disasters-and-emergencies/world/turkey-syria-earthquake/. Accessed 20 Jul 2025.
[5] https://economicsobservatory.com/ukraine-whats-the-global-economic-impact-of-russias-invasion/. Accessed 20 Jul 2025.

events exemplify the range of geopolitical risks, underscoring the importance of designing resilient operational plans for operations of international business.

To cope with these immense challenges, it is critical to identify and understand the operational problems that arise under such disruptive conditions. Operations management (OM) is a major discipline that contributes to disruption management (Dolgui and Ivanov 2021). Its branches span pandemic control, disaster management, humanitarian aid, etc., dedicated to enhancing operational resilience, economic stability, stakeholders' profitability, and public well-being (Sawik 2020). We would thus like to explore how OM helps manage disruptions in this increasingly uncertain era.

1.2. Motivations

The goal of this thesis is to investigate how to scientifically manage logistics and service operations in a disruptive era. In particular, the thesis contains three original studies, and the motivation of each work is as follows.

Diverse and complex disruptions in recent years have triggered a rapid growth in academic research across numerous journals, creating a fragmented landscape that is difficult to navigate. This situation creates a compelling need for a systematic overview. Therefore, the first study in this thesis is motivated by the fundamental need to structure this academic conversation by categorizing the primary sources of modern disruptions, classifying their operational impacts, and reviewing the key problems and methodologies being explored. A central theme that emerges from this literature is the challenge of decision-making under uncertainty, where traditional methods like stochastic programming and robust optimization have significant drawbacks. This methodological gap motivates a further review, which focuses on DRO as a more suitable tool. Recognizing that DRO is unfamiliar to many, we aim to bridge the gap between its advanced theory and its practical application. Its purpose is to explain this powerful methodology and provide a clear guide for its use, thereby equipping researchers and practitioners with a better tool for handling the uncertainty inherent in disruptions.

The COVID-19 pandemic exposed a critical vulnerability in global public health response: A reliance on broad, non-pharmaceutical measures. Faced with a rapidly spreading novel virus, governments around the world implemented sweeping, uniform travel restrictions. While these measures were intended to slow the transmission of the disease, they came at an immense economic and social cost. Supply chains were paralyzed, businesses were shuttered, and the global economy was plunged into recession. This one-size-fits-all approach was largely a product of urgency and the absence of more sophisticated decision-support tools. The immense collateral damage created a clear and pressing need for smarter, more targeted policies. This raises a critical question for logistics and public policy: How can policymakers achieve the necessary public health benefits of travel restrictions while minimizing their devastating side effects? The core difficulty in answering this question lies in the uncertainty surrounding how a new disease will spread, particularly the complex correlation of transmission between different population centers. This high-stakes, real-world problem, characterized by its urgency and profound ambiguity, presents a perfect opportunity to apply advanced analytical methods. This study is motivated by the need to move beyond the broad approaches of the past. Its purpose is to develop a decision-support tool that can help policymakers design more nuanced, effective, and less costly travel restriction policies, providing a vital capability for managing future public health crises.

Beyond the acute crises of pandemics and natural disasters, economic downturns represent another recurring form of disruption that puts companies in difficult strategic positions. In recent years, a notable and controversial strategy has emerged in the service industry, sometimes called a service downgrade strategy (SDS). We have seen this in practice when major airlines reduce in-flight amenities and charge for previously free services, or when hotel chains cut back on daily housekeeping and other guest services to reduce operating costs. While this strategy can offer immediate financial relief in a challenging economic climate, it involves significant risk. It can damage a brand's reputation, alienate loyal customers, and create openings for competitors. This raises a series of complex strategic questions that currently lack a rigorous analytical foundation. When, if ever, is SDS a wise business decision? How should a firm expect its competitors to react? If a rival firm downgrades its service, is it better to follow suit, or to invest in quality to capture dissatisfied customers? Furthermore, how do other strategic tools, such as customer loyalty programs, interact with this decision? These questions are at the intersection of operations management, marketing, and competitive strategy. This final study is motivated by the need to analyze this important and emerging business practice. Its purpose is to model the competitive dynamics of SDS and to provide managers with a clear, analytical framework for navigating these high-stakes decisions in a turbulent economic environment.

1.3. Objectives

This thesis pursues its overarching goal of enhancing operational resilience through three specific and interconnected research objectives, each corresponding to one of the three original studies.

1. The first objective is to provide a structured overview of the recent research on logistics and service operations under disruption. This involves identifying the primary sources of modern disruptions, classifying their operational impacts, and surveying the key problems and analytical methodologies being explored. As decision-making under uncertainty emerges as a central challenge from this review, a special focus is dedicated to DRO, a powerful framework for handling such ambiguity. Therefore, the review aims not only to map the broader research landscape but also to provide an accessible guide to

DRO. The goal is to equip researchers with both a foundational understanding of the field and a more suitable tool for future investigations.

2. The second objective is to develop an analytical framework for designing targeted and more effective intercity travel restriction policies to manage public health crises like pandemics. Motivated by the immense economic and social costs of the broad, uniform restrictions used in practice, this study aims to create a more nuanced approach. The goal is to explicitly model the complex uncertainty of disease spread and to provide policymakers with a model that can generate policies that maximize public health benefits while minimizing negative societal impacts, especially during the critical early stages of an outbreak.
3. The third objective is to examine and formulate competitive dynamics of SDS adopted by firms during economic downturns. As this practice involves significant risks and strategic trade-offs, this study aims to provide a clear analytical framework to understand its implications. The goal is to determine the market conditions under which SDS is a viable strategy, to analyze the competitive interactions between firms, and to provide managers with actionable insights for making these high-stakes decisions in a turbulent economic environment.

1.4. Contributions

This thesis investigates logistics and service operations problems under disruptions by three original studies, and the contribution of each work is summarized as follows.

Chapter 2 conducts a critical literature review. It provides a foundational understanding of logistics and service operations under disruption, with a special focus on the volatile period from 2020 to early 2025. We present a structured statement that reveals three key themes emerging from the latest literature: the primary sources of disruptions and their resulting uncertainties, the critical operational problems that must be addressed, and the analytical methods adopted to resolve these issues. Among these methods, DRO stands out as a powerful framework for decision-making under the uncertainty inherent in these events. Therefore, this chapter also serves as a critical bridge between DRO theory and its practical application in operations management. It provides an accessible guide for practitioners by reviewing DRO applications in key problems like inventory management and sets a clear research agenda, urging the development of novel models to unlock deeper operational insights and enhance resilience.

Chapter 3 conducts an analytical study. It optimizes the optimal targeted intercity travel restriction policies to contain pandemics and contributes to the literature through significant methodological and practical advancements. Methodologically, it pioneers a DRO model that uniquely captures the ambiguous correlation of disease spread among cities. The research successfully reduces this complex, large-scale model into a tractable form and develops a specialized Benders decomposition algorithm, enabling efficient solutions for real-world networks. Practically, the study demonstrates that these targeted policies are two to five times more effective than the uniform restrictions often used in practice, saving more lives with less performance variation. Key insights for policymakers include the critical importance of early implementation and the policy's high effectiveness even under limited budgets, making it especially valuable for developing nations. The model also outperforms classic robust optimization approaches that ignore correlation, proving the value of this more nuanced modeling technique.

Chapter 4 develops an analytical study on service operations under economic downturns. Its contributions are three-fold: i) Novel operational framework: To our knowledge, it is the first analytical study that considers intentionally reducing service qualities as a focal strategy under competition (i.e., SDS) and the corresponding compensation actions. Specifically, we integrate SDS and associated loyalty program design into a unified competitive model, addressing a critical gap in managing cost-cutting amid customer retention. This framework captures real-world practices (e.g., aviation, ride hailing, hospitality) where SDS and loyalty programs are co-dependent. ii) Insightful findings: We derive findings that can challenge existing practices or senses. For example, we disprove the assumption that cost-saving efforts benefit all firms equally. iii) Viable action plans: Our analyses give answers to three "W"s for an operations manager: When to preemptively impose SDS; Whether to adopt SDS given that the rival has already committed to SDS; and What to do with loyalty programs during SDS implementation.

1.5. Thesis Outline

This thesis is structured into five chapters, which collectively present a cohesive body of research developed across three original studies. The document is organized to guide the reader logically from the broad context of the research problem to the specific contributions of each study. **Chapter 1** sets the stage by establishing the contemporary research context. It highlights the increasing frequency and severity of disruptions in the modern world, thereby underscoring the critical significance of developing resilient and efficient logistics and service operations. This chapter outlines the core motivation and objectives that drive the entire doctoral research. **Chapter 2** bridges theories and applications through comprehensive reviews. The first section presents a systematic survey of the recent literature on logistics and service operations under disruption, mapping the current state of knowledge and identifying key research gaps. The second section provides a focused review of DRO, a cutting-edge methodology for modeling uncertainties that arise from disruptive events. Building upon this foundation, the thesis then transitions to two original analytical studies. **Chapter 3** addresses a critical problem in public health logistics, examining how to design optimal targeted intercity travel restriction policies to effectively manage a pandemic. This chapter showcases the application of advanced optimization techniques to a large-scale societal challenge. Subsequently, **Chapter 4** investigates a key strategic problem in service operations. It analyzes the competitive dynamics of service downgrading, exploring when and why firms might adopt such a strategy in response to an economic downturn. This study delves into the strategic trade-offs that companies face in turbulent market conditions. Finally, **Chapter 5** concludes the thesis. This chapter synthesizes the key findings from the three constituent studies, articulates the overall contribution of this doctoral research to the field of operations management, and proposes a detailed agenda for future research stemming from each of the three studies. To ensure the main chapters remain focused and readable, all supplementary materials, extended datasets, and detailed technical proofs are provided in the **Appendices**. **Table 1.1** summarizes research questions and how different chapters answer them.

Table 1.1. The correspondence between research questions and chapters.

Chapter	Research Question(s)	How the Chapter Answers Them
2. Literature & Methodology Review	How can we categorize modern disruptions, and what is the best way to model their inherent uncertainty?	Provides a structured taxonomy of disruptions and operational impacts; offers a specialized guide to DRO (Distributionally Robust Optimization) as a superior tool over traditional methods.
3. Targeted Travel Restrictions	How can policymakers design effective travel restrictions that balance public health benefits with socioeconomic costs?	Develops a DRO-based analytical model that captures city-to-city transmission correlations, proving that targeted policies are 2.5–5 times more effective than uniform lockdowns.
4. Service Downgrading (SDS)	When should a firm adopt SDS during a downturn, and how do competitive dynamics and loyalty programs affect this decision?	Formulates a competitive game-theoretic model integrating SDS and loyalty programs; provides a framework for managers to decide when, whether, and what to do when facing service-cut decisions.

Chapter 2. Literature Review

2.1. Recent Development of Logistics and Service Operations under Disruptions

This sub-chapter aims to review the latest studies on logistics and service operations under disruptions, focusing on two crucial industries for the economy, suppliers, and customers. Using the latest literature, we hope to provide researchers and practitioners with a clear understanding of i) the key disruptions affecting their operations, ii) the major operational problems arising from these disruptions, and iii) available analytical and computational methods for managing operations under disruptions.

2.1.1. Review method

This is a critical review (Wang et al. 2015), in which it is different from a systematic review. We have no intention to exhaustively collect papers from the vast literature. Instead, we focus on reviewing prior studies published from 2020 to early 2025, a period marked by numerous unexpected events. We also focus on the most authoritative journals and hence, the review coverage is the mainstream leading engineering and OM journals (e.g., *IEEE Transactions on Engineering Management*, *Production & Operations Management*, *Manufacturing & Service Operations Management*), based on the standard by Wang et al. (2015). We focus on technical papers that employ analytical modeling or optimization as a solution approach, excluding empirical studies, case studies, or field experiments. The search process utilizes disruption as a compulsory keyword, combined with several optional keywords (e.g., trade war, pandemic, disaster, resilience, and operations). Then, from the obtained initial pool, we manually filter the results to identify papers that explicitly address operational problems under disruptive events in the logistics and service sectors.

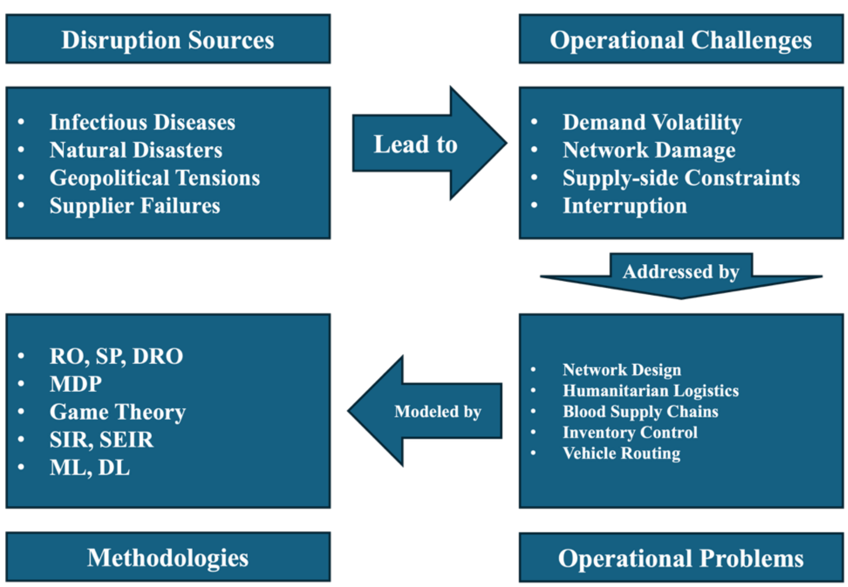

Figure 2.1. A conceptual framework for logistics and service operations under disruptions.

To structure our review and provide a high-level synthesis of the literature, this chapter proposes a conceptual framework shown in Figure 2.1. The framework establishes a clear taxonomy that links the core themes of our review. It illustrates how exogenous **Disruption Sources** create various forms of **Operational Challenges**, which in turn give rise to specific **Operational Problems**. Finally, the framework shows that a portfolio of **Methodologies** is required to effectively model and solve these problems.

2.1.2. Sources of Disruptions

There are three primary sources of disruptions in logistics and service operations over the past few years. While other disruptions exist (e.g., financial crises, terrorism), our review focuses on these three as they represent the most dominant and widely studied categories in the recent engineering and operations management literature. They impose operations with different impacts, resulting in various challenges. This section aims to display these disruptions and analyze their effects. At the end of this section, we summarize our findings in Table 2.1.

2.1.2.1. Infectious diseases and pandemics

The COVID-19 pandemic is the most dominant source of disruption over the past five years. The resulting economic downturns significantly impair logistics and service sectors (Wen et al. 2025). Besides, operational vulnerabilities are relevant to various public health crises, including other infectious diseases like monkeypox, Ebola, and SARS. The lessons learned in fighting against COVID-19 provide a crucial foundation for managing future epidemics. The operational impacts can be categorized into two distinct areas as follows.

Customer demand. Infectious diseases can significantly affect demand (Sawik 2020). During the initial phases of a pandemic, demand for essential goods (e.g., medicines, cleaning supplies, and personal protective equipment) can dramatically surge (Xu et al. 2023). This spike is often driven by a combination of legitimate needs and behavioral factors, which creates a significant bullwhip effect that ripples upstream through the supply chain. Also, demand for non-essential services (e.g., hospitality, tourism, and dine-in restaurants) can collapse quickly as populations are encouraged or mandated to stay home (Bonardi et al. 2023). The demand shrinkage brings immense challenges for forecasting, inventory management, and resource allocation, rendering many traditional models ineffective (Boloori and Saghafian 2023).

Supply-side capacity. Pandemics attack the supply side of logistics and service operations with equal force (Ivanov 2020). Social distancing policies, lockdowns, and widespread worker illness directly reduce the adequate operational capacity of facilities and networks (Chen and Kong 2023, Ouyang et al. 2025). This impacts both physical and human resources. For instance, warehouse and transportation capacity becomes constrained not by a lack of physical assets but by a shortage of available labor. Pandemics directly impact the workforce, as employees become sick, need to quarantine, or must stay home to care for family members (Kaushik and Guleria 2020). This leads to uncertainty in daily labor availability, making scheduling inefficient (Nagurney 2021). Safety protocols, such as social distancing or enhanced cleaning, can also reduce productivity and output. A distribution center might be full of inventory but unable to process orders due to staff shortages. Likewise, global supply chains are affected by the shutdown of manufacturing plants in affected regions and severe congestion at ports and borders resulting from enhanced health screening protocols (Xu et al. 2020). These shocks often lead to supplier reliability uncertainty, where a key supplier may fail to deliver due to localized outbreaks or lockdowns, forcing downstream firms to halt production.

2.1.2.2. Natural disasters

Natural disasters are another critical category of disruptions that significantly affect logistics and service operations (Ye et al. 2020). Hurricanes, earthquakes, floods, wildfires, and other extreme weather can cause sudden and immense damage to operations and infrastructure.

Transportation network integrity. Natural disasters cause severe physical damage to transportation networks. Earthquakes can destroy bridges and create fissures in roads, while hurricanes and floods can make entire road segments impassable (Dukkanci et al. 2023). This leads to severe network connectivity disruption, where the links and nodes of a transportation network fail unpredictably. For logistics and service providers, this means that planned routes become infeasible, travel times become highly uncertain, and entire communities can be cut off from aid. Operators face the challenge of assessing damage and effectively rerouting resources in a broken and constantly changing network. In disruptions, information can become unreliable; for instance, in the initial hours following a disaster, it is hard to determine which roads are passable. The uncertain information of road network structure makes accurate operations impractical (Eftekhar et al. 2022).

Failure of stationary facilities and assets. Natural disasters not only damage transportation links but also the physical facilities essential for operations. Warehouses storing relief supplies can be destroyed, hospitals can be rendered inoperable, and temporary shelters can be compromised (Aghajani et al. 2023). This leads to severe facility capacity uncertainty, where some resources (e.g., storage space, hospital beds, power generation) are suddenly unavailable. Such events are a direct cause of supplier failures, as a catastrophic factory fire or flood can completely halt the flow of materials from a key supplier with little to no warning. The failure can also be cascading; for instance, the loss of power at a hospital renders its medical equipment and beds useless, even if the building itself is intact. This necessitates planning frameworks that are resilient to the failure of critical facilities, accounting for the possibility that prepositioned resources may not be accessible when needed most (Erbeyoğlu and Bilge 2020).

2.1.2.3. Geopolitical tensions: Trade and hot wars

Geographical tension is another critical disruption that has become increasingly important in recent years due to several international events (i.e., the trade war and the hot war). The resulting disruptions include events ranging from geopolitical conflicts and trade disputes to labor strikes and cyberattacks (Fan et al. 2022, Aftabi et al. 2025). The geopolitical risks range from strategic economic competition to acute military conflict, creating new challenges for logistics and service operators, especially those involving international business. A few studies consider operational responses to these complex, human-driven uncertainties.

Strategic Disruption. Trade Wars and Tariffs. The US-China trade war directly imposes cost uncertainty to companies, as the landed cost of goods can change unpredictably subject to new policies (Handfield et al. 2020). A small increase in tariffs can significantly reduce profit margin. The trade war also triggers operators' concerns about the future policy: Will tariffs be permanent? Will they be expanded to other product categories? These concerns affect many decisions such as where to build a new factory and where to buy raw materials. Therefore, companies should diversify away from high-tariff regions to mitigate costs and risks (Lin et al. 2021). The core operational problem becomes one of strategic network design under uncertainty, where firms must balance the cost-efficiency of a concentrated network against the resilience of a diversified one (Sazvar et al. 2021).

Acute disruption. War and sanctions. The war in Ukraine is a more severe form of geopolitical disruption, where operational challenges extend beyond economics to matters of safety and security. The uncertainties in this environment are profound and multi-faceted. Infrastructure destruction and blockades involve the deliberate targeting of critical assets (e.g., ports, railways, and bridges) creating barriers to logistics flows that cannot be overcome simply by incurring higher costs (Cheng et al. 2021). Sudden commodity and energy shocks, driven by the removal of major suppliers like Russia from the global market, create extreme supply uncertainty and price volatility that affect almost every industry. This can manifest as component scarcity, where sanctions or conflict make critical raw materials (e.g., microchips, energy) unavailable, leading to unpredictable and lengthy delivery lead times for a wide range of products. Physical security and access risks pose a constant threat to personnel, assets, and facilities, rendering operations in conflict zones incredibly hazardous and often making withdrawal from the market (McCrie and Lee 2021, Chung et al. 2025).

Other geopolitical and human-driven disruptions. Beyond wars and tariffs, logistics and service operations are vulnerable to other forms of human-driven disruptions that arise from social or political tensions. Labor strikes, particularly at key logistical nodes like ports, can halt the flow of goods for weeks. Strikes cause ships to wait offshore, containers to pile up, and stores to run out of stock; the recovery can be just as disruptive as the strike itself (Leung et al. 2020). Cyberattacks, whether by governments or others, can shut down key logistics systems and halt global operations (August et al. 2024, Kumar et al. 2025). Major product recalls also disrupt supply chains, as companies must quickly handle returns and repairs while under public scrutiny (Chakravarty et al. 2022).

Disruption Source	Impact on the Logistics Industry	Impact on the Service Industry	Key Characteristics / Severity
Infectious diseases	Uncertain travel times, driver/worker shortages, network closures, and supplier unreliability.	Unpredictable demand for services, staff shortages, and facility closures.	Widespread, potentially long-duration, global scope. Impacts both supply and demand simultaneously.
Natural disasters	Damaged roads and ports, warehouse destruction, route blockages, and supplier facility failures/	Damaged facilities (e.g., hospitals), mass casualty incidents, and a surge in demand for aid.	Often geographically localized but acute and severe. Primary impact is on physical infrastructure. Short warning time.
Geopolitical tensions	Volatile tariffs, sanctions, asset seizure risk, route blockades, forced network redesign, and component scarcity.	Service interruptions from cyberattacks, energy and food price shocks, and managing refugees.	Human-driven and strategic. Can be long-term (trade wars) or acute (hot wars). Impacts are often economic or security-related.

Table 2.1. Major sources of disruption in recent years.

2.1.3. Operational Problems under Disruptions

Disruptions not only present challenges to existing operations but also give rise to new and critical operational problems. To better organize these problems, we propose a Decision-level Time-horizon (DT) taxonomy, based on two key dimensions: the **Time Horizon** of the decision (i.e., Proactive vs. Reactive) and the **Decision Level** (i.e., Strategic vs. Operational), as shown in Figure 2. **Proactive** problems focus on preparedness before a disruption, while **Reactive** problems address the response after an event occurs. **Strategic** problems involve long-term decisions like network design, while **Operational** problems focus on short-term execution like routing and inventory control. This section identifies five major operational problems from recent literature within this framework.

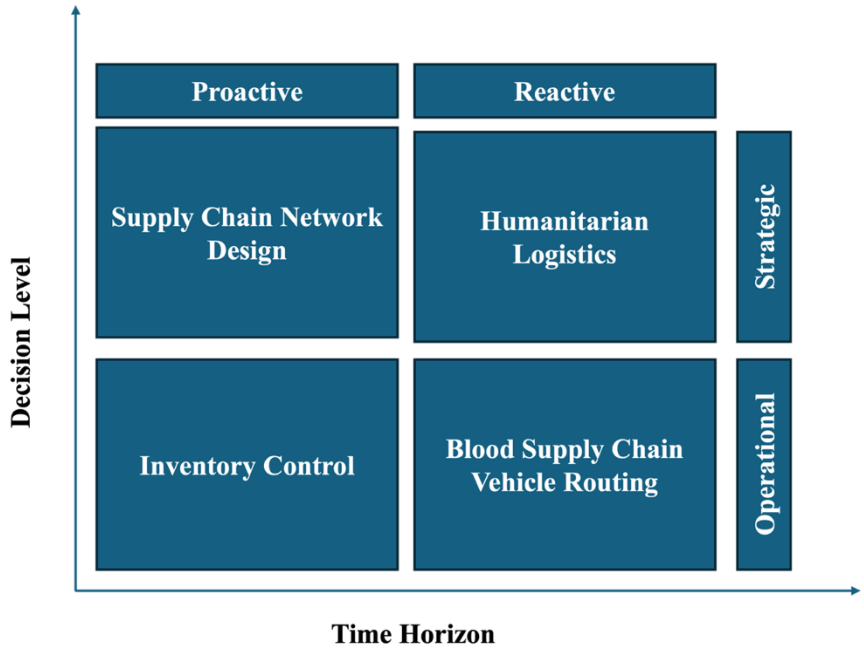

Figure 2.2. Decision-level time-horizon (DT) taxonomy.

2.1.3.1. Strategic-proactive problems

Strategic-proactive problems involve long-term planning and investment decisions made before disruptions occur to build resilience into the system. The primary example in the literature is supply chain network design.

Supply chain network design and sourcing

Network design is a classic problem in operations management. Still, recent natural disasters and geopolitical conflicts (e.g., the Russo-Ukrainian war) have propelled this area back to the forefront with new and urgent challenges. The core problem has shifted from designing a network that is purely cost-efficient to designing one that is resilient and can withstand major disruptions (Huang et al. 2023). This means making long-term decisions about where to put factories and get materials, even though the future is uncertain. These choices are vital as the global setup can decide whether a firm can survive serious events (Noorizadegan et al. 2025).

Modeling war-related risks. One primary stream is modeling tariff uncertainty. The US-China trade war demonstrated that tariffs can be used as a political tool, making the landed cost of goods highly unpredictable. In a modeling perspective, tariffs are treated not as a fixed cost but as an uncertain parameter (Dong and Kouvelis 2020). The solution helps firms decide whether to stay in a high-tariff country, shift to a more expensive but tariff-free alternative, or invest in a flexible capacity that allows them to switch production between countries as trade policies change.

Robust sourcing strategies. Besides costs and tariffs, companies need to consider how stable and reliable other countries are when choosing where to get their supplies (Wu et al. 2024). New models are developed to help companies spread out their suppliers, so they aren't too dependent on just one country or region. This helps protect them from problems that might happen in one specific place (Jafarian et al. 2025).

Comprehensive sanctions and sudden market exit. This kind of disruption is much more serious than a tariff because it can suddenly block access to a market or supplier, sometimes within hours (Sun et al. 2022, Shalpegin et al. 2025). Research on this topic is still new, but it looks at both how to quickly change supply routes and the big financial and operational losses that come from investments and unused assets.

2.1.3.2. Strategic-reactive problems

Strategic-reactive problems involve reconfiguring long-term strategy in the immediate aftermath of a major, system-altering disruption. While less common in the literature than operational responses, this category includes decisions like sudden market exit. A popular reactive problem is the humanitarian logistics problem.

Humanitarian logistics

This is the most direct application of operations management in the face of disruptions, with the goal to efficiently and equitably distribute aid to affected populations in disasters. The field is challenging because decisions must be made under time pressure with highly incomplete information and in chaotic environments. Effective planning directly reduces human suffering and saves more lives (Liu et al. 2025). Operations span both preparedness and response. For preparedness, researchers develop models for prepositioning materials and designing resilient facility networks that can withstand partial failures. Once a disaster has occurred, the focus shifts to reactive response, including planning large-scale evacuations, coordinating the last-mile delivery of aid, and managing temporary shelters.

Equity and fairness. It is now widely recognized that simply delivering the most aid in the shortest time is insufficient if specific communities are left behind. A growing body of literature incorporates fairness metrics into aid distribution models, moving beyond pure efficiency. This can mean goals like reducing the highest unmet needs in all communities, making sure the most vulnerable groups get a minimum level of service, or using methods that balance fairness with efficiency (Li et al. 2024, Zhang et al. 2025b).

2.1.3.3. Operational-proactive problems

These problems involve positioning resources and setting policies in the short-to-medium term to prepare for potential disruptions. Inventory control is the archetypal problem in this category.

3.3.1. Inventory control under uncertainty

Inventory control. It is one of the most classic problems in operations management. Still, emerging disruptions have provided a new context for its application, introducing new layers of complexity. The key decision remains how much quantity stock, but the nature of the uncertainties that must be managed has evolved significantly. While traditional models focus primarily on demand uncertainty, modern inventory problems must simultaneously address uncertainties in supply, lead time, and cost as direct inputs to the decision-making model.

Supply disruptions. This includes the risks that a supplier could suddenly fail due to bankruptcy, natural disaster, or political reasons (Saputro et al. 2021). This has led to a rich literature on multi-sourcing strategies, where firms deliberately source from multiple suppliers, even if some are more expensive, to create redundancy. Models have been developed to determine the optimal allocation of orders across a portfolio of reliable and unreliable suppliers, balancing cost and resilience (Pathy and Rahimian 2023, Fardi et al. 2025).

Uncertain lead times. Problems like port congestion, strikes, and customs delays are happening more often, so delivery times are now unpredictable instead of fixed (Sun et al. 2020). Because of this, inventory models need to figure out how much extra stock to keep on hand to deal with these delays and make sure service stays reliable (Zhang et al. 2020).

Cost uncertainty. When tariffs can change suddenly, companies don't always know how much an order will cost when they place it (Yang and Shi 2023). This has led to new inventory models that take this risk into account. For example, a company might order extra goods before a tariff increase or use a hub in a neutral country to store products and wait until things are more certain (Hezarkhani et al. 2023). Making these choices needs advanced models that combine inventory planning with financial and political risk factors.

2.1.3.4. Operational-reactive problems

Operational-reactive problems focus on the immediate response after a disruption has occurred, where decisions must be made rapidly with incomplete information to alleviate suffering or restore service.

Blood supply chain management

Blood is a vital but highly perishable product in healthcare operations. Its supply chain is especially fragile because disasters can suddenly increase the need for blood while also making it harder for donors to give blood and for deliveries to reach hospitals. Managing blood supplies during these times is a serious challenge that can make a critical difference between life and death.

Blood collection planning. This involves choosing the best places and times to hold mobile blood drives so that as many people as possible donate. This is tricky because it's hard to predict how many donors will show up (Abbasi et al. 2020). After a disaster, things get even harder because roads might be damaged and the collected blood has to be taken to a processing center quickly, before it spoils.

Blood inventory management. Blood storage cannot last long, only a few days. This makes it hard to decide how much blood to store: You need enough to handle sudden increases in demand but storing too much means some will go to waste if it expires (Zhang et al. 2023). Recent studies examine creating better ways to manage blood inventories, using robust optimization methods (Razavi et al. 2021). Some models also look at using new medical technologies (e.g., cryopreserved platelets) which last much longer but cost more. This adds another decision: When it's worth switching to these more durable but expensive options.

Blood distribution. Transporting blood to hospitals is a critical issue, especially during disasters when transport routes may be disrupted (Meneses et al. 2023). Delivery needs to be fast and safe, and the models must handle the urgent and unpredictable demands from different hospitals treating injured people (Hamdan and Diabat 2020).

Vehicle routing under disruptions

The vehicle routing problem is a well-established operational problem, but it becomes much harder under disruptive environments (e.g., disasters). In these situations, vehicle routing is used to plan how to deliver emergency supplies or services. This makes the problem much more complex, with a lot of uncertainty and changing goals.

Uncertain states in transport networks. After a disaster has already taken place, many routes may be unusable, and the status of many roads and facilities may be unknown (Gmira et al. 2021). This means that a routing plan must be created with incomplete information. This has led to the development of robust and adaptive routing models that can handle road interruptions and travel time uncertainty. For instance, a route is planned to include backup alternatives in case the primary path is blocked. Other models focus on dynamic routing, where vehicle paths are updated in real time as new information about the network status becomes available from drones, sensors, or field reports (Mor and Speranza 2022, Abdulrashid et al. 2025, Faramarzi-Oghani et al. 2025).

Emerging technologies. Routing problems are no longer limited to a homogeneous fleet of trucks. Modern disaster response may involve a mixed fleet of traditional vehicles, agile motorcycles for navigating narrow or damaged streets, and autonomous assets, such as drones (Wang et al. 2022). This creates a new class of vehicle routing problems that consider the unique features of these new technologies. For example, when routing drones, models must account for their limited flight range, payload capacity, and the need to plan paths that include stops at charging stations (Dukkanci et al. 2023). Pandemics have also spurred innovation in routing for contactless commerce and hyper-local delivery networks to serve residential areas under lockdown conditions. The integration of these new technologies with traditional logistics assets is a promising and very active area of current research (Yoon et al. 2025, Zhang et al. 2025a).

Position in the DT Taxonomy	Operational Problem	Brief Definition	Major Problem Features
Strategic-Proactive	Network Design	Designing global supply chain structures under geopolitical risks.	Tariff/sanction uncertainty, political instability, diversification vs. cost.
Strategic-Reactive	Humanitarian Logistics	Preparing for or responding to disasters via aid distribution.	Network damage, demand uncertainty, equity, and timeliness.
Operational-Proactive	Inventory Control	Setting inventory levels under conditions of supply and demand uncertainty.	Unknown distributions, lead time variability, and data-driven signals.
Operational-Reactive	Blood Supply Chains	Managing the collection and distribution of perishable blood products.	Perishability, supply and demand uncertainty, and wastage versus shortage.
	Vehicle Routing	Planning vehicle routes on unreliable networks.	Uncertain travel times, link failures, and driver availability.

Table 2.2. Logistics and service operational problems under disruptions.

Operational Problem	Infectious Diseases	Natural Disasters	Geopolitical Tensions	Supplier Failures
Humanitarian Logistics	✓	✓	✓	✓
Network Design	✓	✓	✓	
Blood Supply Chains				✓
Inventory Control	✓	✓	✓	✓
Vehicle Routing		✓	✓	

Table 2.3. Mapping of Disruption Sources to Primary Operational Problems

2.1.4. Major Methodologies

This section reviews the primary methods used to solve operational problems under disruptions, including both analytical modeling and computational approaches. We classify them into five groups, each of which characterizes different problem features and operational objectives.

2.1.4.1. Operational uncertainty

Potential disruptions can bring operational uncertainty, including facility disruptions, unpredictable delivery times, and transportation interruptions. There are three mainstream approaches to modeling uncertainties in operational problems.

Stochastic Programming (SP). SP originated in the 1950s with pioneers like George Dantzig (Cottle et al. 2007). It models uncertain items as random variables and requires complete knowledge of their probability distributions (Birge and Louveaux 2011). When uncertainty only appears in the objective, the objective function is often the expectation of the operational objective. In this case, the problem can be solved by Sample Average Approximation (SAA). SAA is a discretization approach that approximates the original distribution by a representative realization (Kim et al. 2014). Its performance depends on the number and quality of representative realizations. If uncertainty appears in constraints. Such constraints need to be modeled as a chance constraint, which guarantees the fulfillment probability of the constraint above a pre-specified confidence level.

Robust Optimization (RO). RO is a powerful tool where the probability distribution of uncertain items is unknown (Ben-Tal and Nemirovski 2002, Bertsimas et al. 2011). In particular, the uncertain items are modeled only based on their possible realizations, without probabilistic information. A set characterized by constraints is used to model all possible realizations, referred to as an uncertainty set. There are numerous types of uncertainty sets. Choosing a suitable uncertainty set that best characterizes your uncertainty, while balancing tractability, is a central philosophy in RO. When uncertainties appear in the objective function, the goal is to identify the worst-case objective among all possible realizations within the uncertainty sets. When uncertainties appear in constraints, these constraints must ensure fulfillment under all possible realizations of the uncertainties.

Distributionally Robust Optimization (DRO). DRO is an advancement of RO, which not only characterizes possible realizations but also incorporates probabilistic information based on available references (Ouyang and Chung 2025). It can also be regarded as a bridge between SP and RO. The DRO originated from the robust newsvendor problem in the 1950s, pioneered by Scarf (1957), and gained tremendous attention since the 2010s (Delage and Ye 2010). DRO models the probability distribution of an uncertain item by ambiguity sets, which are constructed according to accessible references (e.g., statistical means and variances, empirical distributions, or reference distributions). The objective function is to optimize the expectation of the operational objective (e.g., profit or cost) under the worst-case probability distribution among all possible distributions in the ambiguity set. When uncertainties arise in constraints, they are modeled as a variant of chance constraints. Ambiguity sets contain two major types: moment-based and metric-based. A moment-based ambiguity set often uses lower moments (e.g., mean, variance, covariances) as reference information, while a metric-based ambiguity set generally uses the empirical distribution as reference. Metric-based ambiguity sets can be combined with data-driven approaches, which are very trending in recent literature (Gao and Kleywegt 2023).

2.1.4.2. Competition between players

While much of the disruption literature focuses on a single decision-maker, disruptions can create or intensify competitive interactions that require game-theoretic models. For example, a trade war is inherently a strategic game between nations that impacts firm-level decisions, while a disaster may induce competition for scarce resources among responding organizations. The geographical conflicts in recent years, such as the trade war and hot war, have extended the scope of competition. Competition can occur between countries and impact various decision-making problems. Game theory is the primary tool to model competition in operational problems. We present two game-theoretical models below.

Stackelberg game model. This is a classic model for a leader-follower competition (Carvalho et al. 2024). Consider a strategic decision where one player moves first, and the other then reacts. The leader (e.g., a dominant firm or a government setting a policy) makes the optimal decision, anticipating the response from the follower (e.g., a smaller competitor or a company). In the context of intensified geopolitical conflicts, game theory provides a solution to analyze strategic interplay between nations. This model is especially suitable for analyzing situations in which a government imposes a tariff, knowing that firms will then adjust their sourcing strategies, or a major company sets a price that smaller rivals must adapt to.

Cournot game model. This is a classic model for situations in which two or more firms compete on quantity or amount (Korpeoglu et al. 2020). Consider two logistics companies that need to determine transport capacity on the same route, or two manufacturers deciding how many units of an identical product to produce. In this model, each firm must make its output decision simultaneously, without knowing the other's choice. Each firm makes its decision based on what it expects its rivals to do, aiming to maximize its profit. The market price is then determined by the total quantity produced by all firms combined; if everyone produces too much, the price will drop for every agent. This model captures the core tension between trying to capture market share by creating more and the risk of flooding the market, driving down profits for the entire industry.

2.1.4.3. Multiple stages

Taking proactive actions to hedge against the adverse impacts of potential disruptions is naturally a two-stage decision-making process. For example, governments may allocate evacuation and healthcare resources in specific distribution centers to cope with natural disasters. In this case, determining resource allocation is the first-stage decision, while optimizing resource delivery in the event of an earthquake is the second-stage decision. However, in the real world, decisions may involve multiple stages, which require more sophisticated tools. Two major approaches are the Markov decision process and optimal control theory. In particular, the second method is more powerful in modeling continuous evolution, such as pandemic infections over time. Furthermore, reinforcement learning (RL) is gaining increasing attention as an emerging method to address multi-stage problems.

Markov decision process (MDP). MDP is a stochastic model for sequential decision-making in settings where outcomes are partly random and partly under the control of a decision-maker (Brown et al. 2024). It models a system using a set of states (e.g., current inventory levels), a set of actions available in each state (e.g., replenishment quantities), and a set of transition probabilities that govern the evolution to the next state based on the current state and chosen action. The objective is to find an optimal policy that maximizes a cumulative reward or minimizes a cumulative cost over an extended time horizon. The optimal policy can be regarded as a map from states to actions. MDP is especially suitable for the problems that reveal uncertainties in a discrete fashion (e.g., periodic inventory control, equipment maintenance scheduling).

Optimal control theory. Optimal control theory encompasses various branches, with the primary goal of determining the optimal policy to manage a dynamic system that evolves continuously over time (Li 1993). In contrast to the discrete stages of MDP, the system state in the optimal control theory (e.g., the number of infected individuals in a population) is often described by differential equations. The decision-makers task is to determine the optimal time-varying route for a set of control actions (e.g., vaccination rates or social distancing levels) that guides the system to reach its desired target (e.g., minimizing total infections over a specific period). Its ability to handle continuous state and control variables makes it a potent tool for managing dynamically evolving crises, which explains its extensive use in modeling pandemic responses.

Reinforcement learning (RL). RL has a close connection with MDP and is suitable for situations in which an explicit probabilistic model of the environment (e.g., transition probabilities) is unknown or too complex to formulate (Oroojlooyjadid et al. 2022). In the RL framework, an autonomous agent learns to make optimal decisions through direct interaction with its environment. The implementation is like a trial-and-error process: The agent observes a state, performs an action, and receives a numerical reward or penalty. By repeatedly performing actions and observing the resulting rewards, the agent gradually learns a policy that maximizes its cumulative long-term reward. The policy is also a map from states to actions like MDP. This model-free approach is compelling for tackling highly complex and dynamic operational problems, such as real-time vehicle routing in congested traffic or dynamic pricing in e-commerce, where the underlying system dynamics are complex to specify in advance.

2.1.4.4. Epidemiological evolution

Due to the worldwide spread of COVID-19, the dynamics and evolution of disease spread gained significant attention. Many operations management researchers draw on models in biostatistics to inform their studies. Two epidemiological models are widely used.

Suspected-Infected-Recovered (SIR) model. The SIR model is a simple way to understand how disease can spread through a population (Perakis et al. 2023). It divides people into three groups: Susceptible (S), those who can catch the illness; Infected (I), those who have the disease and can spread it; and Recovered (R), those who have had the disease and are now immune. The model illustrates how people transition from being susceptible to infected and then from an infected state to a recovered status. The speed of this movement depends on the infectiousness of the disease and the rate of recovery, which helps predict how an epidemic might grow and decline.

Suspected-Exposed-Infected-Recovered (SEIR) model. The SEIR model extends the classic SIR model by adding one new group in the population to make the model more realistic (Chen and Kong 2023). In particular, it introduces the Exposed (E) group, which is divided into four stages: Susceptible, Exposed, Infected, and Recovered. The Exposed category is for people who have contracted the illness but are not yet contagious. This accounts for the incubation period of a disease. So, an individual's path is from Susceptible (capable of getting sick) to Exposed (sick but not spreading it), then to Infected (spreading it), and finally to Recovered (immune). This extra stage helps create more accurate predictions for diseases with a delay. The exposed group is especially suitable for modeling a disease that has an obvious Incubation period.

2.1.4.5. Prediction

Instead of modeling potential disruptions and their resulting impacts on operations as random variables, many studies attempt to predict the actual realizations of these uncertainties directly. The prediction process typically considers numerous features and factors related to realizations. Machine learning and deep learning are two dominant approaches to prediction. These approaches originate from computer science but are increasingly used by operations management researchers.

Machine learning (ML). Instead of assuming that uncertainties follow some probabilistic distributions, ML algorithms learn from complex, real-world data to forecast impacts (Chou et al. 2023). For logistics operations, this could involve training a model on historical data of traffic and weather to forecast road travel times during a flood. For service operations, an ML model could analyze public health data and demographic factors to predict healthcare demand during a pandemic. Through identifying patterns across numerous features, these data-driven approaches provide more accurate and granular inputs, such as expected demand surges or likely supplier delays, which are then fed into optimization models to enable more informed and effective operational decisions.

Deep learning (DL). DL is a subfield of ML and is more suitable for addressing unstructured and poor-quality data generated by major disruptions. Its multi-layered neural networks can process raw data, such as images and text, without requiring predefined features (Luo and Choi 2024). For logistics under disruption, this means a deep learning model can analyze real-time satellite imagery to automatically identify and map impassable roads after an earthquake, feeding this crucial information directly into a relief vehicle routing algorithm. For service operations, a DL model can help retailers to uncover early signs of customers' purchasing intensions using thousands of social media posts; a proactive inventory order can thus be made.

Methodology	Best Suited for Disruption Characteristics	Example Application Context
Stochastic Programming	Uncertainty with known/estimable probability distributions. Recurrent disruptions where historical data is available.	Inventory control under seasonal demand volatility; regular port congestion.
Robust Optimization	High uncertainty with unknown probabilities. Focus on worst-case performance guarantees against acute, unforeseen events.	Facility location to withstand severe natural disasters; routing with unpredictable network failures.
Distributionally Robust Optimization	Some distributional information (e.g., moments) is known, but the exact distribution is ambiguous.	Sourcing decisions under tariff uncertainty where the range of policies is known but likelihood is not.
Game Theory	Situations with strategic interactions and competition among multiple decision-makers triggered by a disruption.	Analysing national responses to trade wars; modelling competition for resources among humanitarian agencies.
Reinforcement Learning	Highly complex and dynamic environments where an explicit model is unknown. Decisions learned through trial-and-error.	Real-time vehicle routing in congested post-disruption traffic; dynamic pricing.
Epidemiological Models (e.g., SIR/SEIR)	Modelling the spread dynamics of infectious diseases to inform public health operational responses.	Vaccine allocation, lockdown policy design, and massive screening strategies during a pandemic.

Table 2.4. Alignment of Methodologies with Disruption Characteristics.

2.1.5. Summary

This sub-chapter provides a crucial bridge between academic theory and managerial practice for navigating supply chain disruptions. For operations and engineering managers, this paper serves as a structured guide to enhance organizational resilience in an increasingly volatile world. It synthesizes complex research into a practical conceptual framework, enabling policy makers to systematically diagnose different types of disruptions—from pandemics to geopolitical tensions—and understand their specific impacts on operations.

The proposed DT (Decision-level Time-horizon) taxonomy helps managers classify operational problems, such as network design or inventory control, as either proactive or reactive, strategic or operational. This allows for more targeted and effective decision-making. By mapping specific analytical methodologies, like robust optimization or machine learning, to distinct disruption characteristics, the review equips managers with the knowledge to select the right tools to solve their unique challenges. Ultimately, this research provides a clear roadmap for policy makers to not only respond to current crises but also to proactively build more robust and resilient logistics and service operations for the future.

2.2. Modeling Uncertainties in Operations under Disruptions: Distributionally Robust Optimization

2.2.1. Background

In the real world, operational activities pose various uncertainties, such as uncertain customer demand and product supply. Incorporating these uncertainties into decision making is critical because ignoring them or inappropriately characterizing them could lead to very poor performance in practice. To this end, stochastic programming (SP) addresses uncertainties by explicitly incorporating probability distributions of random variables to maximize expected profits or minimize expected costs (Birge & Louveaux 2011). Robust optimization (RO) is another technique for modeling under uncertainty, which optimizes over the worst-case realization of uncertain parameters (Ben-Tal & Nemirovski 1998).

However, these two approaches have respective shortcomings. SP requires the probability distribution to be explicitly known. In other words, the probability mass function or density function of uncertainty parameter should be accessible. In addition, a model could involve extensive uncertain parameters, forming a high-dimensional random vector. Characterizing the distribution of such a random vector relies on the joint distribution of these uncertain parameters. Deriving such joint distributions is challenging, especially when uncertain parameters exhibit significantly heterogeneous features. Moreover, deriving the explicit form of the expected objective often leads to a high-dimensional integral problem, which is extremely complex and computationally intractable. On the other hand, RO needs no distribution information. The realization of uncertain parameters is considered to belong to an uncertainty set, and the interdependence of these parameters can be captured by imposing constraints on parameters. Despite attractive tractability, RO ignores critical probability distribution features and merely seeks the worst-case realization of all parameters. This is too conservative since the worst-case realization may never happen in practice.

DRO circumvents all these issues by a framework pf modeling any distribution with limited statistical information. DRO assumes that the true distribution belongs to a family of distributions aligning with the accessible distribution features, and makes decisions over the worst-case probability distribution, which is a generalization of both SP and RO (Rahimian & Mehrotra 2022, Long et al. 2024, Xu et al. 2025). When full distribution information is known, DRO reduces to SP, and if no distribution information is available, DRO reduces to RO. In summary, DRO inherits the merits of SP and RO and stands out thanks to its generalization, tractability, and unique ability to handle distributional ambiguity.

2.2.2. Preliminary knowledge of DRO

This section presents how DRO formulates ambiguous distributions and how to solve the resulting models to equip readers with basic knowledge of DRO. For those who are interested in more advanced theoretical results, please refer to the technical review by Lin et al. (2022).

2.2.2.1. Ambiguity sets

The decision in DRO is made under the worst-case probability distribution. Such worst distribution is considered to belong to a set, referred to as ambiguity sets $\mathcal{P}$. According to the features to construct the set, ambiguity sets can be classified into two major classes (i.e., moment- or metric-based).

2.2.2.1.1. Moment-based ambiguity set

This set uses (lower) moments to model ambiguous distributions. Delage and Ye (2010) construct such ambiguity set for a random vector $\tilde{\boldsymbol{\xi}}$ and allow moment uncertainty through the idea of uncertainty sets in the classic robust optimization and linear matrix inequalities. In the below ambiguity set,

$$\mathcal{P} = \left\{ \mathrm{P} \in \mathscr{P}(\Xi) : \left(\mathrm{E}_{\mathrm{P}}\left[\tilde{\boldsymbol{\xi}}\right] - \boldsymbol{\mu} \right)^{\top} \Sigma^{-1} \left(\mathrm{E}_{\mathrm{P}}\left[\tilde{\boldsymbol{\xi}}\right] - \boldsymbol{\mu} \right) \le \gamma_1,\ \mathrm{E}_{\mathrm{P}}\left[\left(\tilde{\boldsymbol{\xi}} - \boldsymbol{\mu}\right)\left(\tilde{\boldsymbol{\xi}} - \boldsymbol{\mu}\right)^{\top} \right] \preceq \gamma_2 \Sigma \right\},$$

where $\Xi \subseteq \mathrm{R}^d$ is the support set of d-dim random vector $\tilde{\boldsymbol{\xi}}$, $\boldsymbol{\mu}$ is the sampled mean vector, $\Sigma \in \mathrm{S}_{++}^{d}$ is an estimated covariance matrix, positive parameters γ_1 and γ_2 are given to control the magnitude of the moment uncertainty. In particular, the true mean is constrained in an ellipsoidal region centering in $\boldsymbol{\mu}$, and the true covariance matrix is bounded above in the sense that the matrix $\gamma_2 \Sigma - \left(\tilde{\boldsymbol{\xi}} - \boldsymbol{\mu}\right)\left(\tilde{\boldsymbol{\xi}} - \boldsymbol{\mu}\right)^{\top}$ is positive semidefinite. Addressing the linear matrix inequalities in this ambiguity set needs semidefinite programming (SDP) techniques, which produce nonlinear reformulation. To facilitate computation, one could use the ambiguity set with a linear structure by Goh & Sim (2010):

$$\mathcal{P} = \left\{ \mathrm{P} \in \mathscr{P}(\Xi) : \mathrm{E}_{\mathrm{P}}\left[\tilde{\boldsymbol{\xi}}\right] = \boldsymbol{\mu},\ \mathrm{E}_{\mathrm{P}}\left[\left| \tilde{\boldsymbol{\xi}} - \boldsymbol{\mu} \right| \right] \le \boldsymbol{\sigma} \right\},$$

where $\boldsymbol{\sigma}$ represents the element-wise absolute deviation. The absolute deviation constraint can be easily replaced by linear constraint, but the correlation between random variables is missing.

2.2.2.1.2. Metric-based ambiguity set

The ambiguity set of this type is constructed based on probability metrics. Given a reference distribution Q, the distance from this distribution to an arbitrary distribution can be evaluated by some metric. The most well-known one is the Wasserstein distance, and the corresponding ambiguity set is called the Wasserstein ambiguity set (Gao & Kleywegt, 2023). The reference distribution is generally the empirical distribution drawn from the historical data:

$$\mathrm{Q} = \frac{1}{N} \sum_{i=1}^{N} \delta_{\boldsymbol{\xi}^i}\left(\tilde{\boldsymbol{\xi}}\right),$$

where $\delta_{\xi^i}(\xi)$ denotes the Dirca delta measure with probability mass on observation ξ^i. Then, the Wasserstein distance based on p-norm between Q and another distribution P is

$$W_p(\mathrm{P},\mathrm{Q}) = \inf_{\Pi\in\mathscr{P}(\Xi\times\Xi)} \left\{ \sqrt[p]{\int_{\Xi\times\Xi} \|\xi-\xi'\|_p^p \,\Pi(d\xi, d\xi')} : \Pi(d\xi,\Xi) = \mathrm{P}(d\xi),\ \Pi(\Xi,d\xi') = \mathrm{Q}(d\xi') \right\},$$

where Π is the join distribution of Q and P, and the marginal distribution of Π is exactly Q and P. With these notations, the Wasserstein ambiguity set is defined as

$$P = \left\{ \mathrm{P}\in\mathscr{P}(\Xi) : W_p(\mathrm{Q},\mathrm{P}) \le \rho \right\},$$

where ρ is the radius of the Wasserstein ball, which controls the magnitude of the distributional ambiguity. It is worth noting that the type-∞ Wasserstein distance has an alternative expression:

$$W_\infty(\mathrm{P},\mathrm{Q}) = \inf\left\{ \Pi\text{-ess}\sup\left\|\tilde{\xi}-\tilde{\xi}'\right\| : \Pi(d\xi,\Xi) = \mathrm{P}(d\xi),\ \Pi(\Xi,d\xi') = \mathrm{Q}(d\xi') \right\},$$

where the essential supremum under the joint distribution Π is defined as

$$\Pi\text{-ess}\sup\left\|\tilde{\xi}-\tilde{\xi}'\right\| = \inf\left\{ \varepsilon : \Pi\left(\left\|\tilde{\xi}-\tilde{\xi}'\right\| > \varepsilon \right) = 0 \right\},$$

which seeks the minimum ε such that the probabilistic constraint holds surely.

Another way to evaluate the difference between two distributions is divergence. The most famous one is ϕ-divergence. Let $\phi:[0,\infty)\to\mathrm{R}$ be a chosen convex function such that $\phi(1)=0$ and by convention that $\phi\left(\frac{0}{0}\right)=0$ and $\phi\left(\frac{a}{0}\right)=\lim_{t\to\infty}\phi(t)$. Then, the ϕ-divergence is defined as

$$I_\phi(\mathrm{P},\mathrm{Q}) = \int_\Xi \phi\left(\frac{\mathrm{P}(d\xi)}{\mathrm{Q}(d\xi)} \right) \mathrm{Q}(d\xi).$$

For two discrete distributions $\mathrm{P}=(p_1,\ldots,p_M)$ and $\mathrm{Q}=(q_1,\ldots,q_M)$. The ϕ-divergence is written as

$$I_\phi(\mathrm{P},\mathrm{Q}) = \sum_{i=1}^{M} q_i \phi\left(\frac{p_i}{q_i} \right).$$

Substituting the well-established Kulback-Leibler divergence function $\phi(t) = t\log t - t + 1$ gives

$$I_{\phi\text{-}KL}(\mathrm{P},\mathrm{Q}) = \sum_{i=1}^{M} p_i \log\frac{p_i}{q_i}.$$

We can construct the KL-divergence ambiguity set as follows (Ben-Tal et al. 2013):

$$P_\varepsilon = \left\{ \mathrm{P}\in\mathscr{P}(\Xi) : I_{\phi\text{-}KL}(\mathrm{P},\mathrm{Q}) \le \varepsilon \right\},$$

where ε is the radius of the KL-divergence ball.

2.2.2.2. Solution approach

Consider a general DRO problem $\min_{\mathbf{x}\in\mathrm{X}} \sup_{\mathrm{P}\in\mathcal{P}} \mathrm{E}_{\mathrm{P}}\left[f\left(\mathbf{x},\tilde{\xi}\right)\right]$ where $\mathbf{x}$ admits a feasible set X. We focus on solving the inner maximization problem given a certain decision $\mathbf{x}$. The cutting-plane method is well-established for such two-layer problem, but this could be time consuming. Another way is to reformulate the inner problem as an equivalent minimization problem by duality theory, and then combine the outer and inner problems into a large minimization problem.

2.2.2.2.1. Primal approach

The primal approach is based on the cutting plane method (Chen et al. 2019). When the tractable reformulation of the inner problem is inaccessible or when the random variable (vector) takes a discrete distribution, the cutting plane method is often adopted. The idea is to find the worst-case distribution for the given decision $\mathbf{x}$ and augment the candidate distribution set by this distribution. At the next iteration, the decision $\mathbf{x}$ is optimized over the updated candidate distribution sets. Consider a random vector $\tilde{\boldsymbol{\xi}}$ with discrete support of M elements. Its distribution can be captured by a vector $\mathbf{p}=\left(p_1,\ldots,p_M\right)$. In the DRO problem,

$$\min_{\mathbf{x}\in\mathrm{X}} \sup_{\mathrm{P}\in\mathcal{P}} \mathrm{E}_{\mathrm{P}}\left[f\left(\mathbf{x},\tilde{\xi}\right)\right]$$

subject to

$$\mathcal{P} =\left\{\mathrm{P}\in\mathscr{P}\left(\Xi\right):\mathrm{E}_{\mathrm{P}}\left[\psi\left(\tilde{\xi}\right)\right]\infty\, 0\right\},$$

which is constrained by an expected linear matrix inequality. Note that function ψ maps the support vector to a matrix, e.g., in the moment-based ambiguity set $\left(\boldsymbol{\xi}-\boldsymbol{\mu}\right)\left(\boldsymbol{\xi}-\boldsymbol{\mu}\right)^{\top}$. Since the distribution is discrete, the ambiguity set can be compactly represented as

$$\mathcal{P} =\left\{\mathbf{p}\geq 0:\sum_{i=1}^{M} p_i=1,\ \sum_{i=1}^{M} p_i\psi\left(\boldsymbol{\xi}^i\right)\infty\, 0\right\}.$$

Initialize the candidate worst-case distribution set by any feasible distribution $P_0=\left\{p_0\right\}$. Denote the worst-case distribution found at iteration t by $\mathbf{p}^t$. At iteration $t+1$, solve the below master problem:

$$\alpha^{t+1}=\min_{\alpha,\mathbf{x}\in\mathrm{X}} \alpha$$

subject to

$$\sum_{i=1}^{M} p_i^t \left[f\left(\mathbf{x}^t, \boldsymbol{\xi}^i\right) + \nabla f\left(\mathbf{x}^t, \boldsymbol{\xi}^i\right)^{\top} \left(\mathbf{x} - \mathbf{x}^t\right) \right] \le \alpha, \ \forall \mathbf{p}^t \in P^{\ t},$$

where X is the feasible set of $\mathbf{x}$, and $P^{\ t}$ is the candidate worst-case distribution set obtained at iteration t. With the resulting master solution $\mathbf{x}^{t+1}$, solve the separation problem to find a new worst-case distribution:

$$v^{t+1} = \max_{\mathbf{p} \ge 0} \sum_{i=1}^{M} p_i f\left(\mathbf{x}^{t+1}, \boldsymbol{\xi}^i\right)$$

subject to

$$\sum_{i=1}^{M} p_i = 1,$$

$$\sum_{i=1}^{M} p_i \psi\left(\boldsymbol{\xi}^i\right) \infty\ 0.$$

If $v^{t+1} > \alpha^{t+1}$, augment the candidate set by $P^{\ t+1} = P^{\ t} \bigcup \left\{\mathbf{p}^{t+1}\right\}$; otherwise, terminate the algorithm.

2.2.2.2.2. Dual approach

The dual approach aims to reformulate the inner maximization problem into an equivalent minimization problem, called tractable reformulation or distributionally robust counterpart. To this end, it is natural to derive the dual of the original inner maximization problem. However, we need to further verify the strong duality to ensure the tightness of the resulting minimization problem.

We begin with the classic moment-based ambiguity set. By Schur's complement, writing the ambiguity set more compactly produces the maximization problem:

$$\sup_{\mathrm{P} \ge 0} \mathrm{E}_{\mathrm{P}}\left[f\left(\mathbf{x}, \tilde{\boldsymbol{\xi}}\right) \right]$$

subject to

$$\mathrm{E}_{\mathrm{P}}\left[\mathrm{I}\left(\tilde{\boldsymbol{\xi}} \in \Xi\right) \right] = 1,$$

$$\mathrm{E}_{\mathrm{P}}\left[\tilde{\boldsymbol{\xi}}\tilde{\boldsymbol{\xi}}^{\top} - \tilde{\boldsymbol{\xi}}\boldsymbol{\mu}^{\top} - \boldsymbol{\mu}\tilde{\boldsymbol{\xi}}^{\top} \right] \infty\ \gamma_2 \Sigma - \boldsymbol{\mu}\boldsymbol{\mu}^{\top},$$

$$\mathrm{E}_{\mathrm{P}}\left[\begin{pmatrix} \Sigma & \tilde{\boldsymbol{\xi}} - \boldsymbol{\mu} \\ \left(\tilde{\boldsymbol{\xi}} - \boldsymbol{\mu}\right)^{\top} & \gamma_1 \end{pmatrix} \right] \pm\ 0.$$

Note that the above three constraints are linear in distribution $\mathbb{P}$. Associate three constraints with dual variables r, Q, and $\begin{pmatrix} P & p \\ p^{\top} & s \end{pmatrix}$, and derive the dual:

$$\min_{r,Q,P,p,s} r + \left\langle Q, \gamma_2 \Sigma - \boldsymbol{\mu}\boldsymbol{\mu}^{\top} \right\rangle + \left\langle P, \Sigma \right\rangle - 2\boldsymbol{\mu}^{\top} p + s\gamma_1$$

subject to

$$f\left(\mathbf{x}, \boldsymbol{\xi}\right) - r - \boldsymbol{\xi}^{\top} Q \boldsymbol{\xi} + 2\boldsymbol{\xi}^{\top} Q \boldsymbol{\mu} + 2\boldsymbol{\mu}^{\top} \boldsymbol{\xi} \leq 0, \ \forall \boldsymbol{\xi} \in \Xi,$$

$$r \in \mathbb{R}, \ Q \succeq 0, \begin{pmatrix} P & p \\ p^{\top} & s \end{pmatrix} \succeq 0.$$

Combining the outer and inner minimization problems produces an SDP problem, which is nonlinear. For simplicity, many studies adopt a linear moment-based ambiguity set. See the following problem:

$$\sup_{\mathbb{P} \geq 0} \mathbb{E}_{\mathbb{P}} \left[f\left(\mathbf{x}, \tilde{\boldsymbol{\xi}}\right) \right]$$

subject to

$$\mathbb{E}_{\mathbb{P}} \left[\mathbb{I}\left(\tilde{\boldsymbol{\xi}} \in \Xi \right) \right] = 1,$$

$$\mathbb{E}_{\mathbb{P}} \left[\tilde{\boldsymbol{\xi}} \right] = \boldsymbol{\mu},$$

$$\mathbb{E}_{\mathbb{P}} \left[\left| \tilde{\boldsymbol{\xi}} - \boldsymbol{\mu} \right| \right] \leq \boldsymbol{\sigma}.$$

Its dual is

$$\min_{\alpha, \boldsymbol{\beta}, \boldsymbol{\gamma}} \alpha + \boldsymbol{\mu}^{\top} \boldsymbol{\beta} + \boldsymbol{\sigma}^{\top} \boldsymbol{\gamma}$$

subject to

$$\alpha + \boldsymbol{\xi}^{\top} \boldsymbol{\beta} + \left| \boldsymbol{\xi} - \boldsymbol{\mu} \right|^{\top} \boldsymbol{\gamma} \geq f\left(\mathbf{x}, \boldsymbol{\xi}\right), \ \forall \boldsymbol{\xi} \in \Xi,$$

$$\alpha \in \mathbb{R}, \ \boldsymbol{\beta} \in \mathbb{R}^{d}, \ \boldsymbol{\gamma} \in \mathbb{R}_{+}^{d},$$

This is a classic robust linear program with a robust constraint $\min_{\boldsymbol{\xi} \in \Xi} \left\{ \alpha + \boldsymbol{\xi}^{\top} \boldsymbol{\beta} + \left| \boldsymbol{\xi} - \boldsymbol{\mu} \right|^{\top} \boldsymbol{\gamma} \right\} \geq f\left(\mathbf{x}, \boldsymbol{\xi}\right)$.

2.2.3. DRO in operational problems

This section presents the application of DRO in three operational problems. We pay special attention to the source of uncertainty and how they are modeled by DRO.

2.2.3.1. Network design

Zhang et al. (2021) optimize the deployment of emergency logistics centers while considering vehicle travel time uncertainty in transporting emergency materials. The uncertain travel time is assumed to lie in a reduced version of the classic moment-based ambiguity set:

$$P = \left\{ \mathrm{P} \in \mathscr{P}(\Xi) : \mathrm{E}_{\mathrm{P}}\left[\tilde{\xi}_{ij}\right] = \mu_{ij},\ \mathrm{E}_{\mathrm{P}}\left[\left(\tilde{\xi}_{ij} - \mu_{ij}\right)^2\right] \le \sigma^2,\ \forall i \in [N], j \in [M] \right\},$$

where the correlation of travel time on different roads is ignored. In addition, the latest delivery time of any affected area is expected to be no later than a given time threshold T with a certain confidence level. This is modeled by the following joint chance constraint:

$$\inf_{\mathrm{P} \in P} \mathrm{P}\left(a_i \left(Z_{ij} - 1 \right) + \tilde{\xi}_{ij} U_{ij} \le T,\ \forall i \in [N], j \in [M] \right) \ge 1 - \varepsilon,$$

where integer variable Z_{ij} is the number of vehicles from center i to area j, binary variable U_{ij} equals 1 if $Z_{ij} \ge 1$, and a_i is the vehicle departure duration at center i.

Noyan et al. (2022) examine the network investment problem, where the survival probability of a node in the network is improved if the investment is given to enhance the facilities at this node. Let $\mathbf{x} \in \{0,1\}^M$ be the binary decision vector that indicates which nodes of all M nodes get investment. The survival probability of node i is ambiguous, denoted by $q_i \in [\overline{q}_i, 1]$. Their decision-dependent ambiguity set is

$$P(\mathbf{x}) = \left\{ \mathbf{p}(\mathbf{x}) = \{p_1, .., p_{2^M}\} : p_j = \prod_{i \in [M]:\, \xi_i^j = 1} \left[(1 - x_i)\overline{q}_i + x_i q_i \right] \prod_{i \in [M]:\, \xi_i^j = 0} \left[(1 - x_i)(1 - \overline{q})_i + x_i (1 - q_i) \right] \right\},$$

where ξ_i^j indicates whether node i in scenario j survives.

2.2.3.2. Fleet management

Li and Chung (2019) note that the demand for relief supplies at a site could be very large, and the fleet must visit the site several times to meet the demand. This introduces the split delivery vehicle routing problem. They model the uncertainty of demand and travel time by the well-established box uncertainty set:

$$\Xi_T = \left\{ t_{ij} \ge 0,\ \forall i, j \in [N] : t_{ij} \in \left[\overline{t}_{ij}, \overline{t}_{ij} + \tilde{t}_{ij} \right],\ \forall i, j \in [N] \right\},$$

where $\overline{t}_{ij}$ is the nominal travel time on arc (i, j) and $\tilde{t}_{ij}$ is uncertain travel delay. The tractable reformulation is obtained by duality theory and the resulting reformulation is solved by heuristics.

Boutilier and Chan (2020) optimize the ambulance fleet in low- and mid-income countries by a location and routing model, which determines both the fleet deployment and routing plans. They use a scenario-wise uncertainty set to model the uncertain demands:

$$\Xi_D = \left\{ \mathbf{d}^1, \ldots, \mathbf{d}^M \right\},$$

which contains M scenarios, and each vector $\mathbf{d}^i$ indicates the demand amount and deployment. They adopt an interdiction-based budged-constrained uncertainty set to model uncertain travel times:

$$\Xi_T = \left\{ t_{ij} \geq 0,\ \forall i, j \in [N] : t_{ij} = \bar{t}_{ij} + \varepsilon_{ij},\ \sum_{i,j \in [N]} \varepsilon_{ij} \leq B,\ \varepsilon_{ij} \geq 0,\ \forall i, j \in [N] \right\},$$

where the nominal travel time $\bar{t}_{ij}$ is the empirical travel time.

Avishan et al. (2023) investigate the supply fleet management problem by determining the vehicle routes and the distribution time spent on visited sites considering travel time uncertainty. The road travel time is modeled by the classic box uncertainty set:

$$\Xi_T = \left\{ t_{ij} \geq 0, \forall i, j \in [N] : t_{ij} = \left(1 + \rho \chi_{ij}\right) \bar{t}_{ij},\ \forall i, j \in [N] \right\},$$

where $\rho \in [0,1]$ and $\bar{t}$ capture the degree of uncertainty and the nominal travel time, whereas $\chi_{ij} \in [-1,1]$ is an uncertain parameter to be optimized. The distribution time spent on any site i is assumed to be affected by the travel time used, which is modeled by the well-known linear decision rule:

$$T_i(\mathbf{t}) = \bar{T}_i + \sum_{i', j \in [N]} \sum_{k \in [K]} \gamma^i_{i'jk} \left(1 + \rho \chi_{ij}\right) \bar{t}_{i'j},$$

where k is the order of site i to be visited, $\bar{T}_i$ and $\gamma^i_{i'jk}$ are coefficients to be optimized.

2.2.3.3. Resource allocation

Ni et al. (2018) determine the inventory levels of distribution centers in the pre-disaster phase to hedge against the demand, facility disruption, and road capacity in the post-disaster phase. They propose a modified absolute mean deviation and budget-constrained uncertainty set to model these uncertain factors. In particular, the random demand is represented by a vector subject to constraints:

$$\Xi_D = \left\{ d \in \mathrm{R}^N_+ : \begin{array}{c} \eta_i = \begin{cases} \left(\bar{d}_i - d_i\right) / \left(\bar{d}_i - d^L_i\right), \text{ if } d_i \leq \bar{d}_i \\ \left(d_i - \bar{d}_i\right) / \left(d^U_i - \bar{d}_i\right), \text{ if } d_i > \bar{d} \end{cases} \\ \sum_{i \in [N]} \eta_i \leq B,\ d_i \in \left[d^L_i, d^U_i\right],\ \forall i \in [N] \end{array} \right\},$$

where $\bar{d}_i = \alpha d_i^L + (1-\alpha) d_i^U$ is a convex combination of demand upper and lower bounds, which can be regarded as the most possible realization of random demand at site i. The correlation of demand at different sites is characterized by a budget-type constraint (Bertsimas and Sim 2004), which indicates that the total normalized deviations are no more than B.

Chan et al. (2018) optimize the deployment of a limited automated external defibrillator to minimize a conditional value at risk type objective. The probability distribution of random cardiac arrest is ambiguous. A service region $\mathscr{X}$ is partitioned into M subareas such that $\mathscr{X} = \bigcup_{i=1}^{M} \mathscr{X}_i$, and each subarea is characterized by some representative cardiac arrest sites $\Xi_i = \{\xi_k \in \mathscr{X}_i, \forall k \in [K_i]\}$. The probability of a cardiac arrest taking place in sub-area i is known and denoted by π_i, i.e., $\mathrm{P}(\xi \in \Xi_i) = \pi_i$. Note that if subareas have overlapped, then it is possible that $\sum_{i\in[M]} \pi_i > 1$. Then, their ambiguity set is defined as

$$P = \left\{ \mathbf{p} \geq 0 : \sum_{k=1}^{K_i} p_k^i = \pi_i, \forall i \in [M] \right\},$$

which is a variant of the marginal distribution-based ambiguity set.

Dalal and Üster (2021) consider uncertain disaster duration and people to be evacuated. They construct scenarios to capture associated uncertain characteristics of evacuation. They use a box uncertainty set:

$$\Xi_{\tilde{\phi}_{id}} = \left[\bar{\phi}_{id}(1-\varepsilon_{id}), \bar{\phi}_{id}(1+\varepsilon_{id}) \right],$$

where $\varepsilon_{id} \in [0,1]$, to model $\tilde{\phi}_{id} \in [0,1]$, which stands for the uncertain proportion of people to be evacuated. They further assume that ε_{id} is a staircase function of the time when operators make decisions; the shorter the time after disasters are, the smaller ε_{id} is.

To ensure the bus resources equally serve all bus routes, Sun et al. (2023) optimize the type and number of buses assigned to each bus route and model passengers' boarding and getting-off amount by DRO. Let $\tilde{\boldsymbol{\xi}} = (\tilde{\mathbf{a}}, \tilde{\boldsymbol{\lambda}})$ be random, where $\tilde{a}_{ij} \in [0,1]$ and $\tilde{\lambda}_{ij}$ are the ratio of passengers getting off at station j after i to all passengers onboard after i, and the number of passengers boarding at station j after i. The random $\tilde{\boldsymbol{\xi}}$ is captured by the type-∞ Wasserstein ambiguity set as follows

$$P_\infty = \left\{ \frac{1}{N} \sum_{i=1}^{N} \delta\left(\tilde{\boldsymbol{\xi}} - \boldsymbol{\xi}^i\right) : \exists \boldsymbol{\xi}^i \in \Xi, \left\| \boldsymbol{\xi}^i - \tilde{\boldsymbol{\xi}}^k \right\| \leq \theta, \forall k \in [N] \right\},$$

where $\{\bar{\xi}^k, \forall k \in [N]\}$ contains N historical observations, and conservativeness is captured by θ. This set mimics the empirical distribution $\frac{1}{N}\sum_{k\in[N]}\delta\left(\tilde{\xi}-\bar{\xi}^k\right)$. However, the worst-case supports are such that the deviation measured in norm from all historical observations is no more than ball radius.

2.2.4. DRO in the newsvendor problem

Inventory management is critical in supply chain management, which affects profits of supply chain agents and customer satisfaction. However, optimizing inventory level faces various uncertainties such as demand fluctuations, supply disruptions, and market volatility. Ignoring them and using a mis-specified inventory level may lead to substantial financial losses and diminished profitability. To address this issue, the newsvendor model is widely used to optimize order quantities in the presence of random demand, especially in the single-period setting.

The newsvendor problem with distributional ambiguity is also referred to as distribution-free newsvendor, which was pioneered by Scarf (1958). This seminal work considers that the distribution of random demand is not explicitly known and instead, is modeled by mean and variance. The objective is to maximize the expected profit under the worst-case distribution:

$$\max_{q} \inf_{\mathrm{P}\in \mathcal{P}} \mathrm{E}_{\mathrm{P}}\left[\Pi\left(q,\tilde{\xi}\right)\right],$$

where q is the order quantity, and $\tilde{\xi}$ is the random demand. The distribution P can be any element of the ambiguity set:

$$\mathcal{P} = \left\{\mathrm{P}\in\mathscr{P}\left(\mathrm{R}_+\right): \mathrm{E}_{\mathrm{P}}\left[\tilde{\xi}\right]=\mu,\ \mathrm{E}_{\mathrm{P}}\left[\left(\tilde{\xi}-\mu\right)^2\right]=\sigma^2\right\}.$$

We review the application of DRO in the newsvendor problem from the following six perspectives.

2.2.4.1. Decision criteria

The decision criteria work as the objective of the newsvendor problem, which not only greatly affects model traceability but also the practical significance of the decision. Perakis and Roels (2008) pioneer the minimax regret decision criterion in the newsvendor problem, which is defined as follows:

$$\min_{y\geq 0} \sup_{\mathrm{P}\in \mathcal{P}} \left\{\max_{x\geq 0} \mathrm{E}\left[\Pi\left(x;\tilde{\xi}\right)\right]-\mathrm{E}\left[\Pi\left(y;\tilde{\xi}\right)\right]\right\},$$

where y is the order quantity minimizing the largest regret, and x is the optimal order quantity under the distribution maximizing the regret. Aside from the moment information, they further characterize distribution by shape information (i.e., mode/range, symmetry, unimodularity).

Jammernegg and Kischka (2009) propose a new decision criterion incorporating risk preference. Their objective is a convex combination of expected profit and conditional value at risk, given a confidence level. Instead of modeling demand distribution by moment information, they adopt the stochastic dominance rule. They assume that some reference random variables are given, and the true demand variable stochastically dominates these reference random variables in first or second order:

$$\tilde{\xi}_A \succ_{(1)} \tilde{\xi}_B : F_A(t) \le F_B(t), \forall t \text{ and } \tilde{\xi}_A \succ_{(2)} \tilde{\xi}_B : \int_{\infty}^{t} F_A(t)\,dt \le \int_{\infty}^{t} F_B(t)\,dt, \forall t,$$

where $\tilde{\xi}_A$ is the true random demand variable and $\tilde{\xi}_B$ is a reference random demand variable. The robustness is achieved by seeking the worst-dominated distribution.

Ng et al. (2012) propose a new decision criterion to maximize satisfaction for a given target:

$$\max_{\tilde{y} \in \mathrm{Y}} \inf_{\mathrm{P} \in P} \max_{u \ge 0} \mathrm{E}_{\mathrm{P}}\left[\min\{u\tilde{y}, 1\}\right],$$

where $\tilde{y}$ is an abstract presentation of service performance.

Zhu et al. (2013) extend the classic minimax regret criterion by a relative minimax regret:

$$\min_{y \ge 0} \sup_{\mathrm{P} \in P} \frac{\max_{x \ge 0} \mathrm{E}_{\mathrm{P}}\left[\Pi\left(x; \tilde{\xi}\right)\right]}{\mathrm{E}_{\mathrm{P}}\left[\Pi\left(y; \tilde{\xi}\right)\right]},$$

which minimizes the worst-case regret ratio. They derive the closed-form optimal order quantity in the single-product case and investigate the impact of random demand support set boundness.

Andersson et al. (2013) extend Scarf's model by the minimax entropy decision criterion:

$$\min_{x \ge 0} \sup_{\mathrm{P} \in P} \int_{\Xi} -f(\xi) \ln\left(f(\xi)\right) d\xi,$$

where Ξ is the support of random demand.

Han et al. (2014) apply mean-variance (MV) risk measure as the objective in Scarf's classic model. To be specific, their objective is the expected profit minus the weighted variance of the profit:

$$\max_{q \ge 0} \inf_{\mathrm{P} \in P} \left\{ \mathrm{E}_{\mathrm{P}}\left[\Pi\left(q, \tilde{\xi}\right)\right] - \lambda \mathrm{E}_{\mathrm{P}}\left[\left(\Pi\left(q, \tilde{\xi}\right) - \mathrm{E}_{\mathrm{P}}\left[\Pi\left(q, \tilde{\xi}\right)\right]\right)^2\right] \right\},$$

where weight λ reflects the magnitude of the decision maker's risk aversion. They derive the closed-form optimal order quantity and the worst distribution.

Chen and Xie (2021) consider the uncertainty of both demand and yield with l-∞ norm Wasserstein ambiguity under decision criteria of minimax regret and Hurwicz measure:

$$\max_{x \ge 0} \left\{ \lambda \sup_{\mathrm{P} \in P} \mathrm{E}_{\mathrm{P}}\left[\Pi\left(x, \tilde{u}, \tilde{v}\right)\right] - (1 - \lambda) \inf_{\mathrm{P} \in P} \mathrm{E}_{\mathrm{P}}\left[\Pi\left(x, \tilde{u}, \tilde{v}\right)\right] \right\},$$

where λ is the weight to balance optimism and pessimism. They derive the optimality condition, regret bound, and a golden section search algorithm to find the optimal order quantity.

2.2.4.2. Problem-specific ambiguity set

This subsection displays some ambiguity sets tailored to problem-specific features, which differentiate from the classic moment- or metric-based ambiguity sets. Qiu et al. (2014) adopt the idea of uncertainty set in RO to model distributional ambiguity. They assume the true distribution lies in an ellipsoid or a box centering in a known distribution and seek the worst distribution in it. Later, Qiu et al. (2017) apply a similar modeling method (i.e., modeling distributional ambiguity by the classic robust optimization method) to a single-product multi-period inventory review problem and derive the optimal inventory policy. However, note that the k-dim probability vector forms a standard simplex:

$$\left\{\mathbf{p} \in \mathrm{R}^k : \sum_{i=1}^k p_i = 1,\ p_i \geq 0,\ i \in [k]\right\},$$

and directly restricting the shape and structure of this simple (i.e., applying box or ellipsoid constraint) is, in my view, unjustified.

Natarajan et al. (2018) introduce second-order partitioned statistics to model distribution asymmetry:

$$\begin{pmatrix} \left(\tilde{\boldsymbol{\xi}} - \boldsymbol{\mu}\right)^+ \\ \left(\boldsymbol{\mu} - \tilde{\boldsymbol{\xi}}\right)^+ \end{pmatrix},$$

where $\tilde{\boldsymbol{\xi}}$ is a random vector, $\boldsymbol{\mu}$ is the mean (or sample mean), and $(\bullet)^+$ is the element-wise maximum operator. This is a high-dimensional analogy of semi-variance of the univariate random variable, which enables newsvendor to address multi-product cases. Since the resulting model involving the asymmetry information is computationally demoing, they derive an approximation algorithm by semidefinite programming. In addition, they drive the closed-form optimal order quantity for the single-product case.

Rahimian et al. (2019) propose a total variation-based ambiguity set to model uncertain demand distribution in a single-product newsvendor problem:

$$P_\gamma = \left\{f : \int_\Xi \left|f(\xi) - f_0(\xi)\right| d\xi \leq 2\varepsilon, \int_\Xi f(\xi)\, d\xi = 1, f(\xi) \geq 0, \forall \xi \in \Xi\right\},$$

where Ξ is the support of random demand $\tilde{\xi}$, $f(\xi)$ is the density function, $f_0(\xi)$ is a reference (nominal) density function, and most importantly, ε is the radius of the total variation ball, which controls the level of robustness. They investigate the impact of ε on the optimal order quantity and how to find the best ε.

Das et al. (2021) construct the ambiguity set with higher moments, i.e., higher than the first two moments. Their ambiguity set incorporating the first N moments is

$$P_N = \left\{ \mathrm{P} \in \mathscr{P}\left(\Xi\right) : \mathrm{E_P}\left[\left(\tilde{\xi}\right)^i\right] = m_i,\ \forall i \in [N] \right\},$$

where m_i is the i-th moment, which is assumed to be known. However, they find that in this case, deriving the closed-form optimal order quantity is impractical. In fact, finding the optimal quantity numerically is also very challenging. They adopt a primal-and-dual approach to iteratively approximate the optimal order quantity in the presence of higher moment constraints. They further point out that Scarf's solution is only optimal for heavy-tailed distribution.

2.2.4.3. Data-driven approach

The data-driven approach based on historical observations is also popular in modeling distribution-free features. It either directly formulates the demand function by data or constructs data-driven ambiguity sets. Saghafian and Tomlin (2016) are the first to combine DRO and data-driven together. The newsvendor first forms his belief on the distribution (e.g., moment) and then progressively updates his belief. They give closed-form solutions under some conditions and show how this method asymptotically approaches the true distribution.

Xu et al. (2022) model the distributional ambiguity of a single random demand by its probability density function (PDF) in a data-driven approach. They propose protection curves to approximate the true PDF and use evolving data to repeatedly update the protection curve. A continuous nonnegative function $c(x)$ is a protection curve of PDF $f(x)$ if

$$\int_y^{\bar{x}} f(x) - c(x)\, dx \geq 0, \forall y \in [\underline{x}, \bar{x}],$$

where $[\underline{x}, \bar{x}]$ is the support interval of random demand. To characterize the distribution features more precisely, they propose several partitioning rules to partition the support interval of the random demand. The partitioned support segments and sampled data are used to construct ambiguity sets. For example, if we believe the PDF is non-decreasing in the interval $[\underline{x}, \bar{x}]$ and the probability of this interval is p_i, then the ambiguity set for this interval is

$$P_{[\underline{x}_i, \bar{x}_i]} = \left\{ \mathrm{P} \geq 0 : \mathrm{P}\left(\underline{x}_i \leq x \leq \bar{x}_i\right) = p_i, f'(x) \geq 0, x \in [\underline{x}, \bar{x}] \right\}.$$

They give the closed-from optimal order quantity under several partitioning rules. They show the asymptotic optimality of this method and point out that this approach is particularly effective for insufficient data.

When launching a new product, the manager often lacks data to predict the demand for this new product. Nevertheless, the demand could be estimated by the historical demand for some comparable products. To this end, Lin et al. (2022) use machine learning to build the demand distribution of the new product using similar products' historical demand. Zhang et al. (2023) use the idea of machine learning to retrieve the relationship between demand and features based on observed data. Given an observation of a collection of features, the corresponding demand is modeled by an ambiguous distribution by the Wasserstein ambiguity set.

2.2.4.4. Price Setting

The price-setting newsvendor is a branch of the newsvendor problem. He and Lu (2021) study the joint pricing and inventory decision for single-product newsvendor problems with ambiguous price-sensitive demand. In particular, the demand either takes a multiplicative form with respect to price: $D=d\left(p\right)\tilde{\varepsilon}$ with $\mathrm{E}\left[\tilde{\varepsilon}\right]=1$, or an additive form: $D=d\left(p\right)+\tilde{\varepsilon}$ with $\mathrm{E}\left[\tilde{\varepsilon}\right]=0$, where $d\left(\bullet\right)$ is the unknown price-demand map and $\tilde{\varepsilon}$ is the random noise. The ambiguous price-demand map is modeled by accessible observations of exercised price and the corresponding demand realization. Under the minimax regret decision criterion, the objective is

$$\min_{y\geq 0,\, p\in\left[\underline{p},\bar{p}\right]} \sup_{d(\bullet)\in P} \left\{ \max_{x\geq 0,\, p'\in\left[\underline{p},\bar{p}\right]} \mathrm{E}\left[\Pi\left(x,p';\tilde{\xi}\right)\right]-\mathrm{E}\left[\Pi\left(y,p';\tilde{\xi}\right)\right]\right\},$$

where P is the ambiguity set for the price-demand map:

$$P=\left\{d\left(\bullet\right)\geq 0\text{: } d\left(\bullet\right) \text{ is contintuious and decreasing agaisnt } p, d\left(p_i\right)=d_i\right\}.$$

They derive the analytical expression of the optimal pricing and order quantity.

2.2.4.5. Multiple products

Ng et al. (2012) pioneer the distribution-free multi-product newsvendor problem with downside substitution. Each demand corresponds to several products classified by the produce grade, and the demand for a lower-grade product can be substituted by an upper-grade product. The demand for each product and the demand proportion of each grade are uncertain, which are modeled by unknown distributions with known means and supports. Since this problem is too complex, it is impossible to derive closed-form optimal solutions. The model is reformulated as a linear program, which can be efficiently solved by commercial solvers.

Ardestani-Jaafari and Delage (2016) interpret the multi-product newsvendor problem in a cost-minimization form and investigate the uncertain piece-wise linear form of the cost function. The piece-wise linear cost function is perturbed by random variables that are modeled by the classic robust optimization method (i.e., modeling support set by an uncertainty set). They further incorporate lower-order moment information of the random perturbation to form a DRO version uncertain cost function. They use SDP to construct an approximation algorithm. Wang et al. (2023) consider a multi-product newsvendor problem subject to an inventory capacity constraint, and the ambiguous distribution is, again, modeled by the first two moments. They derive the closed-form optimal order quantities via the Lagrangian multiplier method.

2.2.4.6. Discrete Demand

Gallego et al. (2001) pioneer the discrete demand distribution in the distribution-free newsvendor problem. They find that the worst distribution can be found by solving a special linear program. In addition, they extend the single-period newsvendor problem to multiple periods and use dynamic programming to solve the resulting model. Ninh et al. (2019) extend this problem by considering two objectives (i.e., maximum expected profit, minimax profit regret). They explore the optimal base structure of the resulting linear program that derives the worst-case distribution. Ninh (2021) further extends this problem by modeling demand as a compound Poisson process and each Poisson random variable in the compound Poisson process is modeled by sampled moment information. The optimal order quantity is obtained by solving a convex relaxation via McCormick's envelope.

2.2.5. Summary

We aim to equip researchers and managers with basic knowledge of DRO and help understand how DRO is applied to OM problems. To this end, we illustrate DRO from the viewpoint of both modeling and solution approaches. Then, we review the application of DRO in three operational problems and point out how DRO models uncertainties arising in these problems. We further dive into the newsvendor problem and analyze how DRO can be combined with various newsvendor features. Before closing this chapter, we try to give researchers and managers more insights.

2.2.5.1. Takeaways for managers

While DRO enjoys versatile abilities to model ambiguous probability distributions, the resulting model is often computationally demanding. This limits its applications in the real world, especially in large-scale problems. Hence, among numerous uncertainties that may affect decision-making, operations managers are advised to identify "truly critical" ones so as to build "simple" models. In addition, the managers can feel free to involve risk attitudes in decision-making as DRO performs good tractability to address various risk metrics (e.g., conditional value at risk and minimax regret).

2.2.5.2. Takeaways for researchers

The theoretical studies of DRO have achieved significant advancements during the past decade, whereas the application-oriented studies only cover a very limited part of these theoretical results. The majority of application-oriented studies adopt a few well-established ambiguity sets (e.g., lower-order moment-based) and reformulation tricks. Problem-specific ambiguity sets that capture unique problem features are still under-explored but have strong practical significance. This may help researchers derive valuable insights to greatly improve problem-specific operations.

2.3. Logistics Operations under Pandemics: Targeted Intercity Travel Restriction Policies

We first review some pandemic control studies to uncover our unique problem features. Then, from a methodological perspective, we review DRO studies and algorithms of stochastic programs with integer recourse.

2.3.1. Pandemic control studies

The global outbreak of COVID-19 inspires various studies on pandemic control. For example, from a strategic viewpoint, Choi (2021) identifies how operations research (OR) can help before, during, and after the pandemic and proposes a sense-and-response OR framework for policymakers. From an operational viewpoint, Xu et al. (2024) develop a two-stage newsvendor model that incorporates updated pandemic information to determine stocking quantities of vaccines. Yin et al. (2024) integrate agent-based simulation and optimization to deploy vaccine centers while considering the dynamics of disease spread. Zan et al. (2024) propose a data-driven approach to allocating testing resources utilizing real-time monitoring data of infectious diseases. Shams Eddin et al. (2025) investigate the effectiveness of large-scale screening at early outbreak and uncover when individual or group testing is more efficient.

Travel restrictions include measures such as social distancing (separation), quarantine, activity control, and intercity migration restriction. We concisely review some studies on each measure. For example, Kaplan (2020) develop a probability model to determine the social distancing standard (i.e., population density) to guarantee the infection risk below a desired level. Birge et al. (2022) propose a mixed-integer linear program to determine the allowed activity levels among urban communities in a city to gradually reduce infections over time. Li and Aprahamian (2024) derive the optimal social separation policy for a social network in a single period and propose a heuristic policy for multiple periods. Lin et al. (2024) employ a set partitioning method to determine the optimal quarantine policies with consideration of spread mitigation and economic impact. Song et al. (2024) adopt a Markov decision process to optimize vaccine supply and social distancing levels in an area, while considering disease spread over multiple periods. Zhou et al. (2024) examine the air travel bubble policy and build a mixed-integer linear program to determine which international flights to resume.

We note that the studies on intercity travel restriction policies are less developed than those on other measures like screening and social distancing. This study enriches this research direction by optimizing the restriction levels imposed on all migration flows among a large network. In addition, most prior studies employ susceptible-infectious-removed (SIR) based models to formulate disease spread in the future (e.g., Song et al. (2024), Yin et al. (2024), Vanli and Tsekeni (2025)). This study provides an alternative approach through modeling potential pandemic deteriorating scenarios using DRO.

2.3.2. DRO studies

DRO is a versatile and trendy technique to model parameter uncertainty in mathematical programs. Unlike stochastic programming, which assumes that the uncertain parameters follow a known probability distribution, DRO only needs some reference information on the distribution (e.g., the first and second moments), and the true distribution is assumed to lie in an ambiguity set characterized by some reference information. There are two major types of ambiguity sets (i.e., moment-based and metric-based). The moment-based ambiguity set characterizes distributions using lower-order statistical information (e.g., means and covariances) of uncertain parameters (Delage and Ye 2010). The set and its variant are adopted in various healthcare management problems like appointment scheduling (Bansal et al. 2021) and surgery admission (Wang et al. 2023). The metric-based ambiguity set contains distributions whose probability metrics (e.g., Wasserstein distance (Gao and Kleywegt, 2023) and divergence (Ben-Tal et al. 2013)) to a given reference distribution are within a prespecified threshold. Among these metrics, the Wasserstein distance-based ambiguity set has gained extensive attention thanks to good tractability and has been used in various operations problems such as vehicle routing (Zhang et al. 2021), allocation (Sun et al. 2022), and hurricane evacuation (Liu et al. 2025).

However, both classic ambiguity sets cannot capture the characteristics of correlation of pandemic deterioration in a precise manner. To be specific, to build a moment-based ambiguity set in our problem, we need to derive the covariance matrix that characterizes the correlation of risk states of any two cities. Producing such covariance matrices is challenging, especially when the number of cities is large. Regarding the metric-based ambiguity sets, a reference distribution is required (e.g., the empirical distribution derived from historical data). However, when a new infectious disease suddenly outbreaks (e.g., the Wuhan outbreak in January 2020), policymakers often lack enough historical data to build a reliable empirical distribution. In addition, since a city could stay in a certain risk state for a long period (e.g., weeks or even months), sampling city risk states at different times may yield similar results, making the resulting empirical distribution unreliable.

Aside from these two ambiguity sets, Agrawal et al. (2012) propose a marginal distribution-based ambiguity set to indirectly model the unknown correlation of random variables. This approach only requires the marginal distribution of each random variable, and thus especially suits the case that there is insufficient data to measure correlation (e.g., by covariance). However, unlike moment- and metric-based ambiguity sets, there is no unified approach to deriving the tractable reformulation of marginal distribution-based ambiguity sets. The solving procedure is strongly problem-specific, i.e., depending on specific structural properties of models. The question left to us is: How to use this technique to model the correlation of disease spread among cities in potential pandemic deterioration, and more importantly, how to solve the resultant model effectively?

2.3.3. Stochastic programs with integer recourse

We find that a computationally tractable counterpart of the original DRO model indeed exists. However, the counterpart is a stochastic program with integer recourse and is very challenging to solve. This is because both the master problem and the recourse problems are both complex integer programs, and the number of recourse problems is large. Two methods are widely adopted in solving stochastic programs with integer recourse (i.e., L-shaped method and Lagrangian relaxation). The L-shaped method is invented by Laporte and Louveaux (1993) to decompose the original model into a master problem and one or multiple subproblem(s). The cuts derived from the subproblems are added to the master problem to control the exploration of the optimal master solution. It is easy to implement and has been used in, for instance, vehicle routing (Laporte et al. 2002) and network design (Sanci and Daskin 2021). Lagrangian relaxation-based methods (Carøe and Schultz 1999) introduce local copies of master decision variables in recourse problems and dualize the critical constraint that protects the consistency of master variables and their local copies. Then, the original model can be decomposed into a master problem and many subproblems, and the information obtained from the subproblems is used to update the Lagrangian multipliers of the critical constraints. This algorithm has various applications such as product pricing (Steeger et al. 2018) and vehicle relocation (Hua et al. 2019).

However, in both methods, we need to solve many integer subproblems at each iteration. If a model has numerous subproblems or the subproblem itself is complex, both methods can be very time-consuming. In the tractable counterpart, any subproblem is at least the same complex as the master problem; moreover, the number of subproblems increases quickly regarding network sizes and risk state classification; directly applying the two classic algorithms could be inefficient. This motivates us to find an efficient algorithm to address large-scale modes arising in real-world applications.

2.4. Service Operations under Economic Downturns: Service Downgrading Strategies

This study relates to two streams of studies: i) service operations and ii) loyalty program operations, which are critical branches of operations management. We concisely review some representative studies in each stream to uncover research gaps.

2.4.1. Service operations

We classify the related service operations literature into three major groups. The first group considers service competition and pricing dynamics. For example, So (2000) examined how service delivery firms optimized pricing and time guarantees in competitive environments, demonstrating that equilibrium decisions depended heavily on firm-specific characteristics. Tsay and Agrawal (2000) analyzed competitive dynamics between two retailers purchasing from a common manufacturer, where the manufacturer set wholesale prices and retailers competed on selling prices. Chiu et al. (2014) derived Nash equilibrium service levels for firms facing service-level-sensitive demand, exploring cases where pre-season inventory was either fixed or endogenously determined. Yu et al. (2018) examined pricing decisions for per-use rental services in the context of service quality differentiation, underscoring the positive effect of differentiation strategy on profitability. The second group focuses on service-level management and resource allocation. For instance, Zanjirani Farahani et al. (2019) investigated deployment problems of urban service facilities in disaster management, highlighting the significance of an intelligent deployment. Siqin et al. (2022) explored how e-platforms selected sales channels and designed service contracts, identifying scenarios where revenue-sharing contracts with fixed fees were optimal. Gu et al. (2023) studied outsourcing and cooperation strategies when third-party bike rebalancing service providers exhibit different service qualities, and derived the conditions under which cooperation is beneficial. The third group pioneers technology-driven service innovations. For example, Xu et al. (2023) demonstrated that WhatsApp-based shopping helped retailers sustain operations and increase physical store demand when offline purchases were restricted. Loeys et al. (2025) developed a novel service contract design problem where IoT sensor data is used to dynamically assess maintenance risk based on actual machine usage during the contract.

Prior studies focused on service upgrades, pricing competition, or technology adoption, but overlooked some critical features: i) No work addressed service downgrading as a deliberate operational tactic to reduce costs. ii) The design of loyalty programs under SDS, which is common in practice, remained unexamined theoretically. iii) Existing competitive models (e.g., Chiu et al. 2014) did not consider how the integration of SDS and loyalty programs affects equilibrium outcomes in contested markets. This study bridges these gaps by analyzing SDS implementation, designing loyalty programs tailored to downgraded services, and modeling competitive interactions, offering novel insights into balancing cost efficiency with customer retention.

2.4.2. Loyalty program operations

Early studies on loyalty program operations laid the foundation for understanding loyalty programs as a strategic tool. Kim et al. (2001) pioneered the application of reward programs in competitive environments, showing how they weaken price competition by creating switching costs. Lewis (2004) introduced dynamic programming to model customer retention, demonstrating that loyalty programs shift consumers from short-term to long-term purchasing behavior. Recent loyalty program operations studies are mainly dedicated to novel operational features. For example, Chun and Ovchinnikov (2019) analyzed spending-based loyalty programs, showing they outperform quantity-based designs by leveraging strategic, status-seeking customers, even improving outcomes for both firms and consumers. Walsman and Dixon (2020) explored paid loyalty programs, revealing that fee-paying members prioritize easy-to-redeem benefits, challenging the assumption that more benefits enhance loyalty. Chun et al. (2020) redefined loyalty program operations by linking loyalty points to balance-sheet liabilities. They showed that firms should adjust point values based on "profit potential", using loyalty programs as buffers against financial uncertainty. Rossi and Chintagunta (2023) provided causal evidence from gasoline markets, showing that loyalty programs raise prices in later periods due to customer lock-in, influencing broader market pricing dynamics. Guo (2023) argued that firms should penalize extra consumption with overage charges (vs. rewarding loyalty with discounts) when high-value consumers' demand frequency is higher (vs. sufficiently lower) than low-value consumers, balancing pricing strategies to retain loyalty and maximize profits. Lim et al. (2024) revealed that customers treat points differently from money, and that heavy point earners would value points more, while occasional earners prefer cash, urging firms to tailor pricing policies to segment-specific mental accounting. Freund and Hssaine (2025) proposed tractable incentive schemes under fairness constraints, ensuring equitable treatment across different customer segments.

These studies treat loyalty programs as a standalone tool for customer retention, whereas ignored the interplay with service strategies that could also enhance profitability or competitiveness. For instance, Kim et al. (2001) and Singh et al. (2008) examined loyalty programs' competitive effects but did not consider any service strategies. Chun et al. (2020) addressed financial liabilities but not compensation for service cuts. Our research bridges this gap by investigating the proper loyalty program design joint with a cost-reduction strategy, which could impair customer satisfaction (i.e., SDS). Note that while Rossi and Chintagunta (2023) and Lim et al. (2024) showed loyalty programs' pricing and behavioral impacts, they failed to identify how such programs offset the demand loss entailed by service strategies.

2.5. Summary of this Chapter

This chapter has established a foundation for this thesis. First, by reviewing the literature on operations under disruption, we identify various operational challenges and display associated recent studies. Then, by reviewing the theory and application of DRO, we identify a powerful tool for managing the associated uncertainty. With a comprehensive understanding of the latest studies, theories, and applications, this research will then proceed from literature reviews to specific operational problems in the real world. In particular, **Chapter 3** will examine a logistics operations problem under pandemics, while **Chapter 4** will investigate a service operations problem under economic downturns, both of which utilize DRO to model uncertainty arising in their contexts.

Chapter 3. Logistics Operations under Pandemics: Targeted Intercity Travel Restriction Policies

3.1. Problem Statement

The review in **Chapter 2** reveals that studies on intercity travel restriction policies are less developed than those on other measures like screening and social distancing. Thus, the analytical study in **Chapter 3** aims to enrich this research direction by optimizing the restriction levels imposed on all migration flows among a large network. Furthermore, this work provides a methodological alternative to the common approach in prior research. Unlike many studies adopting SIR-based models to formulate disease spread (e.g., Song et al. (2024), Yin et al. (2024), Vanli and Tsekeni (2025)), this study employs a DRO framework. This method allows for robust decision-making under uncertainty without needing to precisely forecast the pandemic's evolution, offering a new perspective for managing public health crises and contributing to both the specific literature on travel restrictions and the broader methodological toolkit for pandemic response. The detailed background of the problem studied in this chapter is as follows.

3.1.1. Research background

In human history, infectious diseases, such as plague, cholera, smallpox, Ebola virus, severe acute respiratory syndrome coronavirus (SARS), and Middle East respiratory syndrome coronavirus (MERS), have caused many severe disasters (Piret and Boivin, 2020). For example, the COVID-19 pandemic swept the world in 2020 and has caused over 777 million infections, killing over seven million people (WHO, 2025). Recently, in August 2024, the monkeypox outbreak in Africa was declared as a public health emergency of international concerns (WHO, 2024a). To save people's lives and contain the spread of pandemics, various methods, including pharmaceutical measures and non-pharmaceutical interventions, were introduced. Due to the high contagiousness of viruses, the available pharmaceutical and healthcare resources in many countries, especially in developing countries, are often insufficient to control quickly increased cases. In this situation, non-pharmaceutical interventions, such as masks, massive screening, isolation/quarantine, social distancing, and travel restrictions, have been adopted to fight against pandemics, especially amid the COVID-19 outbreak in 2020 (Zhao et al. 2024).

Travel restrictions are major actions of non-pharmaceutical interventions, which effectively reduce exposure and transmission of viruses by limiting people's movements. It is often adopted to control the early outbreak of severe diseases, especially new infectious diseases (e.g., SARS, Ebola virus, COVID-19) that lack wonder drugs and vaccines (Lai et al. 2020). According to the range impacted, travel restrictions contain two major types (i.e., innercity and intercity). The innercity one decreases people's touch to control local transmission, including such as isolation/quarantine of mild patients, social distancing, and public facility closures. Intercity travel restrictions reduce potential imported infections by limiting inbound migration from risky cities, by means of strict permission (e.g., testing, centralized quarantine, outdoor activity monitoring) on inbound travelers (Chinazzi et al. 2020). For example, in February 2020, the Chinese government imposed the highest-level restrictions of both types in Wuhan, making its inflows, outflows, and local activities reduce by around 77%, 56%, and 55%, respectively (Fang et al. 2020). For another example, just one day after WHO's monkeypox warning, China required inbound travelers from countries/regions in monkeypox outbreaks to declare their status; travelers will get sampling and testing, if contacted with monkeypox cases or have symptoms such as fever, headache, swollen lymph nodes, or rash (China Customs 2024).

While intercity travel restrictions are effective in controlling early outbreaks, a huge amount of cost is often incurred, including but not limited to healthcare resources, labor resources, and negative impacts on the economy and society (Kraemer et al. 2020). For example, the Hong Kong government imposed strict restrictions on inbound visitors from mainland China in January 2020 and then extended the restrictions on international travelers. The total arrivals to Hong Kong in 2020 dropped to 3.57 million from 55.9 million in 2019, attaining the 36-year-lowest level in the tourism sector (South China Morning Post, 2021). In view of the huge cost, can policymakers make full use of a limited budget to maximize their pandemic control abilities by optimizing intercity travel restriction policies (TRPs)?

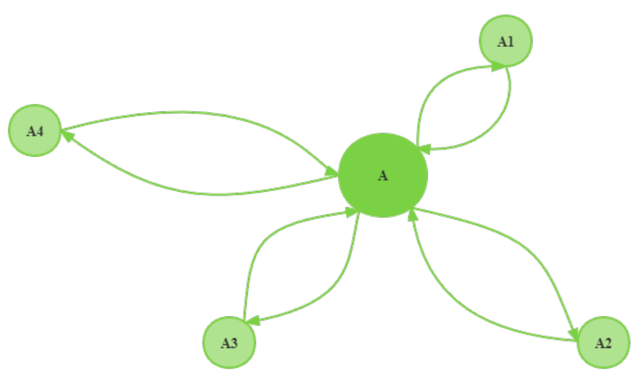

Figure 3.1. An illustrative network with one central city and four satellite cities.

As viruses continuously mutate, often performing higher contagion, what should policymakers do if the imposed TRPs cannot effectively control the outbreak (i.e., deterioration)? For example, the virus that caused WHO's monkeypox warning in August is a much more deadly variant of the clade found in 2022 (WHO, 2024b). Shortly after the 2020 Wuhan big outbreak, COVID-19 swept China, and the central government thus implemented travel restrictions in almost the entire mainland (Yesudhas et al. 2021). In this case, can policymakers determine TRPs in a more proactive manner? In particular, instead of considering the current pandemic control performance only, is it possible to hedge against potential pandemic deteriorating scenarios in the future?

Table 3.1. City risk states in the current outbreak and three pandemic deteriorating scenarios.

City	Current City Risk State	City Risk State (Pandemic Deterioration)		
		Scenario 1	Scenario 2	Scenario 3
A	Medium	Very High	Very High	Very High
A1	Low	High	Very High	Low
A2	Low	High	High	Low
A3	Low	Very High	High	Low
A4	Low	Mid	Mid	Low

To answer the above questions, it is critical to examine the pattern of disease spread. One special feature of disease spread is the correlation resulting from the virus transmission carried by people's migration among cities (Chinazzi et al. 2020). Specifically, people from high-risk cities (i.e., severe pandemics) could seriously worsen the outbreak in the destination cities they traveled to. To illustrate such a correlation, consider the network in **Figure 3.1**, consisting of one central city (i.e., A) and four satellite cities (i.e., A1 to A4). We evaluate the outbreak in a city by four risk states (i.e., low, mid, high, and very high). **Table 3.1** displays the city risk states at the current outbreak and three possible pandemic deteriorating scenarios. Expectedly, the occurring probabilities of Scenarios 1 and 2 should be higher than Scenario 3, since when the outbreak in City A worsens significantly, its adjacent cities are also likely to face deteriorating outbreaks. While it is understandable that scenario 3 has the lowest occurring probability, predicting this probability accurately is difficult. Also, for Scenarios 1 and 2, it is even hard to tell which scenario is more likely to happen, because their risk states are very similar. How to characterize the correlation of disease spread among cities raises a challenging question.

3.1.2. Research questions and major findings

Motivated by these observations from the real world, we propose the following research questions:

1) How to characterize the correlation of disease spread among cities and efficiently solve the resulting model on real-world scales?
2) What is the benefit of modeling the correlation of disease spread among cities in TRPs, and what is the advantage of our TRPs compared to real-world TRPs?
3) What is the insight brought by our TRPs to policymakers when containing pandemics?

To explore these questions, we conduct an optimization study to investigate the optimal targeted policies of intercity travel restrictions and establish the following:

1) We employ a marginal distribution-based ambiguity set to model the correlation of disease spread among cities in pandemic deterioration. The resulting model is a huge-scale mixed integer nonlinear program and is then reduced to an equivalent mixed integer linear problem of moderate scale. To solve large-scale problems, we develop a tailored Benders decomposition algorithm that utilizes a special relation between master- and sub-problem variables. Various enhancement schemes (e.g.,

initial solution/cut construction and Hamming distance cuts) are further adopted to accelerate convergence.

2) Computational experiments demonstrate that compared to a classic robust optimization model without considering the correlation, our model simultaneously achieves higher pandemic control performance and lower performance variation (i.e., “mean-variance dominance”). Moreover, our tailored algorithm can find optimal solutions to large-scale problems efficiently (e.g., 1 hour for 100 cities), enabling policymakers to frequently update their policies (e.g., daily basis) to involve the latest pandemic information.
3) In a case study with real-world pandemic and economic data of Guangdong, China, our policies exhibit 2.5 to 4.9 times the pandemic control performance compared to a uniform travel restriction policy adopted by China, where inbound permission depends on visitors’ origin only. Moreover, the targeted policy is especially better than the uniform policy at the early outbreak stage or when the budget is limited. This emphasizes the urgency of imposing travel restrictions as early as possible if a large-scale spread is anticipated.
4) In the policy budget allocation that all cities get an identical percentage of their GDPs, the cities whose economies heavily depend on tourism may not get enough budget to decrease inbound migration, leading to unfairness. However, the variations of all cities’ pandemic control performances are found to remain moderate (less than 4%) even when reuse efficiencies of anti-epidemic materials significantly change. In other words, our policies indirectly mitigate the unfairness in budget allocation.

3.2. Model and Tractable Reformulation

After stating the problem settings in detail, we formulate this problem by a nonlinear two-stage DRO model. However, since the resulting model appears to be computationally intractable, we drill deeper to uncover problem-specific structural properties and derive a tractable reformulation to facilitate further analysis.

3.2.1. Model settings

Suppose a policymaker is facing the outbreak of a new infectious disease (e.g., the sudden outbreak in Wuhan in January 2020) and plans to contain the disease spread by restricting people’s intercity travel among N cities. These cities are indexed by $[N] \triangleq \{1, \dots, N\}$, and the travel flow from city i to city j is expressed by a directional arc (i, j). The policymaker needs to determine the restriction levels on all travel flows. For each flow, there are L restriction levels, where level 1 is the weakest and level L is the strongest. Imposing level l restriction on flow (i, j) incurs a cost c_{ij}^{l}, and the resulting pandemic control effect (e.g., human lives saved or infection reduced) is evaluated by utility function $u_{ij}(l)$. To capture diminishing marginal reward, we consider a nondecreasing concave utility function $u_{ij}(l)$ in term of restriction levels, following the convention of the utility theory (Kimball, 1993). For city $j \in [N]$, total costs of limiting all inflows cannot exceed a prespecified budget $C_j^{current}$, which reflects city j's healthcare and financial capability.

The use of a concave utility function is empirically justified by the diminishing marginal effectiveness of non-pharmaceutical interventions. Empirical evidence from the early COVID-19 pandemic indicates that initial, targeted restrictions on high-volume travel hubs yield the most substantial reductions in imported cases (Chinazzi et al. 2020). As the restriction level intensifies, the incremental gain in infection reduction goes down because secondary transmission pathways are more complex to mitigate and the virus may already have established a local baseline (Kraemer et al. 2020). This aligns with the first-mile principle in public health policy: early implementation is significantly more effective than late-stage, sweeping measures, which often face a ceiling effect in their ability to further curb the pandemic's trajectory.

As mentioned, an imposed travel restriction policy may not be as effective as expected, and the outbreak could worsen. This could be especially true when a new infectious disease suddenly outbreaks. For example, in late January 2020, Hubei province imposed the strictest travel restriction policy on its capital, Wuhan, to contain the COVID-19 outbreak. However, many infected people had already left the city, causing the virus to appear in neighboring cities like Huanggang and Ezhou. In response, authorities quickly imposed travel restrictions there as well. However, as the virus continued to spread, the entire province was soon placed under massive travel restrictions by early February. This escalation of travel restrictions, from a single city to the entire province, was a direct reaction to the growing infectious disease.

Based on the above practice in the real world, to hedge against potential pandemic deterioration, the current restriction policy is expected to be enhanced in the sense that when the central government reoptimizes TRPs in pandemic deterioration, the previously imposed policies can benefit the new one. Consider the network in **Figure 3.2**, which consists of 2 central cities and 7 satellite cities. Nodes and arcs stand for cities and migration flows; a larger node represents a larger city, and a darker color means that the risk state of that city is higher. Compared with the current outbreak, the situations in city A and all of city group B worsen; the risk states of these five cities move to higher levels. In this case, TRPs should be strengthened, and the cities facing a worsening pandemic need more money to maintain or enhance the previous travel restrictions.

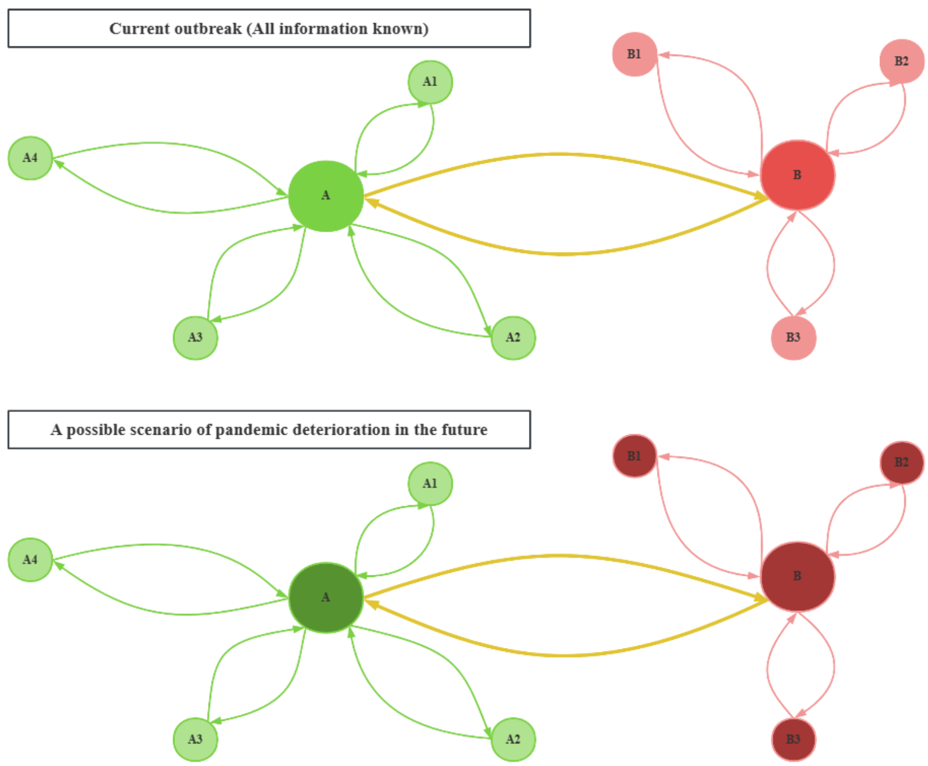

Figure 3.2. A current outbreak situation and a possible pandemic deteriorating scenario.

We can model the above policymaking problem in a two-stage framework: 1) Optimize the current TRPs with available information on the pandemic; 2) then, facing a particular deteriorating scenario, strengthen the TRPs by utilizing new budget and reusable resources of previous TRPs. The decisions at the two stages are linked together through *i*) The strengthening of travel restriction levels, and *ii*) the reusable resources of the first stage. To be specific, if the first-stage restrictions on a flow are level l, the strengthened restriction at the second stage can be one of $\{l,...,L\}$; implementing level l restriction on flow (i,j) at the first stage is expected to save a cost s_{ij}^{l} at the second stage.

3.2.2. Marginal distribution-based ambiguity set

Suppose the risk state of a city is classified by K types (e.g., safe, low-risk, mid-risk, and high-risk). At the first stage, we can evaluate the current outbreak to obtain the risk states of all cities, denoted by $r_j^{current}$, $\forall j \in [N]$. In the second stage, a city's risk state in pandemic deterioration is uncertain and thus is modeled by a random variable $\tilde{r}_j^{later}$, $\forall j \in [N]$. In a compact form, all cities' risk states in pandemic deterioration are captured by a random vector $\tilde{S} = \{\tilde{r}_1^{later},...,\tilde{r}_N^{later}\}$. The support set of $\tilde{S}$ is

$$\Xi = \{\boldsymbol{r} \in \mathbf{Z}^N : K \geq r_j \geq r_j^{current}, \forall j \in [N]\}. \tag{3.1}$$

Note that set Ξ has exponentially many elements (i.e., $|\Xi| = \prod_{j=1}^{N} R_j$, where $R_j = \left|\left\{r_j^{current}, ..., K\right\}\right|$ is the number of possible risk states of city j). The policy budget of a city at the second stage is still risk-state dependent, and in a particular scenario S, the budget of city j is denoted by C_j^{S}.

The discrete random vector $\tilde{S}$ should follow a certain distribution P, which can indirectly reflect the correlation of disease spread among cities. For example, in **Figure 3.1** and **Table 3.1**, the occurring probabilities of scenarios 1 and 2 should be higher than scenario 3. In scenarios 1 and 2, when central city A faces a significantly worsening outbreak, its adjunct cities' situation (e.g., A1 and A2) also becomes worse. However, in scenario 3, when the outbreak in city A deteriorates, all its adjacent cities remain at a low-risk status. This should be likely to happen in practice. Precisely deriving P is very hard. It is the joint distribution of exponentially many scenarios; a policymaker must predict the occurring probability of every single scenario, which is challenging. Therefore, instead of assuming that P takes a known form, we suppose that P belongs to a family of distributions characterized by some critical information. We use an ambiguity set P to include all such distributions.

To specify P, let $\boldsymbol{p}$ be a probability vector associated with support set Ξ; each element of $\boldsymbol{p}$ stands for the occurring probability of a scenario in Ξ. If reflecting the relationship among all scenarios in an exact way, we must specify the value of each element of $\boldsymbol{p}$, which is hard. Instead, we describe $\boldsymbol{p}$ by accessible information. Now, consider a particular city and temporarily ignore the impact of other cities. In this case, the probabilities of this city at different risk states are more practical to predict, as it solely reflects the relative relationship of this city's ability to combat different-level pandemics and need not consider other cities. The ability could be evaluated by, for example, healthcare resources, human resources, and financial support. Then, based on the marginal distribution-based ambiguity set proposed by Agrawal et al. (2012), our ambiguity set P that characterizes the correlation of pandemic deterioration is defined as

$$P = \left\{ \boldsymbol{p} \geq 0 : \sum_{\mathrm{S} \in \Xi} p(\mathrm{S}) = 1, \sum_{\mathrm{S} \in \Xi:\, r_j^k \in \mathrm{S}} p(\mathrm{S}) = q_j^k, \forall j \in [N], k \in [R_j] \right\}, \tag{3.2}$$

where $p(\mathrm{S})$ is the probability of scenario S; r_j^k is the k-th risk state in $[R_j]$; q_j^k is the probability of city j at risk state r_j^k. The critical constraint $\sum_{\mathrm{S} \in \Xi: r_j^k \in \mathrm{S}} p(\mathrm{S}) = q_j^k$ originates from the law of total probability (i.e., $P(A) = \sum_{m \in [M]} P(A \cap B_m)$, where $\{B_m\}_{m \in [M]}$ are all possible outcomes of any other discrete random variable $\tilde{B}$). It indicates that q_j^k equals the sum of probabilities of all scenarios where the risk state of city j equals r_j^k. In doing so, the proposed ambiguity set indirectly models the true joint distribution through the marginal distribution of each city.

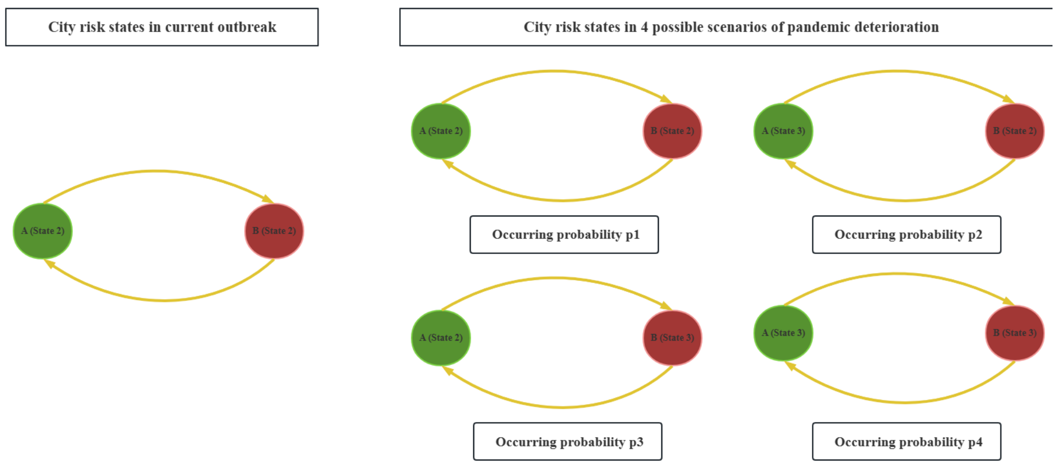

Figure 3.3. Four possible pandemic deteriorating scenarios and their occurring probabilities.

We explain the ambiguity set by an example in **Figure 3.3**. Classify the two cities' risk states as states 1, 2, and 3. In the current outbreak, both cities are at risk state 2 (i.e., $(R_A, R_B) = (2,2)$). When the pandemic deteriorates, there are four possible scenarios: $(2,2)$, $(3,2)$, $(2,3)$, and $(3,3)$. To characterize the joint distribution of these four scenarios, we need a vector $\boldsymbol{p} = (p_1, p_2, p_3, p_4)$, each entry corresponds to the occurring probability of a scenario. Suppose that for city A, we have $q_A^1 = q_A^2 = 0.5$ and $q_B^1 = 0.7$, $q_B^2 = 0.3$ for city B. Note that superscripts of q_A^1 and q_A^2 do not mean that the risk state of city A is 1 or 2, but mean that the risk state is the first one (i.e., 2) and the second one (i.e., 3) of the possible risk state set (i.e., $\{2,3\}$) in pandemic deterioration. Then, the marginal distribution-based ambiguity set characterizes the joint distribution $\boldsymbol{p}$ as follows.

$$p_1 + p_2 = q_A^1 \text{ (City A at risk state 2 joint with City B at risk state 2 or 3)}, \tag{3.3}$$

$$p_3 + p_4 = q_A^2 \text{ (City A at risk state 3 joint with City B at risk state 2 or 3)}, \tag{3.4}$$

$$p_1 + p_3 = q_B^1 \text{ (City B at risk state 3 joint with City A at risk state 2 or 3)}, \tag{3.5}$$

$$p_2 + p_4 = q_B^2 \text{ (City B at risk state 3 joint with City A at risk state 2 or 3)}, \tag{3.6}$$

$$p_1 + p_2 + p_3 + p_4 = 1, \tag{3.7}$$

$$p_1, p_2, p_3, p_4 \geq 0. \tag{3.8}$$

3.2.3. Two-stage DRO model

We now define the decision variables of the intercity travel restriction policymaking problem. Let x_{ij}^l be a binary variable, which equals 1 if level l restriction is imposed on flow (i,j) at the first stage, and 0 otherwise. Let y_{ij}^{l} be a binary variable that equals 1 if level l restriction is imposed on flow (i,j) at the second stage or 0 otherwise. Denote by $u_{ij}^{l}=u_{ij}(l)$ the utility value of imposing level l restriction on flow (i,j). Then, the problem is formulated by the following two-stage DRO model:

$$\textbf{[DR-LM]:}\quad \max_{\boldsymbol{x}}\left\{\sum_{i,j\in[N]}\sum_{l\in[L]}u_{ij}^{l}x_{ij}^{l}+\min_{\mathrm{P}\in\mathcal{P}}\mathrm{E}_{\mathrm{P}}\left[u\left(\boldsymbol{x},\tilde{\mathrm{S}}\right)\right]\right\} \tag{3.9}$$

subject to

$$\sum_{l\in[L]}x_{ij}^{l}=1,\forall i,j\in[N], \tag{3.10}$$

$$\sum_{i\in[N]}\sum_{l\in[L]}c_{ij}^{l}x_{ij}^{l}\leq C_{j}^{current},\forall j\in[N], \tag{3.11}$$

$$x_{ij}^{l}\in\{0,1\},\forall i,j\in[N],l\in[L], \tag{3.12}$$

with the recourse problem given a particular pandemic deteriorating scenario S:

$$u(\boldsymbol{x},\mathrm{S})=\max_{\boldsymbol{y}}\sum_{i,j\in[N]}\sum_{l\in[L]}u_{ij}^{l}y_{ij}^{l} \tag{3.13}$$

subject to

$$\sum_{l\in[L]}y_{ij}^{l}=1,\ \forall i,j\in[N], \tag{3.14}$$

$$\sum\nolimits_{l=k}^{L}y_{ij}^{l}\geq x_{ij}^{k},\ \forall i,j\in[N],k\in[L], \tag{3.15}$$

$$\sum_{i\in[N]}\sum_{l\in[L]}c_{ij}^{l}y_{ij}^{l}-\sum_{i\in[N]}\sum_{l\in[L]}s_{ij}^{l}x_{ij}^{l}\leq C_{j}^{\mathrm{S}},\forall j\in[N], \tag{3.16}$$

$$y_{ij}^{l}\in\{0,1\},\forall i,j\in[N],l\in[L]. \tag{3.17}$$

The objective function (3.9) maximizes the first-stage utility plus the worst-case expected utility of the second stage. Constraints (3.10) assign each migration flow with one restriction policy. Constraints (3.11) protect the policy budget of each city. Given a current restriction decision $\boldsymbol{x}$ and scenario S, the corresponding second-stage utility is derived by program (3.13) to (3.17). Constraints (3.14) match each flow with a single travel restriction policy; constraints (3.15) ensure that the second-stage restriction is no weaker than the previous one. The scenario-dependent budget is protected by constraints (3.16).

3.2.4. Hidden submodularity and optimal scenario reduction

The proposed two-stage DRO model is computationally intractable for two reasons. First, since the probability vector $\boldsymbol{p}$ needs to be optimized for the worst-case distribution, the second-stage objective function is thus bilinear, which makes DR-LM a mixed integer nonlinear program. Second, the model admits an extremely large scale. There are exponentially many possible scenarios in the second stage, which lead to a huge number of recourse problems. We cannot formulate the model explicitly even for small travel networks. This motivates us to find a tailored approach to the tractability issue. After examining the structural properties of DR-LM, we uncover that the worst-case expected utility of the second-stage problem admits a closed-form expression. Deriving such an expression relies on the submodularity hidden in the recourse problem $u(\boldsymbol{x}, \mathrm{S})$. Refer to the following lemma.

Lemma 3.1. *Given a current travel restriction decision* $\boldsymbol{x}$*, if we interpret scenario vector* S *by a modified set form, then the recourse problem* $u(\boldsymbol{x}, \mathrm{S})$ *is "hiddenly" submodular with respect to* S.

Equipped with the submodularity hidden in DR-LM, we can derive the closed form of the worst-case expected utility as follows.

Proposition 3.1. *The original two-stage DRO model DR-LM admits the deterministic equivalence:*

$$\textbf{[DR-LM-I]}: \max_{\boldsymbol{x}} \sum_{i,j\in[N]} \sum_{l\in[L]} u_{ij}^l x_{ij}^l + \sum_{v\in\{0\}\cup[R]} \big(q(v) - q(v+1)\big) u\big(\boldsymbol{x}, \chi^v\big) \tag{3.18}$$

subject to constraints (10) to (17), where $R = \sum_{j\in[N]} R_j$ *is the sum of all cities' possible risk states in pandemic deterioration;* $q(v)$ *is the* v*-th largest occurring probability among all* R *states; and scenario* χ^v *is constructed according to* $q(v)$.

In this Proposition, the constructed pandemic deteriorating scenarios $\{\chi^v, \forall v \in \{0\}\cup[R]\}$ and the corresponding probabilities $\{q(v) - q(v+1), \forall v \in \{0\}\cup[R]\}$ jointly establish the closed-form worst-case probability distribution. The significance of this closed-form expression is three-fold: *i*) The worst-case distribution is independent of the first-stage decision $\boldsymbol{x}$, which is greatly beneficial to applying decomposition algorithms. Specifically, if we devise a decomposition algorithm by stages, while the first-stage decision $\boldsymbol{x}$ is updated iteratively, we need not update the worst-case distribution, which effectively saves computational time. *ii*) DR-LM reduces from a mixed-integer nonlinear program to an integer linear program because the probability vector $\boldsymbol{p}$ in DR-LM, which is unknown and should have been optimized, is now replaced by known probability values. *iii*) The worst-case distribution only contains a moderate number of scenarios (i.e., $1+\sum_{j=1}^N R_j$), which is greatly fewer than the scenarios in support Ξ (i.e., $\prod_{j=1}^N R_j$). For example, given $N = 10$ and $R_j = 2$, we will have $2^{10} = 1024$ recourse problems in DR-LM, while only $2*10+1 = 21$ recourse problems in DR-LM-I, leading to a significant reduction of 1003 scenarios. To conclude, our reduction extracts a small number of critical scenarios from the set Ξ and by assigning appropriate probabilities, maintains the equivalence to the original model. The probabilities of these critical scenarios can be interpreted as the optimal solution to the inner minimization problem in the program (9).

3.3. Tailored Benders Decomposition

The reduced model DR-LM-I is tractable in principle, because it is "linear" and contains a moderate number of recourse problems. However, solving it by classic methods (e.g., the L-shaped method (Laporte and Louveaux, 1993) or Lagrangian relaxation (Carøe and Schultz, 1999)) could be computationally expensive. These algorithms need to solve $R+1$ integer subproblems at each iteration. For large-scale problems, this will still be time-consuming. To circumvent this issue, we develop a tailored Benders decomposition (BD) algorithm, which solves the linear programming (LP) relaxation of the recourse subproblems instead of the original integer program. We further establish several cuts (i.e., initial cuts and Hamming distance cuts) to enhance the convergence of this BD algorithm. The overall algorithmic framework is summarized in the last subsection.

3.3.1. Tight reformulation and decomposition

Since directly solving integer recourse subproblems can be time-consuming, we propose to approximate its optimal value by the LP relaxation of the recourse subproblem. The approximation can be embedded into the classic BD algorithm to attain near-optimal solutions. BD decomposes a mixed-integer linear model into a mixed integer master problem and (one or multiple) LP subproblem(s) (Benders, 1962). The cuts derived from the dual of the LP subproblems are progressively added to the master problem to accelerate convergence. In our problem, because of the gap between the integer subproblems and its LP relaxation, the cuts obtained by the dual can be very weak, and eventually make the algorithm fail to converge. Hence, a natural idea to overcome this issue is to strengthen the LP relaxation to reduce the gap and obtain stronger cuts. We thus propose a tight reformulation as follows.

Our tight reformulation is inspired by the constraint expansion theory (CET), which is well-established in the facility location literature (Revelle, 1993). CET splits a general integer variable into many binary variables and enforces the equivalence of the original integer variable and its associated binary variables through a set of tight linear constraints so as to tighten the formulation. However, the integer variables in our problem are already binary, and CET cannot be directly employed. However, by redefining all binary variables and their coefficients in an incremental form, we find that tight linear constraints can still be imposed. Moreover, CET needs to introduce many auxiliary binary variables, whereas our reformulation admits an identical number of integer variables to the original model.

In the reformulation, x_{ij}^{l} becomes a binary variable that equals 1 if the first-stage restriction on flow (i,j) is no weaker than level l, and 0 otherwise; c_{ij}^{l} and u_{ij}^{l} respectively becomes the cost and utility increased by improving the restriction on flow (i,j) from level $l-1$ to level l. Likewise, in the recourse problem, y_{ij}^{l} becomes a binary variable that equals 1 if the second-stage restriction on flow (i,j) is no weaker than level l, and 0 otherwise; s_{ij}^{l} becomes the cost-saving increment by improving restriction on flow (i,j) from level $l-1$ to level l at the first stage. With the redefined decision variables and parameters, the tight reformulation is

$$\textbf{[DR-LM-II]:}\quad \max_{\boldsymbol{x}} \sum_{i,j\in[N]}\sum_{l\in[L]} u_{ij}^{l}x_{ij}^{l} + \sum_{v\in\{0\}\cup[R]} \big(q(v)-q(v+1)\big)u\big(\boldsymbol{x},\chi^{v}\big) \tag{3.19}$$

subject to

$$\sum_{l\in[L]} x_{ij}^{l} \geq 1, \forall i,j\in[N], \tag{3.20}$$

$$x_{ij}^{l} \geq x_{ij}^{l+1}, \forall i,j\in[N], l\in[L-1], \tag{3.21}$$

$$\sum_{i\in[N]}\sum_{l\in[L]} c_{ij}^{l}x_{ij}^{l} \leq C_{ij}^{current}, \forall j\in[N], \tag{3.22}$$

$$x_{ij}^{l} \in \{0,1\}, \forall i,j\in[N], l\in[L], \tag{3.23}$$

with the recourse problem:

$$u\big(\boldsymbol{x},\chi^{v}\big) = \max_{\boldsymbol{y}} \sum_{i,j\in[N]}\sum_{l\in[L]} u_{ij}^{l}y_{ij}^{l} \tag{3.24}$$

subject to

$$\sum_{l\in[L]} y_{ij}^{l} \geq 1, \forall i,j\in[N], \tag{3.25}$$

$$y_{ij}^{l} \geq y_{ij}^{l+1}, \forall i,j\in[N], l\in[L-1], \tag{3.26}$$

$$y_{ij}^{l} \geq x_{ij}^{l}, \forall i,j\in[N], l\in[L], \tag{3.27}$$

$$\sum_{i\in[N]}\sum_{l\in[L]} c_{ij}^{l}y_{ij}^{l} - \sum_{i\in[N]}\sum_{l\in[L]} s_{ij}^{l}x_{ij}^{l} \leq C_{j}^{\chi^{v}}, \forall j\in[N], \tag{3.28}$$

$$y_{ij}^{l} \in \{0,1\}, \forall i,j\in[N], l\in[L]. \tag{3.29}$$

The reformulation DR-LM-II is equivalent to DR-LM-I in the sense that we can easily retrieve the true restriction policy from the solution to DR-LM-II. Also, from the modeling perspective, DR-LM-II is tight due to the convex hull-defining constraints (21), (26), and (27), which mimic the tight linear constraints in CET. Then, to apply BD to the reformulation, note that DR-LM-II is equivalent to

$$\max_{\boldsymbol{x}} \sum_{i,j\in[N]} \sum_{l\in[L]} u_{ij}^l x_{ij}^l + \sum_{v\in\{0\}\cup[R]} \big(q(v)-q(v+1)\big)\psi^v \tag{3.30}$$

subject to constraints (20) to (23) and

$$\psi^v \le u\left(\boldsymbol{x},\chi^v\right), \forall v\in\{0\}\cup[R]. \tag{3.31}$$

Instead of exactly computing the recourse value, BD approximates it by a bunch of linear inequalities in terms of the master decision $\boldsymbol{x}$ (i.e., cuts). By replacing $u\left(\boldsymbol{x},\chi^v\right)$ with the cuts, we obtain

$$\max_{\boldsymbol{x}} \sum_{i,j\in[N]} \sum_{l\in[L]} u_{ij}^l x_{ij}^l + \sum_{v\in\{0\}\cup[R]} \big(q(v)-q(v+1)\big)\psi^v \tag{3.32}$$

subject to constraints (20) to (23) and

$$\psi^v \le \textit{Benders Cuts}, \forall v\in\{0\}\cup[R]. \tag{3.33}$$

3.3.2. Tailored Benders optimality cuts

While implementing BD, two types of cuts (i.e., optimality and feasibility cuts) could be generated. The optimality cuts strengthen the dual bound and improve the solution quality of the master problem, while the feasibility cuts prevent master solutions that make the resource problem infeasible. Generally, we should consider cuts of both types in the course of BD. Yet, by examining the structural properties of DR-LM-II, we conclude that there is no need to generate feasibility cuts. See the following lemma:

Lemma 3.2. *The DR-LM-II admits complete recourse property, and thus, only Benders optimality cuts are needed.*

Thereafter, we will focus on the derivation of the optimality cuts. To begin, the integer requirement on $\boldsymbol{y}$ will be relaxed, and the binary constraint (29) now becomes variable bound constraints:

$$y_{ij}^l \le 1, \forall i,j\in[N], l\in[L]. \tag{3.34}$$

To derive the dual of the LP relaxation of the recourse problem, define dual variables $\phi_{ij} \le 0, \forall i,j\in[N]$ for constraints (25), $\kappa_{ij}^l \le 0, \forall i,j\in[N], l\in[L-1]$ for constraints (26), $\varpi_{ij}^l \le 0, \forall i,j\in[N], l\in[L]$ for constraints (27), $\sigma_j \ge 0, \forall j\in[N]$ for constraints (28), and $\eta_{ij}^l \ge 0, \forall i,j\in[N], l\in[L]$ for constraints (34). Given a master solution $\overline{\boldsymbol{x}}$, the dual of the LP relaxation of the recourse problem in scenario χ^v is

$$\min_{\phi,\kappa,\varpi,\sigma,\eta} \sum_{i,j\in[N]} \phi_{ij} + \sum_{i,j\in[N]} \sum_{l\in[L]} \overline{x}_{ij}^l \varpi_{ij}^l + \sum_{j\in[N]} \left(C_j^{\chi^v} + \sum_{i\in[N]} \sum_{l\in[L]} s_{ij}^l \overline{x}_{ij}^l \right) \sigma_j + \sum_{i,j\in[N]} \sum_{l\in[L]} \eta_{ij}^l \tag{3.35}$$

subject to

$$\phi_{ij} + \kappa_{ij}^1 + \varpi_{ij}^1 + c_{ij}^1 \sigma_j + \eta_{ij}^1 \ge u_{ij}^1, \forall i,j\in[N], \tag{3.36}$$

$$\phi_{ij} + \kappa_{ij}^{l} - \kappa_{ij}^{l-1} + \varpi_{ij}^{l} + c_{ij}^{l}\sigma_{j} + \eta_{ij}^{l} \geq u_{ij}^{l}, \forall i,j \in [N], l \in \{2,...,L-1\}, \tag{3.37}$$

$$\phi_{ij} + \kappa_{ij}^{L-1} + \varpi_{ij}^{L} + c_{ij}^{L}\sigma_{j} + \eta_{ij}^{L} \geq u_{ij}^{L}, \forall i,j \in [N]. \tag{3.38}$$

These dual variables will be used to construct optimality cuts, which are linear inequalities of master decision $\boldsymbol{x}$ parameterized by dual variables (i.e., $\phi,\kappa,\varpi,\sigma,\eta$). While we have enhanced the optimality cut by strengthening the LP relaxation, the integrality gap still exists. Thus, we try to further enhance optimality. Instead of further improving the formulation, we uncover a new cut strengthening method, which leverages a special link between master variables and recourse variables arising in our tight reformulation DR-LM-II. The link is captured by constraints (27), which enforce $y_{ij}^{l} = 1$ given $x_{ij}^{l} = 1$. Note that such a tight link does not exist in DR-LM-I. The proposition below defines the optimality cut tailored to this special link, which is stronger than the classic Benders optimality cut.

Proposition 3.2. *Given a master decision* $\bar{\boldsymbol{x}}$*, denote by* $\left(\bar{\phi},\bar{\kappa},\bar{\varpi},\bar{\sigma},\bar{\eta}\right)$ *the optimal dual vector of the LP relaxation of the integer recourse problem in scenario* χ^{v}*. Then, the following optimality cut:*

$$\psi^{v} \leq \sum_{i,j\in[N]} \bar{\phi}_{ij} + \sum_{j\in[N]} C_{j}^{\chi^{v}} \bar{\sigma}_{j} + \sum_{i,j\in[N]} \sum_{l\in[L]} \bar{\eta}_{ij}^{l} + \sum_{i,j\in[N]} \left(u_{ij}^{1} - \bar{\phi}_{ij} - \bar{\kappa}_{ij}^{1} - \left(c_{ij}^{1} - s_{ij}^{1}\right)\bar{\sigma}_{j} - \bar{\eta}_{ij}^{1}\right)x_{ij}^{1} + \tag{3.39}$$

$$\sum_{i,j\in[N]} \sum_{l\in[2,...,L-1]} \left(u_{ij}^{l} - \bar{\phi}_{ij} - \bar{\kappa}_{ij}^{l} + \bar{\kappa}_{ij}^{l-1} - \left(c_{ij}^{l} - s_{ij}^{l}\right)\bar{\sigma}_{j} - \bar{\eta}_{ij}^{l}\right)x_{ij}^{l} + \sum_{i,j\in[N]} \left(u_{ij}^{l} - \bar{\phi}_{ij} + \bar{\kappa}_{ij}^{L-1} - \left(c_{ij}^{L} - s_{ij}^{L}\right)\bar{\sigma}_{j} - \bar{\eta}_{ij}^{L}\right)x_{ij}^{L} \quad \text{is}$$

valid and stronger than the classic Benders optimality cut.

3.3.3. Initial cuts and convergence enhancement

Since the initial cuts added to the Benders master problem have a significant impact on the convergence (Rahmaniani et al. 2017), we propose a variable rounding rule to construct good feasible solutions and derive good initial cuts with it. Our rounding rule leverages the structural property of the LP relaxation. See the following lemma:

Lemma 3.3. *Solve the LP relaxation of DR-LM-II and denote the optimal master solution by* $\underline{\boldsymbol{x}}$*. Denote by* $\underline{x}_{ij}^{r}$ *the variable such that* $\underline{x}_{ij}^{r} > 0$ *and* $\underline{x}_{ij}^{r+1} = 0$ *for* $\forall i,j \in [N]$*. We claim that* $\underline{x}_{ij}^{r}$ *is the unique variable that could be fractional in all* $\underline{x}_{ij}^{l}$ *for* $\forall l \in [L]$ *in the LP relaxation.*

The lemma suggests that we can obtain an integer-feasible master solution by rounding the fractional variable $\underline{x}_{ij}^{r}$. Additionally, the lemma implies that the reformulation DR-LM-II is tight in the sense that at most $N\cdot(N-1)$ master variables could be fractional, while the rest $N\cdot(N-1)\cdot(L-1)$ master variables are integers. To determine how to round fractional variables, we define the following criteria:

Definition 1. Heuristically, we evaluate the potential of fractional $\underline{x}_{ij}^{r}$ to be 1 by the following mark:

$$g_{ij}^{r} = u_{ij}^{r} \big/ \left(c_{ij}^{r} - s_{ij}^{r}\right), \forall i, j \in [N], \tag{3.40}$$

where u_{ij}^{r}, c_{ij}^{r}, and s_{ij}^{r} are parameters of utility, cost, and cost-saving in DR-LM-II.

Roughly speaking, the proposed mark can be regarded as the marginal utility per unit of "true" investment since the cost is subtracted by the cost-saving. Round down city j's fractional restriction level variables of inflows; then, let variable $\underline{x}_{ij}^{r}$ with the largest mark g_{ij}^{r} be 1, if the rounding up does not make the cost exceed the policy budget $C_{j}^{current}$. Next, round up the one with the second-largest grade if the remaining budget is enough. Repeat the above procedure until the budget is used up. Denote the master solution obtained by the aforesaid rounding rule by $\boldsymbol{x}^{0}$. Adopt $\boldsymbol{x}^{0}$ as the input of all recourse problems to generate tailored Benders optimality cuts as the initial cuts to warmly start BD.

In the course of running BD, two issues often arise when solving the master problem, which greatly burden computational efficiency (Rahmaniani et al. 2017). First, optimal master solutions could oscillate among several feasible sub-regions, leading to sub-optimality. Second, BD repeatedly yields identical master solutions at early iterations due to limited knowledge provided by the cuts. To circumvent these issues, we add two types of cuts based on the Hamming distance into the master problem (Li and Sun, 2006). The definition of the Hamming distance is as below.

Definition 2. The Hamming distance from binary vector $\boldsymbol{x}^{0}$ to binary vector $\boldsymbol{x}$ is

$$\Delta\left(\boldsymbol{x}, \boldsymbol{x}^{0}\right) = \sum_{i \in S_0} \left(1 - x_i\right) + \sum_{i \in I \setminus S_0} x_i, \tag{3.41}$$

where I is the index set of origin $\boldsymbol{x}^{0}$ and $S_0 = \left\{i \in I : x_i^{0} = 1\right\}$ is the support set of $\boldsymbol{x}^{0}$.

To prevent the oscillation behavior of the master problem, denote the optimal master at iteration t be $\boldsymbol{x}^{t}$, and add the following cut:

$$\Delta\left(\boldsymbol{x}, \boldsymbol{x}^{t}\right) \le \alpha \text{ (Type-I Hamming distance cuts),} \tag{3.42}$$

which limits the feasible region of the master problem at the next iteration within a neighborhood of the preceding optimal master solution, controlled by a prespecified positive integer α. Then, to avoid repetitive behavior, we use the cut:

$$\Delta\left(\boldsymbol{x}, \boldsymbol{x}^{t}\right) \ge 1 \text{ (Type-II Hamming distance cuts),} \tag{3.43}$$

enforcing that the optimal master solution at the next iterations is different from that at previous iterations. Both cuts are added to the master problem to reduce the computational time.

3.3.4. Full algorithm implementation

The tailored BD iteratively solves a sequence of the master- and sub-problems (s). In particular, at each iteration, the master problem is first solved, and the obtained optimal master solution is delivered to subproblems to generate tailored Benders optimality cuts and Hamming distance cuts, which are added to the master problem at the next iteration.

Over the progress, we approximate the true optimality gap ε by $\varepsilon' = \left(\overline{z}' - \underline{z}'\right) / \overline{z}'$, where $\overline{z}'$ and $\underline{z}'$ are pseudo upper and lower bounds, respectively. Specifically, $\overline{z}'$ is the optimal value of the master problem. Note that $\overline{z}'$ may not be the global upper bound due to the existence of Hamming distance cuts. We define the pseudo lower bound by

$$\underline{z}' = \max\left\{\underline{z}', \boldsymbol{u}\boldsymbol{x}^t + \sum_{v\in\{0\}\cup[R]}\left(q(v) - q(v+1)\right)\pi^v\left(\boldsymbol{x}^t\right)\right\}, \tag{3.44}$$

where $\boldsymbol{u}$ is the vector form of restriction utilities, and $\pi^v\left(\boldsymbol{x}^t\right)$ is the dual optimal value of the LP relaxation of the recourse problem v given input $\boldsymbol{x}^t$. It may not be the global lower bound since it is not based on the true recourse value. Nonetheless, we can compute the true gap ε after the main iterations terminate, while the gap ε' is only used to control the progress of the main iterations. To be specific, upon the pseudo gap ε' reducing below a prespecified threshold (e.g., 0.05%), we terminate the iteration. Then, we remove all Hamming distance cuts from the master problem while maintaining all tailored Benders optimality cuts. We solve the resulting master problem and denote its optimal value by $\overline{z}$ (i.e., true upper bound) and optimal solution by $\boldsymbol{x}^*$. The true lower bound can be computed by

$$\underline{z} = \boldsymbol{u}\boldsymbol{x}^* + \sum_{v\in\{0\}\cup[R]}\left(q(v) - q(v+1)\right)u\left(\boldsymbol{x}^*, \chi^v\right). \tag{3.45}$$

The true optimality gap is thus $\varepsilon = \left(\overline{z} - \underline{z}\right) / \overline{z}$. The full algorithm implementation is outlined as follows.

Algorithm 1. Tailored Benders Decomposition for DR-LM-II.

Phase I. Warm Start

1) Generate the initial master solution $\boldsymbol{x}^0$ by the proposed rounding rule of fractional variables.
2) Generate initial tailored Benders optimality cuts by input $\boldsymbol{x}^0$.
3) Generate initial Hamming distance cuts by input $\boldsymbol{x}^0$.

Phase II. Main Iteration

When the approximated gap $\varepsilon' > 0.05\%$ and the computational time $T \le 1800\text{s}$.

1) Solve the Benders master problem to obtain the optimal master solution.
2) Generate tailored Benders optimality cuts and Hamming distance cuts by the optimal master solution.
3) Update pseudo-upper and -lower bounds to compute ε'.

Phase III. Termination

1) Drop all Hamming distance cuts and keep all tailored Benders optimality cuts. Solve the resulting master problem and denote the optimal master solution by $\boldsymbol{x}^*$.

2) With input $\boldsymbol{x}^*$, solve all recourse problems to obtain the optimal recourse solution $\boldsymbol{y}^*$ and recourse value $u\left(\boldsymbol{x}^*, \chi^v\right), \forall v \in \{0\} \cup [R]$.
3) Compute the true optimality gap $\varepsilon = \left(\overline{z} - \underline{z}\right) / \overline{z}$ and total computational time.

3.4. Computational Experiments

This section examines the proposed BD algorithm's computational efficiency in large-scale problems. The DRO model is benchmarked with a classic RO model to quantify the benefit of modeling the correlation of disease spread. The intercity travel networks are drawn from China. Real-world city data, analytically-derived travel flows, hypothesized policy information (i.e., budget and cost), and simulated disease outbreak information are used to design the experiments (see **Appendix.I.1**).

3.4.1. Experimental design

We test the algorithm's performance on different network sizes: $N \in \{30, 40, 50, ..., 100\}$. Since a province in China generally has 20 to 30 cities, we choose 30 as the smallest network size to simulate a provincial policymaker. The largest network consists of 100 cities, which include all large cities with over 500 million population in China. Note that we also tested a huge network of 120 cities. The number of variables in DR-LM-II is nearly 28.8 million. In this case, solving the LP relaxation of DR-LM-II by GUROBI becomes very inefficient, and invalid solutions (i.e., *NaN*) were often returned. These invalid solutions cannot be used to generate initial solutions and initial cuts, so we limit the network size to below 100 cities. Since all municipalities, provincial capitals, and other large cities are included, it should be sufficient to provide reliable references to a national policymaker.

Aside from the network size, we consider policymakers' focus on pandemic control performances at different stages of the outbreak. Specifically, since containing the current outbreak is the major goal while hedging against future deterioration is a plus, it is natural to put different weights on the two stages. Therefore, we modify the objective function as follows:

$$\max_{\boldsymbol{x}} \left\{ \rho \sum_{i,j \in [N]} \sum_{l \in [L]} u_{ij}^l x_{ij}^l + (1-\rho) \min_{\mathrm{P} \in \mathcal{P}} \mathrm{E}_{\mathrm{P}} \left[u\left(\boldsymbol{x}, \tilde{\mathrm{S}}\right) \right] \right\}, \tag{3.46}$$

where ρ is the weight to balance policymakers' foci. $\rho = 0.5$ implies that policymakers regard controlling the current outbreak and hedging against future deterioration equally; $0.5 < \rho < 1$ suggests that hedging against potential deterioration is only a plus. We vary ρ between $\{0.2, 0.5, 0.8\}$ to reflect decision makers' different foci. When $\rho = 0.2 / 0.5 / 0.8$, policymakers will be less/equally/more focused on the current pandemic control performance, while more/equally/less about hedging against potential deterioration in the future.

Regarding algorithm parameters, the main iteration solves the LP relaxation of recourse problems and generates tailored Benders optimality cuts and Hamming distance until the pseudo gap $\varepsilon' \le 0.05\%$. To control the time consumed in the main iteration, we limit the maximum runtime to below 1800s. Regarding the strength of Hamming distance cuts, which control the main iteration's search progress, we refer to **Lemma 3.3**. For each migration flow, at most one of its associated restriction level variables could be fractional. Hence, we can significantly restrict the search space at the next iteration. By letting $\alpha = N$, we allow at most N integer variables to change in the next iteration.

3.4.2. Computational efficiency analysis

All computational results are reported in **Table 3.2**. To be specific, for each group classified by ρ, the total computational time varies from 57.18s (the fastest one) to 3921.70s (the slowest one). For the largest 100-city network, the optimal solution can be attained in 20 minutes. The tested models have 104 to 354 recourse problems, which are much larger than many stochastic programming models. We also find that network sizes affect the computation time significantly, whereas the impact of ρ is not obvious. Computational time obviously increases as the network size increases. However, interestingly, the most time-consuming instance is the network of 90 cities instead of the largest network of 100 cities. Also, the time used in the network of 70 cities is much longer than that of 80 cities. One possible reason could be that in the networks of 70 and 90 cities, some optimality cuts may make the Benders master problem very hard to solve, and these cuts could burden all next iterations significantly.

Table 3.2. Computational performance of the BD algorithm in different network sizes and policy foci.

N	V	**RHO-0.2**			**RHO-0.5**			**RHO-0.8**		
		Gap# (%)	**Gap (%)**	**T (s)**	**Gap# (%)**	**Gap (%)**	**T (s)**	**Gap# (%)**	**Gap (%)**	**T (s)**
30	104	0.04	0.17	68.71	0.03	0.12	80.79	0.01	0.05	57.18
40	145	0.01	0.04	103.02	0.01	0.03	80.33	0.00	0.01	144.89
50	175	0.01	0.59	165.84	0.03	0.37	235.11	0.00	0.16	938.65
60	210	0.04	0.67	523.96	0.03	0.38	614.42	0.00	0.17	481.93
70	244	0.00	0.06	2683.30	0.00	0.04	2776.60	0.02	0.02	802.28
80	288	0.04	0.25	862.05	0.03	0.16	863.44	0.01	0.06	841.87
90	309	0.02	0.79	1284.90	0.00	0.45	3071.60	0.00	0.19	3921.70
100	354	0.00	0.01	1377.10	0.00	0.00	1578.30	0.00	0.00	1399.60
Average		0.02	0.32	883.61	0.02	0.19	1162.57	0.00	0.08	1073.51

Notes. RHO: value of weight ρ; N: number of cities in the network; V: number of scenarios in the recourse problems; Gap# (%): pseudo-gap at the termination of the main iteration (phase II); Gap (%): integrality gap at the termination of the entire BD algorithm (phase III); T (s): total computational time of the main iteration (phase II) and the termination stage (phase III).

In terms of the solution quality, the optimality gaps of all instances are smaller than 1%, ranging from 0.00% to 0.79%. The average value of all gaps is around 0.2%, which can be regarded as a very high-quality, near-optimal solution. Moreover, the algorithm completely closes the gap in two cases, and a total of 11 cases yield a very small gap, all below 0.1%. In these cases, the obtained solutions can be regarded as almost the true optimal ones. We also note that the pseudo gaps are very small in all cases. To be specific, 10 tested instances have zero pseudo gaps. Though this gap is calculated by pseudo upper and lower bounds, from the result, we can see that this gap effectively guides the search of the algorithm. In fact, as discussed, solving integer recourse problems can be very time-consuming, and we find that the time spent on phase III is quite long. If we compute exact upper and lower bounds at each iteration, it will take a very long time, making the efficiency greatly lower. The pseudo gap is an effective tool to guide the search since LP relaxation can be quickly solved.

3.4.3. Comparison with a classic robust optimization model

We further benchmark our DRO model with a classic robust optimization (RO) model that ignores the correlation to examine our modeling benefits. In some pandemic control studies, it is identified that policymakers are risk-averse to the variation of policy performances (Choi 2021). Hence, to simultaneously evaluate policy performance and performance stability, we adopt a mean-variance (MV) framework, which is well-established in logistics and supply chain risk analysis (Sun et al. 2020). Adapted to our problem setting, the MV metric is defined as follows.

Definition 3. Policy X is said to strongly MV-dominate policy Y if *i)* the mean utility of policy X is strictly larger than Y, and *ii)* the utility variance of policy X is strictly smaller than Y. Policy X is said to be MV-non-dominated by policy Y if it performs better in terms of either mean or variance.

Similar to our DRO model, the benchmark RO model also has a two-stage framework, where the second stage contains all possible deteriorating scenarios. However, we will not impose any correlation information. In particular, the ambiguity set P is dropped, and only the support set Ξ stays. We obtain

$$\textbf{[R-LM]:} \quad \max_{\boldsymbol{x}} \left\{ \rho \sum_{i,j\in[N]} \sum_{l\in[L]} u_{ij}^{l} x_{ij}^{l} + (1-\rho) \min_{\mathrm{S}\in\Xi} u(\boldsymbol{x},\mathrm{S}) \right\} \tag{3.47}$$

subject to constraints (3.10) to (3.17). The inner minimization problem can be converted to a maximization problem $\max\left\{\sigma : \sigma \le u(\boldsymbol{x},\mathrm{S}), \forall \mathrm{S} \in \Xi\right\}$, which can be combined with outer maximization. However, since the uncertainty set Ξ contains exponentially many elements, the resulting maximization problem has numerous constraints and cannot be explicitly formulated. This motivates us to find the tractable counterpart of R-LM as follows.

Lemma 3.4. *The robust optimization model R-LM admits the tractable counterpart:*

$$\textbf{[R-LM-I]:} \ \max_{\boldsymbol{x}} \left\{ \rho \sum_{i,j \in [N]} \sum_{l \in [L]} u_{ij}^l x_{ij}^l + (1-\rho) u\left(\boldsymbol{x}, \chi^0\right) \right\} \tag{3.48}$$

subject to constraints (3.10) to (3.17), where χ^0 *is the scenario constructed in Proposition 3.2.*

Denote by $\boldsymbol{x}_{\mathrm{DRO}}$ and $\boldsymbol{x}_{\mathrm{RO}}$ the optimal master solutions to DR-LM-II and R-LM-I, respectively. We evaluate the policy performance of $\boldsymbol{x}_{\mathrm{DRO}}$ and $\boldsymbol{x}_{\mathrm{RO}}$ in simulated deteriorating scenarios. Again, the tests are conducted on different network sizes and performance foci ρ. **Table 3.3** shows all results. First, regarding the policy performance, the fourth and fifth columns display the mean utility in all simulated scenarios. The DRO policies consistently yield higher utilities, and the increases vary from USD 1,186 to USD 4,591,860 (shown in Column Mean-Diff). Remarkably, the maximum increase is up to USD 6 million, and the increases in three instances are over USD 1 million. Even for small networks (e.g., 30 cities), the DRO policy still achieves an increase of over USD 10,000. On the contrary, the classic RO model produces conservative policies, and performs poorly in utilities. The reasoning behind is that only one critical scenario in Ξ truly affects the RO model, whereas our DRO model captures a series of critical scenarios in Ξ. As a remark, we note that some small networks yield higher utilities than large networks. Since network nodes are randomly selected from the 125 candidate cities, when a small network contains many huge population cities, it can yield a higher utility than a large network with fewer populations.

Table 3.3. Comparison of DRO and RO policies in different pandemic deteriorating scenarios.

	N	M	Mean-DRO (10^3)	Mean-RO (10^3)	Mean-Diff	Variance-Diff (10^6)	MV-Dominance
RHO-0.2	30	500	225,699	225,686	12,564	-82,185	Strongly Dominant
	40	1000	356,802	356,800	1,186	-254	Strongly Dominant
	50	1500	665,370	663,353	2,015,571	107,720	Non-Dominated
	60	2000	966,987	966,985	1,442	-72,142	Strongly Dominant
	70	2500	1474,526	1474,518	7,133	-127,909	Strongly Dominant
	90	3500	2595,337	259,074	4,591,860	579,677	Non-Dominated
RHO-0.5	30	500	216,368	216,355	11,714	21,259	Non-Dominated
	40	1000	435,909	435,902	6,772	545,850	Non-Dominated
	50	1500	600,965	600,957	6,983	-291,401	Strongly Dominant
	60	2000	1259,035	1259,031	3,727	115,805	Non-Dominated
	70	2500	1195,996	1195,976	18,786	615,306	Non-Dominated
	90	3500	2052,332	2052,327	3,926	-274,468	Strongly Dominant
RHO-0.8	30	500	208,698	208,685	12,581	-152,210	Strongly Dominant
	40	1000	425,859	425,849	8,829	659,674	Non-Dominated
	50	1500	8636,269	863,618	7,357	256,825	Non-Dominated
	60	2000	1404,056	1404,050	5,491	88,825	Non-Dominated
	70	2500	1073,754	1073,517	235,765	-1838,181	Strongly Dominant
	90	3500	2167,025	2167,022	2,689	-236	Strongly Dominant

Notes. RHO: preference weight; N: number of cities; M: number of simulated deteriorations; Mean-DRO/RO ($): mean utility of all simulated deteriorations under DRO/RO restriction policy; Mean-Diff ($): Mean-DRO minus Mean-RO; Variance-Diff: the variance of the utility under DRO restriction policy minus that under RO policy.

We proceed to the risk hedging abilities of the two policies. In the MV metric, the magnitude of risk is reflected by the variance, and hence, a more robust policy should admit a smaller variance of the utility. The difference in utility variances of the two policies is reported in Column Variance-Diff. The cases where DRO policy yields smaller variance have negative difference values, suggesting that DRO policy better matches policymakers' risk aversion. Remarkably, we find that half of the cases show that the DRO policy is better regarding the risk state. Furthermore, all these cases show that the DRO policy also gives a higher mean utility. By Definition 3, the DRO policy strongly "MV dominates" the RO policy in these cases. Even in the remaining half of the instances, where the DRO policy's variance is higher, since they consistently produce higher utilities, the DRO policy is said to be "MV non-dominated" by the RO policy. Since DRO policies always win in terms of at least one criterion, the DRO policy is thus considered to "MV weakly dominate" the RO policy by Definition 3.

3.4.4. Major experimental findings

The computational results give the following three major findings:

Computational Efficiency. Our BD algorithm can find optimal or near-optimal solutions to various-scale problems in a very efficient manner. Regardless of network sizes, the BD can find almost optimal solutions (with an optimality gap below 1%) within about one hour, which is quick and reasonable for real-world applications. Policymakers can thus periodically update TRPs (e.g., daily) to involve updated pandemic information and make the policy more adaptive.

Performance Robustness. Modeling the correlation features greatly enhances containment performance and meanwhile, maintaining relatively low performance variation. Compared with an RO model without considering this feature, the additional utility brought by our DRO model can be up to USD 6 million, which creates appealing economic rewards.

Model Scalability. Our model can also be used in innercity travel restriction problems, such as activities among urban communities (Birge et al. 2022). In addition, policymakers are advised to exercise caution when putting foci on improving the current pandemic control performance or hedging potential deterioration, since different foci could yield very different restriction policies.

3.5. Societal Impacts and Policy Insights

To examine the societal impacts of TRPs and derive managerial insights for policymakers, we conduct a case study of the COVID-19 outbreak in Guangdong province, China, in early 2020 using publicly available economic and pandemic data. Migration and infection data were collected by combining official municipal yearbooks for total visitor volumes with the Baidu Migration Database to determine intercity flow ratios, which were then averaged over a four-week period to estimate specific city-to-city movements during the early outbreak.

We evaluate the policy impacts on society and individuals from the view of the tourism sector (including hospitality and catering) because TRPs directly reduce the number of intercity travelers and related economic activities. In addition, the official tourism data of all Guangdong cities (e.g., travelers, tourism employment) before and after the pandemic is open online, making our analysis more realistic. To save space, we put our preliminary analysis of the case study in **Appendix.A.I.2**. Its first five parts respectively focus *i)* establishing intercity migration network in Guangdong during the early outbreak, *ii)* quantifying the policy cost suffered by the tourism sector (i.e., economic loss), *iii)* quantifying the policy cost suffered by tourism professionals (i.e., salary loss and unemployment), *iv)* quantifying the pandemic control performance of TRPs through infections reduced or lives saved by decreasing migration flows, and *v)* how to implement TRPs in the real world and estimate policy budgets based on practices in Hong Kong. Next, we will derive managerial insights for policymakers from four perspectives: *i)* policy targeting, *ii)* policy budget efficiency, and *iii)* utilization of reusable resources.

3.5.1. Performance benchmark: Targeted vs. Uniform

In the real world, TRPs depend on the risk state of inbound travelers' origin cities. For example, Hong Kong classified inbound travelers into four groups according to their origins, each of which corresponds to a certain quarantine policy (see **Table h**). China also adopted such origin-based TRPs from 2020 to 2022 (China Government, 2022). All destination cities must adopt the origin-based TRPs and cannot relax according to local conditions. This implies that the TRPs imposed on all outflows from a particular city are identical, regardless of flow destinations. Hence, we refer to such policies as a uniform TRP. In contrast, our TRPs consider not only the origin city risk state but also the destination city policy budget and healthcare resources. The outflows from a particular city can be different, depending on flow destinations. We thus call our policy a targeted TRP. We will compare the infections reduced and the lives saved by the two policies.

To begin, we randomly generate the initial risk states of 21 Guangdong cities. Note that once the initial risk states are given, possible deteriorating scenarios are also specified. In addition, our infection and death model and policy budget model are well defined in terms of risk states. This means that the policymaker only needs to input the initial risk states into our model and then can get the desired TRPs. The city risk states in six initial outbreak scenarios are presented in **Table A3.9**.

We can obtain the uniform TRPs by adding the constraints that force all outflows from city i to get the same TRPs: $x_{ij}^{l} = x_{ik}^{l}, \forall j \neq k \in [N] \setminus \{i\}$. **Table 3.4** reports infections reduced and lives saved by the two policies, where Row T vs. U is the quotient of infections reduced or lives saved by the two policies. Apparently, the pandemic control performance of targeted TRPs greatly outperforms uniform TRPs. In the best case, targeted TRPs reduce imported infections nearly five times as much as uniform TRPs. Even in the worst case, it reduces infections by more than twice as much as uniform TRPs. Similarly, targeted TRPs save 2.6 times to 4.3 times more lives as much as uniform TRPs. The average quotient of infections reduced is 366%, and that of lives saved is 361%, both very high.

Table 3.4. Performance benchmark: Infections reduced/Lives saved by targeted and uniform TRPs.

		Scenario 1	Scenario 2	Scenario 3	Scenario 4	Scenario 5	Scenario 6
Infections Reduced	**Targeted**	7422	8374	8521	8556	8768	16323
	Uniform	1898	1704	3295	2579	2084	5352
	T vs. U	391%	491%	259%	332%	421%	305%
Lives Saved	**Targeted**	552	564	593	574	573	776
	Uniform	143	131	190	159	140	288
	T vs. U	386%	431%	312%	361%	409%	269%

To uncover the situation where targeted TRPs exhibit significantly better pandemic control performance, we dive deep into scenarios whose indicators "T vs. U" are above the average level. Interestingly, for both infections reduced and lives saved, these scenarios are Scenarios 1, 5, and 2 (ranking in increasing order of the indicator value). We note that Scenarios 1 and 2 respectively have two and three cities being at medium risk state, whereas all the other cities are at no risk state. These two scenarios capture the very early outbreak of an infectious disease since the disease only appears in a few cities. We further analyze Scenario 5. It has two cities being medium-risk, four cities being low-risk, and the other cities being no-risk. Scenario 5 captures the disease spread stage after Scenarios 1 and 2, which still belongs to the early outbreak since only 28.5% of cities in Guangdong province face pandemics, and most of them are at low-risk states. These observations imply that targeted TRPs significantly outperform uniform TRPs at the early outbreak of infectious diseases. To verify our inference, we further analyze Scenario 6, which admits the worst "T vs. U" in terms of lives saved and last second worst "T vs. U" in terms of infections reduced. In Scenario 6, eight cities are at medium risk state, and 13 cities are at low-risk state, implying that the disease has spread across the entire Guangdong province. In this case, while targeted TRPs still outperform uniform TRPs, the performance difference is less significant than in the early outbreak. Therefore, policymakers are strongly suggested to impose targeted TRPs as early as possible. Our findings are summarized as follows.

Policy Insight 3.1. *The pandemic control performance (regarding infections reduced or lives saved) of targeted TRPs is several times greater than that of uniform TRPs (2.5 to 4.9 times). The performance* *difference is especially significant at the early outbreak of infectious diseases, and hence policymakers are suggested to impose targeted TRPs as early as possible if large-scale disease spread is anticipated.*

We proceed to analyze the impact of pandemic control objectives (i.e., reducing infections or saving lives) on policy details. To present the policy details in a concise way, we adopt the average restriction levels on the outflows from a particular city imposed by all the other 20 cities. Specifically, let L_{ij} be the restriction level imposed by city j on the outflow from city i. Then, the average restriction level on all outflows from city i is $\frac{1}{20}\sum_{j\in[21]\setminus\{i\}} L_{ij}$. **Table A3.9** and **Table A3.10** report such average restriction levels with the objective of reducing infections or saving lives. We find that targeted TRPs yield significantly different policy details (i.e., travel restriction levels) under the two objectives in all six scenarios. On the contrary, uniform TRPs produce very similar policy details, and the policies in Scenarios 3, 4, and 5 are even identical under the two objectives. To present these observations, we compute the absolute difference between the average restriction levels on outflows from a city under the two objectives, which is displayed in **Table 3.5**. In all six scenarios, the absolute differences of targeted TRPs are positive, all greater than uniform TRPs. Moreover, the absolute differences of uniform TRPs are zero in Scenarios 3, 4, and 5. We thus derive the following insight.

Policy Insight 3.2. *Uniform TRPs are insensitive to pandemic control objectives, which can yield identical policy details (i.e., travel restriction levels) regardless of whether the aim is to reduce infections or save lives. In contrast, targeted TRPs are sensitive and produce distinct policy details under the two objectives, which respond to policymakers' requirements in a more accurate manner.*

Table 3.5. Sum of city-wise absolute differences of average outflow restriction levels

Targeted TRPs / Uniform TRPs					
Scenario 1	**Scenario 2**	**Scenario 3**	**Scenario 4**	**Scenario 5**	**Scenario 6**
3.617 / 2	4.429 / 2	2.333 / 0	4.048 / 0	3.571 / 0	3.143 / 2

3.5.2. Policy budget efficiency

In our case study, the 21 Guangdong cities' policy budgets are inferred based on similar data of Hong Kong (i.e., the ratio of anti-epidemic funds to the GDP in 2021) (see **Table A3.12**). The policy budgets reflect how much the policymaker is willing to pay for its TRPs, mainly regarding economic losses. We next examine the efficiency of policy budgets, in terms of pandemic control performance. Let the policy budget derived from Hong Kong be the base budget. We scale the base budget by different times {1,2,3,4,5,10}, and **Figure 3.4** plots the results, where Budget X1 denotes the base budget. The vertical axis presents the ratio of infections reduced by a certain scaled budget to that by the base budget. Note that the results of Budgets X6 to X9 are obtained by curve fitting.

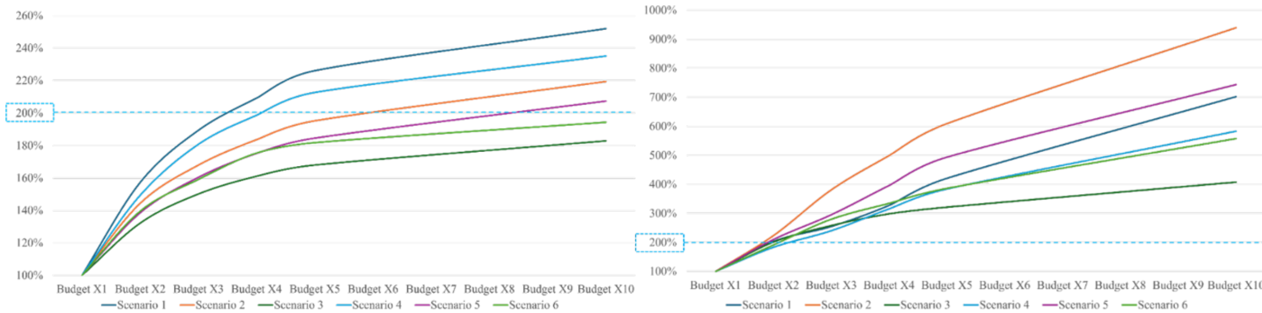

Figure 3.4. The ratios of infections reduced by scaled budgets to that by the base budget (Left: Targeted TRPs; Right: Uniform TRPs).

We find that the performance ratio of targeted TRPs exhibits a concave shape with respect to budget changes. To be specific, let the performance ratio under the base budget (i.e., Budget X1) be 100%. When the budget is doubled, the performance ratios of all six scenarios get obvious increases, varying from 120% to 170%. However, after more budgets are available, the ratio increase becomes slower and slower. When the budget gets ten times (i.e., Budget X10), the minimum ratio is around 180% while the maximum ratio is less than 260%. From a converse perspective, this means that targeted TRPs can achieve most of the pandemic control performance of ten times the base budget with the base budget. Specifically, in the best case (i.e., Scenario 3), Budget X1 achieves over 55% performance of Budget X10. Even in the worst case (i.e., Scenario 1), Budget X1 achieves nearly 40% performance of Budget X10. Regarding uniform TRPs, we note that the performance ratios increase significantly when more budgets are available. For example, in Budget X10, the performance ratio of Scenario 2 is nearly 1000%, which is almost identical to the budget change. Also, in Budget X2, almost each of the six scenarios exhibits a performance ratio of around 200%. The performance ratios of uniform TRPs with respect to budgets are nearly linear in all six scenarios. We thus draw the following.

Policy Insight 3.3. *The performance ratio of targeted TRPs is nearly concave with respect to policy budgets, whereas that of uniform TRPs is nearly linear in budgets. This implies that decreasing the budget of targeted TRPs has much less impact on the pandemic control performance than uniform TRPs. From another perspective, targeted TRPs could achieve most of the pandemic control objective with less budget. Therefore, policymakers with limited budgets are especially recommended to adopt targeted TRPs, thanks to their high budget efficiency.*

We proceed to benchmark the pandemic control performances of the two policies when budgets vary. The vertical axis of **Figure 3.5** reports the ratio of infections reduced by targeted TRPs to that of uniform TRPs. Expectedly, in all six scenarios and all budgets, the ratio is over 100%. However, the performance differences decay when more budgets are available. To be specific, in Budget X10, the performance ratios of the six scenarios range from 100% to 150%. In fact, after Budget X5, the performance ratios are always less than 200%. In contrast, in Budget X1, the maximum ratio is near 500% and the minimum ratio is also over 250%, both very significant. These observations motivate the following insight.

Policy Insight 3.4. *While the pandemic control performance of targeted TRPs is always better than uniform TRPs, the performance difference is especially significant when available policy budgets are limited. This emphasizes the finding that targeted TRPs are especially perfect for policymakers with limited budgets.*

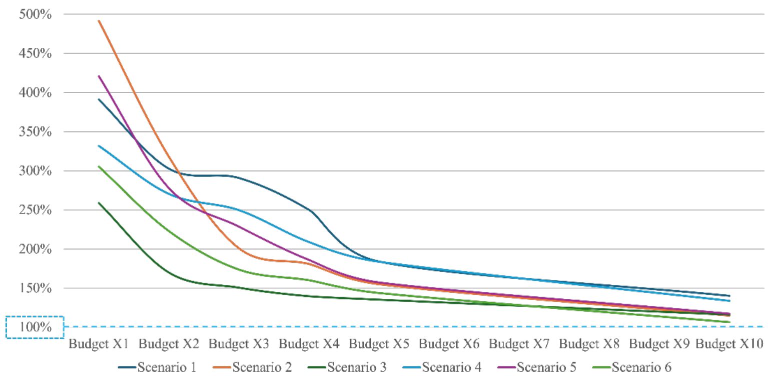

Figure 3.5. The quotients of infections reduced by targeted TRPs and uniform TRPs.

3.5.3. Reuse efficiency of anti-epidemic resources

During pandemics, many resources are reusable. For example, mobile cabin hospitals, facilities at hotels requisitioned by the government for quarantine, thermometers, Cu-Mask (a reusable mask invented by Hong Kong Research Institute of Textiles and Apparel), and training for epidemic prevention workers. When policymakers plan to strengthen TRPs in deteriorating scenarios, these resources can be reused and save a lot of expenses. In our case study, the value of reusable materials is considered to account for 5% of the anti-epidemic investment at the current outbreak. The reuse efficiency ratio (i.e., 5%) partially reflects the governance ability of policymakers when implementing their policies. A more efficient policymaker should be able to make better use of their anti-epidemic materials. Hence, to model different reuse efficiencies, we scale the base reuse ratio by {1,2,3,4,5,10} under the six initial outbreak scenarios to analyze how policy details are affected. Before analyzing experimental results, we present the economic structures of 21 Guangdong cities (see **Table A3.11**).

We note that the tourism sector plays distinct roles in different cities' economies. For example, tourism revenue accounts for only 4.46% of Foshan's GDP, whereas accounting for 46.45% of Meizhou's GDP. The standard deviation of the ratio of tourism revenue to the local economy in 21 cities is up to 12.11%, emphasizing that 21 cities have distinct economic structures. Recall that the policy budgets of all 21 cities are estimated to be a certain ratio to city GDPs (see **Tagle A3.12**). In this case, some cities could get sufficient budgets to decrease inflows (e.g., Foshan), whereas some cities could not limit enough inflows to contain pandemics under the limited budgets (e.g., Meizhou). It is thus expected that pandemic control performances of the 21 cities differ significantly, and the impacts of reuse efficiencies on different cities' performances are also distinct. However, the experimental results imply counter-intuitive findings.

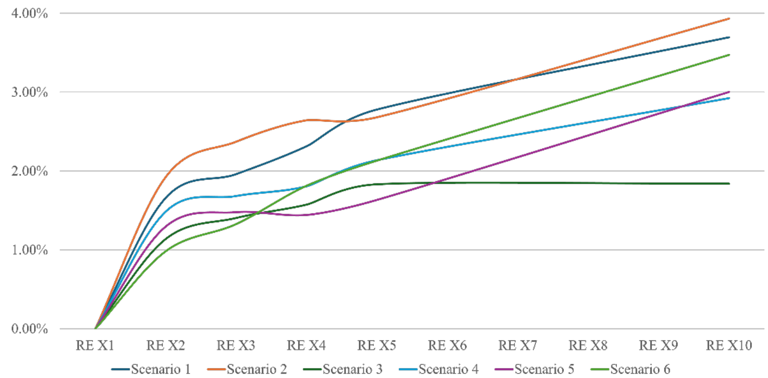

Figure 3.6. Standard deviations of 21 cities' improvements in infections reduced (in percentage).

First, we compute the improvement ratio of pandemic control performance (i.e., infections reduced) when the reuse efficiency ratio rises compared with the base ratio (i.e., 5%). Then, we plot the standard deviation change of the 21 cities' improvement ratios in **Figure 3.6**, where RE X1 denotes the base ratio. Note that standard deviations in all six scenarios in RE X1 are 0% since RE X1 is the base benchmark. From X1 to X2, while the standard deviations of all six scenarios increase significantly, their absolute values are very small (less than 2%). Thereafter, the standard deviations increase very slowly even when RE increases greatly (less than 4% under RE X10). Moreover, differences in the standard deviations of all six scenarios are not obvious. For example, in RE X2, the maximum standard deviation is 1.93% (Scenario 2) and the minimum one is 0.98% (Scenario 6). Under RE X10, where the differences are the most obvious, the maximum one is 3.93% (Scenario 2) and the minimum one is 1.84% (Scenario 3). These observations imply that the pandemic performance variation of the 21 cities remains moderate even when reuse efficiency changes significantly. We thus draw the following insight.

Policy Insight 3.5. *When all cities devote an identical percentage of their GDP to imposing TRPs, this appears unfair for cities whose economies depend highly on tourism since they are not granted enough budgets to decrease inflows. In this case, if policymakers' reuse efficiencies of anti-epidemic materials change, the pandemic control performances of different cities are thus expected to vary significantly. Interestingly, targeted TRPs make the variation of pandemic control performance of all cities remain moderate (less than 4%) even when the reuse efficiency substantially changes. In other words, our targeted TRPs can indirectly mitigate the unfairness in policy budget allocation.*

3.6. Summary of this Chapter

3.6.1. Concluding remarks

This chapter aims to determine targeted intercity TRPs to proactively hedge against potential pandemic deteriorating scenarios. In addition, this problem captures a critical feature of pandemics (i.e., the correlation of disease spread). Since the correlation of spread is hard to precisely forecast, we adopt DRO techniques to model the ambiguous correlation. The resulting DRO model is a huge-scale mixed integer nonlinear program, which is computationally intractable. Utilizing the submodularity of the recourse problem, we derive the worst-case distribution in closed form and reduce the original model to a much smaller integer linear program. To solve large-scale problems in the real world, we design a tailored Benders decomposition algorithm. The algorithm first reformulates the model in a tighter form and uses a special connection between master and recourse variables arising in the reformulation to develop a special optimality cut. We prove that the new cut is stronger than the classic Benders optimality cuts and thus can enhance convergence. To further accelerate the convergence, we make a rounding rule of fractional variables to generate initial feasible solutions and initial cuts. Then, we demonstrate the algorithm efficiency on various scale intercity networks of China and show modeling benefits, compared with a classic RO model ignoring the correlation.

Last, we conduct a societal impact study using real pandemic and economic data of Guangdong province and derive various policy insights. In particular, we show that our proposed policies can yield two to almost five times the pandemic control performance (in terms of infection reduced and human lives saved) compared to a uniform travel restriction policy adopted in practice. Moreover, we reveal that the performance dominance of our policies is especially significant (over triple) in the early stage of a disease outbreak or when limited policy budgets are allowed. Some important managerial insights are generated and recommendations, especially to the policymakers, are proposed.

3.6.2. Managerial implications and actionable recommendations

Managerial insights

1. Superior efficiency: Targeted *Travel Restriction Policies* (TRPs) could outperform the uniform policy by 2.5 to 4.9 times in reducing infections or saving lives.
2. High sensitivity: Targeted TRPs allow for higher precision; unlike uniform policies that remain stagnant, they adapt specifically to whether the objective is health-based (lives saved) or transmission-based (infections reduced).
3. Budget resilience: Targeted TRPs exhibit a concave performance curve, meaning they maintain high efficacy even with limited funding. In contrast, uniform policies lose effectiveness linearly as budgets decrease.

4. Equity & stability: Targeted TRPs indirectly mitigate budget unfairness for tourism-dependent cities and remain stable even when material reuse efficiency fluctuates.

Actionable recommendations

1. Prioritize early intervention: Policy makers should deploy targeted TRPs at the earliest stage of an outbreak to maximize the high performance-gap over uniform measures.
2. Optimize for limited budgets: If resources are scarce, policy makers should avoid uniform cuts; instead, they should shift entirely to targeted TRPs to achieve the majority of control objectives at a lower cost.
3. Define clear objectives: It is crucially important to explicitly define the primary goal (reducing cases vs. saving lives), as targeted models can be precisely calibrated to deliver these distinct outcomes.
4. Promote regional equity: Policy makers should note that using targeted allocations could protect economically vulnerable cities (e.g., those reliant on tourism) from disproportionate pandemic impacts.

3.6.3. An illustrative concrete example of how a policymaker would use the model

Take the Guangdong Provincial Government as an example. It would act as a central coordinator to integrate decentralized data into a robust, targeted strategy. Here are steps to proceed:

Step 1: Local data collection (City level)

Each of the 21 municipal governments (e.g., Guangzhou, Shenzhen, Foshan) is responsible for providing local parameters:

- Marginal distribution estimation: Local health bureaus should estimate the marginal distribution of potential infections within their city based on local hospital capacity and current case counts.
- Budgetary constraints: Each city reports its available budget for enforcing restrictions, such as personnel for checkpoints, monitoring systems, and local quarantine facilities.

Step 2: Central data integration (Provincial level)

The Guangdong Provincial Government aggregates this local information:

- Migration flow estimation: Using data from the Baidu Migration Database and historical yearbooks (as detailed in your study), the provincial government could estimate the flow volume between cities.
- Correlation modeling: The provincial government could use the Distributionally Robust Optimization (DRO) framework to model the ambiguous correlation of disease spread, identifying how an outbreak in a hub like Guangzhou is likely to ripple through the Pearl River Delta network.

Step 3: Optimization and policy execution

The province runs the model using the weighted objectives (0.6 for the current outbreak and 0.4 for potential deterioration):

- Generating targeted mandates: Instead of a blanket lockdown, the model generates specific restriction levels for each city-to-city pair. For example, it may suggest a 70% restriction on travel from Shenzhen to Dongguan but only a 20% restriction from Zhaoqing to Qingyuan.
- Resource allocation: The provincial government can then redistribute anti-epidemic materials to cities where the model identifies the highest marginal utility for infection reduction, ensuring that cities with high tourism dependence or limited budgets are not unfairly penalized.

Chapter 4. Service Operations under Economic Downturns: Service Downgrading Strategies

4.1. Problem Statement

The review in **Chapter 2** uncovers that while prior studies have focused on service upgrades or pricing competition (e.g., Chiu et al. 2014), several critical research gaps exist. First, no work has addressed service downgrading as a deliberate operational tactic to reduce costs. Second, the interplay between service strategies and loyalty programs has been largely overlooked. For instance, studies like Kim et al. (2001) and Singh et al. (2008) examined the competitive effects of loyalty programs but did not consider their joint implementation with service strategies. Others like Chun et al. (2020) addressed financial aspects but not as compensation for service cuts. Thus, the analytical study in **Chapter 4** aims to bridge these gaps by developing a competitive model that analyzes the joint decision of implementing SDS and designing an associated loyalty program, offering novel insights into balancing cost efficiency with customer retention in a contested market. The detailed background of the problem studied in this chapter is as follows.

4.1.1. Research background

The world is facing a major economic downturn, and the competition in the service industry has become increasingly fierce (Hsieh and Rossi-Hansberg, 2023; Lim, 2023). Service companies bear significant challenges in maintaining profitability, which entices them to make changes (Chan et al. 2019, Secchi et al. 2019, Hu et al. 2022). In particular, we observe an emerging practice in which companies downgrade (or even cancel) previously provided services to cut operating costs. For example, many airlines have reduced the variety of beverages and food that can be selected, or even canceled free air meals. Similarly, some hospitality companies have reduced the quality of their breakfast or even canceled free breakfasts. For instance, *Hilton* has removed free breakfast in some US places but provides a certain amount of free dining credits as compensation. We term this emerging practice the *Service Downgrade Strategy* (SDS). SDS has been proven to help service companies save operating costs effectively. For example, *Hilton* reports a cost saving of USD 10 per guest by downgrading food services. Some more SDS examples are shown in **Table 4.1**.

While SDS can help save costs, the downgraded services would inevitably impair customer experience. For example, although many passengers complain about the poor taste of air meals, when some airlines removed free air meals, such actions immediately incurred wide criticism, which damages airlines' image and long-term development. Without effective compensation actions, SDS could lead to demand shrinkages, thereby harming sustainable profitability (Koklic et al. 2017).

Table 4.1. Examples of SDS in the real world.

Companies	Downgraded services
United Airlines	Cancel free air meals for flights within North America.
Jet Airways	Cancel free meals for domestic flights in India.
Air China	Replace snack and drink packages with a bottle of water on short flights.
Southeast Airlines, Air Canada, EasyJet	Charge passengers extra luggage fees.
Marriott	Reducing breakfast quality and downgrading room decoration.
Hyatt Place	Cancel free breakfast in some US places.
Hilton	Cancel free breakfast in some places, but offer dining allowance instead.

To address the above issue, loyalty programs, which have been extensively applied in the service industry, appear to be a promising solution (Singh et al. 2008, Gopalakrishnan et al. 2021). Loyalty programs grant customers "points" as rewards, a kind of token that can be redeemed for souvenirs, free rooms, flight tickets, class upgrades, and other perks. Many giant service companies (e.g., *Hilton*, *Hyatt*, *Cathay Pacific*, and *American Airlines*) operate tailored loyalty programs due to various advantages (Chun and Ovchinnikov 2019, Chun et al. 2020). First, it directly incentivizes re-purchases by encouraging customers to accumulate points to redeem for services or products, which helps cultivate brand loyalty. Second, consumers may find the flexibility to choose the types of services or products to redeem attractive, as they can make selections that align with their preferences and redeem them at their convenience, which also fosters consumer loyalty and satisfaction. Third, companies can provide/acquire the services or products to be redeemed with lower costs or flexibly amend the types of services or products that can be redeemed to realize high cost-efficiency and operational flexibility.

In fact, as we observed in practice, some service companies have adopted loyalty programs as compensation for SDS. For example, *Southern Airlines,* the third largest airline in China, has initiated "Green Fly Program" on short-distance flights. In the program, passengers will receive around 300 flight miles if opting out of air meals. The miles can be redeemed for free tickets, class upgrades, or VIP lounges. The program has helped save over 430,000 meals in 2020, saving around RMB 7.76 million by issuing 120 million miles. The costs of miles (e.g., cost of free tickets, class upgrades, or VIP lounges) are generally much lower than full air meal services. For example, *Southern Airlines*' average cost of an air meal in economy cabins was RMB 26.15 in 2019, while a mile costs only around RMB 0.05. Another example is the *H-World Group*, the second-largest hotel brand in China. Previously, it provided members with room fare discounts. But now, instead of directly granting a fare discount, the fare discounts are transferred into points, being rewarded to customers who pay full fares. They can deduct room charges or purchase hotel products such as pillows and perfume with "cheaper" prices than paying with cash. It is reported that the strategy has received wide popularity, especially among frequent travelers and young customers. However, investing in loyalty programs incurs additional costs, which may contradict the mission to strengthen profitability. Balancing loyalty program cost and customer satisfaction is thus vital. Unfortunately, despite the growing popularity in practice, the analytical study on SDS adoption and associated loyalty program design remains under-explored in the operations literature.

When a company intends to introduce an innovative strategy like SDS, it plays the role of a "leader" that changes the original market status. In a competitive environment, its competitor may follow to adopt SDS or not, subject to its own profit considerations, who reacts as a "follower". The existence of competition makes the payoff of SDS to a company not standalone but also affected by the rival's reaction. Therefore, SDS may exhibit distinct impacts on both the leader and the follower. For example, *Qantas Airlines* revamped its loyalty program in 2020, adding flexible rewards like wine tastings and cooking classes, while its major competitor, Virgin Australia, reduced perks because of financial restructuring. Post-launch, *Qantas* saw a membership surge, while *Virgin Australia* reported a decline in loyalty enrollments. In the US ride-hailing duopoly, *Uber* introduced "Uber One" in 2021, offering discounts and priority support for a monthly fee, while *Lyft*'s "Lyft Pink" lacked comparable benefits. Within a year, *Uber* gained a 3% market size increment, while *Lyft*'s ridership dropped. These instances underscore the significance of anticipating competitors' reaction before deciding whether to move forward with SDS. Understanding this dynamic is vital to making better business decisions in a competitive environment.

4.1.2. Research questions and major findings

Motivated by the real-world practice of SDS, this study aims to explore: i) The SDS adoption strategy (i.e., whether to adopt SDS or not), and ii) the associated loyalty program design (i.e., investment) of two service companies in a competitive environment. The following research questions are proposed:

1. Under competition, when is it wise to adopt SDS, and how to invest in loyalty programs optimally?
2. What are the key factors that can drive a company's SDS adoption?
3. Whether the findings derived from the above questions challenge the existing practices, and how do these findings help a service company stand out in competition?

We build formal Stackelberg service gaming models to answer these questions, and some findings are shown as follows.

1. **Critical role of SDS on equilibrium outcomes**. The equilibrium outcomes (i.e., both, one, or neither company adopts SDS) depend on the *expected post-SDS market sizes* (EPSMs) of the leader and the follower. By comparing their EPSMs with some identified thresholds, we can immediately get the equilibrium outcome (i.e., asymmetric adoption, win-win, or no adoption).
2. **SDS requires increased loyalty program investments to offset customer loss.** A company must invest more in loyalty programs when adopting SDS, even when its rival does nothing. This challenges the practice that some companies cut services but do nothing to loyalty programs or

even cut loyalty budgets simultaneously (e.g., *United Airlines* cut air meals without loyalty program boosts in 2020).

3. **Companies are more likely to adopt SDS after the economy rebounds.** The economic rebound helps alleviate market competition, and a low competition environment is found to drive service enhancement to differentiate a company against rivals (Banker et al. 1998, So 2000). However, our finding is just the opposite: A company in a less competitive environment is more likely to adopt SDS. This finding helps explain some real-world scenarios. For instance, *Air Canada* and *WestJet* reduced various services during the COVID-19 pandemic (e.g., cut free snacks in some flights) to save costs. The competition between them is relatively low as they dominate the domestic market, and some service downgrading measures have lasted until now, even when the pandemic has ended.
4. **Market power asymmetry shapes SDS outcomes**. The same operational efforts may have opposite effects on the leader and the follower. Specifically, a stronger cost-saving ability during SDS implementation will enhance the leader's competitive edge (i.e., strengthen the first-mover advantage). However, this is not the case for the follower because the unique situation in which the follower can benefit from SDS adoption (i.e., the win-win situation) will appear less.

4.2. Basic Model

Our basic model considers the service competition of two companies in terms of SDS adoption and loyalty program investments, which is formulated by a Stackelberg game model. We find that the change in the market size due to SDS plays as the key determinant of the two companies' equilibrium outcomes. We then derive the resulting equilibrium conditions in closed-form and conduct sensitivity analyses to uncover the impacts of critical model factors.

4.2.1. Model settings

We use a real-world example to introduce our problem settings. *Cathay Pacific* and *Hong Kong Airlines* are two dominant airlines in Hong Kong, which operate hundreds of flights from Hong Kong to the world every day. A flight commonly flown by the two airlines can be regarded as a service that is provided by two competing companies. The two airlines provide different flight experiences, entailing different operating costs, and their ticket prices thus also differ. This is a duopoly market where the two players provide similar (but not identical) services. Both *Cathay Pacific and Hong Kong Airlines are well-known full-service airlines, and provide various in-flight services (e.g., air meals and beverages*). However, the recession in recent years has severely impacted the Hong Kong aviation industry[6]. In this situation, if one airline plans

[6] https://www.aljazeera.com/economy/2024/6/21/once-the-pride-of-hong-kong-cathay-pacific-becomes-governments-punchbag/. Accessed 22 Jul 2025.

to implement SDS to survive, it must consider the impact of SDS on its market size together with the other airline's reaction. The question for an airline is hence: i) either to preemptively adopt SDS or ii) to maintain existing services. In the second option, if the rival implements SDS early, the airline must determine whether to follow to adopt SDS or not. The two airlines' final decisions will establish a new norm of aviation services.

Consider a duopoly market in which two companies $i \in \{1,2\}$ provide some services to customers. A company's base market size is denoted by a_i, which is the original market size without introducing SDS. Introducing SDS will decline the base market size due to service downgrading. We characterize the post-SDS market size by a random variable $\hat{a}_i + \tilde{\varepsilon}_i$. To be specific, the constant term $\hat{a}_i$ is EPSM, and $\tilde{\varepsilon}_i$ is random with zero mean and standard deviation δ_i, which captures the uncertainty of customers' reaction to service downgrading. Note that we have $\hat{a}_i + \tilde{\varepsilon}_i \le a_i$ almost surely. On the other hand, a company can invest in its loyalty program to maintain or boost its market so as to mitigate the byproduct of SDS. In particular, the investment and the resulting market size increment follow the well-known exponential cost function (Luo and Choi 2022, Xu et al. 2023), and the market size increment by investment v_i is $(\ln v_i)/\mu_i$, where $\mu_i > 0$ is an exogenously given parameter. Competition between the two companies is captured by $c \in [0,1]$. Note that the economic downturn leads to higher competition, reflected by a larger c [7].

To facilitate presentation, we denote by N and M the case in which a company adopts SDS or not, respectively. Then, a company's expected market size in each case is

$$D_{i,M} = a_i + (\ln v_i)/\mu_i - c(\ln v_{3-i})/\mu_{3-i}, \tag{4.1}$$

$$\tilde{D}_{i,N} = \hat{a}_i + \tilde{\varepsilon}_i + (\ln v_i)/\mu_i - c(\ln v_{3-i})/\mu_{3-i}. \tag{4.2}$$

The above demand functions are concave and increasing in loyalty program investment v_i, while decreasing in the rival company's investment v_{3-i}. The concavity reflects diminishing marginal returns of investments, aligning with real-world practices in the service industry[8,9].

We proceed to model the profit. We denote by ρ_i the marginal profit before introducing SDS, which is the net profit per customer (i.e., revenue minus operating cost per customer). Then, Company i's overall profit considering loyalty program investment in Case M is

$$\Pi_{i,M} = \rho_i D_{i,M} - v_i = \rho_i \left(a_i + (\ln v_i)/\mu_i - c(\ln v_{3-i})/\mu_{3-i}\right) - v_i. \tag{4.3}$$

---

7 https://www.wsj.com/business/airlines/airlines-warn-of-near-term-turbulence-as-recession-fears-loom-0e82fdc4/. Accessed 26 Jul 2025.

8 https://intpolicydigest.org/diminishing-returns-calculated-misery-in-air-travel/. Accessed 21 Jul 2025.

9 https://qedpost.substack.com/p/the-new-age-of-diminishing-returns?utm_campaign=post&utm_medium=web/. Accessed 21 Jul 2025.

Implementing SDS is considered to save a marginal operating cost m_i for Company i, which is the reduced operating cost per customer. In other words, the "marginal profit" in Case N will rise to $\rho_i + m_i$. We formulate Company i's expected profit considering loyalty program investment in Case N by

$$\Pi_{i,N} = \mathrm{E}\left[\left(\rho_i + m_i\right)\tilde{D}_{i,N} - v_i\right] = \left(\rho_i + m_i\right)\left(\hat{a}_i + \left(\ln v_i\right)/\mu_i - c\left(\ln v_{3-i}\right)/\mu_{3-i}\right) - v_i, \tag{4.4}$$

where E is the expectation operator. Note that service price is not considered as a decision variable in the above profit functions, which are based on real-world practices where many service companies have downgraded service quality yet without changing service prices (e.g., flight ticket prices)[10].

We then derive the optimal loyalty program investment in each case in closed-form as follows.

Lemma 4.1. A company's optimal loyalty program investment is $v_{i,N}^* = \left(\rho_i + m_i\right)/\mu_i$ when adopting SDS or $v_{i,M}^* = \rho_i/\mu_i$ when maintaining existing services.

From **Lemma 4.1**, we can see that imposing SDS always incurs a higher loyalty investment compared with the optimal investment without SDS. Since SDS will impair customer experience and lead to a decline in market size, enhancing loyalty programs works as compensation for the market size decrease. However, it is not always good to invest more; there is a unique optimal investment amount, and investing more or less than this amount will not attain the maximum compensation effect. This coincides with the finding by Gu et al. (2022) that investment amount in loyalty programs requires careful analysis.

In terms of the structural properties, the optimal investment amount is increasing in the profitability factor ρ_i or the cost-saving ability factor m_i, while is decreasing in the market sensitivity factor μ_i. Hence, higher profitability or cost-saving ability will make a company pay more (i.e., higher loyalty program investment), which supplements the argument by Nunes and Drèze (2006) that investment amount mainly depends on customer loyalty. In addition, if the market is sensitive to loyalty program enhancements (i.e., bigger μ_i), a company can pay less (i.e., lower investment) when implementing SDS.

4.2.2. Equilibrium analysis

We now analyze a company's decision to preemptively adopt SDS by a two-stage game. **Figure 4.1** displays a decision tree that illustrates the two companies' decision sequence. Without loss of generality, we index the leader (i.e., the one preemptively implementing SDS) by Company 1 and the follower by Company 2. The details of each stage are as follows. At the first stage, Company 1 determines whether to preemptively impose SDS or not, which leads to two branches in the tree. Then, at the second stage, given a particular decision by the leader, Company 2 determines whether to adopt SDS or not, which further leads to two branches. Consequently, the decision tree ends at four leaf nodes: (M,M), (M,N), (N,M), and (N,N),

[10] https://sailawaymagazine.com/cunards-latest-cut-room-service-downgrade-sparks-anger/. Accessed 25 Jul 2025.

where the first and the second elements in the bracket are the leader's and the follower's strategies, respectively. Then, anticipating the follower's reaction, Company 1 can employ well-established backward induction (Li et al. 2015) to uncover whether preemptively committing to SDS is beneficial or not. This gaming process is the well-known two-player Stackelberg game (Lee and Minner, 2024).

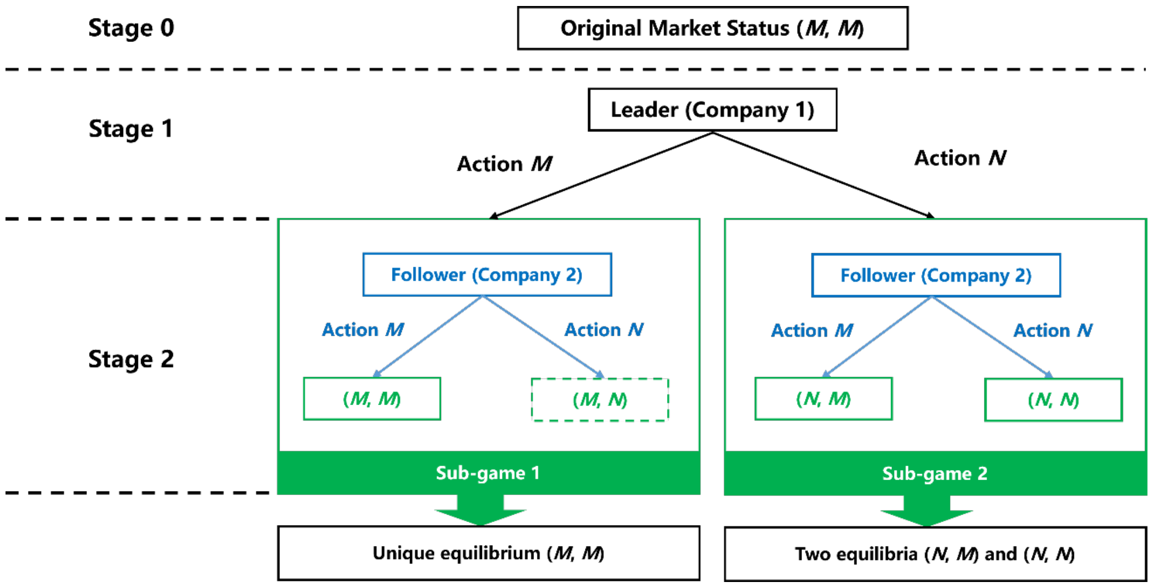

Figure 4.1. The Stackelberg game between the two competing service companies

We first analyze Sub-game 1 in which Company 1 does not preemptively adopt SDS. This situation implies that Company 1 does not intend to deviate from the original market status (M,M). As the leader makes no change to its services, it is expected that the follower will also make no change. In this case, the original market status will be maintained, and (M,M) is the resulting equilibrium outcome. However, theoretically, there exists another node (M,N) where the leader does not adopt SDS while the follower adopts SDS in Sub-game 1. In such a situation, it is Company 2 that preemptively imposes SDS and intends to deviate from the original market status. Therefore, Company 2 will be the true leader, while Company 1 becomes the follower. We can thus simplify the analysis by considering a unique equilibrium (M,M) in Sub-game 1 when the leader is given.

We next analyze Sub-game 2 in which Company 1 preemptively imposes SDS. Company 2 will also adopt SDS only when this action can bring a higher profit. With **Lemma 4.1**, we can readily derive Company 2's optimal loyalty program investment and (expected) profit at nodes (N,M) and (N,N). Since the equilibrium analysis uses the two companies' (expected) profits under different outcomes frequently, we report them and the corresponding optimal loyalty program investments in **Table 4.2** and **Table 4.3**.

Table 4.2. The leader's optimal loyalty program investment and (expected) profit in equilibrium

Outcome	Optimal investment	Optimal (expected) profit

(M,M)	$v^*_{1,(M,M)} = \frac{\rho_1}{\mu_1}$	$\Pi^*_{1,(M,M)} = \rho_1\left(a_1 + \frac{1}{\mu_1}\ln\frac{\rho_1}{\mu_1 e} - \frac{c}{\mu_2}\ln\frac{\rho_2}{\mu_2}\right)$
(N,M)	$v^*_{1,(N,M)} = \frac{\rho_1 + m_1}{\mu_1}$	$\Pi^*_{1,(N,M)} = (\rho_1 + m_1)\left(\hat{a}_1 + \frac{1}{\mu_1}\ln\frac{\rho_1 + m_1}{\mu_1 e} - \frac{c}{\mu_2}\ln\frac{\rho_2}{\mu_2}\right)$
(N,N)	$v^*_{1,(N,N)} = \frac{\rho_1 + m_1}{\mu_1}$	$\Pi^*_{1,(N,N)} = (\rho_1 + m_1)\left(\hat{a}_1 + \frac{1}{\mu_1}\ln\frac{\rho_1 + m_1}{\mu_1 e} - \frac{c}{\mu_2}\ln\frac{\rho_2 + m_2}{\mu_2}\right)$

Table 4.3. The follower's optimal loyalty program investment and (expected) profit in equilibrium

Outcome	Optimal investment	Optimal (expected) profit
(M,M)	$v^*_{2,(M,M)} = \frac{\rho_2}{\mu_2}$	$\Pi^*_{2,(M,M)} = \rho_2\left(a_2 + \frac{1}{\mu_2}\ln\frac{\rho_2}{\mu_2 e} - \frac{c}{\mu_1}\ln\frac{\rho_1}{\mu_1}\right)$
(N,M)	$v^*_{2,(N,M)} = \frac{\rho_2}{\mu_2}$	$\Pi^*_{2,(N,M)} = \rho_2\left(a_2 + \frac{1}{\mu_2}\ln\frac{\rho_2}{\mu_2 e} - \frac{c}{\mu_1}\ln\frac{\rho_1 + m_1}{\mu_1}\right)$
(N,N)	$v^*_{2,(N,N)} = \frac{\rho_2 + m_2}{\mu_2}$	$\Pi^*_{2,(N,N)} = (\rho_2 + m_2)\left(\hat{a}_2 + \frac{1}{\mu_2}\ln\frac{\rho_2 + m_2}{\mu_2 e} - \frac{c}{\mu_1}\ln\frac{\rho_1 + m_1}{\mu_1}\right)$

To ensure Company 2 can also benefit from SDS, we require $\Pi^*_{2,(N,N)} > \Pi^*_{2,(N,M)}$, resulting in an equilibrium outcome (N,N); in contrast, $\Pi^*_{2,(N,N)} \le \Pi^*_{2,(N,M)}$ suggests that SDS cannot improve Company 2's profit, leading to the equilibrium (N,M). Equality $\Pi^*_{2,(N,N)} = \Pi^*_{2,(N,M)}$ yields a critical market threshold in terms of Company 2's EPSM:

$$a_2^{\Delta} = \left(\rho_2 a_2 + \frac{\rho_2}{\mu_2}\ln\frac{\rho_2}{\rho_2 + m_2} + \frac{m_2}{\mu_2}\ln\frac{\mu_2 e}{\rho_2 + m_2} + \frac{cm_2}{\mu_1}\ln\frac{\rho_1 + m_1}{\mu_1}\right)\Big/(\rho_2 + m_2). \tag{4.5}$$

This vital threshold helps us establish the condition under which the follower will commit to SDS in equilibrium. We thus have **Proposition 4.1**.

Proposition 4.1. *In the proposed duopoly Stackelberg service game, the follower (i.e., Company 2) will adopt SDS only when its EPSM is larger than a threshold* a_2^{Δ}.

In this proposition, note that EPSM, as an exogenous factor, measures the market reaction to service downgrading. It directly affects the expected post-SDS profit, thereby affecting the follower's incentive to adopt SDS. This finding also points out the mixed results of SDS. While SDS can save operating costs, it will harm profitability if the market decline is significant (i.e., when $\hat{a}_2 < a_2^{\Delta}$), and the follower should not mimic the leader's strategy in this situation.

Proposition 4.1 helps the leader anticipate the follower's reactions. This enables the leader to derive the conditions under which preemptively adopting SDS is beneficial. In particular, when $\Pi^*_{1,(N,N)} > \Pi^*_{1,(M,M)}$ and $\Pi^*_{2,(N,N)} > \Pi^*_{2,(N,M)}$, Company 1 should preemptively implement SDS and the resulting equilibrium outcome is (N,N). In this symmetric equilibrium, both the leader and the follower can benefit from SDS, which is termed as a win-win situation in the literature (Shi et al. 2022). Equality $\Pi^*_{i,(N,N)} = \Pi^*_{i,(M,M)}$ indicates the critical market threshold in terms of Company 1's EPSM that corresponds to this situation:

$$a^{\Delta}_{1,(N,N)} = \left(\rho_1 a_1 + \frac{\rho_1}{\mu_1}\ln\frac{\rho_1}{\rho_1+m_1} + \frac{m_1}{\mu_1}\ln\frac{\mu_1 e}{\rho_1+m_1} + \frac{c\rho_1}{\mu_2}\ln\frac{\rho_2+m_2}{\rho_2} + \frac{cm_1}{\mu_2}\ln\frac{\rho_2+m_2}{\mu_2}\right)\Big/\left(\rho_1+m_1\right). \tag{4.6}$$

This threshold helps us derive the equilibrium condition for a win-win situation as follows.

Proposition 4.2 (a). *When the EPSMs of Company 1 and Company 2 satisfy $\hat{a}_1 > a^{\Delta}_{1,(N,N)}$ and $\hat{a}_2 > a^{\Delta}_2$ respectively, the leader should preemptively adopt SDS and in this case, the follower will also adopt SDS, resulting in a symmetric equilibrium (N,N).*

When $\Pi^*_{1,(N,M)} > \Pi^*_{1,(M,M)}$ and $\Pi^*_{2,(N,N)} \le \Pi^*_{2,(N,M)}$, Company 1 should also preemptively adopt SDS, whereas Company 2 should not follow since such action cannot bring a higher profit. This leads to an asymmetric equilibrium (N,M). The profit relation $\Pi^*_{1,(N,M)} = \Pi^*_{1,(M,M)}$ yields another market threshold in terms of Company 1's EPSM:

$$a^{\Delta}_{1,(N,M)} = \left(\rho_1 a_1 + \frac{\rho_1}{\mu_1}\ln\frac{\rho_1}{\rho_1+m_1} + \frac{m_1}{\mu_1}\ln\frac{\mu_1 e}{\rho_1+m_1} + \frac{cm_1}{\mu_2}\ln\frac{\rho_2}{\mu_2}\right)\Big/\left(\rho_1+m_1\right). \tag{4.7}$$

We report the equilibrium condition under which only the leader can benefit from SDS as follows.

Proposition 4.2 (b). *When the EPSMs of Company 1 and Company 2 fulfill $\hat{a}_1 > a^{\Delta}_{1,(N,M)}$ and $\hat{a}_2 \le a^{\Delta}_2$ respectively, the leader should preemptively adopt SDS but the follower will not adopt SDS, leading to an asymmetric equilibrium (N,M).*

This proposition uncovers the condition under which the leader admits the first-mover advantage, which is a vital result in the Stackelberg game. In this case, only the leader can benefit from SDS, whereas the follower cannot. In other words, a company can earn a higher profit by preemptively imposing SDS, whereas its rival cannot enhance profitability by SDS. This special equilibrium will happen when the follower's EPSM drops below a threshold while the leader's EPSM stays above a threshold. The implication for a manager is that if SDS only slightly decreases the market size, but significantly harms the rival's market size, she should preemptively impose SDS. For example, *Hong Kong Airlines* is more "economical" than *Cathay Pacific*, and its passengers are less sensitive to service downgrading than *Cathay Pacific*'s; in this situation, *Hong Kong Airlines* may preemptively adopt SDS to enjoy the first-mover advantage.

Last, we try to derive a geometric interpretation of the equilibrium outcomes, making the condition for each outcome clearer. We find that the identified market thresholds for the two companies' EPSMs satisfy the magnitude relation $a_1 > a^{\Delta}_{1,(N,N)} > a^{\Delta}_{1,(N,M)} > 0$ and $a_2 > a^{\Delta}_2 > 0$. With this finding, we qualitatively depict the equilibrium outcomes of the two companies in **Figure 4.2**. In particular, the market thresholds divide the space into several areas, each of which is associated with a certain equilibrium. With this interpretation, a company can immediately get the equilibrium outcome by means of quantifying its EPSM and estimating its rival's EPSM, thereby determining whether to preemptively adopt SDS or not.

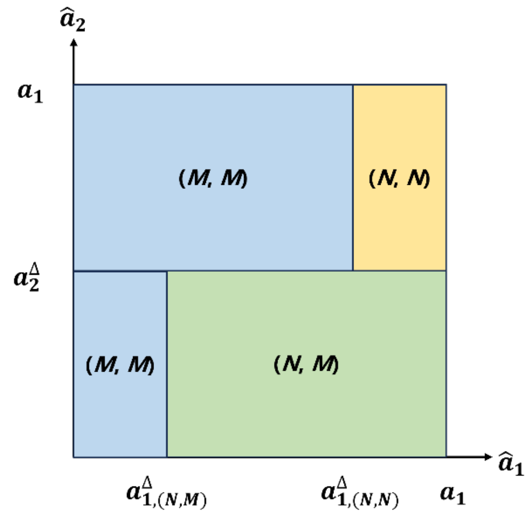

Figure 4.2. Equilibrium outcomes of the proposed duopoly Stackelberg service game (leader: Company 1, follower: Company 2).

4.2.3. Factors driving SDS adoption

In the equilibrium analysis, we find that customers' reaction to service downgrading, measured by EPSM, is the major determinant of equilibrium outcomes. In particular, the market thresholds parameterized by several market factors (e.g., base market size and competition level) establish several critical ranges. By checking the ranges to which the two companies' EPSMs belong, the resulting equilibrium outcome is clear. We now dive deep into the impact of these factors and derive insights for managers.

We begin with the market competition level, which is an exogenous factor. It captures the market environment and is generally not affected by a company's internal actions. As mentioned, the economic downturn in recent years has significantly intensified competition in the service industry, and SDS is an innovative strategy developed in this context. Our analysis reveals the situation in which SDS can enhance the profitability of leaders or both companies in a competitive environment. One may wonder whether SDS is still a valuable strategy when the economy rebounds in the future. The proposition below answers this question.

Proposition 4.3 (a). *When the competition level decreases, the leader's two market thresholds $a_{1,(N,M)}^{\Delta}$ and $a_{1,(N,N)}^{\Delta}$ will drop, and the follower's market threshold a_2^{Δ} will also decline. Meanwhile, $a_{1,(N,N)}^{\Delta}$ decreases faster than $a_{1,(N,M)}^{\Delta}$.*

Let us refer to the geometric interpretation of the equilibrium outcomes in **Figure 4.2**. The decrease of $a_{1,(N,N)}^{\Delta}$ and a_2^{Δ} will obviously expand the area corresponding to the equilibrium (N,N). Such a change means that the two companies will become more likely to reach a win-win situation compared to a market of higher competition. We thus obtain the following.

Finding 4.1. *While SDS was invented amid economic downturns, the two competing companies could both adopt SDS more likely when the economy rebounds, thereby reaching a new norm.*

Then, we focus on the base market sizes of the two service companies, which reflect their market power. Unlike the competition level, the base market size could be affected by a company's operations. We aim to derive insights for managers facing different market powers. See the following.

Proposition 4.3 (b). *When the leader controls a larger market size (i.e., bigger a_1), its two thresholds will increase, in particular, at the equal rate. For the follower, occupying a larger market (i.e., bigger a_2) will also increase its threshold a_2^{Δ}.*

If a_1 rises, the areas of a win-win situation (N,N) and a first-mover advantage situation (N,M) both shrink. It means that the leader becomes less inclined to adopt SDS if its market dominance is enhanced. For the follower, a larger a_2 will also reduce the area (N,N), making SDS less interested. We summarize the findings as follows.

Finding 4.2. *A weak market power (i.e., smaller market size) drives the follower to adopt SDS, whereas strong market power (i.e., larger market size) drives the leader to maintain its existing services.*

Now, we examine the marginal cost reduced by SDS, which reflects a company's operational effectiveness. In practice, the marginal cost saved by SDS depends on what services will be downgraded. In addition, it also relies on a company's operational efficiency; regarding the same services to be downgraded, a more efficient company is expected to save more. The related insights are reported as follows.

Proposition 4.3 (c). *If the leader can save more costs by SDS (i.e., larger m_1), the follower's market threshold a_2^{Δ} will increase. In contrast, if the follower saves more by SDS (i.e., larger m_2), the leader's threshold $a_{1,(N,M)}^{\Delta}$ remains unchanged but $a_{1,(N,N)}^{\Delta}$ will increase.*

This proposition uncovers how a company's operational efficiency affects its rival's strategy. To be specific, when the leader improves its operational efficiency (i.e., larger m_1), its rival will be discouraged from adopting SDS. The win-win situation (N,N) becomes less likely to happen, whereas the first-mover advantage situation (N,M) becomes more likely to happen. In contrast, even if the follower strengthens its cost-saving ability, the leader threshold associated with the first-mover advantage is not affected.

However, the leader's threshold related to the win-win situation will increase, making this situation less likely to form. We conclude the following findings.

Finding 4.3. *The leader can enhance its first-mover advantage by improving the cost-saving ability when implementing SDS. In contrast, the follower cannot weaken the leader's first-mover advantage by strengthening its cost-saving ability; indeed, this action may hinder the occurrence of the win-win situation.*

Last, we investigate how marginal profits affect equilibrium outcomes, which can be deemed as another metric reflecting a company's operational effectiveness. A manager can adjust profitability by optimizing operations. Our findings are as follows.

Proposition 4.3 (d). *When the leader possesses a stronger profitability (i.e., larger ρ_1), the follower's market threshold a_2^{Δ} will increase. When the follower improves profitability (i.e., larger ρ_2), the leader's two thresholds will also increase, while $a_{1,(N,M)}^{\Delta}$ grows faster than $a_{1,(N,N)}^{\Delta}$.*

A larger a_2^{Δ} will decrease the area (N,N) while increasing the area (N,M). This is adverse for the follower since the win-win situation is less likely to occur, while the leader's first-mover advantage is strengthened. In contrast, larger $a_{1,(N,N)}^{\Delta}$ and $a_{1,(N,M)}^{\Delta}$ reduce areas (N,N) and (N,M), respectively. This result is mixed for the follower because it weakens the leader's first-mover advantage but also makes the win-win situation less likely to occur. We further note that $a_{1,(N,M)}^{\Delta}$ grows faster than $a_{1,(N,N)}^{\Delta}$. The adverse impact on the first-mover advantage is thus expected to be more significant than on the win-win situation. We derive the following insight.

Finding 4.4. *Stronger profitability drives the leader to adopt SDS by means of strengthening its first-mover advantage. Stronger profitability exhibits mixed impacts on the follower: it makes it harder for the follower to benefit from SDS, but, at the same time, suppresses the leader's advantage.*

4.3. Extended Studies

The first and second extensions are developed to check the robustness of the findings derived from the basic model. In particular, the first extension replaces the exponential cost function with the well-established quadratic cost function, while the second extension considers decision makers' risk attitudes against profit variation. Then, the third extension drills deeper, aiming to generalize the equilibrium analysis to a situation in which one leader and multiple followers simultaneously exist.

4.3.1. Quadratic cost function

The first extension aims to examine the robustness of the major findings of the basic model when the cost structure of loyalty program investment and the resulting market size increment changes to a quadratic form. To be specific, the exponential cost function in the basic model captures the diminishing reward of loyalty program investment observed in practice. In the literature, there is another well-established cost function that can also capture such diminishing returns; that is, the quadratic cost function (Dou and Choi, 2024). As the two cost functions have some significant differences (e.g., increasing rates and exogenously given parameters), the major findings of the basic model may become invalid, which will be checked in the next analyses.

The quadratic cost function is suitable for our service operations problem because it effectively models the diminishing marginal returns of investments (Kimball, 1993). It reflects the reality that while initial improvements (e.g., in service quality or loyalty programs) are relatively inexpensive, achieving higher-level gains requires progressively larger resource commitments due to increasing organizational friction or resource scarcity. This function is particularly suitable for service competitive games (like the Stackelberg model), where analytical tractability is essential (Tsay and Agrawal, 2000). It would facilitate the derivation of closed-form solutions and analytically tractable insights.

Company i 's market size increment due to loyalty program investment v_i will be $\sqrt{2v_i/k_i}$ under the quadratic cost function, where $k_i > 0$ is an exogenously given parameter. Then, with investment v_i, its overall market size without introducing SDS is

$$D_{i,M} = a_i + \sqrt{2v_i/k_i} - c\sqrt{2v_{3-i}/k_{3-i}}\,, \tag{4.8}$$

and its post-SDS market size is

$$\tilde{D}_{i,N} = \hat{a}_i + \tilde{\varepsilon}_i + \sqrt{2v_i/k_i} - c\sqrt{2v_{3-i}/k_{3-i}}\,. \tag{4.9}$$

The profit in Case M is

$$\Pi_{i,M} = \rho_i D_{i,M} - v_i = \rho_i\left(a_i + \sqrt{2v_i/k_i} - c\sqrt{2v_{3-i}/k_{3-i}}\right) - v_i\,, \tag{4.10}$$

and the expected profit in Case N is

$$\Pi_{i,N} = \mathrm{E}\left[\left(\rho_i + m_i\right)\tilde{D}_{i,N} - v_i\right] = \left(\rho_i + m_i\right)\left(\hat{a}_i + \sqrt{2v_i/k_i} - c\sqrt{2v_{3-i}/k_{3-i}}\right) - v_i\,. \tag{4.11}$$

Same to the basic model, the profit functions are concave and increasing in Company i 's investment v_i, while decreasing in the rival's investment v_{3-i}. The optimal investment in each case under the quadratic cost function is as follows.

Lemma 4.2. *Under the quadratic cost function, regardless of being the leader or the follower, a company's optimal investment is* $v_{i,M}^* = \rho_i^2/2k_i$ *when maintaining existing services or* $v_{i,N}^* = \left(\rho_i + m_i\right)^2/2k_i$ *when adopting SDS.*

This lemma uncovers the same findings as **Lemma 4.1**; that is, investing in loyalty programs with an optimized budget always benefits a company, no matter as the leader or the follower, and imposing SDS always incurs a higher loyalty program investment. In addition, the optimal investment amount is increasing in profitability factor ρ_i or cost-saving ability factor m_i, while decreasing in the factor of market sensitivity to loyalty program investment k_i.

We derive the leader's and the follower's optimal investments and (expected) profits in three possible equilibrium outcomes in **Table 4.4** and **Table 4.5**, respectively. Like the basic model, without loss of generality, we assume Company 1 is the leader and Company 2 is the follower.

Table 4.4. The leader's optimal investment and (expected) profit under the quadratic cost function.

Strategy	Optimal investment	Optimal (expected) profit
(M,M)	$v_{1,(M,M)}^{*}=\dfrac{\rho_1^2}{2k_1}$	$\Pi_{1,(M,M)}^{*}=\rho_1\left(a_1+\dfrac{\rho_1}{k_1}-c\dfrac{\rho_2}{k_2}\right)-\dfrac{\rho_1^2}{2k_1}$
(N,M)	$v_{1,(N,M)}^{*}=\dfrac{(\rho_1+m_1)^2}{2k_1}$	$\Pi_{1,(N,M)}^{*}=(\rho_1+m_1)\left(\hat{a}_1+\dfrac{\rho_1+m_1}{k_1}-c\dfrac{\rho_2}{k_2}\right)-\dfrac{(\rho_1+m_1)^2}{2k_1}$
(N,N)	$v_{1,(N,N)}^{*}=\dfrac{(\rho_1+m_1)^2}{2k_1}$	$\Pi_{1,(N,N)}^{*}=(\rho_1+m_1)\left(\hat{a}_1+\dfrac{\rho_1+m_1}{k_1}-c\dfrac{\rho_2+m_2}{k_2}\right)-\dfrac{(\rho_1+m_1)^2}{2k_1}$

Table 4.5. The follower's optimal investment and (expected) profit under the quadratic cost function.

Strategy	Optimal investment	Optimal (expected) profit
(M,M)	$v_{2,(M,M)}^{*}=\dfrac{\rho_2^2}{2k_2}$	$\Pi_{2,(M,M)}^{*}=\rho_2\left(a_2+\dfrac{\rho_2}{k_2}-c\dfrac{\rho_1}{k_1}\right)-\dfrac{\rho_2^2}{2k_2}$
(N,M)	$v_{2,(N,M)}^{*}=\dfrac{\rho_2^2}{2k_2}$	$\Pi_{2,(N,M)}^{*}=\rho_2\left(a_2+\dfrac{\rho_2}{k_2}-c\dfrac{\rho_1+m_1}{k_1}\right)-\dfrac{\rho_2^2}{2k_2}$
(N,N)	$v_{2,(N,N)}^{*}=\dfrac{(\rho_2+m_2)^2}{2k_2}$	$\Pi_{2,(N,N)}^{*}=(\rho_2+m_2)\left(\hat{a}_2+\dfrac{\rho_2+m_2}{k_2}-c\dfrac{\rho_1+m_1}{k_1}\right)-\dfrac{(\rho_2+m_2)^2}{2k_2}$

We use the same analysis framework in section 3.2 to derive the equilibrium conditions. In **Table 4.6**, we display the critical (expected) profit conditions and the corresponding market thresholds.

Table 4.6. Critical market thresholds under the quadratic cost function.

Condition	Critical market Threshold
$\Pi_{1,(M,M)}^{*}=\Pi_{1,(N,N)}^{*}$	$a_{1,(N,N)}^{\Delta}=\left(\rho_1a_1+\dfrac{c}{k_2}(m_2\rho_1+m_1\rho_2+m_1m_2)-\dfrac{2\rho_1m_1+m_1^2}{2k_1}\right)\Big/(\rho_1+m_1)$
$\Pi_{1,(M,M)}^{*}=\Pi_{1,(N,M)}^{*}$	$a_{1,(N,M)}^{\Delta}=\left(\rho_1a_1+\dfrac{c}{k_2}m_1\rho_2-\dfrac{2\rho_1m_1+m_1^2}{2k_1}\right)\Big/(\rho_1+m_1)$
$\Pi_{2,(N,M)}^{*}=\Pi_{2,(N,N)}^{*}$	$a_2^{\Delta}=\left(\rho_2a_2+\dfrac{c}{k_1}(m_2\rho_1+m_1m_2)-\dfrac{2\rho_2m_2+m_2^2}{2k_2}\right)\Big/(\rho_2+m_2)$

The impacts of market conditions and companies' operational factors on the identified thresholds are summarized in the following proposition.

Proposition 4.4. (a) *The two companies' all market thresholds are increasing in the competition level:* $0<\frac{\partial a^{\Delta}_{1,(N,M)}}{\partial c}<\frac{\partial a^{\Delta}_{1,(N,N)}}{\partial c}$ *and* $0<\frac{\partial a^{\Delta}_{2}}{\partial c}$. **(b)** *Two companies' market thresholds increase in their base market sizes,* $0<\frac{\partial a^{\Delta}_{1,(N,M)}}{\partial a_1}=\frac{\partial a^{\Delta}_{1,(N,N)}}{\partial a_1}$ *and* $0<\frac{\partial a^{\Delta}_{2}}{\partial a_2}$*, where the leader's two thresholds change equally.* **(c)** *The leader's* $a^{\Delta}_{1,(N,M)}$ *is independent of the follower's cost-saving ability but* $a^{\Delta}_{1,(N,N)}$ *is increasing in the follower's cost-saving ability; the follower's* a^{Δ}_{2} *is increasing in the leader's cost-saving ability:* $0=\frac{\partial a^{\Delta}_{1,(N,M)}}{\partial m_2}<\frac{\partial a^{\Delta}_{1,(N,N)}}{\partial m_2}$ *and* $0<\frac{\partial a^{\Delta}_{2}}{\partial m_1}$. **(d)** *The leader's thresholds are increasing in the follower's profitability, and vice versa:* $0<\frac{\partial a^{\Delta}_{1,(N,M)}}{\partial \rho_2}=\frac{\partial a^{\Delta}_{1,(N,N)}}{\partial \rho_2}$ *and* $0<\frac{\partial a^{\Delta}_{2}}{\partial \rho_1}$.

This proposition is a counterpart of **Proposition 4.3** in the basic model. In particular, **Proposition 4.4 (a)** suggests that the as the competition level declines, the leader's threshold $a^{\Delta}_{1,(N,N)}$ decreases faster than $a^{\Delta}_{1,(N,M)}$, and the follower's threshold a^{Δ}_{2} also decreases. In this case, the area corresponds to (N,N) will expand (see **Figure 4.2**), making the two companies more likely to adopt SDS. This is the same as **Finding 4.1** in the basic model. Likewise, we can find that **Propositions 4.4 (b)** and **(c)** are respectively similar to **Propositions 4.3 (b)** and **(c)**, and hence, **Findings 4.2** and **4.3** in the basic model are robust. A slight exception appears in **Proposition 4.4 (d)**, where $\frac{\partial a^{\Delta}_{1,(N,M)}}{\partial \rho_2}=\frac{\partial a^{\Delta}_{1,(N,N)}}{\partial \rho_2}>0$ in the extension but $\frac{\partial a^{\Delta}_{1,(N,M)}}{\partial \rho_2}>\frac{\partial a^{\Delta}_{1,(N,N)}}{\partial \rho_2}>0$ in the basic model. While the changing rates of the two thresholds in terms of ρ_2 are different from the basic model, the leader's two thresholds still increase in ρ_2, and thus, we can obtain a similar result to **Finding 4.4**. The impact of model parameters is summarized as follows.

Finding 4.5. *When the relation between investment and market size increment changes from the exponential cost function to the quadratic cost function, the major findings in the basic model (i.e.,* ***Findings 4.1*** *to 4.4) are still valid.*

4.3.2. Risk attitudes and distributional ambiguity

The second extension is also for robustness checking, studying the situation in which the two companies possess certain risk attitudes (i.e., risk-averse or risk-seeking) against profit variation. Profit variation is due to the uncertainty of the post-SDS market size. As estimating the exact distribution of post-SDS market size can be hard, we will further consider its distributional ambiguity. In particular, a risk-averse company prefers the strategy with a more stable performance, whereas a risk-seeking company admits performance variation to gamble for a higher profit. Both risk attitudes are common in the real world. For example, Marriott proposed an asset-light model that focuses on franchising and management contracts rather than owning hotels to reduce cash flow risk[11]. During the COVID-19 pandemic, most airlines scaled back their operations, whereas Ryan Air increased its fleet and flights; it gambled on a post-pandemic travel surge, accepting short-term losses[12]. The post-SDS market size is uncertain, captured by EPSM $\hat{a}_i$ plus a random variable $\tilde{\varepsilon}_i$. Modeling the post-SDS market size's uncertainty is, in nature, characterizing the distribution of $\tilde{\varepsilon}_i$. A precise estimation of the distribution is challenging in practice, and an estimated distribution may mismatch the latest environment. For example, *Hilton*'s CEO argued that customer demand changed significantly due to the pandemic and that historical distributions may not be suitable anymore[13]. We thus consider the distributional ambiguity of $\tilde{\varepsilon}_i$, which models its distribution by the mean and variance.

In the literature, there are various metrics to evaluate decision-makers' risk attitudes, such as value at risk (Luciano et al. 2003, Tapiero 2005), conditional value at risk (Wu et al. 2006), and the mean-variance approach (Chiu and Choi 2016). Among them, the mean-variance approach is widely applied in service operations problems, thanks to its traceability and interpretability. For example, with this approach, Choi et al. (2020) studied shipping service companies' risk attitudes, especially risk-seeking behavior, under a volatile and competitive environment. We adopt this powerful approach in this extension. Regarding the distributional ambiguity, it is well investigated by the DRO literature. The key idea is to model possible distributions of the random variable(s) of interest by accessible statistical information. A commonly used statistical information is lower moments, in particular, mean and variance (Delage and Ye 2010). While DRO is well-established, its application in service operations is limited. A closely relevant work is dedicated to Fu et al. (2018), which designed a profit-sharing contract for a decentralized supply chain in which customer demands and selling prices possess ambiguous distributions. This extension adopts mean-variance information to model $\tilde{\varepsilon}_i$'s distributional ambiguity.

We quantify Company i's risk attitude by a parameter λ_i. The standard deviation of the company's profit is denoted by SD_i. Then, under the mean variance framework, the company aims to maximize the expected profit plus the profit standard deviation weighted by risk sensitivity λ_i (i.e., $\Pi_i + \lambda_i SD_i$). For a

[11] https://www.amminvest.com/how-marriotts-business-model-generates-high-returns-and-excess-cash-flow/. Accessed 21 Jul 2025.

[12] chrome-extension://efaidnbmnnnibpcajpcglclefindmkaj/https://investor.ryanair.com/wp-content/uploads/ 2022/07/Ryanair-2022-Annual-Report.pdf/. Accessed 21 Jul 2025.

[13] https://seekingalpha.com/article/4573510-vici-properties-vs-realty-income-best-reit-for-2023/. Accessed 21 Jul 2025.

risk-neutral company (i.e., $\lambda_i = 0$), its objective will reduce to Π_i, same as the basic model. For a risk-averse (i.e., $\lambda_i < 0$) or risk-seeking (i.e., $\lambda_i > 0$) company, its objective will decrease or increase given a larger profit variation. The magnitude of λ_i captures the degree of risk sensitivity.

Following the convention of DRO, $\tilde{\varepsilon}_i$'s distribution P_i belongs to an ambiguity set defined as below:

$$P_i = \left\{ \mathrm{P} \in \mathscr{P}(\Xi) : \mathrm{E}_{\mathrm{P}}\left[\varepsilon_i\right] = 0,\ \underline{\delta}_i^2 \le \mathrm{E}_{\mathrm{P}}\left[\tilde{\varepsilon}_i^2\right] \le \bar{\delta}_i^2 \right\}, \tag{4.12}$$

where $\underline{\delta}_i$ and $\bar{\delta}_i$ is the lower and upper bound of $\tilde{\varepsilon}_i$'s standard deviation; set $\mathscr{P}(\Xi)$ contains all possible distributions over the given support set Ξ. For notational simplicity, we will still adopt the quadratic cost function, which has been analyzed thoroughly in section 4.1.

Given an SDS decision and loyalty program investment, DRO seeks the worst-case distribution in P_i , which yields the smallest objective: $\mathrm{P}_i^* = \arg\min_{\mathrm{P}_i \in P_i} \left\{ \Pi_i + \lambda_i SD_i \right\}$. Obtaining such a worst-case distribution and objective often calls for computational approaches. However, after drilling deeper into the structures of the ambiguity set and the mean-variance objective, we derive the worst-case objective in closed form as follows.

Theorem 4.1. *Company i's worst-case mean-variance objective given* loyalty program *investment v_i after adopting SDS admis the following closed-form expression:*

$$U_{i,N}(v_i) = (\rho_i + m_i)\left(\hat{a}_1 + \sqrt{2v_i/k_i} - c\sqrt{2v_{3-i}/k_{3-i}}\right) - v_i + \lambda_i(\rho_i + m_i)\delta_i, \tag{4.13}$$

where $\delta_i = \mathrm{I}(\lambda_i < 0)\bar{\delta}_i + \mathrm{I}(\lambda_i > 0)\underline{\delta}_i$ and $\mathrm{I}(\cdot)$ is the indicator.

The closed-form expression of the worst-case objective value under the mean-variance framework is concave and increasing in Company i's loyalty program investment v_i, while decreasing in the rival's investment v_{3-i}, which is the same as the profit function in the basic model. We further derive the optimal investments and worst-case objectives of the leader and the follower in three equilibrium outcomes in **Table 4.7** and **Table 4.8**, respectively. We can see that when considering risk attitudes and distributional ambiguity, imposing SDS also needs a higher loyalty program investment, which is exactly the same as the finding in **Lemma 4.1**.

Table 4.7. The leader's optimal loyalty program investment and worst-case objective.

Strategy	Optimal investment	Worst-case objective
(M,M)	$v_{1,(M,M)}^{RISK*} = \dfrac{\rho_1^2}{2k_1}$	$U_{1,(M,M)}^* = \rho_1\left(a_1 + \dfrac{\rho_1}{k_1} - c\dfrac{\rho_2}{k_2}\right) - \dfrac{\rho_1^2}{2k_1}$
(N,M)	$v_{1,(N,M)}^{RISK*} = \dfrac{(\rho_1 + m_1)^2}{2k_1}$	$U_{1,(N,M)}^* = (\rho_1 + m_1)\left(\hat{a}_1 + \dfrac{\rho_1 + m_1}{k_1} - c\dfrac{\rho_2}{k_2}\right) - \dfrac{(\rho_1 + m_1)^2}{2k_1} + \lambda_1(\rho_1 + m_1)\delta_1$

(N,N)	$v_{1,(N,N)}^{RISK*}=\frac{(\rho_1+m_1)^2}{2k_1}$	$U_{1,(N,N)}^{*}=(\rho_1+m_1)\left(\hat{a}_1+\frac{\rho_1+m_1}{k_1}-c\frac{\rho_2+m_2}{k_2}\right)-\frac{(\rho_1+m_1)^2}{2k_1}+\lambda_1(\rho_1+m_1)\delta_1$

Table 4.8. The follower's optimal loyalty program investment and worst-case objective.

Strategy	Optimal investment	Worst-case objective
(M,M)	$v_{2,(M,M)}^{RISK*}=\frac{\rho_2^2}{2k_2}$	$U_{2,(M,M)}^{*}=\rho_2\left(a_2+\frac{\rho_2}{k_2}-c\frac{\rho_1}{k_1}\right)-\frac{\rho_2^2}{2k_2}$
(N,M)	$v_{2,(N,M)}^{RISK*}=\frac{\rho_2^2}{2k_2}$	$U_{2,(N,M)}^{*}=\rho_2\left(a_2+\frac{\rho_2}{k_2}-c\frac{\rho_1+m_1}{k_1}\right)-\frac{\rho_2^2}{2k_2}$
(N,N)	$v_{2,(N,N)}^{RISK*}=\frac{(\rho_2+m_2)^2}{2k_2}$	$U_{2,(N,N)}^{*}=(\rho_2+m_2)\left(\hat{a}_2+\frac{\rho_2+m_2}{k_2}-c\frac{\rho_1+m_1}{k_1}\right)-\frac{(\rho_2+m_2)^2}{2k_2}+\lambda_2(\rho_2+m_2)\delta_2$

It is unexpected that all optimal investments are identical to those without considering risk attitudes and distributional ambiguity. A quick answer is that the objective's risk-sensitive part is invariable in terms of the investment decision under the moment-based ambiguity set. However, note that this finding may not be true for other ambiguity sets like Wasserstein ambiguity sets (Gao and Kleywegt 2023) or other risk metrics like conditional value at risk (Rockafellar and Uryasev, 2000).

Following the analysis framework in section 3.2, we obtain critical market thresholds for the leader and the follower by comparing the worst-case mean-variance objectives in different equilibrium outcomes, which are detailed in **Table 4.9.**

Table 4.9. Critical market thresholds considering risk attitudes and distributional ambiguity.

Condition	Critical market threshold
$U_{1,(M,M)}^{*}=U_{1,(N,M)}^{*}$	$a_{1,(N,M)}^{RISK\Delta}=\left(\rho_1a_1+c\frac{m_1\rho_2}{k_2}-\frac{m_1(2\rho_1+m_1)}{2k_1}-\lambda_1(\rho_1+m_1)\delta_1\right)\Big/(\rho_1+m_1)$
$U_{1,(M,M)}^{*}=U_{1,(N,N)}^{*}$	$a_{1,(N,N)}^{RISK\Delta}=\left(\rho_1a_1+c\frac{m_1\rho_2}{k_2}+c\frac{(\rho_2+m_2)m_1}{k_2}-\frac{m_1(2\rho_1+m_1)}{2k_1}-\lambda_1(\rho_1+m_1)\delta_1\right)\Big/(\rho_1+m_1)$
$U_{2,(N,M)}^{*}=U_{2,(N,N)}^{*}$	$a_{2}^{RISK\Delta}=\left(\rho_2a_2+c\frac{(\rho_1+m_1)m_2}{k_1}-\frac{m_2(2\rho_2+m_2)}{2k_2}-\lambda_2(\rho_2+m_2)\delta_2\right)\Big/(\rho_2+m_2)$

The difference of the above thresholds from those without considering risk attitudes and distributional ambiguity is just the residual term $-\lambda_i\delta_i$, which is a constant. Considering these two features makes the thresholds increase for a risk-averse company (i.e., $\lambda_i<0$), while decrease for a risk-seeking company (i.e., $\lambda_i>0$). Since such a difference only affects the magnitude of the thresholds, following the analyses presented before (we thus omit the details), it is easy to show that the major findings are still valid. However, due to the existence of the residual terms, the thresholds can be negative, which becomes meaningless. We thus develop the following condition.

Proposition 4.5. *For a risk-seeking company, if it is the leader, its risk sensitivity must be controlled below:*

$$\lambda_1 < \left(\rho_1 a_1 + c\frac{m_1\rho_2}{k_2} - \frac{m_1(2\rho_1 + m_1)}{2k_1} \right) \Big/ (\rho_1 + m_1)\delta_1 ; \tag{4.14}$$

if being the follower, its risk sensitivity must be controlled below:

$$\lambda_2 < \left(\rho_2 a_2 + c\frac{(\rho_1 + m_1)m_2}{k_1} - \frac{m_2(2\rho_2 + m_2)}{2k_2} \right) \Big/ (\rho_2 + m_2)\delta_2 . \tag{4.15}$$

For a risk-neutral or averse company (i.e., $\lambda_i \le 0$), its risk-sensitive part in the mean-variance objective is always nonnegative, so there is no need to control risk sensitivity. However, the objective can be negative for a risk-seeking company so its risk sensitivity must be upper bounded. This coincides with the sense that a company can only gamble moderately; otherwise, too aggressive gambling can harm. Moreover, since risk-averse companies' thresholds increase by the same magnitude, (M, M) becomes more likely to happen, while (N, N) becomes less likely to happen. In contrast, since risk-seeking companies' thresholds decrease by the same magnitude, (M, M) becomes less likely to happen, while (N, N) becomes more likely to happen. We summarize all the above analyses as follows.

Finding 4.6. *The major findings in the basic model are still valid when considering companies' risk attitudes and the distributional ambiguity of the post-SDS market size. A new finding is that risk-averse companies become less likely to adopt SDS, while risk-seeking companies become more likely to adopt SDS. Risk-seeking companies' risk sensitivity has an upper bound to restrict too aggressive gambling actions.*

Last, we analyze how factors δ_i and λ_i, which respectively reflect market volatility and risk sensitivity, affect companies' incentive to adopt SDS. Their impacts are summarized below.

Proposition 4.6. *When standard deviation δ_i or risk sensitivity $|\lambda_i|$ increases, regardless of being the leader or the follower, a risk-seeking company's market thresholds decline, while a risk-averse company's thresholds rise. Importantly, a company's all thresholds change at an identical rate.*

For the leader, since $a^{\Delta}_{1,(N,M)}$ and $a^{\Delta}_{1,(N,N)}$ change equally, the win-win situation (N, N) and a first-mover advantage situation (N, M) both become less likely to happen for risk-averse companies, while more likely to happen for risk-seeking companies. A bigger a^{Δ}_2 makes the win-win situation in which the follower benefits from SDS less (more) likely to happen under risk-averse (-seeking) attitudes. We can thus get the following finding.

Finding 4.7. *Increased volatility of post-SDS market sizes or risk sensitivity (in terms of absolute value) drives risk-seeking companies to adopt SDS while discouraging risk-averse companies from adopting SDS.*

4.3.3. One leader and multiple followers

The last extension moves beyond the classic duopoly market and aims to generalize the analysis to a competitive environment in which a leader faces multiple followers. Such a situation can be found where a service is operated by several companies. For example, the ride-hailing service in China has one dominant operator Didi (owning over 50% market share) and dozens of minor operators such as Gaode and Caocao[14]. DoorDash controls around 60% of the food delivery market in the US, while Uber Eats and Grubhub control most of the remaining[15]. In these situations, when the dominant service company intends to implement a new strategy (e.g., SDS), it needs to anticipate the other companies' reactions, which can be captured by a one-leader and multi-follower Stackelberg game model. In the next analyses, we will see that deriving closed-form equilibrium conditions is incredibly challenging, even if all followers are homogeneous. Nevertheless, we still derive the sufficient conditions for two symmetric equilibria.

In service operation literature, studies on the one-leader and multi-follower Stackelberg game are limited. A closely relevant study is attributed to Jin and Ryan (2012), which examined the pricing and service level design of a supply chain of one buyer and multiple suppliers. However, the decision in our problem is more complex, requiring a distinct analysis technique.

Let ρ_0, m_0, a_0, $\hat{a}_0+\tilde{\varepsilon}_0$, and k_0 denote the leader's marginal profit, saved marginal cost, base market size, post-SDS market size, and cost parameter. We consider $K \geq 2$ homogeneous followers for tractability and they have common ρ, m, a, $\hat{a}+\tilde{\varepsilon}$, and k. The competition level between an arbitrary company and its rivals is $c \in [0,1/K]$. We define a binary variable x_0 which equals one if the leader adopts SDS or zero otherwise, and a non-negative continuous variable v_0 to stand for the leader's investment. For follower $i \in \{1,...,K\}$, we define x_i and v_i in the same way. Then, the leader's expected profit is:

$$\Pi_0(x_0,v_0)=(\rho_0+m_0x_0)\left(\hat{a}_0x_0+a_0(1-x_0)+\sqrt{2v_0/k_0}-c\sum_{i=1}^{K}\sqrt{2v_i/k}\right)-v_0, \tag{4.16}$$

and the expected profit of the follower i is:

$$\Pi_i(x_i,v_i)=(\rho+mx_i)\left(\hat{a}x_i+a(1-x_i)+\sqrt{2v_i/k}-c\sqrt{2v_0/k_0}-c\sum_{j=1,j\neq i}^{K}\sqrt{2v_j/k}\right)-v_i. \tag{4.17}$$

The optimal investment exhibits a similar characteristic to the previous models. By the concavity of the profit functions, we derive the optimal investment in closed form as follows.

[14] https://www.sixthtone.com/news/1015043/. Accessed 21 Jul 2025.
[15] https://secondmeasure.com/datapoints/food-delivery-services-grubhub-uber-eats-doordash-postmates/. Accessed 21 Jul 2025.

Lemma 4.3. *The leader's optimal* loyalty program *investment is* $v_0^* = \rho_0^2/2k_0$ *when* $x_0 = 0$ *, or* $v_0^* = (\rho_0 + m_0)^2/2k_0$ *when* $x_0 = 1$. *The follower* i *'s optimal* loyalty program *investment is* $v_i^* = \rho^2/2k$ *when* $x_i = 0$*, or* $v_i^* = (\rho + m)^2/2k$ *when* $x_i = 1$.

Interestingly, both the leader's and the followers' optimal investments are totally identical to those in the one-leader and one-follower game. This again underscores the insight that no matter how rivals modify service strategies, a company always benefits from investing in loyalty programs with an optimized budget.

From the modeling perspective, since the optimal loyalty program investment depends on the binary decision, the market size increment also depends on the binary decision, which can be expressed as:

$$\sqrt{2v_0/k_0} = \frac{\rho_0}{k_0}(1-x_0) + \frac{\rho_0 + m_0}{k_0} x_0, \tag{4.18}$$

$$\sqrt{2v_i/k} = \frac{\rho}{k}(1-x_i) + \frac{\rho + m}{k} x_i. \tag{4.19}$$

We can thus eliminate variables v_0 and v_i from the profit functions as follows:

$$\begin{aligned}\Pi_0(x_0) = (\rho_0 + m_0 x_0)\left[\left(a_0 + \frac{\rho_0}{k_0}\right)(1-x_0) + \left(\hat{a}_0 + \frac{\rho_0 + m_0}{k_0}\right)x_0 - c\sum_{j=1}^{K}\left(\frac{\rho}{k}(1-x_i) + \frac{\rho+m}{k}x_i\right)\right] \\ - \frac{\rho_0^2}{2k_0}(1-x_0) - \frac{(\rho_0 + m_0)^2}{2k_0}x_0,\end{aligned} \tag{4.20}$$

$$\begin{aligned}\Pi_i(x_i) = (\rho + m x_i)\left[\left(a + \frac{\rho}{k}\right)(1-x_i) + \left(\hat{a} + \frac{\rho+m}{k}\right)x_i - c\left(\frac{\rho_0}{k_0}(1-x_0) + \frac{\rho_0 + m_0}{k_0}x_0\right)\right. \\ \left. - c\sum_{j=1, j\neq i}^{K}\left(\frac{\rho}{k}(1-x_j) + \frac{\rho+m}{k}x_j\right)\right] - \frac{\rho^2}{2k}(1-x_i) - \frac{(\rho+m)^2}{2k}x_i,\end{aligned} \tag{4.21}$$

which contain binary decisions only. With these reduced expressions, we formulate the follower i 's optimal reaction to the leader and the other followers as follows:

$$\begin{aligned}&\max_{x_i \in \{0,1\}} \Pi_i(x_i; x_0, \ldots, x_{i-1}, x_{i+1}, \ldots, x_K) = \\ &(\rho + m x_i)\left[\left(a + \frac{\rho}{k}\right)(1-x_i) + \left(\hat{a} + \frac{\rho+m}{k}\right)x_i - c\left(\frac{\rho_0}{k_0}(1-x_0) + \frac{\rho_0 + m_0}{k_0}x_0\right)\right. \\ &\left. - c\sum_{j=1, j\neq i}^{K}\left(\frac{\rho}{k}(1-x_j) + \frac{\rho+m}{k}x_j\right)\right] - \frac{\rho^2}{2k}(1-x_i) - \frac{(\rho+m)^2}{2k}x_i.\end{aligned} \tag{4.22}$$

Given the leader's decision, A follower is assumed to maintain current services if adopting SDS does not bring a positive profit increase. The proposed game model admits nonlinear payoff functions and discrete decisions, which need not lead to Nash equilibria. We thus establish sufficient conditions for symmetric Stackelberg equilibria where the leader and all followers either keep or adopt SDS. See the following theorem.

Theorem 4.2. *The following conditions are sufficient to guarantee the symmetric Stackelberg equilibrium where both the leader and all followers maintain existing services:*

$$0<\hat{a}_0 \le \left(\rho_0 a_0 + cK\frac{\rho m_0}{k} - \frac{m_0^2+2\rho_0 m_0}{2k_0}\right)\Big/\left(\rho_0+m_0\right), \tag{4.23}$$

$$0<\hat{a} \le \left(mc\left(\frac{\rho_0+m_0}{k_0}+\left(K-1\right)\frac{\rho}{k}\right)-\rho a-\frac{m^2+2m\rho}{2k}\right)\Big/\left(\rho+m\right). \tag{4.24}$$

The following conditions are sufficient to guarantee the Stackelberg equilibrium where the leader and all followers adopt SDS:

$$\hat{a}_0 > \left(a_0\rho_0 - \frac{m_0^2+2\rho_0 m_0}{2k_0} + \frac{cK}{k}\left(\rho m_0+\rho_0 m+m m_0\right)\right)\Big/\left(\rho_0+m_0\right)>0, \tag{4.25}$$

$$\hat{a} > \left(\rho a + c\frac{m\rho_0+m m_0}{k_0}+\left(cK-c-\frac{1}{2}\right)\frac{m^2+2m\rho}{k}\right)\Big/\left(\rho+m\right)>0. \tag{4.26}$$

Since all followers are homogeneous, it is intuitive that they should make an identical decision in equilibrium. However, we find that in a special case, homogeneous followers can make distinct decisions in equilibrium. Briefly speaking, this will happen if the followers who adopt SDS have the same profit as those without adopting SDS, and the profit is greater than the case where all followers reject SDS. Moreover, in this special equilibrium, the number of followers adopting SDS is not an arbitrary value, but a certain number characterized by several model parameters. This finding is reported by the following theorem.

Theorem 4.3. *If there exists an integer* $K^* \in \{1,\ldots,K-1\}$ *such that*

$$K^*-1 = k\frac{\rho a+\left(\rho+m\right)\hat{a}}{cm^2} - k\frac{\rho_0+m_0}{mk_0} - \frac{\rho}{m}\left(K-2-\frac{1}{c}\right)+\frac{1}{2c} \tag{4.27}$$

and if the leader's and the followers' EPSMs are larger than the thresholds below:

$$\hat{a}_0 > \left(\rho_0 a_0 - \frac{2m_0\rho_0+m_0^2}{2k_0}+\left(\rho_0+m_0\right)cK^*\frac{m}{k}+cK\frac{\rho m_0}{k}\right)\Big/\left(\rho_0+m_0\right)>0, \tag{4.28}$$

$$\hat{a} > \left(\rho a + mc\frac{\rho_0+m_0}{k_0} - \frac{\left(1+2c\right)\left(m^2+2m\rho\right)}{2k}+\left(\rho+m\right)cK^*\frac{m}{k}+cK\frac{\rho m}{k}\right)\Big/\left(\rho+m\right)>0, \tag{4.29}$$

then it will be sufficient to guarantee the equilibrium where the leader and K^* *followers adopt SDS while the remaining* $K-K^*$ *followers reject SDS.*

Note that this special equilibrium contains $\binom{K}{K^*} = \frac{K!}{\left(K-K^*\right)!K^*!}$ possible realizations since it only regulates the number of followers who adopt SDS but does not restrict which followers should do so. The findings in **Theorem 4.2** are similar to those of the previous models. In particular, if the decline of market size due to SDS is incredibly significant, then the leader and all followers reject SDS. In contrast, if the market drops are acceptable, all companies will adopt SDS.

4.4. Summary of This Chapter

4.4.1. Concluding remarks

This study explores the joint implementation of SDS and the associated loyalty program design of two companies in a competitive environment. In the basic model, we build a duopoly Stackelberg service game model, where the two companies compete in SDS adoption and loyalty program investments. We uncover three equilibrium scenarios: two of them are symmetric, while the other one is asymmetric. We derive the equilibrium condition for each scenario. Specifically, by comparing the two companies' EPSMs with some identified thresholds, we can immediately obtain the corresponding equilibrium scenario. We further analyze four market factors (i.e., competition level, profitability, cost-saving ability, and market power) and discover how they drive or hinder commitment to SDS. In the extended models, three new operational features are explored: i) a quadratic cost structure of loyalty program investment, ii) the distributional ambiguity of the post-SDS market size and companies' risk attitudes, and iii) the one-leader and multi-follower competition. They validate the robustness of some findings in the basic model and uncover new insights.

4.4.2. Managerial implications and actionable recommendations

First, this study establishes viable action plans for operations managers to impose SDS and to redesign loyalty programs by answering three "W"s. Second, we challenge some common beliefs and give novel alternative choices. Third, our findings help explain business practices arising in the real world.

- **Answers to three "W"s.** i) ***When to preemptively impose SDS:*** A company should make a preemptive action only when its EPSM and its rival's EPSM respectively fall into two special ranges, which are characterized by the critical market thresholds uncovered by this study. If the two EPSMs disobey these conditions, preemptive commitment cannot create the first-mover advantage. ii) ***Whether to adopt SDS given that the rival has already committed to SDS:*** The follower company in this service game should mimic the leader to impose SDS only when its own SDS is larger than another critical market threshold. iii) ***What to do with*** loyalty programs ***during SDS implementation:*** A company should always pair loyalty program enhancement with SDS implementation. This is true even when the rivals do nothing (i.e., no SDS, no loyalty program change). However, the investment in loyalty programs must respect an optimized budget revealed by this study.

- **Novel choices.** i) ***Avoid preemptive SDS as a default:*** Many companies regard the first-mover advantage as a winning formula and thus rush to launch new strategies. However, our analyses uncover that preemptive commitment to SDS matters only when both companies' EPSMs belong to some special ranges. Therefore, it is essential to analyze not only market reaction but also rival's response. ii) ***Low competition actually calls for SDS:*** Firms often avoid cost cuts in stable markets. However, we find that SDS is indeed ideal for a company in a low competitive environment.
- **Explanation for real-world practices.** Our theoretical findings may explain why some service companies intentionally reduce service quality and their competitors' behavior. For example, i) ***American Airlines*** removed free air meals and free seat selection in 2020 and accordingly revamped its loyalty program "AAdvantage", with extra bonuses and other benefits. This practice aligns with our finding that imposing SDS requires a higher loyalty program investment (**Lemmas 4.1**, **4.2**, and **4.3**). ii) ***Air Canada*** and ***WestJet*** have jointly dominated Canada's domestic aviation market since the early 2000s. Their duopoly solidified further after 2010, as smaller competitors struggled to scale, leaving the two airlines in control of 85% of domestic capacity for over a decade. Their long-standing dominance results in relatively low competition. However, they have reduced various services since the 2020s, particularly post-pandemic. For example, *Air Canada* eliminated free seat selection for basic fares, removed free snacks/drinks on short-haul flights, and introduced surge pricing on high-demand routes. *WestJet* reduced customer service staff, cancelled free snacks in economy, and introduced strict baggage fees. This coincides with our finding that low competition unexpectedly drives the adoption of SDS (**Proposition 4.3(a)**). iii) ***Marriott*** canceled the default daily housekeeping service in most of its mid-tier brands (e.g., *Courtyard*, *Fairfield Inn*, *Residence Inn*) in 2022. Instead, housekeeping was provided only every 3 to 5 days unless guests called for cleaning service. In contrast, *Hyatt* maintained daily housekeeping at mid-tier brands (e.g., *Hyatt Place*, *Hyatt House*), marketing itself as "committed to full-service hospitality". Likewise, *Hilton*'s mid-tier hotels (e.g., *Hampton Inn*, *Garden Inn*) retained daily cleaning, emphasizing "no compromise" in service. **Proposition 4.3** may explain why *Hilton* and *Hyatt* did not mimic *Marriott*. The proposition reveals that the first-mover advantage will appear if the EPSMs of the players under competition fall into certain ranges. In *Marriott*'s case, housekeeping frequency affects customer experience, but it is not the unique determinant for customers' choice; other factors like hotel facilities and brand reputation matter. While customers are sensitive to reduced housekeeping service, the "sensitivity" may be restricted to certain ranges, corresponding

to the case in which preemptive SDS adoption is vital.

Chapter 5. Conclusion

5.1. Concluding remarks

This doctoral research was motivated by a central and increasingly urgent question in the field of operations and engineering management: How can organizations make effective decisions in an environment characterized by frequent and significant disruptions? From global health crises to economic instability, such events introduce profound uncertainty, challenging the core functions of logistics and service operations. This thesis addresses this question by developing studies to enhance operational resilience. Across three studies, the research progresses from a broad assessment of the field to the focused application of advanced methods for specific, critical problems.

The first study reviews the latest literature on operations under disruption. This helps chart the landscape of contemporary challenges, identify how major events like the COVID-19 pandemic, natural disasters, and geopolitical tensions translate into tangible operational issues, such as demand volatility and network failures. This preliminary review highlights the potential of DRO as a promising tool for decision-making under uncertainty. Consequently, we further develop an accessible primer for both researchers and managers, explaining how DRO can be used to model problems where the underlying probability distributions are unknown or ambiguous.

The second study applies DRO to a pressing societal problem: the strategic implementation of intercity travel restrictions during a pandemic. Acknowledging the inherent uncertainty in disease propagation, a DRO model was developed to design a targeted restriction policy. The model's objective was to maximize public health benefits while minimizing economic harm. When tested with real-world data from China, the proposed targeted policy demonstrated significantly superior performance compared to the uniform restrictions commonly adopted in practice, especially during the critical early phases of an outbreak.

The third study shifts the focus from public policy to private-sector strategy in a competitive environment. This study examines how two competing firms navigate an economic downturn, focusing on the strategic decision to implement service downgrading and the design of accompanying loyalty programs. Using a game-theoretic model, the research identifies the equilibrium conditions under which firms would choose different strategies. The analysis reveals how market factors—such as the intensity of competition, firm profitability, and market power—drive these crucial strategic trade-offs during periods of economic instability.

Viewed together, these studies form a cohesive research narrative. They begin with a broad survey of the problem domain, select a powerful analytical tool, and apply it to generate actionable insights for both public and private sector decision-makers. The unifying theme of this thesis is that by explicitly and intelligently accounting for uncertainty, we can develop strategies that are fundamentally more robust and effective.

5.2. Future Research

Like all research, this thesis has its limitations, and our three studies can be extended in the future. In what follows, we will propose some potential research directions.

Regarding **Chapter 2**, the current review focuses on the recent studies on logistics and service operations under disruptions and the application of DRO in various operational problems. Future studies on operations under disruptions could consider the following three directions:

- There is a critical need to model acute geopolitical shocks like hot wars, moving beyond trade disputes. This includes studying the effects of sanctions, asset seizures, and the cascading nature of interconnected disruptions (Bimpikis et al. 2019).
- Expand the scope of operational contexts by developing models for humanitarian logistics in active conflict zones (Peters et al. 2021), with a focus on protecting aid workers, and exploring the crucial link between operational disruptions and a firm's financial health.
- Future research may leverage data-driven and interdisciplinary approaches, incorporating real-time data and models (Wiberg et al. 2025). Create hybrid frameworks that combine machine learning for forecasting, optimization for decision-making, and game theory for competitive analysis.

While DRO has been applied to many operational problems, there are still some possible future directions. We report four ideas to proceed in the future:

- Develop tailored ambiguity sets for the problem context. The available reference information for constructing ambiguity sets depend on the problem context. In some situations, there could be some special reference information. It is encouraged to utilized problem-specific information to construct effective ambiguity sets (Noyan et al. 2022).
- Design adaptive decision criteria for the operational objective. The decision criteria basically rely on operations managers' objective. It is encouraged to communicate with managers to understand their need. On the other hand, Decision criteria greatly affect tractability, so it is encouraged to wisely choose a criterion (Wang et al. 2023b).
- Reduce a complex model to a simple equivalence effectively. DRO models often face computational and tractable issues. A common approach is to derive a tractable counterpart via duality theory. However, this is not always the case (Fan and Hanasusanto 2024).
- Develop efficient computational methods. Even if a tractable counterpart can be obtained, when solving large-scale models, the computational efficiency can be low. It is thus encouraged to design efficient computational approach (Sadana and Delage 2023).

Regarding **Chapter 3**, the current research considers the optimal targeted travel restriction policy under pandemics, and future studies could be conducted following the below pointers:

- The model's inputs could be significantly improved by using artificial intelligence (Choi et al. 2022) and data analytics (Liu et al. 2023) to predict each city's risk state. Rather than relying on static probabilities, machine learning models could dynamically forecast risk by integrating real-time data streams like population mobility, public health capacity, vaccination rates, and even wastewater surveillance data, providing a more accurate and timely description.
- A dynamic, multi-period framework could be developed where policies are updated periodically as new information becomes available (Hu et al. 2025). This would create an adaptive control system where the optimization model recalibrates travel restrictions weekly or bi-weekly, allowing for a more agile and responsive pandemic management strategy. This adaptive approach could also endogenize local response capabilities, modeling how a city's own investments in testing or healthcare directly influence its risk profile over time.
- Future work could incorporate a multi-objective optimization framework to explicitly manage the inherent trade-offs in pandemic response (Robinson et al. 2023). Instead of focusing on a single objective under a budget, this approach would simultaneously optimize for public health outcomes, economic vitality, and social equity. This would provide policymakers with a clearer view of the Pareto frontier, allowing them to make more informed decisions by understanding the precise trade-offs between saving lives and preserving economic activity.

Regarding **Chapter 4**, the current study investigates under what conditions intentionally downgrading service quality may benefit service operators, which can be further extended in four directions:

- Future models could incorporate follower heterogeneity in a multi-follower Stackelberg game. In reality, competing firms possess different market shares, brand reputations, and cost structures. Analyzing a market with asymmetric followers would be more technically challenging but would yield more realistic insights into how firms with varying levels of market power react to a leader's strategic moves (Carvalho et al. 2024).
- The current work pioneers the use of DRO for demand ambiguity but assumes demands are independent (Bakshi and Mohan, 2024). A valuable extension would be to model the correlation between competing firms' demands, as a service change by one company directly impacts its rivals.
- The prediction of the post-SDS market size could be enhanced by leveraging big data technologies (Choi et al. 2018). Future models could incorporate real-time data from social media or customer reviews to dynamically forecast the market's reaction to a service change, providing a more precise estimation of the demand shock.
- Future research could explore alternative competitive structures beyond the static Stackelberg model (Borgs et al. 2014). A multi-period dynamic game, for instance, would be a valuable

extension to capture the long-term effects of service and loyalty decisions, such as the gradual erosion or rebuilding of brand equity over time.

References

Abbasi B, Babaei T, Hosseinifard Z, Smith-Miles K, Dehghani M (2020) Predicting solutions of large-scale optimization problems via machine learning: A case study in blood supply chain management. Computers & Operations Research 119:104941.

Abdulrashid I, Zanjirani Farahani R, Mammadov S, Khalafalla M (2025) Transport behavior and government interventions in pandemics: A hybrid explainable machine learning for road safety. Transportation Research Part E: Logistics and Transportation Review, 193, 103841.

Aftabi N, Li D, Sharkey, TC (2025) An integrated cyber-physical framework for worst-case attacks in industrial control systems. *IISE Transactions*, published online.

Aghajani M, Torabi SA, Altay N (2023) Resilient relief supply planning using an integrated procurement-warehousing model under supply disruption. Omega 118:102871.

Agrawal S, Ding YC, Saberi A, Ye Y (2012) Price of correlations in stochastic optimization. Operations Research, 60(1), 150-162.

Andersson J, Jörnsten K, Nonås SL, Sandal L, Ubøe J (2013). A maximum entropy approach to the newsvendor problem with partial information. European Journal of Operational Research, 228(1), 190-200.

Andoh EA, Yu H (2023) A two-stage decision-support approach for improving sustainable last-mile cold chain logistics operations of COVID-19 vaccines. Annals of operations research 328(1):75-105.

Angelus A, Özer Ö (2022) On the large-scale production of a new vaccine. Production and Operations Management 31(7):3043-3060.

Araz OM, Choi TM, Olson DL, Salman FS (2020) Role of analytics for operational risk management in the era of big data. Decision Sciences 51(6):1320-1346.

Ardestani-Jaafari A, Delage E (2016). Robust optimization of sums of piecewise linear functions with application to inventory problems. Operations Research, 64(2), 474-494.

August T, Noh D, Shamir N, Shin H (2024) Cyberattacks, operational disruption, and investment in resilience measures. Management Science.

Avishan F, Elyasi M, Yanıkoğlu, İ, Ekici A, Özener O Ö (2023). Humanitarian relief distribution problem: An adjustable robust optimization approach. Transportation Science, 57(4), 1096-1114.

Banker RD, Khosla, Sinha KK (1998) Quality and competition. Management Science 44(9):1179-1192.

Bakshi N, Mohan S (2024). Information dependency in mitigating disruption cascades. Manufacturing & Service Operations Management, 26(6), 2050-2066.

Bansal A, Berg B, Huang YL (2021) A distributionally robust optimization approach for coordinating clinical and surgical appointments. IISE transactions, 53(12), 1311-1323.

Battisti E, Alfiero S, Leonidou E (2022) Remote working and digital transformation during the COVID-19 pandemic: Economic–financial impacts and psychological drivers for employees. Journal of Business Research 150:38-50.

Benders JF (1962) Partitioning procedures for solving mixed-variables programming problems. Numerische mathematik, 4(1), 238-252.

Ben-Tal A, Nemirovski A (1998). Robust convex optimization. Mathematics of Operations Research, 23(4), 769-805.

Ben-Tal A, Nemirovski A (2002) Robust optimization–methodology and applications. Mathematical programming 92:453-480.

Ben-Tal A, Den Hertog D, De Waegenaere A, Melenberg B, Rennen G (2013) Robust solutions of optimization problems affected by uncertain probabilities. Management Science, 59(2), 341-357.

Bertsimas D, Brown DB, Caramanis C (2011) Theory and applications of robust optimization. SIAM review 53(3):464-501.

Bimpikis K, Candogan O, Ehsani S (2019) Supply disruptions and optimal network structures. Management Science, 65(12), 5504-5517.

Birge JR, Louveaux F (2011). Introduction to stochastic programming: Springer Science & Business Media.

Birge JR, Candogan O, Feng Y (2022) Controlling epidemic spread: Reducing economic losses with targeted closures. Management Science, 68(5), 3175-3195.

Birge JR, Capponi A, Chen P-C (2023) Disruption and rerouting in supply chain networks. Operations Research 71(2):750-767.

Boloori A, Saghafian S (2023) Health and economic impacts of lockdown policies in the early stage of COVID-19 in the united states. Service Science 15(3):188-211.

Bonardi JP, Gallea Q, Kalanoski D, Lalive R (2023) Managing pandemics: How to contain COVID-19 through internal and external lockdowns and their release. Management Science 69(9):5316-5335.

Borgs C, Candogan O, Chayes J, Lobel I, Nazerzadeh H (2014) Optimal multiperiod pricing with service guarantees. Management Science, 60(7), 1792-1811.

Boutilier JJ, Chan TCY (2020). Ambulance emergency response optimization in developing countries. Operations Research, 68(5), 1315-1334.

Brown S, Sinha S, Schaefer AJ (2024) Markov decision process design: A framework for integrating strategic and operational decisions. Operations Research Letters 54:107090.

Carlsson JG, Behroozi M, Mihic K (2018) Wasserstein distance and the distributionally robust TSP. Operations Research, 66(6), 1603-1624.

Carøe CC, Schultz R (1999) Dual decomposition in stochastic integer programming. Operations Research Letters, 24(1-2), 37-45.

Carvalho M, Dragotto G, Feijoo F, Lodi A, Sankaranarayanan S (2024) When Nash meets stackelberg. Management Science, 70(10), 7308-7324.

Chakravarty A, Saboo AR, Xiong G (2022) Marketing's and operations' roles in product recall prevention: Antecedents and consequences. Production and Operations Management 31(3):1174-1190.

Chan TCY, Shen ZJM, Siddiq A (2018). Robust defibrillator deployment under cardiac arrest location uncertainty via row-and-column generation. Operations Research, 66(2), 358-379.

Chan CW, Green LV, Lekwijit S, Lu L, Escobar G (2019) Assessing the impact of service level when customer needs are uncertain: An empirical investigation of hospital step-down units. Management Science 65(2):751-775.

Charpin R, Cousineau M (2025) Friendshoring: How geopolitical tensions affect foreign sourcing, supply base complexity, and sub-tier supplier sharing. International Journal of Operations & Production Management 45(5):1006-1031.

Chen Z, Sim M, Xu H (2019). Distributionally robust optimization with infinitely constrained ambiguity sets. Operations Research, 67(5), 1328-1344.

Chen Z, Xie W (2021). Regret in the newsvendor model with demand and yield randomness. Production and Operations Management, 30(11), 4176-4197.

Chen J, Yao J, Zhang Q, Zhu X (2023a) Global disaster risk matters. Management Science 69(1):576-597.

Chen Z, Kong G (2023b) Hospital admission, facility-based isolation, and social distancing: An SEIR model with constrained medical resources. Production and Operations Management 32(5):1397-1414.

Cheng C, Adulyasak Y, Rousseau L-M (2021) Robust facility location under demand uncertainty and facility disruptions. Omega 103:102429.

China Govenrment (2022) COVID-19 quarantine and test policy. Accessed 15 Jun 2025, https://www.gov.cn/xinwen/2022-11/21/content_5728107.htm/.

China Customs (2024) Announcement on preventing monkeypox from spreading into China. Accseed 2025 March 13, http://xiamen.customs.gov.cn/manzhouli_customs/566020/3392762/566021/6045737/index/.

Chinazzi M, Davis JT, Ajelli M, Gioannini C, et al (2020) The effect of travel restrictions on the spread of the 2019 novel coronavirus (COVID-19) outbreak. Science, 368(6489), 395-400.

Chiu CH, Choi TM, Li Y, Xu L (2014) Service competition and service war: A game-theoretic analysis. Service Science 6(1):63-76.

Chiu CH, Choi TM (2016) Supply chain risk analysis with mean-variance models: A technical review. Annals of Operations Research 240(2):489-507.

Choi TM (2020a) Innovative “bring-service-near-your-home” operations under corona-virus (COVID-19 /SARS-COV-2) outbreak: Can logistics become the messiah? Transportation Research Part E: Logistics and Transportation Review 140:101961.

Choi TM (2021) Fighting against COVID-19: What operations research can help and the sense-and-respond framework. Annals of Operations Research, Mar 5, 1-17.

Choi TM, Wallace SW, Wang Y (2018) Big data analytics in operations management. Production and operations management, 27(10), 1868-1883.

Choi TM, Chung SH, Zhuo X (2020) Pricing with risk-sensitive competing container shipping lines: Will risk seeking do more good than harm? Transportation Research Part B: Methodological 133:210-229.

Choi TM, Kumar S, Yue X, Chan HL (2022) Disruptive technologies and operations management in the industry 4.0 era and beyond. Production and Operations Management 31(1):9-31.

Chou YC, Chuang HHC, Chou P, Oliva R (2023) Supervised machine learning for theory building and testing: Opportunities in operations management. Journal of Operations Management 69(4):643-675.

Chun SY, Ovchinnikov A (2019) Strategic consumers, revenue management, and the design of loyalty programs. Management Science 65(9):3969-3987.

Chun SY, Iancu DA, Trichakis N (2020) Loyalty program liabilities and point values. Manufacturing & Service Operations Management 22(2):257-272.

Chung SH, Tse YK, Choi TM (2015) Managing disruption risk in express logistics via proactive planning. Industrial Management & Data Systems 115(8):1481-1509.

Chung SH, Wallace SW, Wen X (2025) Data driven operational risk management. *Annals of Operations Research* 348(2), 777-781.

Cottle R, Johnson E, Wets R (2007) George b. Dantzig (1914–2005). Notices of the AMS 54(3):344-362.

Dalal J, Üster H (2021). Robust emergency relief supply planning for foreseen disasters under evacuation-side uncertainty. Transportation Science, 55(3), 791-813.

Das B, Dhara A, Natarajan K (2021). On the heavy-tail behavior of the distributionally robust newsvendor. Operations Research, 69(4), 1077-1099.

Delage E, Ye Y (2010) Distributionally robust optimization under moment uncertainty with application to data-driven problems. Operations research 58(3):595-612.

Dolgui A, Ivanov D (2021) Ripple effect and supply chain disruption management: New trends and research directions. International Journal of Production Research 59(1):102-109.

Dong L, Kouvelis P (2020) Impact of tariffs on global supply chain network configuration: Models, predictions, and future research. Manufacturing & Service Operations Management 22(1):25-35.

Dou G, Choi TM (2024) Compete or cooperate? Effects of channel relationships on government policies for sustainability. European Journal of Operational Research 313(2), 718-732.

Dukkanci O, Koberstein A, Kara BY (2023) Drones for relief logistics under uncertainty after an earthquake. European Journal of Operational Research 310(1):117-132.

Eftekhar M, Jeannette Song J-S, Webster S (2022) Prepositioning and local purchasing for emergency operations under budget, demand, and supply uncertainty. Manufacturing & Service Operations Management 24(1):315-332.

Erbeyoğlu G, Bilge Ü (2020) A robust disaster preparedness model for effective and fair disaster response. European Journal of Operational Research 280(2):479-494.

Fan D, Zhou Y, Yeung AC, Lo CK, Tang C (2022) Impact of the us–china trade war on the operating performance of us firms: The role of outsourcing and supply base complexity. Journal of Operations Management 68(8):928-962.

Fan X, Hanasusanto GA (2024) A decision rule approach for two-stage data-driven distributionally robust optimization problems with random recourse. INFORMS Journal on Computing, 36(2), 526-542.

Fang H, Wang L, Yang Y (2020) Human mobility restrictions and the spread of the Novel Coronavirus (2019-nCoV) in China. Journal of Public Economics, 191, 104272.

Faramarzi-Oghani S, Neghabadi PD, Zanjirani Farahani R (2025) Failed Deliveries in Last-Mile Logistics: A Taxonomy and Research Roadmap. IEEE Transactions on Engineering Management, published online.

Fardi K, Ghasemzadeh F, Zanjirani Farahani R, Asgari N, Laker B, Ruiz R (2025) The impact of frequency and magnitude of natural disasters on inventory prepositioning. European Journal of Operational Research, 322(2), 511-540.

Freund D, Hssaine C (2025) Fair incentives for repeated engagement. Production and Operations Management 34(1):16-29.

Fu Q, Sim CK, Teo CP (2018) Profit sharing agreements in decentralized supply chains: A distributionally robust approach. Operations Research 66(2):500-513.

Gallego G, Ryan JK, Simchi-Levi D (2001). Minimax analysis for finite-horizon inventory models. IIE Transactions, 33(10), 861-874.

Gao R, Kleywegt A (2023) Distributionally robust stochastic optimization with wasserstein distance. Mathematics of Operations Research 48(2):603-655.

Gmira M, Gendreau M, Lodi A, Potvin J-Y (2021) Managing in real-time a vehicle routing plan with time-dependent travel times on a road network. Transportation Research Part C: Emerging Technologies 132:103379.

Goh J, Sim M (2010). Distributionally robust optimization and its tractable approximations. Operations Research, 58(4-part-1), 902-917.

Gopalakrishnan A, Jiang Z, Nevskaya Y, Thomadsen R (2021) Can non-tiered customer loyalty programs be profitable? Marketing Science 40(3):508-526.

Gu W, Luan X, Song Y, Shang J (2022) Impact of loyalty program investment on firm performance: Seasonal products with strategic customers. European Journal of Operational Research 299(2), 621-630.

Gu W, Yu X, Zhang S, Yan X, Wang C (2023) To outsource or not: Bike-share rebalancing strategies under the service quality deviation of a third party. European Journal of Operational Research 310(2), 847-859.

Guo L (2023a) Overage charge or loyalty discount: When should extra consumptions be penalized or rewarded? Marketing Science 42(3):614–633.

Guo X, Kuang Y, Ng CT (2023b). To centralize or decentralize: Mergers under price and quality competition. Production and Operations Management, 32(3), 844-862.

Gupta S, Modgil S, Meissonier R, Dwivedi YK (2021) Artificial intelligence and information system resilience to cope with supply chain disruption. IEEE Transactions on Engineering Management 71:10496-10506.

Gupta S, Starr MK, Zanjirani Farahani R, Asgari N (2022) OM forum—pandemics/epidemics: Challenges and opportunities for operations management research. Manufacturing & Service Operations Management 24(1):1-23.

Hamdan B, Diabat A (2020) Robust design of blood supply chains under risk of disruptions using lagrangian relaxation. Transportation research part E: logistics and transportation review 134:101764.

Han Q, Du D, Zuluaga LF (2014). Technical note—A risk- and ambiguity-averse extension of the max-min newsvendor rrder formula. Operations Research, 62(3), 535-542.

Handfield RB, Graham G, Burns L (2020) Corona virus, tariffs, trade wars and supply chain evolutionary design. International Journal of Operations & Production Management 40(10):1649-1660.

He R, Lu Y (2021). A robust price-setting newsvendor problem. Production and Operations Management, 30(1), 276-292.

Hekimoğlu MH, Park JH, Kazaz B (2024) Service at risk in delivery operations. Decision Sciences 55(1):33-56.

Hezarkhani B, Arisian S, Mansouri A (2023) Global agricultural supply chains under tariff-rate quotas. Production and Operations Management 32(11):3634-3649.

Hodgson MJ (1990) A flow-capturing location-allocation model. Geographical Analysis, 22(3), 270-279.

Hsieh CT, Rossi-Hansberg E (2023) The industrial revolution in services. Journal of Political Economy Macroeconomics 1(1):3-42.

Hu K, Allon G, Bassamboo A (2022) Understanding customer retrials in call centers: Preferences for service quality and service speed. Manufacturing & Service Operations Management 24(2):1002-1020.

Hu J, Chen Z, Wang S (2025) Budget-driven multiperiod hub location: A robust time-series approach. Operations Research, 73(2), 613-631.

Hua Y, Zhao D, Wang X, Li X (2019) Joint infrastructure planning and fleet management for one-way electric car sharing under time-varying uncertain demand. Transportation Research Part B: Methodological, 128, 185-206.

Huang Y, Lin C, Liu S, Tang H (2023) Trade networks and firm value: Evidence from the us-china trade war. Journal of International Economics 145:103811.

Ivanov D (2020) Predicting the impacts of epidemic outbreaks on global supply chains: A simulation-based analysis on the coronavirus outbreak (COVID-19 /SARS-COV-2) case. Transportation Research Part E: Logistics and Transportation Review 136:101922.

Ivanov D, Dolgui A (2022) The shortage economy and its implications for supply chain and operations management. International Journal of Production Research 60(24):7141-7154.

Jain N, Girotra K, Netessine S (2022) Recovering global supply chains from sourcing interruptions: The role of sourcing strategy. Manufacturing & Service Operations Management 24(2):846-863.

Jafarian A, Granberg TA, Zanjirani Farahani R (2025) The effect of geographic risk factors on disaster mass evacuation strategies: A smart hybrid optimization. Transportation Research Part E: Logistics and Transportation Review, 193, 103825.

Jammernegg W, Kischka P (2009). Risk preferences and robust inventory decisions. International Journal of Production Economics, 118(1), 269-274.

Jia JS, Lu X, Yuan Y, Xu G, Jia J, Christakis NA (2020) Population flow drives spatio-temporal distribution of COVID-19 in China. Nature, 582(7812), 389-394.

Jin Y, Ryan JK (2012) Price and service competition in an outsourced supply chain. Production and Operations Management 21(2):331-344.

Kaplan EH (2020) OM Forum—COVID-19 scratch models to support local decisions. Manufacturing & Service Operations Management, 22(4), 645-655.

Kaushik M, Guleria N (2020) The impact of pandemic COVID-19 in workplace. European Journal of Business and Management 12(15):1-10.

Kim BD, Shi M, Srinivasan K (2001) Reward programs and tacit collusion. Marketing Science 20(2):99-120.

Kim S, Pasupathy R, Henderson SG (2014) A guide to sample average approximation. Handbook of simulation optimization:207-243.

Kimball MS (1993) Standard risk aversion. Econometrica, 61(3), 589-611.

Kochhar R, Sechopoulos S (2022) COVID-19 pandemic pinches finances of America's lower- and middle-income families. Pew Research.

Koklic MK, Kukar-Kinney M, Vegelj S (2017) An investigation of customer satisfaction with low-cost and full-service airline companies. Journal of Business Research 80:188-196.

Korpeoglu CG, Körpeoğlu E, Cho S-H (2020) Supply chain competition: A market game approach. Management Science 66(12):5648-5664.

Kraemer MUG, Yang CH, Gutierrez B, Wu CH, et al (2020) The effect of human mobility and control measures on the COVID-19 epidemic in China. Science, 368(6490), 493-497.

Kumar K, Pandey NK, Verre F, Shah R (2025) Cybersecurity Challenges in the Digitization and Integration of Renewable Energy Systems: A Review. *IEEE Transactions on Engineering Management*, published online.

Kwon YW, Sheu JB, Talluri S, Yoon J, Yoo SH (2024) Performance of quantity discount contract under supply and demand disruptions. IEEE Transactions on Engineering Management 71:5782-5797.

Lai S, Ruktanonchai NW, Zhou L, Prosper O, et al (2020) Effect of non-pharmaceutical interventions to contain COVID-19 in China. Nature, 585(7825), 410-413.

Laporte G, Louveaux F (1993) The integer L-shaped method for stochastic integer programs with complete recourse. Operations Research Letters, 13(3), 133-142.

Laporte G, Louveaux F, van Hamme L (2002) An integer L-shaped algorithm for the capacitated vehicle routing problem with stochastic demands. Operations Research, 50(3), 415-423.

Lee E, Minner S (2024) How power structure and markup schemes impact supply chain channel efficiency under price-dependent stochastic demand. European Journal of Operational Research 318(1), 297-309.

Leung WS, Li J, Sun J (2020) Labor unionization and supply-chain partners' performance. Production and Operations Management 29(5):1325-1353.

Lewis M (2004) The influence of loyalty programs and short-term promotions on customer retention. Journal of Marketing Research 41(3):281-292.

Li D (1993) On general multiple linear-quadratic control problems. IEEE Transactions on Automatic Control 38(11):1722-1727.

Li D, Sun X (2006) Nonlinear integer programming (Springer Science & Business Media).

Li Y, Lin Z, Xu L, Swain A (2015) "Do the electronic books reinforce the dynamics of book supply chain market?"– A theoretical analysis. European Journal of Operational Research 245(2), 591-601.

Li YL, Chung SH (2019). Disaster relief routing under uncertainty: A robust optimization approach. IISE Transactions, 51(8), 869-886.

Li Y, Wen X, Choi TM, Chung SH (2022) Optimal establishments of massive testing programs to combat COVID-19: A perspective of parallel-machine scheduling-location (scheloc) problem. IEEE Transactions on Engineering Management 71:13380-13395.

Li H, Delage E, Zhu N, Pinedo M, Ma S (2024a) Distributional robustness and inequity mitigation in disaster preparedness of humanitarian operations. Manufacturing & Service Operations Management 26(1):197-214.

Li S, Aprahamian H (2024b) An optimization-based framework to minimize the spread of diseases in social networks with heterogeneous nodes. IISE Transactions, 56(2), 128-142.

Lim W (2023) Transformative marketing in the new normal: A novel practice-scholarly integrative review of business-to-business marketing mix challenges, opportunities, and solutions. Journal of Business Research 160:113638.

Lim F, Chun SY, Satopää V (2024) Loyalty currency and mental accounting: Do consumers treat points like money? Manufacturing & Service Operations Management 26(5):1878-1896.

Lin Y, Fan D, Shi X, Fu M (2021) The effects of supply chain diversification during the COVID-19 crisis: Evidence from Chinese manufacturers. Transportation Research Part E: Logistics and Transportation Review 155:102493.

Lin F, Fang X, Gao Z (2022a) Distributionally robust optimization: A review on theory and applications. Numerical Algebra, Control and Optimization 12(1):159-212.

Lin S, Chen Y, Li Y, Shen Z-JM (2022b). Data-driven newsvendor problems regularized by a profit risk constraint. Production and Operations Management, 31(4), 1630-1644.

Lin J, Aprahamian H, El-Amine H (2024) Optimal unlabeled set partitioning with application to risk-based quarantine policies. IISE Transactions, 56(2), 143-155.

Liu E, Barker K, Chen H (2022) A multi-modal evacuation-based response strategy for mitigating disruption in an intercity railway system. Reliability Engineering & System Safety 223:108515.

Liu H, Perera SC, Wang JJ, Leonhardt JM (2023) Physician engagement in online medical teams: A multilevel investigation. Journal of Business Research, 157, 113588.

Liu J, Xiong Y, Deng Y, Wang S (2025) Data-driven reliable shelter location during hurricane evacuation. IISE Transactions, published online.

Loeys S, Boute RN, Antonio K (2025) The use of IoT sensor data to dynamically assess maintenance risk in service contracts. European Journal of Operational Research published online.

Long DZ, Qi J, Zhang A (2024) Supermodularity in two-stage distributionally robust optimization. Management Science, 70(3), 1394-1409.

Luciano E, Peccati L, Cifarelli DM (2003) VaR as a risk measure for multiperiod static inventory models. International Journal of Production Economics 81-82:375-384.

Luo S, Choi TM (2022) E-commerce supply chains with considerations of cyber-security: Should governments play a role? Production and Operations Management 31(5):2107-2126.

Luo S, Choi TM (2024) Great partners: How deep learning and blockchain help improve business operations together. Annals of Operations Research 339(1):53-78.

Lv Z, Qiao L, Mardani A, Lv H (2022) Digital twins on the resilience of supply chain under COVID-19 pandemic. IEEE Transactions on Engineering Management, 71:10522-10533.

Mak HY, Dai T, Tang CS (2022) Managing two-dose COVID-19 vaccine rollouts with limited supply: Operations strategies for distributing time-sensitive resources. Production and operations management 31(12):4424-4442.

McCrie R, Lee S (2021) Security operations management (Butterworth-Heinemann).

McEntire DA (2021) Disaster response and recovery: Strategies and tactics for resilience (John Wiley & Sons).

Meneses M, Santos D, Barbosa-Póvoa A (2023) Modelling the blood supply chain. European journal of operational research 307(2):499-518.

Modgil S, Singh RK, Foropon C (2022) Quality management in humanitarian operations and disaster relief management: A review and future research directions. Annals of operations research:1-54.

Mor A, Speranza MG (2022) Vehicle routing problems over time: A survey. Annals of Operations Research 314(1):255-275.

Nagurney A (2021) Supply chain game theory network modeling under labor constraints: Applications to the COVID-19 pandemic. European journal of operational research 293(3):880-891.

Natarajan K, Sim M, Uichanco J (2018). Asymmetry and ambiguity in newsvendor models. Management Science, 64(7), 3146-3167.

Nayal K, Raut RD, Queiroz MM, Priyadarshinee P (2023) Digital supply chain capabilities: Mitigating disruptions and leveraging competitive advantage under COVID-19. IEEE Transactions on Engineering Management 71:10441-10454.

Nemirovski A, Shapiro A (2007). Convex approximations of chance constrained programs. SIAM Journal on Optimization 17(4): 969-996.

Ng TS, Fowler J, Mok I (2012). Robust demand service achievement for the co-production newsvendor. IIE Transactions, 44(5), 327-341.

Ni W, Shu J, Song M (2018). Location and Emergency Inventory Pre-Positioning for Disaster Response Operations: Min-Max Robust Model and a Case Study of Yushu Earthquake. Production and Operations Management, 27(1), 160-183.

Ninh A, Hu H, Allen D (2019). Robust newsvendor problems: effect of discrete demands. Annals of Operations Research, 275(2), 607-621.

Ninh A (2021). Robust newsvendor problems with compound Poisson demands. Annals of Operations Research, 302(1), 327-338.

Niu B, Zhang J, Shen Z (2023) Could early warning combat demand disruption caused by endemics and pandemics? Benefit and dilemma analysis. IEEE Transactions on Engineering Management 71:13285-13295.

Noorizadegan M, Seifi A, Esmaeeli H, Zanjirani Farahani R (2025) Preemptive facility interdiction under damage uncertainty. Transportation Research Part E: Logistics and Transportation Review, 197, 104081.

Noyan N, Rudolf G, Lejeune M (2022) Distributionally robust optimization under a decision-dependent ambiguity set with applications to machine scheduling and humanitarian logistics. INFORMS Journal on Computing, 34(2), 729-751.

Nunes JC, Drèze X (2006) Your loyalty program is betraying you. Harvard business review 84(4), 124.

Oroojlooyjadid A, Nazari M, Snyder LV, Takáč M (2022) A deep q-network for the beer game: Deep reinforcement learning for inventory optimization. Manufacturing & Service Operations Management 24(1):285-304.

Ouyang X, Chung SH (2025a) DRO in operations: An introduction. Encyclopedia in operations management (Elsevier).

Ouyang X, Chung SH, Choi TM (2025b) Optimal targeted intercity travel restriction policies. Working paper.

Paciarotti C, Valiakhmetova I (2021) Evaluating disaster operations management: An outcome-process integrated approach. Production and operations management 30(2):543-562.

Pathy SR, Rahimian H (2023) A resilient inventory management of pharmaceutical supply chains under demand disruption. Computers & Industrial Engineering 180:109243.

Perakis G, Roels G (2008). Regret in the newsvendor model with partial information. Operations Research, 56(1), 188-203.

Perakis G, Singhvi D, Skali Lami O, Thayaparan L (2023) COVID-19: A multi-wave SIR-based model for learning waves. Production and Operations Management 32(5):1471-1489.

Peters K, Silva S, Gonçalves R, Kavelj M, Fleuren, et al. (2021) The nutritious supply chain: optimizing humanitarian food assistance. INFORMS Journal on Optimization, 3(2), 200-226.

Piret J, Boivin G (2020) Pandemics throughout history. Front Microbiol 11, 631736.

Qiu R, Shang J, Huang X (2014). Robust inventory decision under distribution uncertainty: A CVaR-based optimization approach. International Journal of Production Economics, 153, 13-23.

Qiu R, Sun M, Lim YF (2017). Optimizing (s, S) policies for multi-period inventory models with demand distribution uncertainty: Robust dynamic programing approaches. European Journal of Operational Research, 261(3), 880-892.

Rahimian H, Bayraksan G, Homem-de-Mello T (2019). Controlling risk and demand ambiguity in newsvendor models. European Journal of Operational Research, 279(3), 854-868.

Rahimian H, Mehrotra S (2022). Frameworks and results in distributionally robust optimization. Open Journal of Mathematical Optimization, published online.

Rahmaniani R, Crainic TG, Gendreau M, Rei W (2017).The Benders decomposition algorithm: A literature review. European Journal of Operational Research, 259(3), 801-817.

Razavi N, Gholizadeh H, Nayeri S, Ashrafi TA (2021) A robust optimization model of the field hospitals in the sustainable blood supply chain in crisis logistics. Journal of the Operational Research Society 72(12):2804-2828.

Revelle C (1993) Facility siting and integer-friendly programming. European Journal of Operational Research, 65(2), 147-158.

Rezapour S, Zanjirani Farahani R, Tajik N (2021) Impact of timing in post-warning prepositioning decisions on performance measures of disaster management: A real-life application. European Journal of Operational Research 293(1):312-335.

Robinson KF, DuFour MR, Fischer JL, et al. (2023). Lessons Learned in Applying Decision Analysis to Natural Resource Management for High-Stakes Issues Surrounded by Uncertainty. Decision Analysis, 20(4), 326-342.

Rockafellar RT, Uryasev S (2000) Optimization of conditional value-at-risk. Journal of Risk 2:21-42.

Rossi F and Chintagunta PK (2023) Consumer loyalty programs and retail prices: Evidence from gasoline markets. Marketing Science 42(4):794-818.

Sadana U, Delage E (2023) The value of randomized strategies in distributionally robust risk-averse network interdiction problems. INFORMS Journal on Computing, 35(1), 216-232.

Saghafian S, Tomlin B (2016). The newsvendor under demand ambiguity: Combining data with moment and tail information. Operations Research, 64(1), 167-185.

Sanci E, Daskin MS (2021) An integer L-shaped algorithm for the integrated location and network restoration problem in disaster relief. Transportation Research Part B: Methodological, 145, 152-184.

Saputro TE, Figueira G, Almada-Lobo B (2021) Integrating supplier selection with inventory management under supply disruptions. International Journal of Production Research 59(11):3304-3322.

Sawik T (2020) Supply chain disruption management (Springer).

Sazvar Z, Tafakkori K, Oladzad N, Nayeri S (2021) A capacity planning approach for sustainable-resilient supply chain network design under uncertainty: A case study of vaccine supply chain. Computers & industrial engineering 159:107406.

Scarf HE, Arrow K, Karlin S (1957) A min-max solution of an inventory problem (Rand Corporation Santa Monica).

Scarf H (1958). A min max solution of an inventory problem. Studies in the mathematical theory of inventory and production.

Secchi E, Roth A, Verma R (2019) The impact of service improvisation competence on customer satisfaction: Evidence from the hospitality industry. Production and Operations Management 28(6):1329-1346.

Shalpegin T, Kumar A, Browning TR (2025) Undiversity, inequity, and exclusion in supply chains: The unintended fallout of economic sanctions and consumer boycotts. Production and Operations Management 34(4):829-836.

Shams Eddin M, El-Amine H, Aprahamian H (2025) The impact of early large-scale screening on the evolution of pandemics. IISE Transactions, 57(5), 509-523.

Sheth JN, Uslay C (2023) The geopolitics of supply chains: Assessing the consequences of the Russo-Ukrainian war for b2b relationships. Journal of Business Research 166:114120.

Shi P, Helm JE, Heese HS, Mitchell AM (2021) An operational framework for the adoption and integration of new diagnostic tests. Production and Operations Management 30(2):330-354.

Shi X, Tang J, Dong C (2022) Should a domestic firm carve out a niche in overseas markets? Value of purchasing agents. European Journal of Operational Research 300(1), 85-94.

Singh SS, Jain DC, Krishnan TV (2008) Research note—customer loyalty programs: Are they profitable? Management Science 54(6):1205-1211.

Siqin T, Choi TM, Chung SH (2022) Optimal E-tailing channel structure and service contracting in the platform era. Transportation Research Part E: Logistics and Transportation Review 160:102614.

So KC (2000) Price and time competition for service delivery. Manufacturing & Service Operations Management 2(4):392-409.

Song J, Yang W, Zhao C (2024) Decision-dependent distributionally robust Markov decision process method in dynamic epidemic control. IISE Transactions, 56(4), 458-470.

South China Morning Post (2021) Hong Kong fourth wave: Just 3.57 million arrivals in 2020 amid coronavirus pandemic. Accessed 15 Jun 2025, https://www.scmp.com/news/hong-kong/hong-kong-economy/article/.

Steeger G, Lohmann T, Rebennack S (2018) Strategic bidding for a price-maker hydroelectric producer: Stochastic dual dynamic programming and Lagrangian relaxation. IISE Transactions, 50(11), 929-942.

Sun X, Chung SH, Choi TM, Sheu JB, Ma HL (2020) Combating lead-time uncertainty in global supply chain's shipment-assignment: Is it wise to be risk-averse? Transportation Research Part B: Methodological 138:406-434.

Sun YY, Li M, Lenzen M, Malik A, Pomponi F (2022a) Tourism, job vulnerability and income inequality during the COVID-19 pandemic: A global perspective. Annals of Tourism Research Empirical Insights, 3(1), 100046.

Sun J, Makosa L, Yang J, Darlington M, Yin F, Jachi M (2022b) Economic sanctions and shared supply chains: A firm-level study of the contagion effects of smart sanctions on the performance of nontargeted firms. European Management Review 19(1):92-106.

Sun L, Xie W, Witten T (2023) Distributionally robust fair transit resource allocation during a pandemic. Transportation Science, 57(4), 954-978.

Tapiero CS (2005) Value at risk and inventory control. European Journal of Operational Research 163(3):769-775.

Tsay AA, Agrawal N (2000) Channel dynamics under price and service competition. Manufacturing & Service Operations Management 2(4):372-391.

Uichanco J (2022) A model for prepositioning emergency relief items before a typhoon with an uncertain trajectory. Manufacturing & Service Operations Management 24(2):766-790.

Vanany I, Ali MH, Tan KH, Kumar A, Siswanto N (2021) A supply chain resilience capability framework and process for mitigating the COVID-19 pandemic disruption. IEEE Transactions on Engineering Management 71:10358-10372.

Vanli OA, Tsekeni DE (2025) Inference of human contact networks based on epidemic data. IISE Transactions on Healthcare Systems Engineering, 15(1), 15-31.

Walsman MC, Dixon MJ (2020) Fee-based loyalty programs: An empirical investigation of benefit redemption behavior and its effects on loyalty. Service Science 12(2-3):100-118.

Wang Y, Wallace SW, Shen B, Choi TM (2015) Service supply chain management: A review of operational models. European Journal of Operational Research 247(3):685-698.

Wang Y, Wang Z, Hu X, Xue G, Guan X (2022) Truck–drone hybrid routing problem with time-dependent road travel time. Transportation Research Part C: Emerging Technologies 144:103901.

Wang Y, Xiao L, Luo XG (2023a). On the optimal solution of a distributionally robust multi-product newsvendor problem. Journal of the Operational Research Society, 1-15.

Wang Y, Zhang Y, Zhou M, Tang J (2023b) Feature-driven robust surgery scheduling. Production and Operations Management, 32(6), 1921-1938.

Wen X, Ouyang X, Choi TM, Chung SH (2025) Less is more in service operations: When is it wise to offer less? Working paper.

WHO (2024a) WHO declares mpox global health emergency. Accessed 15 Jul 2025, https://www.bbc.com/news /articles/cvg35w27gzno/.

WHO (2024b) Mpox. Accessed 15 Jul 2025, https://www.who.int/news-room/fact-sheets/detail/mpox/.

WHO (2025) WHO COVID-19 dashboard. Accessed 15 Jul 2025, https://data.who.int/dashboards/covid19/.

Wiberg H, Dai T, Lam H, Kulkarni R (2025) Synergizing Artificial Intelligence and Operations Research: Perspectives from INFORMS Fellows on the Next Frontier. INFORMS Journal on Data Science.

Wu J, Yue W, Yamamoto Y, Wang S (2006) Risk analysis of a pay to delay capacity reservation contract. Optimization Methods and Software 21(4):635-651.

Wu L, Wu X, Yi S (2024) Tariff hedging with a new supplier? An analysis of sourcing strategies under competition. Production and Operations Management 33(4):903-921.

Xu Z, Elomri A, Kerbache L, El Omri A (2020) Impacts of COVID-19 on global supply chains: Facts and perspectives. IEEE engineering management review 48(3):153-166.

Xu L, Zheng Y, Jiang L (2022). A robust data-driven approach for the newsvendor problem with nonparametric information. Manufacturing & Service Operations Management, 24(1), 504-523.

Xu L, Zhang C, Xu Z, Long DZ (2025) A Nonparametric Robust Optimization Approach for Chance-Constrained Knapsack Problem. SIAM Journal on Optimization, 35(2), 739-766.

Xu X, Siqin T, Chung SH, Choi TM (2023) Seeking survivals under COVID-19: The WhatsApp platform's shopping service operations. Decision Sciences 54(4):375-393.

Xu X, Sethi SP, Chung SH, Choi TM (2024) Ordering COVID-19 vaccines for social welfare with information updating: Optimal dynamic order policies and vaccine selection in the digital age. IISE Transactions 56(7):729-745.

Yang L, Cui S, Wang Z (2022) Design of COVID-19 testing queues. Production and Operations Management 31(5):2204-2221.

Yang J, Shi J (2023) Discrete-item inventory control involving unknown censored demand and convex inventory costs. Production and Operations Management 32(1):45-64.

Ye Y, Jiao W, Yan H (2020) Managing relief inventories responding to natural disasters: Gaps between practice and literature. Production and Operations Management 29(4):807-832.

Yesudhas D, Srivastava A, Gromiha MM (2021) COVID-19 outbreak: History, mechanism, transmission, structural studies and therapeutics. Infection, 49(2), 199-213.

Yin X, Bushaj S, Yuan Y, Büyüktahtakın, İ E (2024) COVID-19: Agent-based simulation-optimization to vaccine center location vaccine allocation problem. IISE Transactions, 56(7), 699-714.

Yoon J, Alkhudary R, Talluri S, Féniès P (2025) Risk management and macroeconomic disruptions in supply chains: The role of blockchain, digital twins, generative AI, and quantum computing. *IEEE Transactions on Engineering Management*, published online.

Yu Y, Dong Y, Guo X (2018) Pricing for sales and per-use rental services with vertical differentiation. European Journal of Operational Research 270(2), 586-598.

Zanjirani Farahani R, Fallah S, Ruiz R, Hosseini S, Asgari N (2019) OR models in urban service facility location: A critical review of applications and future developments. European Journal of Operational Research 276(1):1-27.

Zhang F, Wu X, Tang CS, Feng T, Dai Y (2020a) Evolution of operations management research: From managing flows to building capabilities. Production and Operations Management 29(10):2219-2229.

Zhang H, Chao X, Shi C (2020b) Closing the gap: A learning algorithm for lost-sales inventory systems with lead times. Management Science 66(5):1962-1980.

Zhang Y, Zhang Z, Lim A, Sim M (2021a) Robust data-driven vehicle routing with time windows. Operations Research, 69(2), 469-485.

Zhang Z, Luo Z, Baldacci R, Lim A (2021b). A benders decomposition approach for the multivehicle production routing problem with order-up-to-level policy. Transportation Science, 55(1), 160-178.

Zhang W, Shao C, Hu B, Zhou J, Cao M, Xie K, Siano P, Li W (2022) Proactive security-constrained unit commitment against typhoon disasters: An approximate dynamic programming approach. IEEE Transactions on Industrial Informatics 19(5):7076-7087.

Zhang C, Ayer T, White CC, Bodeker JN, Roback JD (2023) Inventory sharing for perishable products: Application to platelet inventory management in hospital blood banks. Operations Research 71(5):1756-1776.

Zhang L, Yang J, Gao R (2024). Optimal robust policy for feature-based newsvendor. Management Science, 70(4), 2315-2329.

Zhang T, Jia F, Chen L (2025a) Blockchain adoption in enabling disruptive supply chain finance innovation: Towards a research agenda. *IEEE Transactions on Engineering Management*, published online.

Zhang R, Xie C, Long DZ (2025b) A data-driven robust optimization model for repositioning problem in bike-sharing systems. Transportation Research Part E: Logistics and Transportation Review, 201, 104192.

Zhao N, Yao S, Thomadsen R, Wang CB (2024) The impact of government interventions on COVID-19 spread and consumer spending. Management Science, 70(5), 3302-3318.

Zheng M, Dong S, Wang Q, Xia T, Pan E (2023) Sourcing decisions with time-varying emergency order costs and production disruption during environmental enforcement campaigns. IEEE Transactions on Engineering Management 71:6874-6886.

Zhou Y, Li S, Kundu T, Choi TM, Sheu JB (2025) Travel bubble policies for air traffic restoration during pandemics. Risk Analysis, 45(1), 14-39.

Zhu Z, Zhang J, Ye Y (2013). Newsvendor optimization with limited distribution information. Optimization Methods and Software, 28(3), 640-667.

Appendices

Appendix I. Supplementary Information

I.1. Intercity Migration Network in China

China has hundreds of cities, enabling us to construct large-scale intercity travel networks. We choose 125 big cities of over 400 million people, ranging from 406 million to 3,017 million, including all metropolitans like Shanghai, Beijing, and Shenzhen. The migration flows between any two cities are simulated by the well-established gravity model (Hodgson, 1990). In particular, let W_i and W_j denote the population of city i and j, and d_{ij} denote the travel distance between. The flows between these two cities are approximated by

$$flow_{ij} = W_i W_j / d_{ij}^{1.5}.$$

During the COVID-19 pandemic, the city risk states in China were classified into four levels (i.e., no-, low- mid-, and high-risk). We add another one risk state to capture the severe state like the Wuhan outbreak in early 2020. The travel restriction levels on migration flows are considered to be Level 1 to Level 5, weakest to strongest. For simplicity, the reduction of a particular migration flow, $flow_{ij}$, due to respective five restriction levels are assumed to be 10%, 30%, 50%, and 70% of $flow_{ij}$.

Regarding the policy cost, the daily average spending per person in 2022 was around USD 9.3 in mainland (China Government 2023). We consider a two-week travel restriction duration, and hence, the consumption loss per person is about USD 130. Let $TL_j = 130\sum_{i\in[N]} flow_{ij}$ be the total consumption loss due to inflow reduction to city j. The risk state-dependent policy budget is considered to be proportional to the total consumption loss (see **Table A3.1**). The costs saved by the implemented restriction on a flow in pandemic deterioration are assumed to be 10% of the current cost. Regarding the objective function, we adopt a squared root function regarding policy cost, which is nondecreasing and concave. Let c_{ij} be the cost of restricting flow (i, j). The resulting utility is $u_{ij} = 130 flow_{ij}\sqrt{c_{ij}/130 flow_{ij}}$.

Table A3.1. City Risk State Dependent Policy Budgets.

City Risk State	Policy Budget
No Risk	Zero
Low Risk	10%* TL_j
Medium Risk	20%* TL_j
High Risk	30%* TL_j
Very High-Risk	50%* TL_j

We simulate the city risk states at the current outbreak by randomly selecting one of low- and mid-risk, with equal probabilities. Regarding possible risk states in pandemic deterioration, suppose a city is at medium risk at the current outbreak. Then, its possible risk states in the future are either medium-, high-, or very-high-risk, implying that the pandemic in this city stays stable or worsens. The probabilities of these states are also randomly generated.

I.2. Supplements to Societal Impact Study

The policymaker in the remaining study is the provincial government of Guangdong, which coordinates the province-wide TRPs for 21 cities. Unless stated, the weights of the pandemic control performance are 0.6 and 0.4, respectively for the current outbreak and potential deterioration scenarios in the future.

I.2.1. Migration in Guangdong in Early COVID-19 Outbreak

Guangdong province is the most developed area in South China, with a territory of 177,900 km^2 and a GDP of USD 1.83 trillion in 2023 (China Briefing, 2023). Around 127.07 million people live there in 21 cities of various development levels, including two metropolitans (i.e., Guangzhou and Shenzhen) (Statista 2023). Hence, the insights derived from Guangdong are expected to help countries of similar territorial, economic, and population scales (e.g., many Western European countries, South Korea, Brazil, and Florida State). With the date of the Wuhan Lockdown (i.e., 2020 January 23) as the midpoint, we consider a four-week duration (i.e., from 2020 January 09 to 2020 February 06) to simulate the early outbreak of COVID-19 in Guangdong. We want to examine the efficacy of the intercity TRPs applied to this early outbreak. While inbound travelers to Guangdong cities come from around the globe, we focus on intercity migration within Guangdong only.

We obtain the accurate numbers of inbound travelers (for tourism purposes only) to 21 Guangdong cities by the Statistical Yearbook of Economy (China Breau of Statistics 2024) and Social Development officially issued by municipal governments. These inbound travelers come from the entire mainland China and overseas. To identify the inbound travelers from Guangdong cities, we adopt the Baidu Migration Database (2024). The database records the daily ratio of inflows from any city to a certain destination to the total inflows of that destination city since the beginning of 2019. We use the average value of such ratios during the four-week period as the surrogate ratio to compute the migration flows between two cities. For example, the total inbound travelers to Guangzhou in 2020 was 41.83 million. Then, on average, the four-week period has total inflows of 3.22 million (52 weeks per year). The average inflow ratio from Shenzhen is 6.7%. The total inflows from Shenzhen to Guangzhou are thus 3.22*6.7%=0.216 million. In doing so, we obtain the migration flows between any two Guangdong cities during the early outbreak.

I.2.2. Policy Costs Suffered by the Tourism Sector

While various sectors can be impacted by intercity TRPs, the tourism sector could be the most affected industry, since travel with tourism purposes greatly decreases (Polemis 2021). Analyzing the impacts of TRPs on the tourism sector is a promising reference to the policy impacts on the entire economy. The TRP of a certain level will reduce the inbound travelers to a city. We next establish the relationship between the inflows reduced and the tourism sector revenue reduced by real-world data. To begin, we extract the tourism revenues and inbound travelers of 21 Guangdong cities in 2019 and 2020 (see **A3.2**). Since Guangdong imposed various TRPs during the entire 2020, both revenue and travelers dropped significantly in 2020. The drop ratios are reported in Columns Revenue Drop (%) and Traveler Drop (%). Notably, we uncover that the revenue drop ratio is not proportional to the traveler drop ratio, exhibiting a nonlinear relationship. For example, the travelers to Dongguan declined by 13%, whereas the revenue drop ratio was up to 46.6%, over triple. The same observation appears in Heyuan, whose traveler drop was 33.1% and the revenue drop was 89.1%. In other words, in a converse view, the sector revenue grows increasingly faster with travelers.

Table A3.2. Parameters of traveler inflow and tourism revenue model.

City	Tourism Revenue 2019 (CNY 10^9)	Tourism Revenue 2020 (CNY 10^9)	Sector Revenue Drop (%)	Inbound Travelers 2019 (10,000)	Inbound Travelers 2020 (10,000)	Traveler Drop (%)	Weight λ
Shenzhen	1715.45	1383.76	19.3	6718.03	4998.81	25.6	0.7949
Guangzhou	4457.69	2679.07	39.9	6767.94	4182.59	38.2	0.7615
Foshan	479.28	325.05	32.2	2099.39	1757.19	16.3	0.6185
Dongguan	684.10	366.70	46.4	4456.57	3876.53	13.0	0.4934
Huizhou	570.00	250.78	56.0	6541.0	2220.69	66.0	1.0740
Zhuhai	541.55	187.63	65.4	4618.21	1514.69	67.2	0.9070
Maoming	476.09	88.62	81.4	1551.29	801.00	48.4	0.3306
Jiangmen	146.79	103.34	29.6	1243.61	989.91	20.4	0.6696
Zhongshan	190.89	120.45	36.9	1103.50	817.69	25.9	0.6602
Zhanjiang	201.64	147.60	26.8	1254.02	1058.39	15.6	0.6508
Shantou	568.81	234.92	58.7	2346.42	1396.12	40.5	0.5810
Zhaoqing	371.22	68.67	81.5	1434.04	501.70	65.0	0.4851
Jieyang	362.75	37.01	89.8	2354.50	265.61	88.7	0.8612
Qingyuan	155.65	90.90	41.6	1077.44	826.40	23.3	0.5997
Yangjiang	349.50	161.12	53.9	2711.76	1705.70	37.1	0.6027
Shaoguan	98.54	60.80	38.3	803.69	596.34	25.8	0.6477
Meizhou	551.34	106.96	80.6	4997.47	1264.36	74.7	0.7008
Chaozhou	398.25	199.93	49.8	2629.47	1607.34	38.9	0.6655
Shanwei	172.58	69.02	60.0	971.50	505.44	48.0	0.6466
Heyuan	357.66	53.35	85.1	4020.57	635.41	84.2	0.8797
Yunfu	345.46	221.02	36.0	3537.99	2304.36	34.9	0.7593

We thus consider the well-established exponential cost function (Luo and Choi 2022, Guo et al. 2023) for modeling the observed nonlinear relationship. In the classic exponential cost function, we have $c = e^{\lambda d}$, where d denotes total inflows, c is revenue, and λ controls the increase rate. To better adapt our problem, we modify the classic one as follows:

$$R_{poster-TRPs} = R_{prior-TRPs}\left(e^{\lambda r} - 1\right).$$

In particular, $R_{prior-TRPs}$ is the sector revenue before imposing TRPs, which is known, and $R_{poster-TRPs}$ is the revenue after TRPs. The variable $r = Inflows_{poster} / Inflows_{prior}$ is the ratio of inflows after TRPs to that before, and parameter λ controls the revenue sensitivity to inflow change. We obtain the critical parameter λ by the real tourism data in 2019 and 2020 as follows:

$$\lambda = \log\left(\frac{R_{2020}}{R_{2019}} + 1\right) \Big/ \frac{Inflows_{2020}}{Inflows_{2019}}.$$

In doing so, we derive λ of the 21 cities by their historical tourism data.

To implement the model, consider a migration flow (i, j) and suppose it reduces by 50% after TRPs. The resulting revenue is thus $R_{prior-TRPs}^{(i,j)}\left(e^{\lambda_j \cdot 50\%} - 1\right)$, where $R_{prior-TRPs}^{(i,j)}$ is the revenue of city j related to travelers from city i. Since there is no official statistical data on this, we estimate such flow-dependent revenue similarly in Section 6.1.1 by the Baidu Migration Database. For example, the four-week average inflow ratio from Shenzhen to Guangzhou is 6.7%, and the total revenue of Guangzhou in 2019 is CNY 4.46×10^{12}. Then, the resulting revenue is

$$R_{prior-4\text{weeks}}^{(\text{Shenzhen,Guangzhou})} = \text{CNY}4.46 \times 10^{12} \times 6.6\% \times \tfrac{4}{52} = \text{CNY}22.98 \times 10^{9}.$$

I.2.3. Policy Costs Suffered by Tourism Professionals

The direct impacts of TRPs on individuals are loss of income or unemployment. Regarding the unemployment brought by TRPs, we follow Sun et al. (2022), where the unemployed tourism workers are considered to be proportional to tourism revenue decline as follows:

$$U = E\left(1 - \frac{R_{post-TRPs}}{R_{prior-TRPs}}\right),$$

where E is the number of total employees before imposing TRPs. For example, Guangzhou had 566.35 thousand tourism professionals at the end of 2019, and its tourism revenue dropped by 39.9% in 2020. The resulting unemployment is thus $566.35 \times 39.9\% = 225.97$ thousand. We further note that the effective duration of TRPs also affects unemployment. In particular, while TRPs immediately reduce travelers and revenue, unemployment may not immediately occur. To capture this feature, we modify the original unemployment model as follows:

$$U = E\left(2 - e^{\lambda r}\right)\left(e^{\beta w} - 1\right).$$

In particular, the term $2 - e^{\lambda r} = 1 - \left(e^{\lambda r} - 1\right)$ is drawn from our inflow-revenue model, which reflects the revenue drop. The weight $e^{\beta w} - 1$ captures the impact of the effective duration of TRPs on unemployment.

When the effective duration equals zero (i.e., $w=0$), the weight also equals zero. We consider when the duration is half a year, the weight becomes one (i.e., $e^{26\beta}-1=1$). In this case, the model coincides with the original one. In other words, as the effective duration increases, the impacts of TRPs on unemployment become more obvious. Note that parameter β can be city dependent; that is, different cities have different sensitivities to policy effective durations. For simplicity, for all 21 cities, we adopt a uniform value $\lambda=\frac{1}{26}\log 2\approx 2.66\%$.

Table A3.3. Employment and incomes of tourism professionals in the 21 Guangdong cities.

City	Tourism Employment 2019 (10^4)	Estimated Unemployment after TRPs	Disposable Income 2019 (CNY 10^4)	Salary Loss (CNY 10^4)	Relief Fund Cost (CNY 10^4)
Shenzhen	59.124	4,628	6.488	3,752.86	3,752.86
Guangzhou	56.635	9,147	6.830	7,810.10	7,810.10
Foshan	23.390	3,047	5.625	2,142.15	2,142.15
Dongguan	28.825	5,414	5.653	3,825.70	3,825.70
Huizhou	1.080	245	3.975	121.58	121.58
Zhuhai	10.213	2,702	5.594	1,889.13	1,889.13
Maoming	0.944	311	2.460	95.61	95.61
Jiangmen	0.827	99	3.367	41.68	41.68
Zhongshan	1.926	288	5.275	189.75	189.75
Zhanjiang	0.620	67	2.499	21.01	21.01
Shantou	8.148	1,936	2.822	682.99	682.99
Zhaoqing	0.749	247	2.612	80.69	80.69
Jieyang	0.182	66	2.182	18.04	18.04
Qingyuan	6.133	1,033	2.606	336.37	336.37
Yangjiang	4.019	877	3.231	354.16	354.16
Shaoguan	0.612	95	2.755	32.66	32.66
Meizhou	5.190	1,693	2.387	505.31	505.31
Chaozhou	0.269	54	2.330	15.82	15.82
Shanwei	0.154	37	2.443	11.42	11.42
Heyuan	4.943	1,702	2.229	474.37	474.37
Yunfu	0.484	71	2.231	19.68	19.68

The lives of tourism workers who lost their jobs during the COVID-19 pandemic were significantly impacted by TRPs. In fact, tourism professionals are sensitive to income change as they are often in the mid and lower income tier of a city, and unemployment could lead to more pain in their lives (Kochhar and Sechopoulos 2022). To quantify the cost suffered by unemployed people, we assume the average time needed to find a new job is 1.5 months, and hence, the economic loss of each employed worker is at least a 1.5-month salary. The monthly salary is drawn from the average disposable income of a city in 2019. For example, the average annual disposable income of Guangzhou was CNY 68,300 in 2019. An unemployed tourism worker in Guangzhou lost at least CNY 8,538. Our unemployment model shows that around 9,147 tourism workers will lose their jobs due to the four-week TRPs. Their economic loss is CNY 78.1 million.

We note that the economic cost paid by individuals is far less than that of the sector (i.e., business owners). This may underestimate the cost paid by individuals since TPRs only decrease business owners' profits but cut all income of an unemployed person. To help unemployed people, many governments established unemployment relief funds during the pandemic. For example, in the U.S., one can get unemployment benefits the first week they become unemployed, up to a maximum of 26 weeks (i.e., around 6 months) in a year (US Center on Budget and Policy 2025). Hence, policymakers should consider not only the economic cost paid directly by unemployed people but also unemployment compensation to pay. In our case study, we consider a 1.5-month compensation. The 1.5-month relief fund costs are reported in the last column in **Table A3.3**. The compensation cost also reflects policymakers' concern for people's livelihood and social welfare. A more humanitarian policymaker could put more relief fund costs into the model.

I.2.4. Evaluation of Pandemic Control Performances

We quantify the performance of our intercity TRPs through the infections reduced. To this end, we need to model the relationship between inflows and imported infections. In this research direction, Jia et al. (2020) apply log-transformation to aggregate inflows from Wuhan and accumulative infections at destination cities from 2020 early January to February 19 (see **Figure A3.1**). They find that after the log-transformation, the infections are approximately linearly related to the inflows, and hence propose a multiplicate exponential model, which captures various features (e.g., inflows from Wuhan, city GDP, and population).

For simplicity, we adopt a reduced version of their model, which captures inflow volume and origin city risk state only. In particular, let x_{ji} be the inflows of $\left(j,i\right)$. The imported infections in city i are modeled by $\log\left(y_{ji}\right)=c_j+\alpha_j\log\left(x_{ji}\right)$, where parameters c_j and α_j are related to the risk state of origin city j. This simplified model aligns with the fact that when the origin city is highly risky (i.e., larger α_j), its outflows could cause more infections at destination cities. To estimate c_j and α_j of different risk-state cities, we refer to the infection data of Jia et al. (2020). In **Figure A3.1**, red dots are cities adjacent to Wuhan, which face the most serious outbreak. We use them to estimate the parameters of very high risky cities. In contrast, light purple dots contain cities far away from Wuhan, and their outbreak is much more controllable. We use them to estimate the parameters of low risky cities. Parameters of inflow origin cities of different risk states are shown in **Table A3.4**.

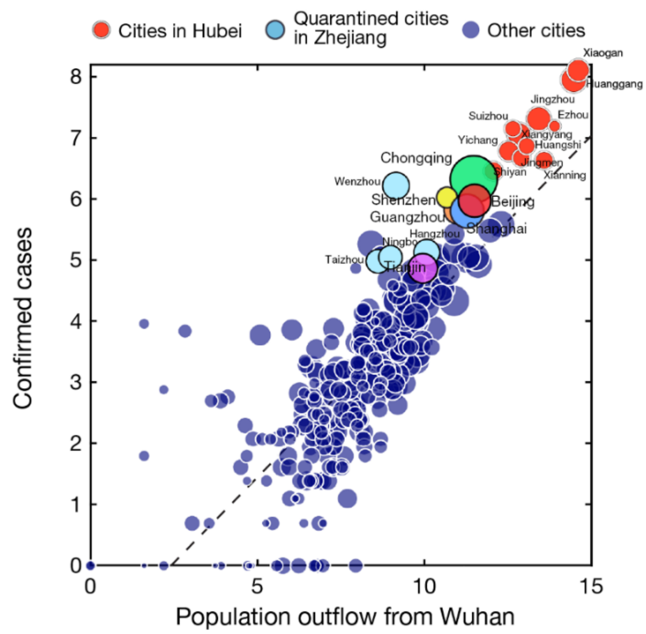

Figure A3.1. Infections of mainland cities and inflows from Wuhan by 19 February 2020.

Table A3.4. Infection model parameters regarding the risk states of inflow origin cities.

Risk State of Inflow Origin City	c	α
Low risk	-0.596	0.465
Medium risk	-0.751	0.531
High risk	-1.136	0.602
Very high risk	-1.552	0.692

Given imported infections, we further compute the resulting deaths by means of the Case Fatality Rate (CFR), which is the ratio of deaths to confirmed cases. Yang et al. (2020) use a linear regression approach to model CFR by the COVID-19 data at the early outbreak in mainland China (i.e., from January 10 to February 03, 2020). They consider four datasets, which correspond to different outbreak states: i) Wuhan, ii) Hubei Province, iii) mainland China except for Hubei, and iv) mainland China. Each data set yields an associated linear regression model. The deaths of a city are considered to depend on the pandemic control ability (e.g., healthcare resources) of this city. Hence, we use these four models to formulate the deaths in cities of different pandemic control abilities. The highest ability is denoted by Level IV, whereas the lowest one is Level I. Given the total infections caused by all inflows to city i, denoted by y_i, the possible deaths are modeled by

$$z_i = \begin{cases} 0.05246 y_i + 1.668, \text{ Level I} \\ 0.02099 y_i + 4.418, \text{ Level II} \\ 0.01413 y_i + 0.076, \text{ Level III} \\ 0.00149 y_i + 2.299, \text{ Level IV} \end{cases}.$$

In summary, our infection model determines the number of imported infections by inflows and the risk state of flow origin city, whereas our death model characterizes total infections and healthcare resources of destination cities. We evaluate the pandemic control ability of a city by healthcare staff per thousand people (see **Table A3.5**).

Table A3.5. Healthcare staff and pandemic control abilities.

City	Healthcare Staffs 2020 (10,000)	Population 2019 (10,000)	Healthcare Staffs per 1,000 people	Pandemic Control Ability Level
Guangzhou	17.78	1530.59	11.62	Level IV
Zhuhai	2.07	202.37	10.22	Level IV
Shenzhen	13.03	1343.88	9.70	Level IV
Shaoguan	2.48	303.04	8.18	Level III
Zhongshan	2.72	338.00	8.04	Level III
Huizhou	3.88	488.00	7.94	Level III
Foshan	6.09	815.86	7.47	Level III
Dongguan	5.89	846.45	6.96	Level III
Heyuan	2.15	310.56	6.92	Level III
Yangjiang	1.72	257.09	6.69	Level III
Qingyuan	2.59	388.58	6.68	Level III
Zhaoqing	2.64	418.71	6.31	Level III
Meizhou	2.65	438.30	6.05	Level III
Jiangmen	2.75	463.03	5.95	Level II
Zhanjiang	4.24	736.00	5.75	Level II
Maoming	3.67	641.15	5.72	Level II
Shantou	2.83	566.48	4.99	Level I
Yunfu	1.15	254.52	4.51	Level I
Jieyang	2.72	610.50	4.46	Level I
Shanwei	1.28	301.50	4.25	Level I
Chaozhou	1.12	265.98	4.19	Level I

I.2.5. Policy Implementation: Budget and Inbound Permission

We next consider the budget to implement TRPs. Due to the absence of some critical data on Guangdong cities, we infer the policy budget by means of insights derived from Hong Kong, which is adjacent to Guangdong, and also applied long-term TRPs to inbound travelers from the mainland and overseas. As mentioned, when a policymaker faces a severe outbreak, more resources (e.g., labor and healthcare resources) are expected to be invested in controlling pandemics. In this case, the policymaker is willing to limit more inbound travelers to reduce potential imported infections.

We estimate the policy budget by the ratio of anti-epidemic investment to city GDPs. In particular, in 2020, the most challenging year, the Hong Kong government built an anti-epidemic fund of HKD 348.27 billion to fight against COVID-19 (HK Government 2023), accounting for around 12.44% of its GDP in 2019. The tourism sector, as one of the four pillar industries of Hong Kong, is considered to evenly share ¼ of this anti-epidemic found, which accounts for about 3.2% of the GDP. The government implemented strict TRPs for inbound travelers all over the world in 2020. The arrivals to Hong Kong declined by around

93.6% in comparison with 2019 (HK Tourism Board 2023). Based on these observations, we roughly infer that when facing a severe outbreak, a policymaker is willing to invest 3.2% of the city's GDP and sacrifice 95% of inflows, in terms of the cost of the tourism sector. This inference of policy budget and inflow reduction works as the upper bound of that in our case study. Based on the analysis of Hong Kong, analogically, a city in Guangdong province is considered to adopt the following budget when it is in a certain risk state (see **Table A3.6**). In fact, Hong Kong's GDP for 2020 witnessed a 4.99% decline from 2019. Since the decline came from various sectors, it should be reasonable that a four-week travel restriction reduces GDP by 0.27% at most.

Table A3.6. City risk state dependent policy budgets.

City Risk State	Whole-Year Policy Budget (% of GDP 2019)	Four-week Policy Budget (% of GDP 2019)
Low risk	1.0%	0.09%
Medium risk	2.0%	0.17%
High risk	2.5%	0.21%
Very high risk	3.2%	0.27%

We next illustrate the implementation of TRPs. While in the previous analysis, we interpret the impact of TRPs on inbound travelers by a reduction ratio, implementing TRPs is not simply to limit the quota of travelers from certain cities. We refer to the TRPs of the Hong Kong government, which contain a series of actions (e.g., testing, quarantine, and monitoring). These actions are complex, time-consuming, and expensive, significantly discouraging inbound travelers and finally reducing inflow. In particular, according to TRPs effected in June 2021, Hong Kong classifies the risk states of inbound travelers' origin cities into four groups (HK Government 2023b). Each group corresponds to a certain quarantine duration, self-monitoring duration, and tests (see **Table A3.7** for details). These measures are expensive, especially quarantine in a hotel. The average price per night of Hong Kong hotels in 2021 is around HKD 836 (Statista 2023), and hence, a 21-day quarantine costs around HKD 17,566. These expensive measures greatly decrease the number of inbound travelers to Hong Kong.

Table A3.7. TRPs of Hong Kong for inbound travelers in June 2021.

TRPs	Origin Cities
1. Undergo compulsory quarantine for 21 days in a designated quarantine hotel 2. Undergo 4 tests during compulsory quarantine; 3. Self-monitoring in the subsequent 7 days; 4. Compulsory testing on the 26th day of arrival in Hong Kong at any Community Testing Centre (CTC).	Group A (Extremely and very high-risk), e.g., **Brazil, India, Nepal, Philippines, South Africa, Ireland, and Indonesia.**
1. Undergo compulsory quarantine for 21 days in a designated quarantine hotel; 2. Undergo 4 tests during compulsory quarantine.	Group B (High-risk), e.g., Italy, Japan, the United States of America, and Vietnam

1. Undergo compulsory quarantine for 14 days in a designated quarantine hotel; 2. Undergo 3 tests during compulsory quarantine; 3. Self-monitoring in the subsequent 7 days; 4. Compulsory testing on the 16th and 19th days of arrival in Hong Kong.	Group C (Medium-risk), e.g., Mainland China, Taiwan, and Maco.
1. Undergo compulsory quarantine for 7 days in a designated quarantine hotel; 2. Undergo 2 tests during compulsory quarantine; 3. Self-monitoring in the subsequent 7 days; 4. Compulsory testing on the 12th day of arrival in Hong Kong.	Group D (Low-risk), e.g., Australia and New Zealand.

Back to the policy in Guangdong, we consider five travel restriction levels (see **Table A3.8**). Level 1 means no restriction while Level 5 is the highest restriction. The reduction ratio can be origin-destination dependent, and a policymaker can make a more accurate estimation. For simplicity, we consider a uniform reduction ratio here; that is, imposing a certain level of TRP leads to the same reduction ratio for all flows.

Table A3.8. Impacts of TRPs on the number of inbound travelers.

TRPs	Inflows Reduced
Level 1	0%
Level 2	50%
Level 3	70%
Level 4	80%
Level 5	95%

I.2.6. Supplement tables in the policy study

Table A3.9. Initial risk states of 21 Guangdong cities in six simulated scenarios.

City	Initial City Risk State (1: Low, 2: Medium, 3: High, 4: Very High)					
	Scenario 1	Scenario 2	Scenario 3	Scenario 4	Scenario 5	Scenario 6
Guangzhou	3	1	1	3	1	3
Shaoguan	1	1	1	1	2	2
Shenzhen	3	1	1	3	1	3
Zhuhai	1	1	3	1	1	2
Shantou	1	1	1	1	1	2
Foshan	1	3	1	1	3	3
Jiangmen	1	1	1	1	1	2
Zhanjiang	1	1	1	1	1	3
Maoming	1	1	1	1	1	2
Zhaoqing	1	1	1	1	1	2
Huizhou	1	1	1	1	1	2
Meizhou	1	1	1	1	1	2
Shanwei	1	1	3	2	1	2
Heyuan	1	1	1	1	2	2
Yangjiang	1	1	3	2	1	3
Qingyuan	1	1	1	1	2	2
Dongguan	1	3	1	1	2	3
Zhongshan	1	1	1	2	1	2
Chaozhou	1	1	1	1	1	3
Jieyang	1	3	1	1	3	2
Yunfu	1	1	3	1	1	3

Table A3.10. Average restriction levels on outflows from a city with the objective of reducing infections.

City	Average Restriction Levels on Outflows: Targeted/Uniform					
	Scenario 1	Scenario 2	Scenario 3	Scenario 4	Scenario 5	Scenario6
Guangzhou	1.24 / 1	1.05 / 1	1.00 / 1	1.29 / 1	1.00 / 1	1.33 / 1
Shaoguan	1.76 / 2	1.67 / 1	1.81 / 2	1.67 / 1	1.95 / 2	1.76 / 2

Shenzhen	1.43 / 1	1.05 / 1	1.14 / 1	1.48 / 1	1.05 / 1	1.48 / 1
Zhuhai	1.57 / 1	1.33 / 1	1.86 / 1	1.43 / 1	1.43 / 1	1.62 / 2
Shantou	1.71 / 1	1.62 / 1	1.76 / 1	1.67 / 1	1.71 / 1	1.76 / 1
Foshan	1.19 / 1	1.62 / 1	1.29 / 1	1.19 / 1	1.71 / 1	1.67 / 1
Jiangmen	1.57 / 1	1.48 / 1	1.67 / 2	1.48 / 1	1.57 / 1	1.52 / 1
Zhanjiang	1.62 / 1	1.52 / 1	1.76 / 1	1.57 / 1	1.62 / 1	1.90 / 1
Maoming	1.48 / 1	1.43 / 1	1.57 / 1	1.52 / 1	1.48 / 1	1.57 / 1
Zhaoqing	1.67 / 1	1.57 / 1	1.62 / 1	1.48 / 1	1.67 / 1	1.71 / 1
Huizhou	1.57 / 1	1.29 / 1	1.48 / 1	1.29 / 1	1.33 / 1	1.52 / 1
Meizhou	1.62 / 1	1.33 / 1	1.67 / 1	1.52 / 1	1.48 / 2	1.76 / 2
Shanwei	1.71 / 2	1.67 / 2	1.95 / 2	1.95 / 2	1.81 / 1	1.81 / 1
Heyuan	1.57 / 1	1.71 / 1	1.62 / 1	1.62 / 1	1.90 / 1	1.81 / 1
Yangjiang	1.52 / 1	1.76 / 2	1.95 / 2	1.90 / 2	1.71 / 2	1.86 / 2
Qingyuan	1.57 / 2	1.67 / 2	1.76 / 1	1.62 / 2	1.90 / 1	1.81 / 2
Dongguan	1.00 / 1	1.62 / 1	1.19 / 1	1.10 / 1	1.38 / 1	1.67 / 1
Zhongshan	1.24 / 1	1.14 / 1	1.43 / 1	1.67 / 1	1.24 / 1	1.33 / 1
Chaozhou	1.67 / 1	1.76 / 1	1.76 / 1	1.71 / 1	1.67 / 1	1.90 / 1
Jieyang	1.67 / 1	1.76 / 1	1.76 / 1	1.43 / 1	1.76 / 1	1.71 / 1
Yunfu	1.86 / 1	1.76 / 1	1.90 / 1	1.67 / 1	1.71 / 1	1.86 / 2

Table A3.10. Average restriction levels on outflows from a city with the objective of saving lives.

City	Average Restriction Levels on Outflows: Targeted/Uniform					
	Scenario 1	Scenario 2	Scenario 3	Scenario 4	Scenario 5	Scenario6
Guangzhou	1.38 / 1	1.24 / 1	1.10 / 1	1.33 / 1	1.14 / 1	1.43 / 1
Shaoguan	1.86 / 1	1.81 / 2	1.95 / 2	2.00 / 1	1.95 / 2	1.95 / 2
Shenzhen	1.48 / 1	1.29 / 1	1.19 / 1	1.48 / 1	1.29 / 1	1.43 / 1
Zhuhai	1.81 / 1	1.76 / 1	1.95 / 1	1.81 / 1	1.71 / 1	1.95 / 2
Shantou	1.90 / 1	1.86 / 1	1.81 / 1	1.90 / 1	1.95 / 1	1.76 / 1
Foshan	1.24 / 1	1.57 / 1	1.33 / 1	1.43 / 1	1.76 / 1	1.67 / 1
Jiangmen	1.81 / 1	1.81 / 1	1.71 / 2	1.71 / 1	1.71 / 1	1.71 / 1
Zhanjiang	1.86 / 1	1.71 / 1	1.90 / 1	1.81 / 1	1.71 / 1	2.05 / 1
Maoming	1.57 / 1	1.52 / 1	1.76 / 1	1.62 / 1	1.57 / 1	1.90 / 1
Zhaoqing	1.76 / 1	1.90 / 1	1.86 / 1	1.81 / 1	1.95 / 1	1.90 / 1
Huizhou	1.67 / 1	1.43 / 1	1.52 / 1	1.52 / 1	1.67 / 1	1.62 / 1
Meizhou	1.86 / 1	1.67 / 1	1.71 / 1	1.76 / 1	1.76 / 2	1.90 / 2
Shanwei	1.95 / 2	1.76 / 2	2.10 / 2	2.05 / 2	2.00 / 1	1.95 / 2
Heyuan	1.81 / 1	1.95 / 1	1.90 / 1	1.81 / 1	2.10 / 1	2.00 / 1
Yangjiang	1.76 / 2	2.00 / 2	2.05 / 2	1.95 / 2	1.76 / 2	2.00 / 2
Qingyuan	1.86 / 2	1.86 / 1	1.86 / 1	1.81 / 2	1.95 / 1	1.86 / 2
Dongguan	1.19 / 1	1.67 / 1	1.24 / 1	1.24 / 1	1.43 / 1	1.71 / 1
Zhongshan	1.52 / 1	1.43 / 1	1.62 / 1	1.71 / 1	1.52 / 1	1.62 / 1
Chaozhou	1.81 / 1	2.00 / 1	1.81 / 1	1.90 / 1	1.90 / 1	2.05 / 1
Jieyang	1.81 / 1	1.95 / 1	1.86 / 1	1.71 / 1	1.90 / 1	1.90 / 1
Yunfu	1.95 / 1	1.95 / 1	2.05 / 1	1.90 / 1	1.90 / 1	2.05 / 1

Table A3.11. Economic structures of 21 Guangdong cities.

City	2019 Tourism Revenue (CNY 10^9)	2019 City GDP (CNY 10^9)	Ratio of Tourism to Economy (%)
Guangzhou	4457.69	23628.60	18.87
Shaoguan	98.54	1353.49	7.47
Shenzhen	1715.45	26927.09	6.37
Zhuhai	541.55	3435.89	15.76
Shantou	568.81	2694.08	21.11
Foshan	479.28	10751.02	4.46
Jiangmen	146.79	3146.64	4.66
Zhanjiang	201.64	3065.00	6.58
Maoming	476.09	3252.34	14.64
Zhaoqing	371.22	2248.80	16.51
Huizhou	570.00	4177.41	13.64
Meizhou	551.34	1187.00	46.45
Shanwei	172.58	1080.30	15.98
Heyuan	357.66	1080.03	33.12
Yangjiang	349.50	1292.18	24.42
Qingyuan	155.65	1698.20	9.17
Dongguan	684.10	9482.50	7.21
Zhongshan	190.89	3101.10	6.16

Chaozhou	398.25	1080.94	36.84
Jieyang	362.75	2101.77	17.26
Yunfu	345.46	921.96	37.47

Appendix II. Mathematical Proofs

II.1. Mathematical Proofs for Chapter 3

Proof of Lemma 3.1. Submodularity is initially defined regarding a set function. We cannot directly adopt the definition of submodularity to analyze the recourse problem $u(\boldsymbol{x}, \mathrm{S})$ because the expression of scenario S reads a vector form rather than a set form. Thus, we will first interpret S in a set form and then prove the submodularity. Given $\mathrm{S} = \{r_1^{k_1}, \ldots, r_N^{k_N}\}$, we define its counterparts by means of power sets as

$$\hat{\mathrm{S}} \in \left\{ 2^{\{1,2,\ldots,r_j^{k_j}-1\}} \cup \{r_j^{k_j}\}, \forall j \in [N] \right\}.$$

Note that S and $\hat{\mathrm{S}}$ have the same impact on the total utility in a modified form of $u(\boldsymbol{x}, \cdot)$. To see that, note that the utility maximization problem $u(\boldsymbol{x}, \cdot)$is separable, and hence we reformulate each city's utility maximization problem as the following program:

$$u_j\left(\boldsymbol{x}, \hat{\mathrm{S}}\right) = \max_{\boldsymbol{y}_j} \sum_{i \in [N]} \sum_{l \in [L]} u_{ij}^l y_{ij}^l$$

subject to

$$\sum_{l \in [L]} y_{ij}^l = 1, \forall i \in [N],$$

$$\textstyle\sum_{l=k}^{L} y_{ij}^l \geq x_{ij}^k, \quad \forall i \in [N], k \in [L],$$

$$\sum_{i \in [N]} \sum_{l \in [L]} c_{ij}^l y_{ij}^l - \sum_{i \in [N]} \sum_{l \in [L]} s_{ij}^l x_{ij}^l \leq c_j + \max\left\{ c_j^{R_1} \mathrm{I}\left(r_j^1\right), \ldots, c_j^{R_j} \mathrm{I}\left(r_j^{R_j}\right) \right\},$$

$$y_{ij}^l \in \{0,1\}, \forall i \in [N], l \in [L].$$

In particular, c_j is the budget of city j at the first stage and $\hat{c}_j^k$ is the budget increment compared with c_j when the risk state is r_j^k at the second stage; that is, $c_j^k = c_j + \hat{c}_j^k$. The indicator $\mathrm{I}\left(r_j^k\right)$ equals one only if r_j^k's corresponding element in $\hat{\mathrm{S}}$ is also one. In set $\hat{\mathrm{S}}$, although a city could be associated with several risk states, by constraints (52), only the highest risk state truly impacts the restriction budget. Hence, we reach $u(\boldsymbol{x}, \mathrm{S}) = u\left(\boldsymbol{x}, \hat{\mathrm{S}}\right)$. Next, we aim to show $u(\boldsymbol{x}, \mathrm{S})$ is "hiddenly" submodular in vector S by showing that $u\left(\boldsymbol{x}, \hat{\mathrm{S}}\right)$ is submodular in set $\hat{\mathrm{S}}$. To this end, we need the following two definitions.

Definition a. Given two pandemic deteriorating scenarios S_1 and S_2, we say $\mathrm{S}_1 \subseteq \mathrm{S}_2$ if there exist $\hat{\mathrm{S}}_1$ and $\hat{\mathrm{S}}_2$ such that $\hat{\mathrm{S}}_1 \subseteq \hat{\mathrm{S}}_2$.

Definition b. Given a risk state r and a scenario S, we say $r \in \mathrm{S}$ if there exists $\hat{\mathrm{S}}$ such that $r \in \hat{\mathrm{S}}$.

Now, consider two sets satisfying $\mathrm{S}_1 \subseteq \mathrm{S}_2 \subseteq 2^{\Omega}$ and an arbitrary element $r \in 2^{\Omega} \setminus \mathrm{S}_2$ (i.e., a particular risk state), where set $\Omega = \left\{ r_j \in \left[R_j \right], \forall j \in \left[N \right] \right\}$ contains all cities' possible risk states in pandemic deterioration. To verify the submodularity, by one of the definitions of submodular functions (Nemhauser et al. 1978), it suffices to show

$$u\left(\boldsymbol{x}, \mathrm{S}_1 \cup \{r\}\right) - u\left(\boldsymbol{x}, \mathrm{S}_1\right) \geq u\left(\boldsymbol{x}, \mathrm{S}_2 \cup \{r\}\right) - u\left(\boldsymbol{x}, \mathrm{S}_2\right), \ \forall r \in 2^{\Omega} \setminus \mathrm{S}_2 .$$

Without loss of generality, we assume r captures the risk state of city j. Let $r_j^{k_A} \in \mathrm{A}$ be the highest risk state in state set A of city j, and let $r_j^{k_B} \in \mathrm{B}$ be the highest risk in another state set B such that $\mathrm{A} \subseteq \mathrm{B}$. Then, it follows that $r_j^{k_A} \leq r_j^{k_B}$ by definition We face three possible situations:

a) When $r \leq r_j^{k_A}$, it holds that

$$\begin{aligned} u\left(\boldsymbol{x}, \mathrm{S}_1 \cup \{r\}\right) - u\left(\boldsymbol{x}, \mathrm{S}_1\right) &= u_j\left(\boldsymbol{x}, \mathrm{S}_1 \cup \{r\}\right) - u_j\left(\boldsymbol{x}, \mathrm{S}_1\right) = 0 \\ &= u_j\left(\boldsymbol{x}, \mathrm{S}_2 \cup \{r\}\right) - u_j\left(\boldsymbol{x}, \mathrm{S}_2\right) = u\left(\boldsymbol{x}, \mathrm{S}_2 \cup \{r\}\right) - u\left(\boldsymbol{x}, \mathrm{S}_2\right). \end{aligned}$$

b) When $r_j^{k_A} \leq r \leq r_j^{k_B}$, it holds that

$$\begin{aligned} u\left(\boldsymbol{x}, \mathrm{S}_1 \cup \{r\}\right) - u\left(\boldsymbol{x}, \mathrm{S}_1\right) &= u_j\left(\boldsymbol{x}, \mathrm{S}_1 \cup \{r\}\right) - u_j\left(\boldsymbol{x}, \mathrm{S}_1\right) \geq 0 \\ &= u_j\left(\boldsymbol{x}, \mathrm{S}_2 \cup \{r\}\right) - u_j\left(\boldsymbol{x}, \mathrm{S}_2\right) = u\left(\boldsymbol{x}, \mathrm{S}_2 \cup \{r\}\right) - u\left(\boldsymbol{x}, \mathrm{S}_2\right). \end{aligned}$$

c) When $r_j^{k_B} \leq r$, it holds that

$$\begin{aligned} u\left(\boldsymbol{x}, \mathrm{S}_1 \cup \{r\}\right) - u\left(\boldsymbol{x}, \mathrm{S}_1\right) &= u_j\left(\boldsymbol{x}, \mathrm{S}_1 \cup \{r\}\right) - u_j\left(\boldsymbol{x}, \mathrm{S}_1\right) = \\ &= u_j\left(\boldsymbol{x}, \mathrm{S}_2 \cup \{r\}\right) - u_j\left(\boldsymbol{x}, \mathrm{S}_2\right) = u\left(\boldsymbol{x}, \mathrm{S}_2 \cup \{r\}\right) - u\left(\boldsymbol{x}, \mathrm{S}_2\right) \geq 0 . \end{aligned}$$

We thus conclude the set function $u\left(\boldsymbol{x}, \hat{\mathrm{S}}\right)$ is submodular in set $\hat{\mathrm{S}}$, and accordingly, the utility function $u\left(\boldsymbol{x}, \mathrm{S}\right)$ is "hiddenly" submodular in S. (*Q.E.D.*)

Proof of Proposition 3.1. While the key idea of the following proof is inspired by Lu et al. (2015), the random variables in our problem (i.e., the risk states of all cities at the second stage) admit much more complex realizations, which is not binary as in Lu et al. (2025). In addition, due to the hidden submodularity arising in our problem, the resulting proof is more technically demanding. The proof relies on a pair of constructed primal and dual solutions; the solutions admit the identical objective value and thus are respectively optimal by strong duality.

To begin, we construct an auxiliary set χ^v. Rank all cities' possible risk states in the decreasing order of their occurring probability. Express the resulting sequence $\{r(1),...,r(R)\}$ by L. The occurring probability of the v-th risk state in L (i.e., $r(v)$) is denoted by $q(v)$. For any $v \in [R]$, we extract the first v risk states in L to form a set $\{r(1),...,r(v)\}$. Note that if several risk states (e.g., $r(m), r(n),...,r(w)$) in this set such that $m < n < ... < w$ correspond to an identical city, we assign the value of the last risk state $r(w)$ to all previous ones (i.e., $r(m) \equiv r(n) \equiv ... = r(w)$). The resulting set is denoted by χ^v. We can interpret χ^v as the counterpart of a scenario by the way in the proof of **Lemma 3.1**. Also, define $\chi^v = \varnothing$ which corresponds to a scenario identical to the current outbreak. To help understand the structure of χ^v, consider the two-city network in section 3.2 with marginal distributions $\boldsymbol{q}_A = \{q_A^1 = q_A^2 = 0.5\}$ and $\boldsymbol{q}_B = \{q_B^1 = 0.7, q_B^2 = 0.3\}$. Ranking these four risk states in the decreasing order of probabilities $\{0.7, 0.5, 0.5, 0.3\}$ gives the sequence $\mathrm{L} = \{q_B^1, q_A^1, q_A^2, q_B^2\}$. By definition, the ordered risk state sequence reads that $q(1) = q_B^1$, $q(2) = q_A^1$, $q(3) = q_A^2$, and $q(4) = q_B^2$. Note that since $q_A^1 = q_A^2 = 0.5$, their positions are interchangeable. Then, the corresponding four constructed auxiliary sets write $\chi^1 = \{q_B^1\}$, $\chi^2 = \{q_B^1, q_A^1\}$, $\chi^3 = \{q_B^1, q_A^2, q_A^2\}$, and $\chi^3 = \{q_B^2, q_A^2, q_A^2, q_B^2\}$.

Now, given an arbitrary current restriction decision $\bar{\boldsymbol{x}}$, we aim to show

$$\min_{\mathrm{P} \in P} \mathrm{E}_{\mathrm{P}}\left[u\left(\bar{\boldsymbol{x}}, \tilde{\mathrm{S}}\right)\right] = \sum_{v \in \{0\} \cup [R]} \left(q(v) - q(v+1)\right) u\left(\bar{\boldsymbol{x}}, \chi^v\right).$$

The worst-case probability distribution can be derived by the following linear program:

$$\min_{\boldsymbol{p}} \sum_{\mathrm{S} \in \Xi} p(\mathrm{S}) u(\boldsymbol{x}, \mathrm{S})$$

subject to

$$\sum_{\mathrm{S} \in \Xi:\, r_j^k \in \mathrm{S}} p(\mathrm{S}) = q_j^k,\ \forall j \in [N], k \in [R_j],$$

$$\sum_{\mathrm{S} \in \Xi} p(\mathrm{S}) = 1,$$

$$p(\mathrm{S}) \geq 0,\ \forall \mathrm{S} \in \Xi.$$

The dual of this program is

$$\max_{\boldsymbol{\pi},\gamma} \sum_{j\in[N]} \sum_{k\in[R_j]} q_j^k \pi_j^k + \gamma$$

subject to

$$\gamma + \sum_{r_j^k \in \mathrm{S}} \pi_j^k \le u(\bar{\boldsymbol{x}}, \mathrm{S}),\ \forall \mathrm{S} \in \Xi,$$

which has exponentially many constraints because the support set Ξ has exponentially many elements.

Primal Feasibility. Construct primal solutions $p(v) = q(v) - q(v+1)$ for set $\chi^v, \forall v \in \{0\} \bigcup [R]$ and $p(\mathrm{S}) = 0$ for all the other states where $q(0) = 1$ and $q(R+1)$ by definition. Let $o(r_j^k)$ denote the index for the risk state r_j^k in the sequence L. Then, the first primal constraint can be written as

$$\begin{aligned}\sum_{\mathrm{S}\in\Xi:\, r_j^k \in \mathrm{S}} p(\mathrm{S}) &= \sum_{v=o(r_j^k)}^{R} p(\chi^v) = \sum_{v=o(r_j^k)}^{R} q(v) - q(v+1) \\ &= q\left(o\left(r_j^k\right)\right) - q(R+1) = q\left(o\left(r_j^k\right)\right) = q_j^k,\end{aligned}$$

where the first equality holds by the structure of the set χ^v. The second primal constraint holds by

$$\sum_{\mathrm{S}\in\Xi} p(\mathrm{S}) = \sum_{v=0}^{R} q(v) - q(v+1) = q(0) - q(R+1) = 1,$$

meaning that the constructed solution forms a probability distribution. Hence, the constructed primal solution satisfies primal feasibility.

Dual Feasibility. Construct dual solution $\pi(v) = u(\boldsymbol{x}, \chi^v) - u(\boldsymbol{x}, \chi^{v-1}),\ \forall v \in [R]$ and $\gamma = u(x, \chi^0)$. Given a particular scenario S, rank its risk states in the decreasing order of occurring probabilities and denote the resulting sequence by $\left\{o(\bar{r}(1)),\ldots,o(\bar{r}(N))\right\}$. Construct set ξ^v whose i-th entry equals the i-th term of χ^v if $i \le v \wedge r(i) \in \mathrm{S}$ or 0 otherwise. It follows that $\xi^v \subseteq \chi^v$ since ξ^v only contains the entries of χ^v that are also in S. We can represent the dual constraints as

$$\begin{aligned}\sum_{r_j^k \in S} \pi_j^k + \gamma &= \sum_{v=1}^{N}\left(u\left(\boldsymbol{x}, \chi^{o(\bar{r}(v))}\right) - u\left(\boldsymbol{x}, \chi^{o(\bar{r}(v))-1}\right)\right) + u\left(\boldsymbol{x}, \chi^0\right) \\ &\le \sum_{v=1}^{N}\left(u\left(\boldsymbol{x}, \xi^{o(\bar{r}(v))}\right) - u\left(\boldsymbol{x}, \xi^{o(\bar{r}(v))-1}\right)\right) + u\left(\boldsymbol{x}, \chi^0\right) \\ &= \sum_{v=1}^{N}\left(u\left(\boldsymbol{x}, \xi^{o(\bar{r}(v))}\right) - u\left(\boldsymbol{x}, \xi^{o(\bar{r}(v-1))}\right)\right) + u\left(\boldsymbol{x}, \chi^0\right) \\ &= u\left(\boldsymbol{x}, \xi^{o(\bar{r}(N))}\right) - u\left(\boldsymbol{x}, \xi^{o(\bar{r}(0))}\right) + u\left(\boldsymbol{x}, \chi^0\right)\end{aligned}$$

$$=u\left(\boldsymbol{x},\xi^{o(\bar{r}(N))}\right)-u\left(\boldsymbol{x},\xi^{0}\right)+u\left(\boldsymbol{x},\chi^{0}\right)$$

$$=u\left(\boldsymbol{x},\xi^{o(\bar{r}(N))}\right)=u\left(\boldsymbol{x},\mathrm{S}\right),$$

where the first inequality follows by the submodularity of $u\left(\boldsymbol{x},\cdot\right)$; the second to the last equalities hold by the structure of ξ^{v}. Hence, the constructed dual solution satisfies dual feasibility.

Optimality. We now show the primal solution and the dual solution admit the identical objective value. Expanding the primal and dual objective functions gives

$$\sum_{\mathrm{S}\in\Xi}p\left(\mathrm{S}\right)u\left(\boldsymbol{x},\mathrm{S}\right)=\sum_{v=0}^{R}p\left(\xi^{v}\right)u\left(\boldsymbol{x},\chi^{v}\right)$$

$$=\sum_{v=0}^{R}\left(q\left(v\right)-q\left(v+1\right)\right)u\left(\boldsymbol{x},\chi^{v}\right)$$

$$=q\left(0\right)u\left(\boldsymbol{x},\chi^{0}\right)-q\left(R+1\right)u\left(\boldsymbol{x},\chi^{R}\right)+\sum_{v=1}^{R}q\left(v\right)\left(u\left(\boldsymbol{x},\chi^{v}\right)-u\left(\boldsymbol{x},\chi^{v-1}\right)\right)$$

$$=u\left(\boldsymbol{x},\chi^{0}\right)+\sum_{v=1}^{R}q\left(v\right)\left(u\left(\boldsymbol{x},\chi^{v}\right)-u\left(\boldsymbol{x},\chi^{v-1}\right)\right)$$

$$=\gamma+\sum_{v=1}^{R}q\left(v\right)\pi\left(v\right)$$

$$=\gamma+\sum_{j\in[N]}\sum_{k\in[R_j]}q_j^k\pi_j^k,$$

where the third equality holds by the definitions $\gamma=u\left(\boldsymbol{x},\chi^{0}\right)$ and $q\left(R+1\right)=0$. As the constructed primal and dual admit the identical objective value, by strong duality, they are both optimal. (*Q.E.D.*)

Proof of Lemma 3.2. The complete recourse property implied that given any current restriction decision $\bar{\boldsymbol{x}}$, the recourse problem $u\left(\bar{\boldsymbol{x}},\mathrm{S}\right)$ is always feasible and has a bounded optimal value. Regarding feasibility, consider an arbitrary solution $\bar{\boldsymbol{x}}$ satisfying all master constraints. We claim that $\bar{\boldsymbol{x}}$ is also feasible for the recourse problem. It is easy to see that if $\boldsymbol{y}=\bar{\boldsymbol{x}}$, constraints (25) to (27) will be protected. As for constraint (28), its left-hand-side (LHS) writes

$$\sum_{i\in[N]}\sum_{l\in[L]}c_{ij}^l y_{ij}^l-\sum_{i\in[N]}\sum_{l\in[L]}s_{ij}^l\bar{x}_{ij}^l=\sum_{i\in[N]}\sum_{l\in[L]}c_{ij}^l\bar{x}_{ij}^l-\sum_{i\in[N]}\sum_{l\in[L]}s_{ij}^l\bar{x}_{ij}^l=C_j^{current}-\sum_{i\in[N]}\sum_{l\in[L]}s_{ij}^l\bar{x}_{ij}^l$$

$$\leq C_j^{\chi^v}-\sum_{i\in[N]}\sum_{l\in[L]}s_{ij}^l\bar{x}_{ij}^l\leq C_j^{\chi^v},\ \forall j\in[N],$$

where the first inequality holds by the fact $C_j^{current} \le C_j^{\chi^v}$. Hence, $\boldsymbol{y} = \bar{\boldsymbol{x}}$ is a feasible recourse solution. Regarding the boundness, let $\bar{\mathrm{Y}}$ be the feasible set of the resource problem given the master solution $\bar{\boldsymbol{x}}$, and denote by $\mathrm{Conv}\left(\bar{\mathrm{Y}}\right)$ its convex hull. Clearly, this is a tight set (i.e., closed and bounded) as $\bar{\mathrm{Y}}$ has finitely many elements. The recourse problem can be written as $\max\left\{\boldsymbol{by} : \boldsymbol{y} \in \mathrm{Conv}\left(\bar{\mathrm{Y}}\right)\right\}$. By the Weierstrass' theorem and $\mathrm{Conv}\left(\bar{\mathrm{Y}}\right)$ being nonempty, optimizing a continuous function over a tight set suggests that its optimal value exists, and the value is finite. Since for any master solution, the recourse problem is always feasible and bounded, there is no need to generate Benders feasibility cuts, and only optimality cuts are needed to guarantee convergence. (*Q.E.D.*)

Proof of Proposition 3.2. For ease of presentation, we drop scenario index v in the proof. Also, given a master solution $\boldsymbol{x}$, we present the LP relaxation of the recourse problem and its dual in abstract forms $\max\left\{\boldsymbol{uy} : \boldsymbol{Ty} + \boldsymbol{Ax} = \boldsymbol{c}\right\}$ and $\min\left\{\boldsymbol{\pi}\left(\boldsymbol{c} - \boldsymbol{Ax}\right) : \boldsymbol{\pi T} \ge \boldsymbol{u}\right\}$. At an iteration, let $\bar{\boldsymbol{\pi}}$ be the optimal dual vector for the corresponding recourse problem. We need to show that the optimality cut induced by $\bar{\boldsymbol{\pi}}$ is valid for any feasible master solution. Now, consider a subgraph variable ψ such that $\psi \le b\left(\boldsymbol{x}, \chi\right)$. It follows that

$$
\begin{aligned}
\psi \le u\left(\boldsymbol{x}, \chi\right) &= \max_{\boldsymbol{Ty} = \boldsymbol{c} - \boldsymbol{Ax},\, \boldsymbol{y} \text{ integer}} \boldsymbol{uy} \\
&= \max_{\boldsymbol{y} \text{ is integer}} \min_{\boldsymbol{\pi}} L\left(\boldsymbol{y}, \boldsymbol{\pi}\right) = \max_{\boldsymbol{y} \text{ is integer}} \min_{\boldsymbol{\pi}} \boldsymbol{uy} + \boldsymbol{\pi}\left(\boldsymbol{c} - \boldsymbol{Ax} - \boldsymbol{Ty}\right) \\
&= \boldsymbol{uy}^* + \boldsymbol{\pi}^*\left(\boldsymbol{c} - \boldsymbol{Ax} - \boldsymbol{Ty}^*\right) \\
&\le \boldsymbol{uy}^* + \bar{\boldsymbol{\pi}}\left(\boldsymbol{c} - \boldsymbol{Ax} - \boldsymbol{Ty}^*\right) \\
&= \boldsymbol{uy}^* + \bar{\boldsymbol{\pi}}\left(\boldsymbol{c} - \boldsymbol{Ax} - \boldsymbol{Ty}^*\right) \\
&= \left(\boldsymbol{u} - \bar{\boldsymbol{\pi}}\boldsymbol{T}\right)\boldsymbol{y}^* + \bar{\boldsymbol{\pi}}\left(\boldsymbol{c} - \boldsymbol{Ax}\right) \\
&\le \left(\boldsymbol{u} - \bar{\boldsymbol{\pi}}\boldsymbol{T}\right)\boldsymbol{x} + \bar{\boldsymbol{\pi}}\left(\boldsymbol{c} - \boldsymbol{Ax}\right) \\
&= \bar{\boldsymbol{\pi}}\boldsymbol{c} + \left(\boldsymbol{u} - \bar{\boldsymbol{\pi}}\boldsymbol{T} - \bar{\boldsymbol{\pi}}\boldsymbol{A}\right)\boldsymbol{x}.
\end{aligned}
$$

In the above, $L\left(\boldsymbol{y}, \boldsymbol{\pi}\right)$ represents the Lagrangian function with respect to $\boldsymbol{y}$ and $\boldsymbol{\pi}$ by dualizing constraint $\boldsymbol{Ty} + \boldsymbol{Ax} = \boldsymbol{c}$, while fully respecting the integer requirement on $\boldsymbol{y}$. Note that the variable bounds on $\boldsymbol{y}$ (i.e., $0 \le \boldsymbol{y} \le 1$) is included in constraints $\boldsymbol{Ty} + \boldsymbol{Ax} = \boldsymbol{c}$. The second and third equalities hold for properties of the Lagrangian function. Let $\boldsymbol{y}^*$ and $\boldsymbol{\pi}^*$ denote the optimal recourse decision and the optimal dual vector in the Lagrangian problem; the fourth equality thus holds. Replacing $\boldsymbol{\pi}^*$ with $\bar{\boldsymbol{\pi}}$, by the optimality of $\boldsymbol{\pi}^*$, yields the second inequality. It holds that $\boldsymbol{u}-\bar{\boldsymbol{\pi}}\boldsymbol{T}\le 0$ by the dual feasibility of $\bar{\boldsymbol{\pi}}$. Also, note that $\boldsymbol{y}^*\ge\boldsymbol{x}$ by constraints (27). We thus conclude $\left(\boldsymbol{u}-\bar{\boldsymbol{\pi}}\boldsymbol{T}\right)\boldsymbol{y}^*\le\left(\boldsymbol{u}-\bar{\boldsymbol{\pi}}\boldsymbol{T}\right)\boldsymbol{x}$, which implies that the third inequality holds. This proves the cut derived by $\bar{\boldsymbol{\pi}}$ is valid for arbitrary $\boldsymbol{x}$. We next show our cut is stronger than the classic Benders optimality cut. By $\boldsymbol{x}\ge 0$ and $\boldsymbol{u}-\bar{\boldsymbol{\pi}}\boldsymbol{T}\le 0$, the residual term satisfies $\left(\boldsymbol{u}-\bar{\boldsymbol{\pi}}\boldsymbol{T}\right)\boldsymbol{x}\le 0$, which implies

$$\left(\boldsymbol{u}-\bar{\boldsymbol{\pi}}\boldsymbol{T}\right)\boldsymbol{x}+\bar{\boldsymbol{\pi}}\left(\boldsymbol{c}-\boldsymbol{A}\boldsymbol{x}\right)\le\bar{\boldsymbol{\pi}}\left(\boldsymbol{c}-\boldsymbol{A}\boldsymbol{x}\right).$$

Note that the RHS of the above inequality is exactly the major term of the classic Benders optimality cut (i.e., $\psi^v\le\bar{\boldsymbol{\pi}}\left(\boldsymbol{c}-\boldsymbol{A}\boldsymbol{x}\right)$) and the LHS is our tailored cut. Therefore, our cut can establish a tighter (i.e., smaller) upper bound on the optimal objective value, compared with the classic cut. By substituting abstract notations in the cut by concrete parameters in DR-LM-II and the dual, we can obtain the cut in the proposition, which completes the proof. (*Q.E.D.*)

Remark. Wang and Jacquillat (2020) proposed a Benders optimality cut tailored to a similar relationship in master and recourse problems, say dual integer cut. Note that our derivation and proof of cut validity follow a very different argument. Briefly speaking, our design originates from the Lagrangian problem of general optimization models (and hence, the model itself needs not be LP, IP, or MIP), while their cut is based on the notation of reduced costs in LP. In addition, we propose a clearer way to verify the cut validity. We refer the readers of interest to Theorem 1 of their paper for more details of the difference.

Proof of Lemma 3.3. We prove by contradiction and recursion. Given a fractional variable $\underline{x}_{ij}^r$, we have $\underline{x}_{ij}^{r+1}=0$ by definition, and $\underline{x}_{ij}^l=0,\forall l\in\left\{r+2,...,L\right\}$ by constraint (26). Suppose that $\underline{x}_{ij}^{r-1}$ is also fractional. We can construct a new feasible solution by relocating a small amount of restriction cost from $\underline{x}_{ij}^r$ to $\underline{x}_{ij}^{r-1}$. Recall that the utility function $u_{ij}\left(l\right)$ is nondecreasing and concave in restriction level l. In this case, the cost relocation will yield a larger utility at the first stage. We can repeat the cost relocation procedure until $\underline{x}_{ij}^{r-1}=1$ or $\underline{x}_{ij}^r=0$. Meanwhile, we need to consider the impact of such cost relocation on the recourse value. We expect to show such cost relocation will increase or at least not decrease recourse value without violating the recourse feasibility.

Denote $\underline{\boldsymbol{y}}$ by the optimal recourse solution to the LP relaxation of DR-LM-II. Since the cost relocation decreases $\underline{x}_{ij}^r$ and increases $\underline{x}_{ij}^{r-1}$, the inequality $\underline{y}_{ij}^{r-1}\ge\underline{x}_{ij}^{r-1}$ in constraints (27) and (28) could be violated.

For the value of $\underline{y}_{ij}^{r-1}$, we have three possible cases: *i*) if $\underline{y}_{ij}^{r-1}=1$, then the cost relocation has no impact on the feasibility of constraint (27); *ii*) if $\underline{x}_{ij}^{r-1}=\underline{y}_{ij}^{r-1}<1$, we can also relocate a small cost from $\underline{y}_{ij}^{r}$ to $\underline{y}_{ij}^{r-1}$ such that $\underline{y}_{ij}^{r-1}\geq\underline{x}_{ij}^{r-1}$ holds; *iii*) if $\underline{x}_{ij}^{r-1}<\underline{y}_{ij}^{r-1}<1$, we can relocate sufficiently small cost at the first stage so that $\underline{y}_{ij}^{r-1}\geq\underline{x}_{ij}^{r-1}$ holds. As for constraints (3.28), the below table shows that the subproblem constraint still holds after the cost relocation.

Table A3.12. Change of terms in constraints (28) after cost relocation.

Case	$\sum_{i\in[N]}\sum_{l\in[L]}c_{ij}^{l}\underline{y}_{ij}^{l}$	$\sum_{i\in[N]}\sum_{l\in[L]}s_{ij}^{l}\underline{x}_{ij}^{l}$	**Recourse Value**
i	No change	Increase	No change
ii	No change	Increase	Increase
iii	Increase	Increase	Increase

The constructed solution by cost relocation is feasible and yields a larger objective value, which contradicts the optimality of $(\underline{\boldsymbol{x}},\underline{\boldsymbol{y}})$. Therefore, we conclude that $\underline{x}_{ij}^{r-1}$ cannot be fractional. Then, by a similar argument and constructing recursion, we can further show that $\underline{x}_{ij}^{l},\forall l\in\{1,...,r-2\}$ cannot be fractional. This completes the proof. (*Q.E.D.*)

Proof of Lemma 3.4. The inner minimization problem of R-LM is to find the worst-case scenario to decrease the utility as much as possible. Note that R-LM is a relaxation of DR-LM since the distribution pattern constrained by ambiguity set P is absent. Since DR-LM satisfies relatively complete recourse, R-LM also satisfies relatively complete recourse. This finding allows us to directly examine the impact on the utility under different S without violating feasibility. Suppose there exists a scenario χ^{v} that decreases the utility more than χ^{0}. We group the cities with increased risk states compared with χ^{0} into an index set N. Then, for any $j\in\mathrm{N}$ and any first-stage restriction decision $\bar{\boldsymbol{x}}$, we have $u_j\left(\bar{\boldsymbol{x}},\chi^{v}\right)\geq u_j\left(\bar{\boldsymbol{x}},\chi^{0}\right)$ due to $C_j^{\chi^{v}}\geq C_j^{\chi^{0}}$, which contradicts the optimality. Hence, we conclude that χ^{0} is the worst-case realization among all possible scenarios. (*Q.E.D.*)

II.2. Mathematical Proofs for Chapter 4

Proof of Lemma 4.1. The profit function of adopting or rejecting SDS is concave in loyalty program investment v_i . To see this, the second-order derivatives of the profit functions in v_i show that $\frac{\partial^2 \Pi_{i,M}}{\partial v_i^2} = -\frac{\rho_i}{\mu_i v_i^2} < 0$ and $\frac{\partial^2 \Pi_{i,N}}{\partial v_i^2} = -\frac{\rho_i + m_i}{\mu_i v_i^2} < 0$, which are strictly negative, since v_i and all parameters are non-negative. With the first-order optimality condition, we can thus derive the optimal investment: $\frac{\partial \Pi_{i,M}}{\partial v_i} = \frac{\rho_i}{\mu_i v_i} - 1 = 0$ and $\frac{\partial \Pi_{i,N}}{\partial v_i} = \frac{\rho_i + m_i}{\mu_i v_i} - 1 = 0$. Solving the two equations yields the optimal investment when maintaining existing services (Case M) or adopting SDS (Case N): $v_{i,M}^* = \frac{\rho_i}{\mu_i}$, and $v_{i,N}^* = \frac{\rho_i + m_i}{\mu_i}$. (*Q.E.D.*)

Proof of Proposition 4.1. When Company 1 attempts to adopt SDS, Company 2 will follow the strategy, only when this action strictly improves profit, i.e., $\Pi_{2,(N,N)}^* > \Pi_{2,(N,M)}^*$. In contrast, $\Pi_{2,(N,N)}^* \le \Pi_{2,(N,M)}^*$ suggests that Company 2 will maintain existing services. We thus find a critical condition $\Pi_{2,(N,N)}^* = \Pi_{2,(N,M)}^*$. Solving equality $(\rho_2 + m_2)\left(\hat{a}_2 + \frac{1}{\mu_2}\ln\frac{\rho_2 + m_2}{\mu_2 e} - \frac{c}{\mu_1}\ln\frac{\rho_1 + m_1}{\mu_1}\right) = \rho_2\left(a_2 + \frac{1}{\mu_2}\ln\frac{\rho_2}{\mu_2 e} - \frac{c}{\mu_1}\ln\frac{\rho_1 + m_1}{\mu_1}\right)$ gives a critical market threshold $a_2^{\Delta} = \left(\rho_2 a_2 + \frac{\rho_2}{\mu_2}\ln\frac{\rho_2}{\rho_2 + m_2} + \frac{m_2}{\mu_2}\ln\frac{\mu_2 e}{\rho_2 + m_2} + \frac{c m_2}{\mu_1}\ln\frac{\rho_1 + m_1}{\mu_1}\right)\Big/(\rho_2 + m_2)$. Hence, when $\hat{a}_2 > a_2^{\Delta}$, Company 2 will strictly benefit from SDS. (*Q.E.D.*)

Proof of Proposition 4.2. Suppose that Company 2 has incentives to adopt SDS. Company 1 should finalize SDS commitment only when $\Pi_{1,(N,N)}^* > \Pi_{1,(M,M)}^*$; otherwise, Company 1 will still maintain existing services. We obtain the condition $\Pi_{1,(N,N)}^* = \Pi_{1,(M,M)}^*$ and $(\rho_1 + m_1)\left(\hat{a}_1 + \frac{1}{\mu_1}\ln\frac{\rho_1 + m_1}{\mu_1 e} - \frac{c}{\mu_2}\ln\frac{\rho_2 + m_2}{\mu_2}\right) = \rho_1\left(a_1 + \frac{1}{\mu_1}\ln\frac{\rho_1}{\mu_1 e} - \frac{c}{\mu_2}\ln\frac{\rho_2}{\mu_2}\right)$. Solving it gives $a_{1,(N,N)}^{\Delta} = \left(\rho_1 a_1 + \frac{\rho_1}{\mu_1}\ln\frac{\rho_1}{\rho_1 + m_1} + \frac{m_1}{\mu_1}\ln\frac{\mu_1 e}{\rho_1 + m_1} + \frac{c\rho_1}{\mu_2}\ln\frac{\rho_2 + m_2}{\rho_2} + \frac{c m_1}{\mu_2}\ln\frac{\rho_2 + m_2}{\mu_2}\right)\Big/(\rho_1 + m_1)$. Thus, when $\hat{a}_1 > a_{1,(N,N)}^{\Delta}$, Company 1 will strictly benefit from adopting SDS.

If Company 2 is not motivated to adopt SDS, Company 1 can directly analyze the profit when unilaterally adopting SDS. The condition $\Pi_{1,(N,M)}^* = \Pi_{1,(M,M)}^*$ gives the equality

$\left(\rho_1+m_1\right)\left(\hat{a}_1+\frac{1}{\mu_1}\ln\frac{\rho_1+m_1}{\mu_1 e}-\frac{c}{\mu_2}\ln\frac{\rho_2}{\mu_2}\right)=\rho_1\left(a_1+\frac{1}{\mu_1}\ln\frac{\rho_1}{\mu_1 e}-\frac{c}{\mu_2}\ln\frac{\rho_2}{\mu_2}\right)$, and the critical market threshold $a_{1,(N,M)}^{\Delta}=\left(\rho_1 a_1+\frac{\rho_1}{\mu_1}\ln\frac{\rho_1}{\rho_1+m_1}+\frac{m_1}{\mu_1}\ln\frac{\mu_1 e}{\rho_1+m_1}+\frac{cm_1}{\mu_2}\ln\frac{\rho_2}{\mu_2}\right)\Big/\left(\rho_1+m_1\right)$. When the follower is not motivated to adopt SDS, the condition $\hat{a}_1>a_{1,(N,M)}^{\Delta}$ implies that the leader will finally adopt SDS. (*Q.E.D.*)

Proof of Proposition 4.3. To analyze the impact of competition level c on the critical thresholds, we cast the threshold value as a function in c and compute the first derivative in c. For Company 1, we get $\frac{\partial a_{1,(N,M)}^{\Delta}}{\partial c}=\frac{m_1}{\mu_2\left(\rho_1+m_1\right)}\ln\frac{\rho_2}{\mu_2}$ and $\frac{\partial a_{1,(N,N)}^{\Delta}}{\partial c}=\frac{\rho_1}{\mu_2\left(\rho_1+m_1\right)}\ln\frac{\rho_2+m_2}{\rho_2}+\frac{m_1}{\mu_2\left(\rho_1+m_1\right)}\ln\frac{\rho_2+m_2}{\mu_2}$. Comparing them uncovers $0<\frac{\partial a_{1,(N,M)}^{\Delta}}{\partial c}<\frac{\partial a_{1,(N,N)}^{\Delta}}{\partial c}$. For Company 2, we have $\frac{\partial a_2^{\Delta}}{\partial c}=\frac{m_2}{\mu_1\left(\rho_2+m_2\right)}\ln\frac{\rho_1+m_1}{\mu_1}>0$. Hence, a larger c makes all the three thresholds increase while $a_{1,(N,N)}^{\Delta}$ increases faster than $a_{1,(N,M)}^{\Delta}$. Next, the first derivatives of Company 1's threshold in a_1 is $\frac{\partial a_{1,(N,N)}^{\Delta}}{\partial a_1}=\frac{\partial a_{1,(NM,M)}^{\Delta}}{\partial a_1}=\rho_1>0$. A larger a_1 makes the two thresholds increase at the same rate. For Company 2, $\frac{\partial a_2^{\Delta}}{\partial a_2}=\rho_2>0$ implies a_2^{Δ} increases with a_2.

Regarding the impact of the rival's cost-saving ability, for Company 1, we have $\frac{\partial a_{1,(N,M)}^{\Delta}}{\partial m_2}=0$ and $\frac{\partial a_{1,(N,N)}^{\Delta}}{\partial m_2}=\frac{cm_1}{\mu_2\left(\rho_2+m_2\right)\left(\rho_1+m_1\right)}+\frac{c\rho_1}{\mu_2\left(\rho_2+m_2\right)\left(\rho_1+m_1\right)}$. It is clear that $\frac{\partial a_{1,(N,N)}^{\Delta}}{\partial m_2}>\frac{\partial a_{1,(N,M)}^{\Delta}}{\partial m_2}=0$. For Company 2, its critical market threshold a_2^{Δ} is affected by the leader's cost-saving ability m_1 as follows

$$\frac{\partial a_2^{\Delta}}{\partial m_1}=\frac{cm_2}{\mu_1\left(\rho_2+m_2\right)\left(\rho_1+m_1\right)}>0.$$

Last, regarding the impact of the marginal profit of a company's rival, for Company 1, we have $\frac{\partial a_{1,(N,M)}^{\Delta}}{\partial \rho_2}=\frac{cm_1}{\mu_2\rho_2\left(\rho_1+m_1\right)}$ and $\frac{\partial a_{1,(N,N)}^{\Delta}}{\partial \rho_2}=\frac{cm_1}{\mu_2\left(\rho_2+m_2\right)\left(\rho_1+m_1\right)}+\frac{c\rho_1}{\mu_2\left(\rho_2+m_2\right)\left(\rho_1+m_1\right)}-\frac{c\rho_1}{\mu_2\rho_2\left(\rho_1+m_1\right)}=\frac{cm_1}{\mu_2\left(\rho_2+m_2\right)\left(\rho_1+m_1\right)}-\frac{c\rho_1 m_1}{\mu_2\rho_2\left(\rho_2+m_2\right)\left(\rho_1+m_1\right)}$. Comparing these derivatives gives the relationship: $\frac{\partial a_{1,(N,M)}^{\Delta}}{\partial \rho_2}>\frac{\partial a_{1,(N,N)}^{\Delta}}{\partial \rho_2}>0$. For Company 2, we have $\frac{\partial a_2^{\Delta}}{\partial \rho_1}=\frac{cm_2}{\mu_1\left(\rho_2+m_2\right)\left(\rho_1+m_1\right)}>0$. (*Q.E.D.*)

Proof of Theorem 4.1. Given Company i's investment v_i, its worst-case mean-variance objective under the moment-based ambiguity set can be derived by the following optimization problem:

$$U_{i,N}(v_i)=\min_{\mathrm{P}_i\in P_i}\mathrm{E}_{\mathrm{P}}\left[(\rho_i+m_i)\tilde{D}_{i,N}-v_i\right]+\lambda_i\sqrt{\mathrm{E}_{\mathrm{P}}\left[\left((\rho_i+m_i)\tilde{D}_{i,N}-v_i-\mathrm{E}_{\mathrm{P}}\left[(\rho_i+m_i)\tilde{D}_{i,N}-v_i\right]\right)^2\right]}$$

$$=\min_{\mathrm{P}_i\in P_i}(\rho_i+m_i)\left(\hat{a}_1+\sqrt{2v_i/k_i}-c\sqrt{2v_{3-i}/k_{3-i}}\right)-v_i+\lambda_i\sqrt{\mathrm{E}_{\mathrm{P}}\left[\left((\rho_i+m_i)\varepsilon_i\right)^2\right]}$$

$$=(\rho_i+m_i)\left(\hat{a}_1+\sqrt{2v_i/k_i}-c\sqrt{2v_{3-i}/k_{3-i}}\right)-v_i+\begin{cases}\lambda_i(\rho_i+m_i)\overline{\delta}_i,\ if\ \lambda_i<0\\ \lambda_i(\rho_i+m_i)\underline{\delta}_i,\ if\ \lambda_i>0\end{cases}.$$

Define $\delta_i=\mathrm{I}(\lambda_i<0)\overline{\delta}_i+\mathrm{I}(\lambda_i>0)\underline{\delta}_i$. Then, we obtain the compact expression as desired. (*Q.E.D.*)

Proof of Proposition 4.5. To ensure the thresholds of a company are always meaningful, we need the condition for the leader $\min\left\{a_{1,(N,N)}^{RISK\Delta},\ a_{i,(N,M)}^{RISK\Delta}\right\}>0$, implying $a_{1,(N,M)}^{RISK\Delta}=\left(\rho_1a_1+c\dfrac{m_1\rho_2}{k_2}-\dfrac{m_1(2\rho_1+m_1)}{2k_1}-\lambda_1(\rho_1+m_1)\delta_1\right)\Big/(\rho_1+m_1)>0$. For the follower, we need $a_2^{RISK\Delta}=\left(\rho_2a_2+c\dfrac{(\rho_1+m_1)m_2}{k_1}-\dfrac{m_2(2\rho_2+m_2)}{2k_2}-\lambda_2(\rho_2+m_2)\delta_2\right)\Big/(\rho_2+m_2)>0$. Rearranging the above inequality yields the desired condition. (*Q.E.D.*)

Proof of Proposition 4.6. Taking the derivative of the threshold functions regarding demand volatility δ_i gives $\dfrac{\partial a_{1,(M,M)}^{RISK\Delta}}{\partial\delta_1}=\dfrac{\partial a_{1,(M,M)}^{RISK\Delta}}{\partial\delta_1}=-\dfrac{\lambda_1m_1}{\rho_1+m_1}$ and $\dfrac{\partial a_2^{RISK\Delta}}{\partial\delta_2}=-\dfrac{\lambda_2m_2}{\rho_2+m_2}$, which are positive for risk-averse companies (i.e., $\lambda_i<0$) and negative for risk-seeking companies (i.e., $\lambda_i>0$). Taking the derivative of the threshold functions regarding the magnitude of the risk sensitivity parameter $|\lambda_i|$ gives $\dfrac{\partial a_{1,(N,M)}^{RISK\Delta}}{\partial\delta_1}=\dfrac{\partial a_{1,(N,N)}^{RISK\Delta}}{\partial\delta_1}=-\dfrac{m_1\delta_1}{\rho_1+m_1}\mathrm{sgn}(\lambda_1)$ and $\dfrac{\partial a_2^{RISK\Delta}}{\partial\delta_2}=-\dfrac{m_2\delta_2}{\rho_2+m_2}\mathrm{sgn}(\lambda_2)$, which are positive for a risk-averse company (i.e., $\mathrm{sgn}(\lambda_i)=-1$) or negative for a risk-seeking company (i.e., $\mathrm{sgn}(\lambda_i)=1$). (*Q.E.D.*)

Proof of Theorem 4.2. Expanding the profit function of follower i gives

$$\max_{x_i\in\{0,1\}}\Pi_i(x_i;x_0,...,x_{i-1},x_{i+1},...,x_K)=\rho\left(a+\frac{\rho}{k}\right)-\rho\left(a+\frac{\rho}{k}\right)x_i+\rho\left(\hat{a}+\frac{\rho+m}{k}\right)x_i-\rho c\left(\frac{\rho_0}{k_0}(1-x_0)+\frac{\rho_0+m_0}{k_0}x_0\right)$$

$$-\rho c\sum_{j=1,j\neq i}^{K}\left(\frac{\rho}{k}\left(1-x_j\right)+\frac{\rho+m}{k}x_j\right)+m\left(a+\frac{\rho}{k}\right)\left(x_i-x_i^2\right)+m\left(\hat{a}+\frac{\rho+m}{k}\right)x_i^2$$

$$-mc\left(\frac{\rho_0}{k_0}\left(1-x_0\right)+\frac{\rho_0+m_0}{k_0}x_0\right)x_i-mc\sum_{j=1,j\neq i}^{K}\left(\frac{\rho}{k}\left(1-x_j\right)+\frac{\rho+m}{k}x_j\right)x_i-\frac{\rho^2}{2k}\left(1-x_i\right)-\frac{\left(\rho+m\right)^2}{2k}x_i,$$

which is quadratic in x_i. Since $x_i\in\{0,1\}$, it is clear that $x_i=x_i^2$. We can thus reduce the quadratic profit function to a linear one:

$$\max_{x_i\in\{0,1\}}\Pi_i\left(x_i;x_0,...,x_{i-1},x_{i+1},...,x_K\right)=\rho a+\frac{\rho^2}{2k}-\rho c\left(\frac{\rho_0}{k_0}\left(1-x_0\right)+\frac{\rho_0+m_0}{k_0}x_0+\sum_{j=1,j\neq i}^{K}\left(\frac{\rho}{k}\left(1-x_j\right)+\frac{\rho+m}{k}x_j\right)\right)$$

$$+x_i\left[\rho a+\left(\rho+m\right)\hat{a}+\frac{m^2+2m\rho}{2k}-mc\left(\frac{\rho_0}{k_0}\left(1-x_0\right)+\frac{\rho_0+m_0}{k_0}x_0+\sum_{j=1,j\neq i}^{K}\left(\frac{\rho}{k}\left(1-x_j\right)+\frac{\rho+m}{k}x_j\right)\right)\right].$$

In this reformulated profit function, if the coefficient of x_i is positive, then $x_i=1$. If the coefficient is negative, it is clear $x_i=0$. When the coefficient equals 0, we regulate $x_i=0$ by convention.

Equipped with the reduced profit function, we next analyze the first symmetric Stackelberg equilibrium where both the leader and all followers reject SDS. When the leader adopts SDS, if the maximum of the critical coefficient is still non-positive for all followers, it will be sufficient to guarantee that all followers will reject SDS. Since the coefficient is decreasing against the number of followers who adopt SDS, the maximum is attained exactly at which all followers reject SDS. Letting $x_0=1$ and $x_j=0,\forall j\in\{1,...,K\}\setminus\{i\}$, we get $\rho a+\left(\rho+m\right)\hat{a}+\frac{m^2+2m\rho}{2k}-mc\left(\frac{\rho_0+m_0}{k_0}+\left(K-1\right)\frac{\rho}{k}\right)\leq 0$ and a common upper bound on the followers' EPSM: $\hat{a}\leq\left(mc\left(\frac{\rho_0+m_0}{k_0}+\left(K-1\right)\frac{\rho}{k}\right)-\rho a-\frac{m^2+2m\rho}{2k}\right)\Big/\left(\rho+m\right)$.

In addition, to ensure equilibrium $\left(0,\mathbf{0}\right)$ truly forms, the leader must get no benefit from unilaterally adopting SDS (i.e., $\Pi_0\left(0,\mathbf{0}\right)\geq\Pi_0\left(1,\mathbf{0}\right)$). This condition writes

$\rho_0\left(a_0+\frac{\rho_0}{k_0}-cK\frac{\rho}{k}\right)-\frac{\rho_0^2}{2k_0}\geq\left(\rho_0+m_0\right)\left(\hat{a}_0+\frac{\rho_0+m_0}{k_0}-cK\frac{\rho}{k}\right)-\frac{\left(\rho_0+m_0\right)^2}{2k_0}$, which implies an upper bound on the leader's EPSM: $\hat{a}_0\leq\left(\rho_0a_0+cK\frac{\rho m_0}{k}-\frac{m_0^2+2\rho_0m_0}{2k_0}\right)\Big/\left(\rho_0+m_0\right)$. Furthermore, these two bounds must be positive so that they are meaningful: $\rho_0a_0+cK\frac{\rho m_0}{k}-\frac{m_0^2+2\rho_0m_0}{2k_0}>0$ and $mc\left(\frac{\rho_0+m_0}{k_0}+\left(K-1\right)\frac{\rho}{k}\right)-\rho a-\frac{m^2+2m\rho}{2k}>0$.

Regarding the other symmetric Stackelberg equilibrium where both the leader and all followers adopt SDS, after the leader adopts SDS, if the minimum of the critical coefficient is positive for all followers, it will be sufficient to guarantee that all followers adopt SDS. The minimum is attained exactly at which all followers adopt SDS. Letting $x_0 = 1$ and $x_j = 1, \forall j \in \{1,...,K\} \setminus \{i\}$, we get condition

$\rho a + (\rho + m)\hat{a} + \frac{m^2 + 2m\rho}{2k} - mc\left(\frac{\rho_0 + m_0}{k_0} + (K-1)\frac{\rho + m}{k}\right) > 0$, which gives a common lower bound on the followers' EPSM: $\hat{a} > \left(mc\left(\frac{\rho_0 + m_0}{k_0} + (K-1)\frac{\rho + m}{k}\right) - \rho a - \frac{m^2 + 2m\rho}{2k}\right) \Big/ (\rho + m)$.

To ensure equilibrium $(1,\mathbf{1})$ truly forms, both the leader and all followers must strictly benefit from SDS. For the leader, its profit should satisfy $\Pi_0(1,\mathbf{1}) > \Pi_0(0,\mathbf{0})$:

$(\rho_0 + m_0)\left(\hat{a}_0 + \frac{\rho_0 + m_0}{k_0} - cK\frac{\rho + m}{k}\right) - \frac{(\rho_0 + m_0)^2}{2k_0} > \rho_0\left(a_0 + \frac{\rho_0}{k_0} - cK\frac{\rho}{k}\right) - \frac{\rho_0^2}{2k_0}$, which suggests a lower bound on the leader's EPSM: $\hat{a}_0 > \left(a_0\rho_0 - \frac{m_0^2 + 2\rho_0 m_0}{2k_0} + \frac{cK}{k}(\rho m_0 + \rho_0 m + m m_0)\right) \Big/ (\rho_0 + m_0)$.

Regarding the profit condition for the followers, supposing that follower i unilaterally deviate from equilibrium $(1,\mathbf{1})$ by becoming $x_i = 0$, its profit is $\rho a + \frac{\rho^2}{2k} - \rho c\left(\frac{\rho_0}{k_0} + \sum_{j=1, j \neq i}^{K}\left(\frac{\rho}{k}(1 - x_j) + \frac{\rho + m}{k}x_j\right)\right)$, which is decreasing against the number of rivals who adopt SDS. The profit attains the maximum exactly at which all rivals reject SDS, and all followers reject SDS in this case. Hence, the condition $\Pi_i(1,\mathbf{1}) > \Pi_i(1,\mathbf{0})$ is sufficient to guarantee that all followers adopt SDS:

$(\rho + m)\left(\hat{a} + \frac{\rho + m}{k} - c\frac{\rho_0 + m_0}{k_0} - c(K-1)\frac{\rho + m}{k}\right) - \frac{(\rho + m)^2}{2k} > \rho\left(a + \frac{\rho}{k} - c\frac{\rho_0 + m_0}{k_0} - c(K-1)\frac{\rho}{k}\right) - \frac{\rho^2}{2k}$, which implies a common lower bound on the followers' EPSM:

$\hat{a} > \left(\rho a + c\frac{m\rho_0 + m m_0}{k_0} + \left(cK - c - \frac{1}{2}\right)\frac{m^2 + 2m\rho}{k}\right) \Big/ (\rho + m)$.

Also, the above two bounds must be positive so that they are meaningful:

$a_0\rho_0 - \frac{m_0^2 + 2\rho_0 m_0}{2k_0} + \frac{cK}{k}(\rho m_0 + \rho_0 m + m m_0) > 0$ and $\rho a + c\frac{m\rho_0 + m m_0}{k_0} + \left(cK - c - \frac{1}{2}\right)\frac{m^2 + 2m\rho}{k} > 0$. (*Q.E.D.*)

Proof of Theorem 4.3. When follower i rejects SDS (i.e., $x_i = 0$), its profit is

$$\Pi_i\left(0;x_0,...,x_{i-1},x_{i+1},...,x_K\right)=\rho a+\frac{\rho^2}{2k}-\rho c\left(\frac{\rho_0}{k_0}\left(1-x_0\right)+\frac{\rho_0+m_0}{k_0}x_0+\sum_{j=1,j\neq i}^{K}\left(\frac{\rho}{k}\left(1-x_j\right)+\frac{\rho+m}{k}x_j\right)\right),$$

and when follower i adopts SDS (i.e., $x_i=1$), its profit is

$$\Pi_i\left(1;x_0,...,x_{i-1},x_{i+1},...,x_K\right)=2\rho a+\left(\rho+m\right)\hat{a}+\frac{\rho^2}{2k}+\frac{m^2+2m\rho}{2k}$$
$$-\left(\rho c+mc\right)\left(\frac{\rho_0}{k_0}\left(1-x_0\right)+\frac{\rho_0+m_0}{k_0}x_0+\sum_{j=1,j\neq i}^{K}\left(\frac{\rho}{k}\left(1-x_j\right)+\frac{\rho+m}{k}x_j\right)\right),$$

both of which are decreasing against the number of its rivals who adopt SDS. Casting the number of rivals who adopt SDS as the variable, the above two profit functions are both linear but with different slopes and intercepts. If these two linear functions intersect at some point in the interval $\left[1,K-1\right]$, then before this point, one strategy will be dominant, whereas the other strategy becomes dominant after this critical point. At this intersection point, the followers who adopt SDS admit an identical profit to those who reject SDS, and hence all followers are indifferent about unilaterally changing their decisions in this case.

Denote by $\left(1,\mathbf{1}^{K^*},\mathbf{0}^{K-K^*}\right)$ the case where the leader and K^* followers adopt SDS and $K-K^*$ followers reject SDS. We consider the condition that all followers have the same profit:

$$\left(\rho+m\right)\left(\hat{a}+\frac{\rho+m}{k}-c\frac{\rho_0+m_0}{k_0}-c\left(K^*-1\right)\frac{\rho+m}{k}-c\left(K-K^*\right)\frac{\rho}{k}\right)-\frac{\left(\rho+m\right)^2}{2k}$$
$$=\rho\left(a+\frac{\rho}{k}-c\frac{\rho_0+m_0}{k_0}-cK^*\frac{\rho+m}{k}-c\left(K-K^*-1\right)\frac{\rho}{k}\right)-\frac{\rho^2}{2k}.$$

Solving this equation gives the number of followers who adopt SDS:

$$K^*-1=k\frac{\rho a+\left(\rho+m\right)\hat{a}}{cm^2}-k\frac{\rho_0+m_0}{mk_0}-\frac{\rho}{m}\left(K-2-\frac{1}{c}\right)+\frac{1}{2c}.$$

To ensure $\left(1,\mathbf{1}^{K^*},\mathbf{0}^{K-K^*}\right)$ truly forms, the leader and all followers must strictly benefit from their decisions. For the leader, the profit condition $\Pi_0\left(1,\mathbf{1}^{K^*},\mathbf{0}^{K-K^*}\right)>\Pi_0\left(0,\mathbf{0}\right)$ should hold:

$$\left(\rho_0+m_0\right)\left(\hat{a}_0+\frac{\rho_0+m_0}{k_0}--cK^*\frac{\rho+m}{k}-c\left(K-K^*\right)\frac{\rho}{k}\right)-\frac{\left(\rho_0+m_0\right)^2}{2k_0}>\rho_0\left(a_0+\frac{\rho_0}{k_0}-cK\frac{\rho}{k}\right)-\frac{\rho_0^2}{2k_0},$$

which implies a lower bound on the leader's EPSM:

$$\hat{a}_0>\left(\rho_0a_0-\frac{2m_0\rho_0+m_0^2}{2k_0}+\left(\rho_0+m_0\right)cK^*\frac{m}{k}+cK\frac{\rho m_0}{k}\right)\Big/\left(\rho_0+m_0\right).$$

Regarding the profit condition for each follower, since all followers admit the same profit, we need only to consider $\Pi_i\left(x_i=1,\left(x_0=1,\mathbf{1}^{K^*-1},\mathbf{0}^{K-K^*}\right)\right)>\Pi_i\left(x_i=0,\left(x_0=1,\mathbf{0}^{K-1}\right)\right)$:

$$(\rho+m)\left(\hat{a}+\frac{\rho+m}{k}-c\frac{\rho_0+m_0}{k_0}-c\left(K^*-1\right)\frac{\rho+m}{k}-c\left(K-K^*\right)\frac{\rho}{k}\right)-\frac{(\rho+m)^2}{2k}$$

$$>\rho\left(a+\frac{\rho}{k}-c\frac{\rho_0+m_0}{k_0}-c(K-1)\frac{\rho}{k}\right)-\frac{\rho^2}{2k},$$

which implies a common lower bound on the followers' EPSM:

$$\hat{a}>\left(\rho a+mc\frac{\rho_0+m_0}{k_0}-\frac{(1+2c)\left(m^2+2m\rho\right)}{2k}+(\rho+m)cK^*\frac{m}{k}+cK\frac{\rho m}{k}\right)\Big/(\rho+m).$$

Furthermore, these bounds should be positive so that they are meaningful:

$$\rho_0 a_0-\frac{2m_0\rho_0+m_0^2}{2k_0}+\left(\rho_0+m_0\right)cK^*\frac{m}{k}+cK\frac{\rho m_0}{k}>0,$$

$$\rho a+mc\frac{\rho_0+m_0}{k_0}-\frac{(1+2c)\left(m^2+2m\rho\right)}{2k}+(\rho+m)cK^*\frac{m}{k}+cK\frac{\rho m}{k}>0.$$

Last, we argue that any follower cannot improve its profit by unilaterally changing its decision. For a follower who originally rejected SDS, substituting the value of K^* into its critical coefficient gives

$$\rho a+(\rho+m)\hat{a}+\frac{m^2+2m\rho}{2k}-mc\left(\frac{\rho_0+m_0}{k_0}+\left(K-K^*-1\right)\frac{\rho}{k}+K^*\frac{\rho+m}{k}\right)=-\frac{cm}{k}(\rho+m)<0.$$

Hence, unilaterally changing its decision to $x_i=1$ will decrease the profit. Likewise, for a follower who originally adopted SDS, its critical coefficient is

$$\rho a+(\rho+m)\hat{a}+\frac{m^2+2m\rho}{2k}-mc\left(\frac{\rho_0+m_0}{k_0}+\left(K-K^*\right)\frac{\rho}{k}+\left(K^*-1\right)\frac{\rho+m}{k}\right)=\frac{m\rho}{k}(1-2c)>0,$$

where the last inequality holds by $c\le 1/K$ and $K\ge 2$ by assumptions. Therefore, unilaterally changing its decision to $x_i=0$ will decrease the profit. We thus conclude that $\left(1,\mathbf{1}^{K^*},\mathbf{0}^{K-K^*}\right)$ is a valid Stackelberg equilibrium. (*Q.E.D.*)

References

Baidu Migration Database (2024). Overall migration trend of China. Accessed 30 May 2025, https://qianxi.baidu.com/.

China Briefing (2023). China 2023 Economic Growth Breakdown. Accessed 30 May 2025, https://www.china-briefing.com/news/china-2023-economic-growth-breakdown-gdp-statistics-and-targets-by-province/.

China Breau of Statistics (2024). China statistics yearbook. Accessed 30 May 2025, https://www.stats.gov.cn/sj/ndsj/.

China Government (2023) Economic stastiscial data. Accessed 30 May 2025, http://www.stats.gov.cn/sj/zxfb/202302/t20230203_1901715.html/.

Guo X, Kuang Y, Ng CT (2023) To centralize or decentralize: Mergers under price and quality competition. Production and Operations Management, 32(3), 844-862.

HK Government. (2023a) Anti-epidemic fund. Accessed 30 Jul 2025, https://www.coronavirus.gov.hk/eng/anti-epidemic-fund.html/.

HK Government (2023b) Inbound travel policy. Accessed 30 July 2025, https://www.coronavirus.gov.hk/eng/inbound-travel.html/.

HK Tourism Board (2023) Tourism statistics. Accessed 30 May 2025, https://www.discoverhongkong.com/eng/hktb/newsroom/tourism-statistics.html/.

Hodgson MJ (1990) A flow-capturing location-allocation model. Geographical analysis, 22(3), 270-279.

Jia JS, Lu X, Yuan Y, Xu G, Jia J, Christakis NA (2020) Population flow drives spatio-temporal distribution of COVID-19 in China. Nature, 582(7812), 389-394.

Kochhar R, Sechopoulos S (2022) COVID-19 pandemic pinches finances of America's lower-and middle-income families.

Lu M, Ran L, Shen ZJM (2015) Reliable facility location design under uncertain correlated disruptions. Manufacturing & Service Operations Management 17(4):445-455.

Luo S, Choi TM (2022) E-commerce supply chains with considerations of cyber-security: Should governments play a role? Production and Operations Management, 31(5), 2107-2126.

Nemhauser GL, Wolsey LA, Fisher ML (1978) An analysis of approximations for maximizing submodular set functions—I. Mathematical programming 14(1):265-294.

Polemis ML (2021) National lockdown under COVID-19 and hotel performance. Annals of Tourism Research Empirical Insights, 2(1), 100012.

Statista (2023a) Total population of Guangdong province in China from 2013 to 2023. Accessed 30 July 2025, https://www.statista.com/statistics/1033846/china-population-of-guangdong/.

Statista (2023b) Average hotel room rate in Hong Kong from December 2018 to November 2021, by tariff level. Accessed 30 July 2025, https://www.statista.com/statistics/956217/hong-kong-average-hotel-room-rate-by-tariff-level/.

Sun YY, Li M, Lenzen M, Malik A, Pomponi F (2022) Tourism, job vulnerability and income inequality during the COVID-19 pandemic: A global perspective. Annals of Tourism Research Empirical Insights, 3(1), 100046.

US Center on Budget and Policy. (2025) Policy basics: How many weeks of unemployment compensation are available? Accessed 30 July 2025, https://www.cbpp.org/research/economy/how-many-weeks-of-unemployment-compensation-are-available/.

Wang K, Jacquillat A (2020) A stochastic integer programming approach to air traffic scheduling and operations. Operations Research 68(5):1375-1402.

Yang S, Cao P, Du P, Wu Z, Zhuang Z, Yang L, et al. (2020). Early estimation of the case fatality rate of COVID-19 in mainland China: a data-driven analysis. Annals of translational medicine, 8(4), 128.